

**DNA Repair and the Cytotoxic
Effects of Cisplatin and DNA
Thiobases**

By

Andrew James Massey

A thesis submitted for the degree of Ph.D.

at

The University of London

August 2001

Imperial Cancer Research Fund
Clare Hall Laboratories
South Mimms
Potters Bar
Herts
EN6 3LD

and

Department of Biology
University College London
WC1E 6BT

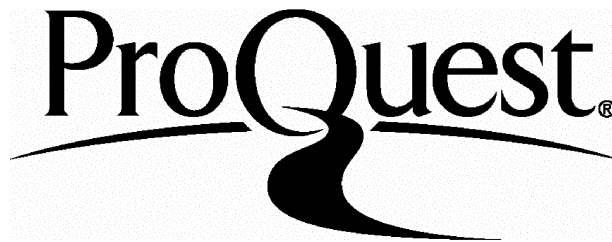
ProQuest Number: U641964

All rights reserved

INFORMATION TO ALL USERS

The quality of this reproduction is dependent upon the quality of the copy submitted.

In the unlikely event that the author did not send a complete manuscript and there are missing pages, these will be noted. Also, if material had to be removed, a note will indicate the deletion.



ProQuest U641964

Published by ProQuest LLC(2015). Copyright of the Dissertation is held by the Author.

All rights reserved.

This work is protected against unauthorized copying under Title 17, United States Code.
Microform Edition © ProQuest LLC.

ProQuest LLC
789 East Eisenhower Parkway
P.O. Box 1346
Ann Arbor, MI 48106-1346

Abstract

DNA Mismatch Repair (MMR) modulates the cytotoxicity of the therapeutic agent cisplatin. Two model systems: cisplatin sensitive *Escherichia coli dam* mutants and the ovarian carcinoma cell line A2780 were used to investigate the possible selection of MMR defects in cisplatin resistance.

Cisplatin sensitivity in *dam* mutants is partially reversed by a mutation in either the *mutS* or *mutL* MMR genes. Bacteria selected for cisplatin resistance were either *dam* revertants or *dam mmr* mutants. The latter displayed a partial decrease in sensitivity although some variants were comparable to wild type in this respect. This suggests the contribution of additional factors to cisplatin resistance.

Several independently selected variants of the ovarian tumour line A2780 were 1.5 to 3-fold less sensitive to cisplatin. All were proficient for mismatch repair. Two factors were identified that contributed to resistance - reduced levels of platination indicative of a protective mechanism and possible defects in p21 induction after cisplatin treatment.

Thiopurines are used in the treatment of leukaemia. Active DNA mismatch repair is required for 6-thioguanine (S^6G) toxicity. S^6G is incorporated into DNA and requires *in vivo* methylation at the S-6 position for lethality. The deoxynucleoside, 4-thiothymidine (S^4TdR), was evaluated as a potential chemotherapeutic agent. S^4TdR was incorporated into DNA and was S-methylated. Unlike S^6G , it showed no mismatch repair dependent toxicity. DNA S^4meT does not code ambiguously during replication. This property probably underlies its failure to interact with MMR.

S^4TdR absorbs light in the UVA range. UVA was synergistically toxic to human cells grown in S^4TdR . The thiopyrimidine sensitised normal fibroblasts approximately 100-fold to UVA. DNA adducts, possibly resembling (6-4) pyrimidine pyrimidone photoproducts, are implicated in this synergistic toxicity because S^4TdR conferred a 1000-fold sensitisation to UVA light in nucleotide excision repair deficient fibroblasts. Both S^6G and S^4dUdR also display synergistic cytotoxicity with UVA. The photochemical properties of thiobases may offer a novel therapeutic option.

Table of Contents

Abstract	2
Table of Contents	3
List of Tables	7
List of Figures	8
Acknowledgements	10
Publications	11
List of Abbreviations	12
Chapter 1 : Introduction	14
Repair of DNA Damage	14
Mechanisms of Direct Damage Reversal	16
Photoreactivation	16
Alkyltransferases	16
Excision Resynthesis Mechanisms	17
Base Excision Repair	17
Double Strand Break Repair	18
Homology Directed Repair	18
Single Strand Annealing	21
Non-Homologous End Joining	23
Nucleotide Excision Repair	24
Global Genome Repair	26
Transcription Coupled Repair	26
Cockayne Syndrome	28
Trichothiodystrophy	28
Mismatch Repair	29
The Bacterial Paradigm of Mismatch Repair	29
Strand Discrimination in <i>E. coli</i>	30
Mammalian Mismatch Repair	32
Strand Discrimination in Human MMR	33
Mismatch Repair Gene Mutations and Cancer	35
DNA Mismatch Repair and Acquired Resistance to DNA Damaging Agents	36
Methylating Agents	36
6-thioguanine	37
Model for O ⁶ meG / S ⁶ meG Processing by MMR	39
Other DNA Damaging Agents	39
Cisplatin	40
Cellular Responses to Cisplatin	43
Effects on DNA Replication	43
Effects on Transcription	44
Effects on Telomeres	44
Repair of Cisplatin Adducts	44

Binding by HMG Proteins	44
Acquired Resistance to Cisplatin	45
MMR	45
Alternative Factors that Contribute to Acquired Resistance to Cisplatin	49
Thiobases and Thionucleosides	51
Phototherapy and Photodynamic Therapy	55
Aims of Thesis	57
Chapter 2 : Materials and Methods	58
Materials	58
Bacterial Techniques	58
Maintenance of Stocks	58
Cisplatin Survival Curves	58
Preparation of Cisplatin	59
Selection of Cisplatin Resistant <i>E. coli</i>	59
Preparation and Digestion of Genomic DNA	59
Cell Culture Techniques	60
Maintenance of Cell Cultures	60
Cell Storage	60
Generation of Cell Cultures From Single Cells	61
Selection of Cisplatin Resistant Clones	61
Dialysis of Foetal Calf Serum	61
Cell Survival by Colony Formation Assay	61
Cisplatin	61
S ⁴ TdR and UVA	62
S ⁶ G and UVA	62
Lymphoblastoid Growth Curves	62
UVA Irradiation	62
Mutation Frequency	62
Inhibition of Cell Growth by Aminopterin	63
Molecular and Cellular Biology Techniques	63
Measurement of Protein Concentrations in Aqueous Solution	63
Determination of Nucleic Acid Concentrations in Aqueous Solutions	64
Cell Extracts	64
Stillman Replication Extract	64
For DE81 Paper TK Assay	64
For Gel Retardation Assay	64
For Western Blots	65
Preparation of Genomic DNA	65
HPLC and PCR	65
Platination Levels	65
Determination of DNA-S ⁴ TdR by HPLC	65
Thymidine Kinase Assays	66
By DE81 Paper	66
By TLC	66
Thymidine Phosphorylase Assay	66
Synthesis of S ⁴ T and S ⁴ meT Containing Oligonucleotides	67
Gel Retardation Assay	67
Substrate oligonucleotides	67

Primer Extension Assay	68
<i>In vitro</i> Mismatch Repair Assay	68
Western Blotting	69
Antibodies	69
PCR Amplification and DNA Sequencing of p53	70
DNA Sequencing Reactions	71
Fluorescence Associated Cell Sorting (FACS) Analysis	71
Levels of DNA Platination in Cultured Human Cells After Cisplatin Treatment	72
Determination of Reduced Glutathione Levels	72
Chapter 3: Results I	74
Role of DNA Mismatch Repair in Cisplatin Sensitivity of <i>Escherichia coli</i> Defective in the DNA Adenine Methylase (<i>dam</i>) Gene	
Determination of Secondary Characteristics of <i>dam E. coli</i>	74
Verification of Selection Strategy	76
Sensitivity of <i>dam</i> and <i>dam mutL/S E. coli</i> to Cisplatin	77
Selection for Cisplatin Resistance in a <i>dam</i> Genetic Background	80
Extent of Cisplatin Resistance in Selected Clones	83
Summary	86
Discussion	88
Models for MMR Involvement in O ⁶ meG and Cisplatin DNA Damage Processing	89
Chapter 4: Results II	94
Acquired Resistance to Cisplatin in the Ovarian Tumour Cell Line A2780	
Generation of Clonal Variants of A2780 Resistant to Cisplatin	94
Cisplatin Resistance of A2780 Clonal Variants	96
Mismatch Repair Status of Clonal Variants	98
p53 Response in Cisplatin-resistant Variants	98
Mutations in the p53 Gene	104
Codon 72 Polymorphisms and Cisplatin Resistance	109
DNA Platination Levels in A2780 Clonal Variants	109
GSH, A Protective Mechanism Against DNA Damage Induced by Cisplatin	111
Cell Cycle Analysis of A2780 Clonal Variants After Cisplatin Treatment	113
Mechanism of p21 Inactivation in Group 2 Clonal Variants	115
Summary	115
Discussion	117
Chapter 5: Results III	123
The Interaction Between DNA Mismatch Repair and the Thiopyrimidine, 4-Thiothymidine	
Cytotoxicity of S ⁴ TdR	124
Metabolism of S ⁴ TdR	124
S ⁴ TdR Incorporation into DNA	129
S-methylation of S ⁴ TdR	130
Coding Properties of S ⁴ TdR and S ⁴ meTdR During DNA Synthesis	133
Thermal Stability of S ⁴ T:A Base Pairs	134

Mutagenicity of S ⁴ TdR	134
Recognition of S ⁴ TdR and S ⁴ meTdR Base Pairs by hMutS α	137
Summary	141
Discussion	142
Chapter 6: Results IV	149
4-thiothymidine And Other DNA Thiobases As UVA Photosensitisers	
Synergistic Toxicity of 4-thiothymidine and UVA Light	149
Synergistic Toxicity Requires Active Thymidine Kinase	151
Effects of NER Deficiency on the Cytotoxicity of S ⁴ TdR and UVA	151
An Indication of Possible Lethal DNA Lesion - XP129	154
Effects of Defective MMR on S ⁴ TdR / UVA Toxicity	154
Exogenous Thymidine Inhibits the Synergistic Toxicity	157
Effect of Thymidylate Synthase Inhibitors on S ⁴ TdR / UVA Toxicity	158
4-thiodeoxyuridine as a Photosensitiser	161
Photosensitising Effects of DNA-6-thioguanine	161
Modulation of S ⁶ G / UVA Toxicity by NER	163
S ⁶ G / UVA Toxicity in MMR-proficient Fibroblasts	163
Summary	165
Discussion	166
Mechanism of S ⁴ TdR and UVA Cytotoxicity	166
S ⁶ G and UVA Light - A Common Cytotoxic Mechanism for Thiobases and UVA?	169
Possible Clinical Implications	172
Skin Cancer in Patients Receiving Azathioprine - A Role for S ⁶ G and UVA Light?	173
References	176
Appendix	192
FACs Data for Figure 4.9	192
Apoptosis Data for Figure 4.10	193

List of Tables

Table 1.1 Comparison of DNA Adducts Formed by Cis- and Transplatin	43
Table 1.2 Cisplatin Resistance in Ovarian Carcinoma Cell Lines	45
Table 1.3 Cisplatin Resistance in MMR Defective Cell Lines	46
Table 3.1 Genotypes of <i>E. coli</i> K-12 strains	75
Table 3.2 Mutator phenotypes of <i>E. coli</i> K-12 Defective in Mismatch Repair	76
Table 3.3 Summary of Secondary Phenotypes	76
Table 3.4 Sensitivity of <i>dam</i> and <i>dam mutL/S E. coli</i> to Cisplatin	80
Table 3.5 Secondary Phenotypes of Cisplatin Selected <i>E. coli</i>	82
Table 3.6 Summary of Cisplatin Resistance of Clones Selected for Cisplatin Resistance	83
Table 4.1 Comparative Cytotoxicity in Cisplatin Resistant Clones	96
Table 4.2 DNA Platination Levels in A2780 Clonal Variants	111
Table 5.1 Mutation Frequency Induced by S ⁴ TdR	137
Table 6.1 Summary of D ₃₇ Values	165

List of Figures

Fig 1.1	Sources and Consequences of Endogenous DNA Damage	15
Fig 1.2	Model for Base Excision Repair	19
Fig 1.3	Model for the Repair of Double-strand Breaks in <i>E. coli</i>	20
Fig 1.4	Repair of DSBs by Mammalian Cells	22
Fig 1.5	Overlapping Pathways of DSB Repair	25
Fig 1.6	DNA Damage Induced by UVC	25
Fig 1.7	Model for NER of Non-transcribed DNA (Global Genome Repair) in Mammalian Cells	27
Fig 1.8	Model of Methylation-dependent Mismatch Repair in <i>E. coli</i>	31
Fig 1.9	Initiation of Mismatch Repair in Mammalian Cells	34
Fig 1.10	Contribution of MMR to Methylating Agent Tolerance	38
Fig 1.11	Proposed Model for the Involvement of MMR in O ⁶ meG or S ⁶ meG Toxicity	40
Fig 1.12	Platinum (II) Compounds and DNA Damage	42
Fig 1.13	Effects of p53 and MMR Defects on Cisplatin Sensitivity in A2780	47
Fig 1.14	Cellular Responses to DSBs Mediated by the ATM/ATR Kinases	47
Fig 1.15	Structure of the <i>p53</i> Gene and p53 Protein	50
Fig 1.16	S ⁶ G, S ⁴ TdR and S ⁴ UdR Metabolism <i>in vivo</i>	52
Fig 1.17	Structure and Absorption Spectra of TdR, S ⁴ TdR, S ⁶ G and S ⁴ meTdR	53
Fig 1.18	Thiobases and UVA	54
Fig 3.1	Phenotypic Characterisation of Wild Type and Mutant Strains	78
Fig 3.2	Cisplatin Cytotoxicity in <i>dam</i> and <i>dam mutL/S</i> Mutant <i>E. coli</i>	79
Fig 3.3	Secondary Characteristics of GM113 Selected with Cisplatin	81
Fig 3.4	Secondary Characteristics of GM3819 Selected With Cisplatin	84
Fig 3.5	Cisplatin Cytotoxicity in Clones Selected for Resistance to Cisplatin	85
Fig 3.6	Secondary Characteristics of Clones G1 to G5	87
Fig 3.7	Cisplatin Sensitivity of G clones	87
Fig 3.8	Role of Mismatch Repair in the Processing of O ⁶ meG	92
Fig 3.9	Origin of Double-strand Breaks Induced by Cisplatin-DNA Adducts	93
Fig 4.1	Cisplatin Cytotoxicity in A2780 Clonal Variants	97
Fig 4.2	Analysis of Mismatch Repair Function	99
Fig 4.3	Analysis of p53 and p21 Levels After Induction With Cisplatin	101
Fig 4.4	p53 Induction in CP3A and CP7A by Different Forms of DNA Damage	102
Fig 4.5	Downstream Targets of p53 - Induction of MDM2 and Bax by Cisplatin	103
Fig 4.6	PCR Amplification of the <i>p53</i> Gene	105
Fig 4.7	Direct Genomic Sequencing of <i>p53</i>	108
Fig 4.8	Analysis of the Codon 72 Polymorphism in A2780 Clonal Variants	110
Fig 4.9	Determination of DNA-Platinum Levels After Treatment With Cisplatin	112
Fig 4.10	GSH Levels in A2780 Clonal Variants Before and After Cisplatin Treatment	112
Fig 4.11	Cell Cycle Response to Cisplatin in A2780 Clonal Variants	114
Fig 4.12	Cisplatin Induced Apoptosis in A2780 Clonal Variants	116
Fig 4.13	Induction of p21 Protein Levels by <i>n</i> -butyric Acid	116

Fig 4.14	Model for the involvement of p21 in the G2/M checkpoint control	121
Fig 5.1	Cytotoxicity of S ⁴ TdR	125
Fig 5.2	Inhibition of Phosphorylation of [¹⁴ C]TdR by Cold TdR or S ⁴ TdR	125
Fig 5.3	Direct Phosphorylation of TdR and S ⁴ TdR by [³² P]γATP	127
Fig 5.4	Degradation of Nucleosides by Thymidine Phosphorylase	128
Fig 5.5	Incorporation of S ⁴ TdR into Genomic DNA	130
Fig 5.6	<i>In situ</i> Methylation of a S ⁴ TdR Containing Oligonucleotide by Methyl Iodide	132
Fig 5.7	S ⁴ TdR Does Not Increase Sensitivity to Either S _N 1 or S _N 2 Methylating Agents	132
Fig 5.8	Coding Properties of S ⁴ TdR and S ⁴ meTdR	135
Fig 5.9	Extension of Terminal Base Pairs by Exonuclease-deficient Klenow Fragment	136
Fig 5.10	hMutSα Binding to a 34mer Containing S ⁴ TdR or S ⁴ meTdR Base Pairs	139
Fig 5.11	hMutSα Binding to a 31mer Containing S ⁴ TdR or S ⁴ meTdR Base Pairs	140
Fig 5.12	Structure of Base-pairing Confirmations	147
Fig 6.1	Synergistic Toxicity of S ⁴ TdR and UVA Light in MRC5VA Fibroblasts	150
Fig 6.2	S ⁴ TdR / UVA Cytotoxicity Depends on Active TK	152
Fig 6.3	Sensitivity of NER-defective XP Fibroblasts to S ⁴ TdR / UVA	153
Fig 6.4	Sensitivity of XP129 to S ⁴ TdR / UVA	155
Fig 6.5	Effects of Defective MMR in S ⁴ TdR / UVA Toxicity	156
Fig 6.6	Inhibition of S ⁴ TdR / UVA Toxicity by Exogenous TdR	159
Fig 6.7	Use of TS Inhibitors to Increase the Cytotoxicity of S ⁴ TdR / UVA	160
Fig 6.8	S ⁴ UdR as an Alternative Photosensitiser	162
Fig 6.9	S ⁶ G Sensitises XP12ROB4 Cells to UVA	162
Fig 6.10	Involvement of NER in Processing S ⁶ G-DNA Photoproducts	164
Fig 6.11	Modulation of S ⁶ G / UVA Cytotoxicity in MMR-proficient MRC5VA Cells	164
Fig 6.12	Structure of Photodimers Induced in Oligonucleotides Containing a TpS ⁴ T Dimer	168
Fig 6.13	Structure of TpdS ⁶ I Dinucleotide After UVA Irradiation	168
Fig 6.14	Azathioprine and Skin Cancer	175

Acknowledgements

I would like to thank Dr. Peter Karran, my principal supervisor, for all his help and patience over the last four years, not only in the laboratory but also during the preparation of this manuscript. I am grateful to the other members of the laboratory, both past and present, for their help however large or small. I would especially like to thank Pauline Branch for her help with the cell culture and Peter Macpherson for carrying out the *in vitro* mismatch repair assay.

A special thanks must go to Dr. Yao-Zhong Xu, now of the Open University, for synthesising and providing the 4-thiothymidine, and the 4-thioT and 4-methylthioT containing oligonucleotides. The help of the oligonucleotide synthesis service here at Clare Hall for their aid in this process is gratefully acknowledged. I am also grateful to Drs. M. Marinus, J. Essigmann and B. Sedgwick for kindly providing *E. coli* strains, M. Bignami and G. Aquilina for the HeLa Clone 7 and Clone 7#7 cell lines, and C. O'Neill for carrying out the AAS analysis.

Last, but by no means least, I would like to thank everybody here at Clare Hall and at L.I.F. for their support. I am especially grateful to everybody at the Clare Hall Cell Services laboratory for all their cell work, D. Davies for carrying out the FACs analysis and the Equipment Park for running the sequencing reactions. Thanks to you all.

Publications

Massey, A., Xu, Y.-Z. and Karran, P. Photoactivation of DNA Thiobases as a Novel Therapeutic Option (2001). *Current Biology* 11, 1142-1146.

Massey, A., Xu, Y.-Z. and Karran, P. Ambiguous Coding is Required for the Lethal Interaction Between Damaged Bases and DNA Mismatch Repair. *Submitted Mutation Research, October 2001.*

List of Abbreviations

2-AP	2-aminopurine
5FdUMP	5-fluorodeoxyuridine monophosphate
5FUdR	5-fluorodeoxyuridine
5meC	5-methylcytosine
6-MP	6-mercaptopurine
A	aminopterin
AP	apurinic / apyrimidinic
ATP	adenosine 5-triphosphate
Aza	azathioprine
BER	base excision repair
bp	base pair
BrUdR	5-bromodeoxyuridine
CPD	cyclobutane pyrimidine dimer
CS	Cockayne syndrome
dATP	deoxyadenosine triphosphate
DFCS	dialysed foetal calf serum
dGTP	deoxyguanosine triphosphate
dH ₂ O	deionised water
DNA	deoxyribonucleic acid
dNTP	deoxyribonucleotide triphosphate
DSB	double strand break
dsDNA	double-stranded DNA
DTNB	5,5'-dithiobis(2-nitrobenzoic acid)
dUMP	deoxyuridine 5-monophosphate
EDTA	disodium ethylenediaminetetraacetic acid
EtBr	ethidium bromide
FCS	foetal calf serum
GGR	global genome repair
GSH	glutathione (reduced)
H	hypoxanthine
HDR	homology directed repair
Hepes	<i>N</i> -2-hydroxyethylpiperazine- <i>N'</i> -2-ethane sulphonic acid
HGPRT	hypoxanthine guanine phosphoribosyl transferase
HNPCC	hereditary nonpolyposis colorectal cancer
HR	homologous recombination
IDL	insertion-deletion loop
IR	ionising radiation
IUdR	5-iododeoxyuridine
Kb	kilobase
MeI	methyl iodide

MGMT	O ⁶ -methylguanine DNA methyltransferase
MLH	MutL homologue
MMR	mismatch repair
MMS	methylmethane sulphonate
MNNG	<i>N</i> -methyl- <i>N'</i> -nitro- <i>N</i> -nitrosoguanidine
MNU	<i>N</i> -methyl- <i>N</i> -nitrosourea
MSH	MutS homologue
MSI	microsatellite instability
MT	metallothionein
NER	nucleotide excision repair
NHEJ	non-homologous end joining
O ⁴ meT	O ⁴ -methylthymine
O ⁶ meG	O ⁶ -methylguanine
PAGE	polyacrylamide gel electrophoresis
PBS	phosphate buffered saline
PCR	polymerase chain reaction
PDT	photodynamic therapy
PMS	post-meiotic segregation
PR	photoreactivation
RNA	ribonucleic acid
rpm	revolutions per minute
S ⁴ meTdR	4-methylthiothymidine
S ⁴ TdR	4-thiothymidine
S ⁴ UdR	4-thiodeoxyuridine
S ⁶ G	6-thioguanine
S ⁶ meG	6-methylthioguanine
SAM	<i>S</i> -adenosylmethionine
SDS	sodium dodecyl sulphate
SSA	single-strand annealing
ssDNA	single-stranded DNA
TCR	transcription coupled repair
TdR	thymidine
Thy	thymine
TK	thymidine kinase
TMP	thymidine 5-monophosphate
Tris	tris[hydroxymethyl]amino-methane(2-amino-2-hydroxy-methylpropane-1,2-diol)
TS	thymidylate synthetase
TTD	trichothiodystrophy
TTP	thymidine 5-triphosphate
U	units
UV	ultraviolet
x g	gravitational force
XP	xeroderma pigmentosum

Chapter 1

Introduction

When DNA was first identified as the store of the cell's genetic information, it was assumed that this macromolecule must be extremely stable in order to maintain its integrity. DNA, however, is not as stable as we would hope and is under constant attack from both inside and outside the cell. These are summarised in Fig 1.1. Cell metabolism can cause many forms of DNA change including hydrolytic base loss, deamination, oxidative damage, base methylation and base misincorporation during replication. Naturally occurring radiation including ultraviolet light (UV) and ionising radiation (IR) are additional exogenous sources of DNA damage. Finally, components of our lifestyles, such as smoking, cause damage to our DNA. Unrepaired DNA damage can lead to mutation and in higher organisms to the subsequent malignant transformation of cells and the development of cancer. Paradoxically, DNA damage is a common mechanism by which many chemotherapy drugs exert their cytotoxic effects. Efficient pathways of repair have evolved to take care of UV, H₂O, O₂ and methylation induced DNA damage and their ability to repair other forms of damage is coincidental.

Repair of DNA Damage

DNA repair mechanisms can be subdivided into two major categories:

(1) Direct damage reversal

- Photoreactivation
- Alkyltransferases

(2) Excision resynthesis

- Base Excision Repair (BER)
- Double Strand Break (DSB) Repair
- Nucleotide Excision Repair (NER)
- Mismatch Repair (MMR)

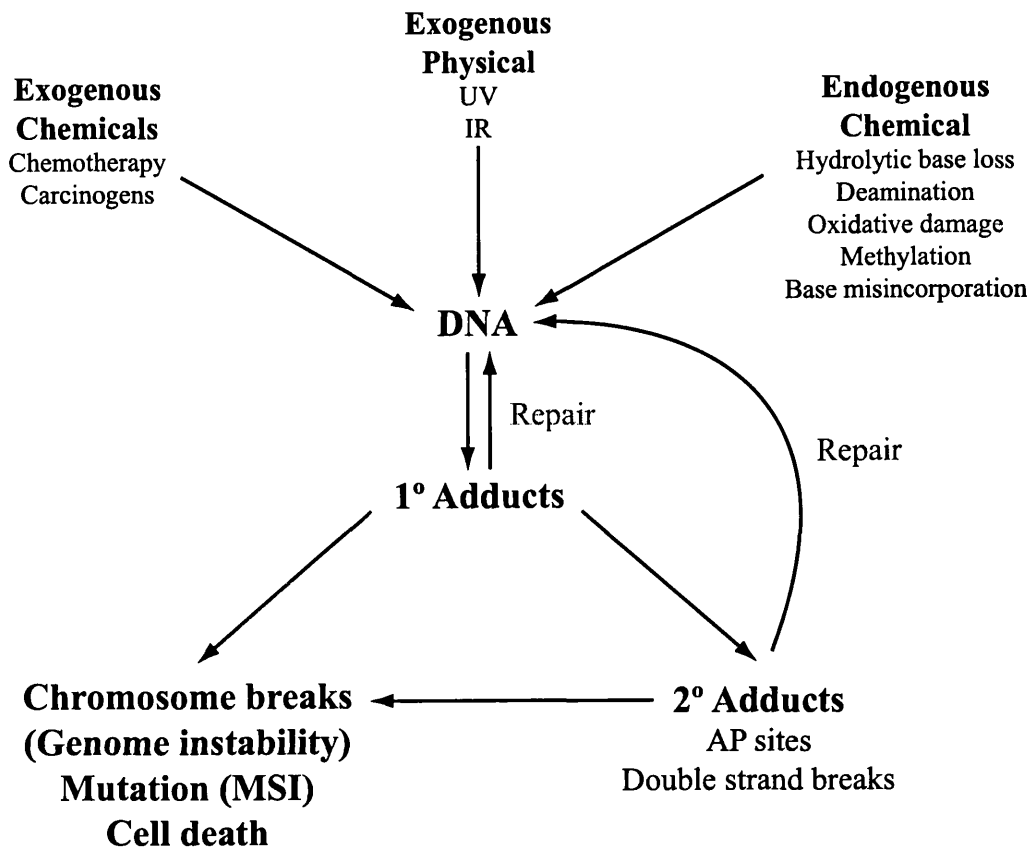


Figure 1.1 Sources and Consequences of Endogenous DNA Damage

The importance of DNA repair is highlighted by the conservation of the basic repair pathways across the evolutionary tree. However, the complexity of specific mechanisms increases with the organism's complexity. This brief survey of the major DNA repair pathways is based on (Friedberg *et al.*, 1995).

Mechanisms of Direct Damage Reversal

Photoreactivation (PR)

Photoreactivation involves the direct reversal of UV-induced DNA damage. It is catalysed by the photolyase enzyme and requires light of $\lambda > 300\text{nm}$. PR has evolved to repair a major product of UV-induced DNA damage, *cis-syn*-cyclobutane pyrimidine dimers (CPD, see Fig 1.6 for structures) and also exhibits, albeit at a decreased rate, some activity on *trans-syn*-cyclobutane pyrimidine dimers. Despite the presence of photolyase in most organisms, its activity is missing from placental mammals.

Alkyltransferases

S_N1 methylating agents, such as *N*-methyl-*N*-nitrosourea (MNU) and *N*-methyl-*N'*-nitro-*N*-nitrosoguanidine (MNNG), and some chemotherapeutic agents, like Temozolomide (TMZ), induce significant methylation of the O⁶ position of DNA-guanine and the O⁴ position of DNA-thymidine (see Fig 1.10A). If unrepaired, both DNA-O⁶-methylguanine (O⁶meG) and DNA-O⁴-methylthymine (O⁴meT) are potentially mutagenic through their ability to miscode. The direct chemical reversal of this methylation damage is achieved by the enzyme O⁶-methylguanine methyltransferase (MGMT; cells deficient in MGMT are often referred to as Mex⁻ or Mer⁻). The enzyme directly, and irreversibly, transfers the methyl group from the O⁶ position of G or the O⁴ position of T to a cysteine residue in the active site. For this reason, MGMT is sometimes referred to as a suicide repair enzyme. Repair of O⁶meG by MGMT is about 10⁴-fold more efficient than that of O⁴meT.

Excision Resynthesis Mechanisms

Base Excision Repair

For recent reviews of BER see (Lindahl *et al.*, 1997; Lindahl and Wood, 1999). The main role of BER is to facilitate the precise and rapid repair of a variety of DNA lesions caused by spontaneous hydrolytic depurination of DNA, deamination of cytosine and 5-methylcytosine (5meC), reaction of oxygen and hydroxyl radicals with DNA, and methylation. The basic mechanism is summarised in Fig 1.2. Essentially, an altered DNA base is removed by a DNA glycosylase and the resulting abasic site (AP-site) is repaired by the concerted action of an AP endonuclease, a DNA polymerase, and a DNA ligase. The enzymes that initiate the process of BER, the DNA glycosylases, show, in general, quite a high degree of substrate specificity. Despite limited structural homology, these enzymes show a common mechanism of action. This involves diffusion along the minor groove of DNA until a specific type of base damage is reached. The enzyme then kinks the DNA backbone, flips out the abnormal nucleoside residue into a specific recognition pocket, and mediates cleavage. There is some redundancy between glycosylases for the repair of some DNA lesions. For example, at least five different activities have been identified that can remove uracil from DNA.

After removal of the damaged base, the glycosylase may stay clamped to the DNA acting as a site of recruitment for the AP endonuclease APE1. APE1 cleaves the sugar-phosphate backbone on the 5' side and in the major pathway of BER (Fig 1.2A) then recruits POL β . POL β has intrinsic AP-lyase as well as polymerase activity and thus can remove the 5-deoxyribosephosphate (dRp) before inserting the correct base. The polymerase but not the AP-lyase activity of POL β is dispensable. Repair is completed once the LIG3-XRCC1 complex has ligated the nick. Terminal sugar-phosphate residues with a more complex structure may be resistant to cleavage by the AP-lyase activity of POL β . In these cases, strand displacement may occur (Fig 1.2B) involving POL β or another polymerase such as POL δ to fill in a gap several nucleotides long. The displaced flap is then cleaved by FEN1 and these reactions are

stimulated by PCNA which is believed to play a scaffolding role similar to XRCC1 in the other pathway. DNA ligase 1 (LIG1) then ligates the nick completing repair.

Double Strand Break Repair

DNA double-strand breaks (DSBs) are a common form of DNA damage and can be induced by a wide variety of processes including IR, some chemicals and chemotherapy drugs, processing of regions of ssDNA, and indirectly through the collapse of blocked replication forks.

Homology Directed Repair

Homology directed repair in somatic cells is very similar to the process of homologous recombination (HR). The function of HR is to repair chromosomal DSBs deliberately introduced as part of the normal process of meiosis to produce haploid cells. As a consequence, many of the enzymes used to facilitate HR are also common to the process of HDR. As HDR utilises a second intact copy of the chromosome to facilitate repair, repair by this pathway is extremely accurate.

An understanding of the mechanism of recombinational repair has come from studying *E. coli* (for a recent review see (Masson and West, 2001)). In *E. coli*, almost 20 gene products are required for normal levels of recombination and many play well-defined roles in either initiation, DNA-DNA interactions leading to homologous contacts and strand exchange, branch migration and Holliday junction resolution. The basic mechanism for the repair of DSBs in *E. coli* is illustrated in Fig 1.3. Recombination is initiated by the RecBCD complex that exhibits both DNA helicase as well as ssDNA and dsDNA nuclease activities. RecBCD binds to the DSB and then travels along the DNA leading to the resection of the DSB until χ sequences are reached generating 3' overhanging ssDNA tails. These tails are acted upon by RecA, a powerful recombinase, catalysing the invasion of the ssDNA tail into a homologous duplex to form a Holliday junction.

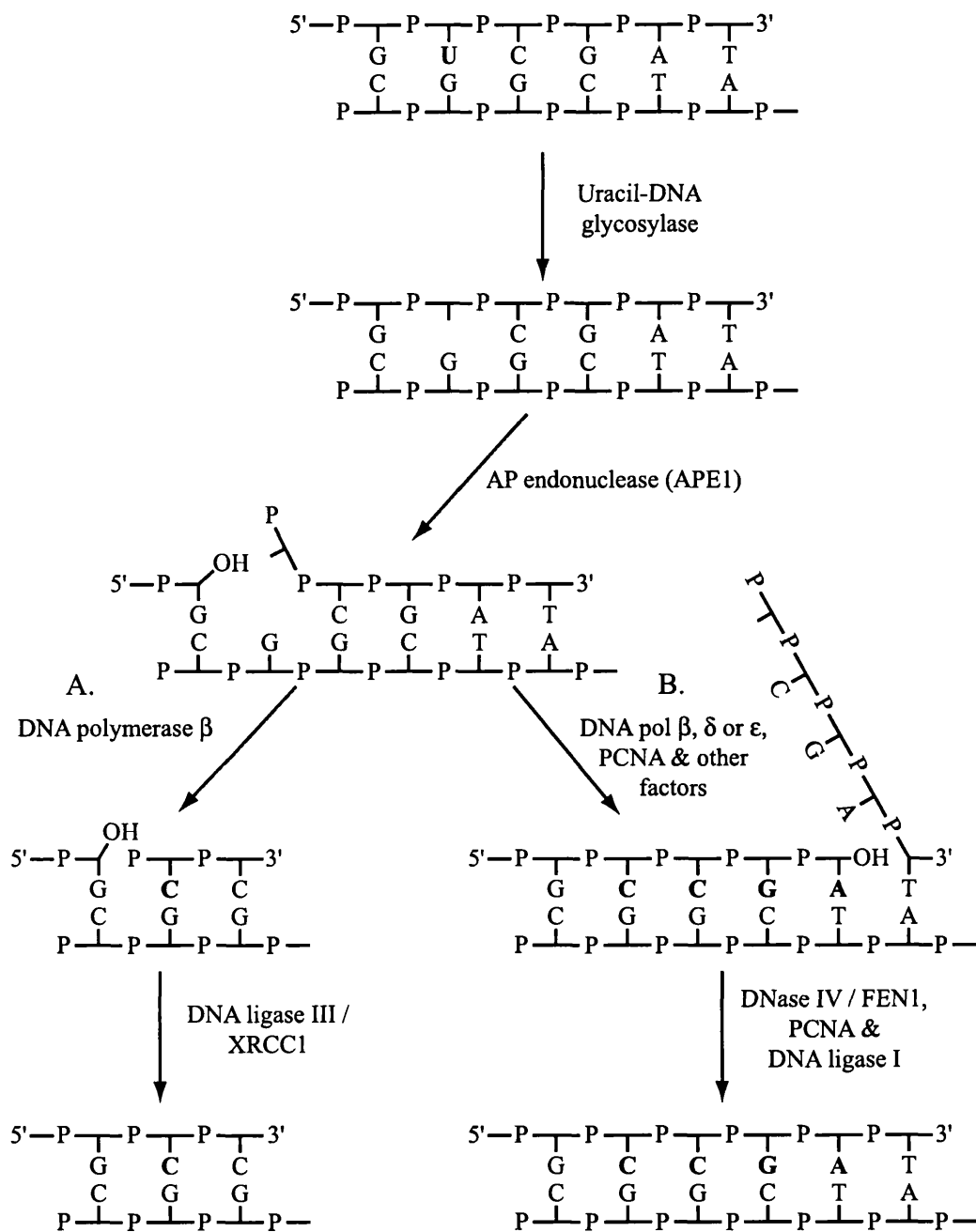


Figure 1.2 Model for Base Excision Repair

The altered base residue (in this case a Uracil) is removed by a glycosylase to leave an abasic site. This abasic site is then cleaved by the AP-endonuclease APE1. The major pathway (A) involves the removal of the 5'-dRp moiety by the AP-lyase activity of POL β followed by the insertion of the correct nucleotide. Repair is completed by ligation of the nick by the LIG3-XRCC1 complex. When the 5-sugar-phosphate is resistant to cleavage by the AP-lyase activity, strand displacement and resynthesis, catalysed by POL β or δ , may occur (B). The displaced strand is then cleaved by FEN1 and the newly synthesised DNA ligated by LIG1.

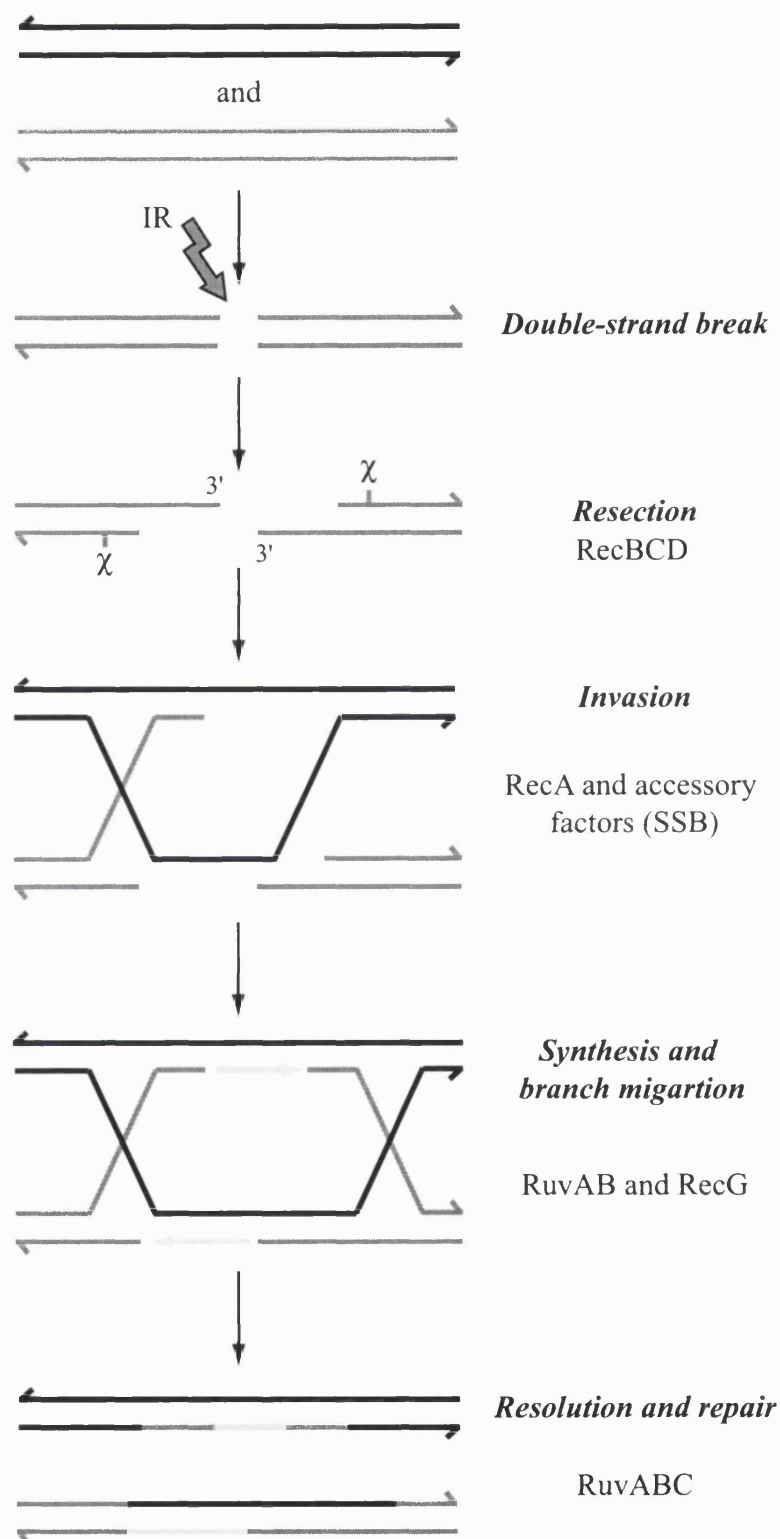


Figure 1.3 Model for the Repair of Double-strand Breaks in *E. coli*

Two homologous duplexes are indicated in black and grey respectively with half arrows denoting 3' termini. Light grey lines indicate newly synthesised DNA. The recombination product indicated in the final step is only one of several possible outcomes dependent upon the resolution of the Holliday junction.

Inter-linked molecules are further processed by RuvAB and RecG (through a process known as branch migration) and DNA synthesis to replace any lost information. Finally, resolution of the Holliday junction by RuvABC, and DNA ligation complete the repair process.

S. cerevisiae has proved a useful model for studying HDR in eukaryotic cells. HDR is carried out by the RAD52 epistasis group of proteins and includes the products of the *RAD50-55*, *RAD57*, *RAD59*, *MRE11* and *XRS2* genes (see (Baumann and West, 1998) for recent review). This, and the identification of human homologues, has provided valuable insights into the mammalian mechanism.

In mammalian cells, strand exchange is catalysed by the hRad51 protein in a reaction stimulated by hRad52 (which has dsDNA end-binding activity) and RPA (Fig 1.4). hRad51 is the human homologue of the *E. coli* RecA protein. In addition, hRad54, hRad55 and hRad57 are required for the efficient formation of Holliday structures. Further processing by branch migration, Holliday-junction resolution and DNA ligation completes repair. An interesting recent development is the realisation that the products of the breast cancer susceptibility genes *BRCA1* and *BRCA2* are involved in the processes of DSB repair. hRad51 has been shown to co-localise with Brca1 and Brca2 into foci also containing PCNA after DNA damage. Both *Brca1*^{-/-} and *Brca2*^{-/-} mouse fibroblasts show a high level of spontaneous chromosome aberrations and exhibit some sensitivity to double-strand break inducing agents.

Single Strand Annealing

SSA relies on regions of DNA homology within the same molecule to align the DNA strands to be rejoined. Unlike HDR, SSA can be seen as an error prone repair pathway as it can lead to the loss of quite large regions of DNA sequence. DSB end processing and the detection of overlapping homology is performed by the hRad50/Nbs1/hMre11 complex. Resection and annealing by this complex creates single-stranded tails which are trimmed before ligation possibly by the XPF-ERCC1 structure specific nuclease (human homologues of scRAD1/RAD10). In yeast this process also requires the MSH2 and MSH3 proteins especially when the tails are short.

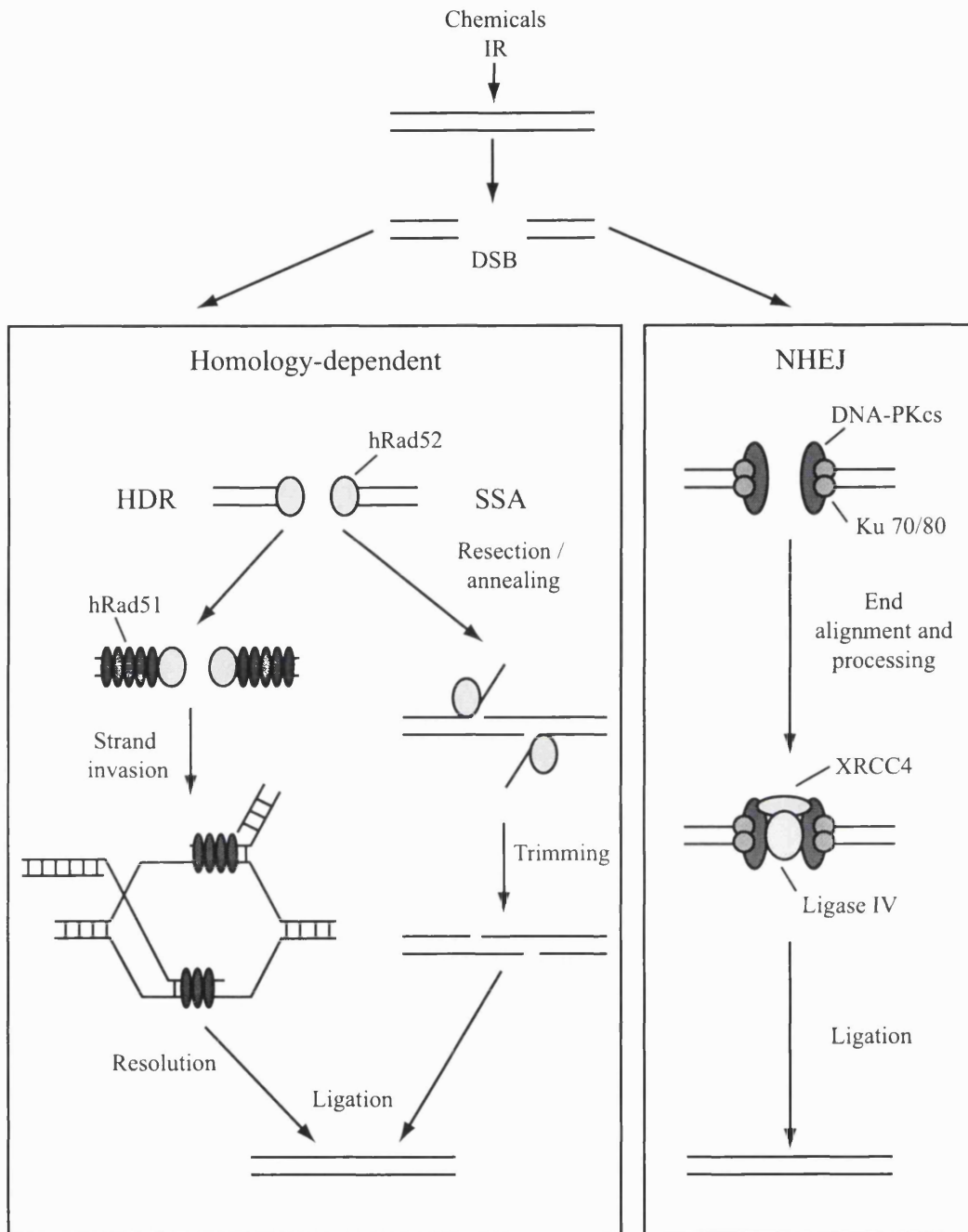


Figure 1.4 Repair of DSBs by Mammalian Cells

The ends of a DSB introduced by either IR or other sources are bound by either Rad52 or the Ku 70/80 heterodimer. Strand invasion of the intact sister chromatid is catalysed by hRad51 initiating repair by homologous recombination. Resection and annealing of short regions of complementary sequence leads to repair by the SSA pathway. Trimming of non-complementary single-stranded tails and ligation completes repair.

In the NHEJ pathway, Ku70/80 recruits DNA-PK_{cs} and repair is completed by the XRCC4-DNA ligase IV complex.

Non-Homologous End Joining

NHEJ is the major pathway by which mammalian cells repair DSBs. Its importance is highlighted by the high degree of conservation of this pathway's components between *S. cerevisiae* and man. For recent reviews of this pathway see (Critchlow and Jackson, 1998; Khanna and Jackson, 2001). In human cells, NHEJ involves the proteins Ku70, Ku80, DNA-PK_{cs}, XRCC4 and Ligase 4. These factors, however, are insufficient to catalyse efficient end-joining *in vitro* and additional factors have yet to be identified. Interestingly, inositol phosphate (IP₆) has recently been shown to bind DNA-PK_{cs} and stimulate end-joining *in vitro*.

Ku70 and 80 form a heterodimer that shows a strong affinity for binding to double-stranded DNA ends. DSB repair by NHEJ is probably initiated by the binding of Ku70/80 to the ends of the break. This may protect the ends from further degradation and bring them into close enough proximity for ligation. Ku 70/80 then recruits DNA-PK_{cs} to the break where the complexes form a bridge between the two ends. DNA-PK_{cs} is a member of the PI-3 kinase like protein kinases (which also includes ATM and ATR). When bound with Ku (in the presence of DNA ends), DNA-PK_{cs} is activated and it phosphorylates several proteins including other end-joining components and signalling molecules such as p53. The relevance of these phosphorylation events is, however, not completely understood. End trimming and gap filling to generate ligatable ends by as yet identified components may then occur before the ends are ligated by XRCC4-LIG4. Cells with defects in components of the NHEJ pathway are sensitive to killing by ionising radiation. In addition, many of the components of NHEJ are necessary for the process of V(D)J recombination used to generate antibody diversity in B-cells. For example, mice defective in DNA-PK_{cs} show a severe combined immunodeficiency (SCID) phenotype and are also sensitive to IR.

Many of the proteins involved in the repair of DSBs show overlapping functions not only in the different pathways of DSB repair but also with other repair pathways. For example, hMSH2 and hMSH3 may be involved in the processing of the overlapping tails generated by SSA. In addition, these proteins form the hMutSβ mismatch recognition complex involved in the repair of looped DNA structures

generated by replication slippage. A summary of these potentially overlapping functions is illustrated in Fig 1.5.

Nucleotide Excision Repair

NER has evolved to deal with DNA damage induced by UV-light, predominantly UVB. DNA absorbs maximally in the UVC range at around 260nm and when exposed to such wavelengths, adjacent pyrimidines become covalently linked. Light of longer wavelength (including both UVB and UVA) can also generate the same sort of DNA damage albeit at a lower frequency (Kielbassa and Epe, 2000; Runger *et al.*, 2000). Two major forms of DNA damage can be induced by light of such wavelengths. Cyclobutane pyrimidine dimers (Fig 1.6A) are formed between two adjacent pyrimidines by the saturation of their respective 5,6 double bonds to form a four-membered cyclobutyl ring. The second class are known as (6-4) pyrimidine pyrimidone dimers and are formed predominantly at CC, TC and less frequently TT (but not CT, (Friedberg *et al.*, 1995)) sequences (Fig 1.6B). Linkage between the C-6 position of one pyrimidine and the C-4 position of the adjacent pyrimidine generates the four-membered ring oxetane. The oxetane is unstable and rapidly converts to the (6-4) pyrimidine pyrimidone dimer. Subsequent irradiation of the DNA with wavelengths of around 300nm can convert the (6-4) form to its Dewar isomer. NER not only repairs UV-induced damage but can act on a wide variety of bulky, helix distorting lesions. It appears that NER does not recognise particular adducts but the DNA distortion induced by these adducts. The more distorting a lesion, the more efficient its repair by NER appears to be.

Identification of the major components of human NER has been made possible by virtue of a rare, recessively inherited autosomal disorder, xeroderma pigmentosum (XP). Patients suffering from XP are characterised by the early onset of severe photosensitivity, a high incidence of skin cancer and, in some cases, neurological abnormalities. Cells derived from these patients have identified seven complementation groups, XP-A to XP-G, each group defective in a different component of the repair pathway. An additional group, XP-variant (XP-V), is not defective in NER but instead lacks a DNA polymerase (POL η) involved in DNA damage bypass.

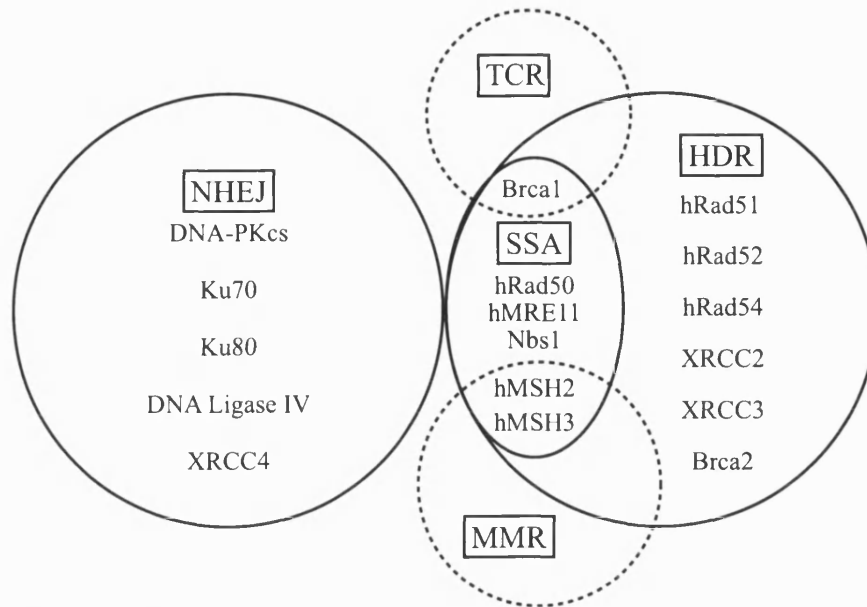
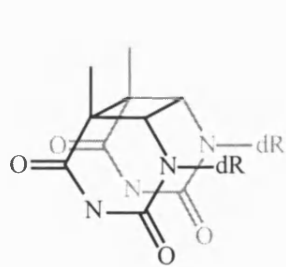


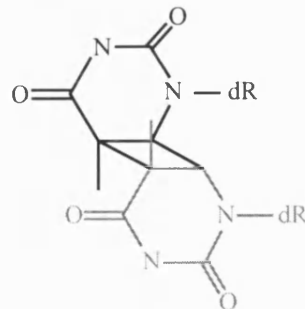
Figure 1.5 Overlapping Pathways of DSB Repair

Proteins in the left circle are those indicated to be involved in NHEJ and those in the right, homology-dependent repair. SSA, which requires some homology, is depicted as a subpathway of HDR. Possible overlaps between SSA and TCR or MMR are indicated but it should be noted that no evidence exists, as of yet, for an involvement of mammalian MMR in SSA.

A.

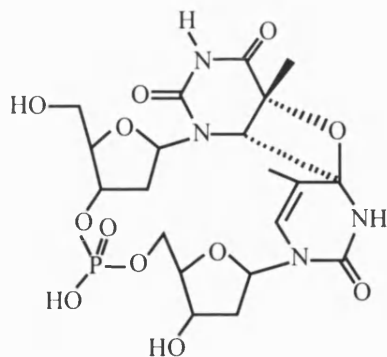


cis-syn (T-T)

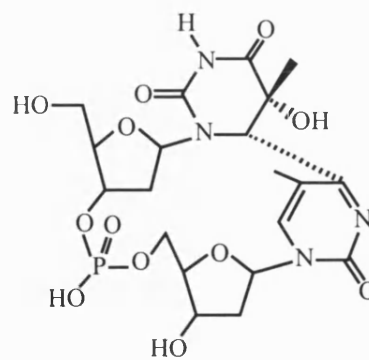


trans-syn (T-T)

B.



Oxetane



(6-4) pyrimidine-pyrimidone dimer

Figure 1.6 DNA Damage Induced by UVC

A. Cyclobutane Pyrimidine Dimers. The two major forms of thymine dimer are indicated.

B. Oxetane and (6-4) pyrimidine pyrimidone photoproducts. TpT dimers are illustrated.

Two modes of NER exist: repair of lesions in the entire genome (referred to as global genome repair, GGR) and repair of transcription-blocking lesions present in transcribed DNA strands (called transcription-coupled repair, TCR). Many of the XP-complementation group proteins are common to both pathways. Two recent reviews (Batty and Wood, 2000; de Laat *et al.*, 1999) have covered this work in great detail.

Global Genome Repair

GGR functions to remove DNA lesions from the bulk of the genome and is summarised in Fig 1.7. Distortions in the DNA helix due to bulky DNA adducts are recognised by the XPC-hHR23B complex leading to partial opening of the DNA helix. This slightly open DNA structure allows entry of TFIIH in concert with XPA and RPA to the site of damage. XPD and XPB, two of the subunits of TFIIH, are a 5'→3' and a 3'→5' helicase respectively. ATP dependent unwinding by the two helicases now occurs leading to the formation of the pre-incision complex (PIC). The helicases probably stall when one of them encounters the DNA lesion and this may serve to identify the damaged strand. XPG then makes an incision 2-9 phosphodiester bonds 3' of the lesion followed by an ERCC1-XPF incision 16-25 phosphodiester bonds 5' to the lesion. The oligonucleotide containing the lesion (24-32 nucleotides) is then released and the gap filled by a PCNA dependent polymerase (POL δ or ϵ) and sealed by a DNA ligase regenerating an intact DNA duplex.

Transcription Coupled Repair

DNA damage recognition by XPC-hHR23B is dispensable for TCR. Instead, stalling of the elongating RNA POL II at the DNA lesion probably serves as the signal for recruitment of repair factors. TCR also requires, in addition to XPA, XPG, ERCC1-XPF, TFIIH and RPA, the two Cockayne syndrome (CS) proteins CSA and CSB. In the postulated mechanism, the advancing RNA polymerase stalls at a DNA lesion. The RNA polymerase may either be displaced by CSA, CSB, TFIIH, XPA and RPA or the polymerase may "back up" allowing access of these factors to the damaged strand. As before, the action of the two TFIIH helicases (XPB and XPD) cause the ATP dependent formation of the PIC and this is cleaved, as before, by the 3' and 5' nucleases XPG and ERCC1-XPF. The strand containing the damage is released and the gap filled as before.

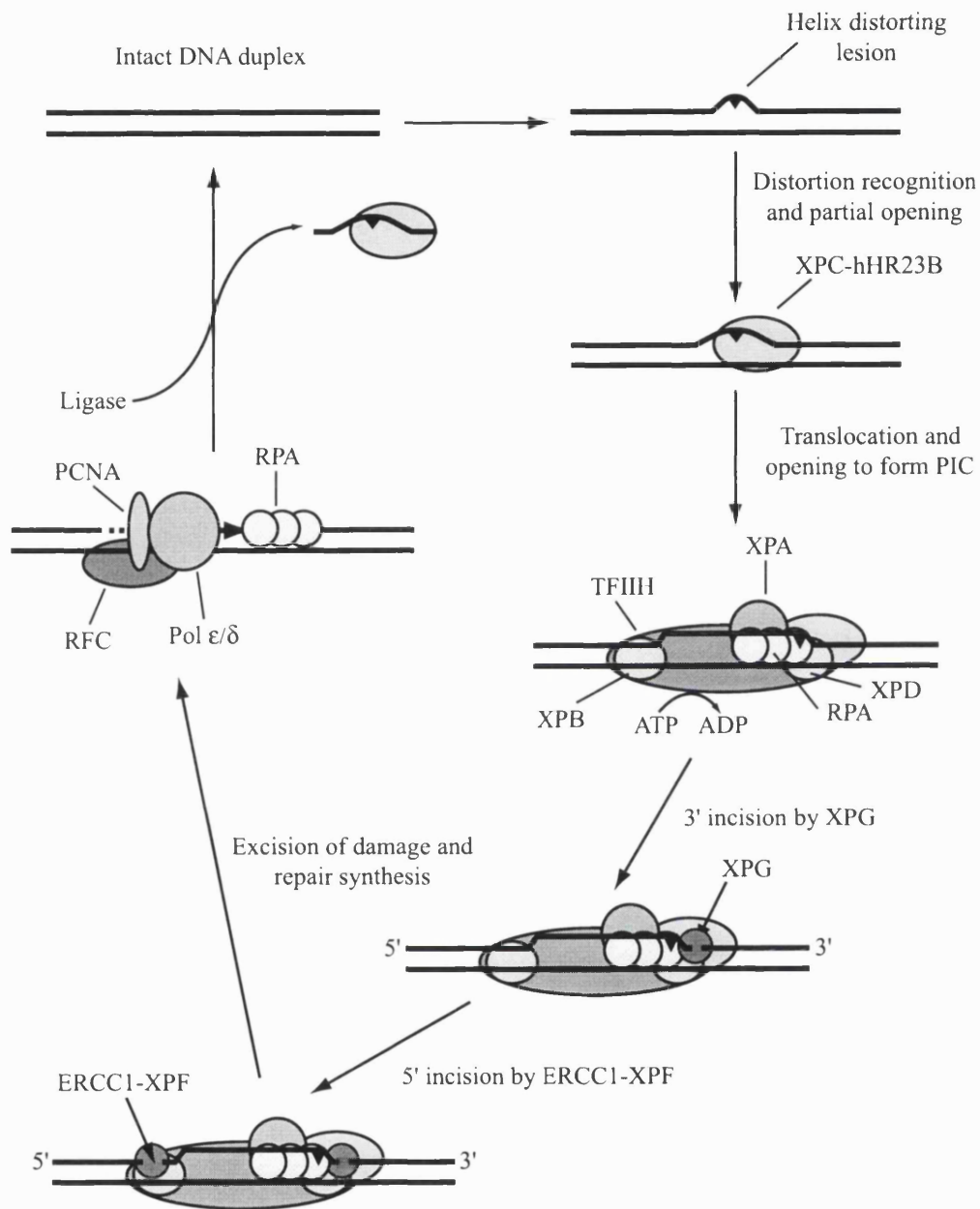


Figure 1.7 Model for NER of Non-transcribed DNA (Global Genome Repair) in Mammalian Cells

See text for further details

Two additional UV-sensitive human syndromes, like xeroderma pigmentosum, defective in NER are associated with human disease (reviewed in (Bootsma *et al.*, 1998; de Boer and Hoeijmakers, 2000)).

Cockayne Syndrome

CS is a very pleiotropic disorder and CS patients display, in general, skeletal abnormalities, mental retardation and progressive neurological degeneration. Surprisingly, these patients do not show a pre-disposition to the development of skin cancer. CS cells display increased killing by DNA damaging agents, including UV, due to a defect in TCR. Two complementation groups exist for "classic CS" - CS-A and CS-B and the associated genes code for two proteins CSA and CSB. The clinical phenotype of CS patients cannot be attributed to defects in NER as these symptoms are not exhibited by patients with defects that completely abolish NER, such as those in XPA. It is suggested that perhaps CS-A and CS-B patients have a transcription deficiency, induced possibly by DNA damage, that contribute to the clinical symptoms.

Trichothiodystrophy (TTD)

TTD is an autosomal recessive disorder characterised by sulphur-deficient brittle hair, ichthyosis (fish-like scales on the skin), and mental and physical retardation. TTD is a rare syndrome and patients exhibit broad clinical heterogeneity. Many other described syndromes, including Pollitt syndrome, Tay's syndrome, Amish brittle hair syndrome, Sabina's syndrome and Marinesco-Sjorgen syndrome belong to the broad TTD spectrum. Patients with TTD fall into three complementation groups: defects in *XPB*, defects in *XPD* and defects in an as yet unidentified gene named *TTD-A*. Interestingly, the mutations in *XPB* and *XPD* in TTD patients do not give rise to classical XP. Mutations in these proteins may not only affect the NER function of TFIIH but may also affect both the basal transcription function and/or the stability of TFIIH (de Boer and Hoeijmakers, 2000). The degree to which this happens may reflect the wide variation in clinical symptoms exhibited by TTD patients.

The three diseases of XP, CS and TTD are not always distinct and all show extensive clinical heterogeneity. Patients in the same complementation group do not always

show the same phenotype. Mutations in the complementation group XP-D, for example, can give patients the clinical phenotype of XP, XP/CS or TTD (Bootsma *et al.*, 1998). This is probably a reflection of the underlying effects of the mutation on not only NER but also transcription.

Mismatch Repair

The mismatch repair (MMR) system plays a crucial role in protecting the integrity of the genome through its ability to repair mismatched bases. MMR operates both during DNA replication and recombination. The post-replication repair of DNA polymerisation errors is probably its best known function. However, recognition of homologous DNA sequences during recombination and the repair of mismatches or subsequent abortion of these recombination attempts is also an important function of MMR. This anti-recombinogenic property is suggested to control speciation. Repair by MMR involves the excision of a tract of DNA containing the mismatch of up to 1Kb in length. In order to discriminate this from the short excision patches generated by some DNA glycosylases that repair mismatches (for example TDG), this process is referred to as "Long Patch" MMR. Another important concept in MMR is the ability of the enzyme complexes to discriminate the parental strand from the newly synthesised daughter strand. Failure to do so could lead to the fixing of mutations. For an extensive in depth recent review of MMR see (Harfe and Jinks-Robertson, 2000).

The Bacterial Paradigm of Mismatch Repair

The methyl-directed pathway of MMR in *E. coli* is probably the best understood and has been completely reconstituted *in vitro*. This process involves three dedicated proteins MutS, MutL and MutH as well as a helicase (Helicase II), exonucleases (Exo I, Exo VII or RecJ), DNA polymerase (Pol III) and DNA ligase. The basic pathway is outlined in Fig 1.8. A homodimer of MutS serves as the mismatch recognition factor and MutS binds to mismatches with a much greater affinity than to homoduplex DNA. Deletion studies indicate that the C-terminal portion of MutS is important for dimerisation and mismatch binding occurs through the N-terminal domain. A P-loop nucleoside triphosphate binding domain has also been identified

in the C-terminal half. The crystal structure of *E. coli* MutS bound to a G:T mismatch has recently been solved (Lamers *et al.*, 2000). While MutS may bind as a homodimer, this crystal structure study has shown that it functions as a structural heterodimer; that is, the two subunits have different functions. Only one MutS subunit binds the mismatch but both contact the DNA forming a clamp. The helix-turn-helix domain situated in the C-terminus is important for protein dimerisation. The ATPase and DNA binding sites are formed by utilising domains from both subunits and can be viewed as composite sites. Disruption of the dimerisation domain subsequently abolishes both ATPase activity and DNA binding.

Binding of the MutS homodimer to the mismatch triggers an ATP-dependent conformational change in MutS followed by the ATP-driven, bi-directional translocation along the DNA. This generates a looped out DNA structure (resembling the Greek letter Ω) with the mismatched base at the top of the loop and the protein complexes at the bottom. MutS is able to interact with two double helices and probably binds to both sides of the looped structure. The role of MutL in the process is not known. MutL recognises and binds to MutS as a homodimer. The addition of MutL accelerates this process of bi-directional translocation and MutL may catalyse the conformational change of MutS or recognise the conformationally changed MutS and promote translocation away from the mismatch (Jiricny, 1998). MutL has also been assigned the role of "molecular matchmaker" and is thought to mediate the interaction of MutH with MutS and the loading of Helicase II. Translocation occurs along the DNA until a strand discrimination signal is reached. This activates the endonucleolytic activity of the strand discrimination factor MutH and introduces a single-strand nick in the daughter strand. Degradation of this newly synthesised strand by Exo I (3'→5') or Exo VII/RecJ (5'→3') with Helicase II to just beyond the mismatch can then occur. Pol III holoenzyme and DNA ligase seal the gap and complete repair.

Strand Discrimination in E. coli

The DNA adenine methylase (Dam) protein can methylate the 6-position of adenine in the DNA of *E. coli* at the sequence GATC (Barras and Marinus, 1989). This sequence serves as the strand discrimination signal in *E. coli*. MutH cleaves DNA 5' to the G in GATC.

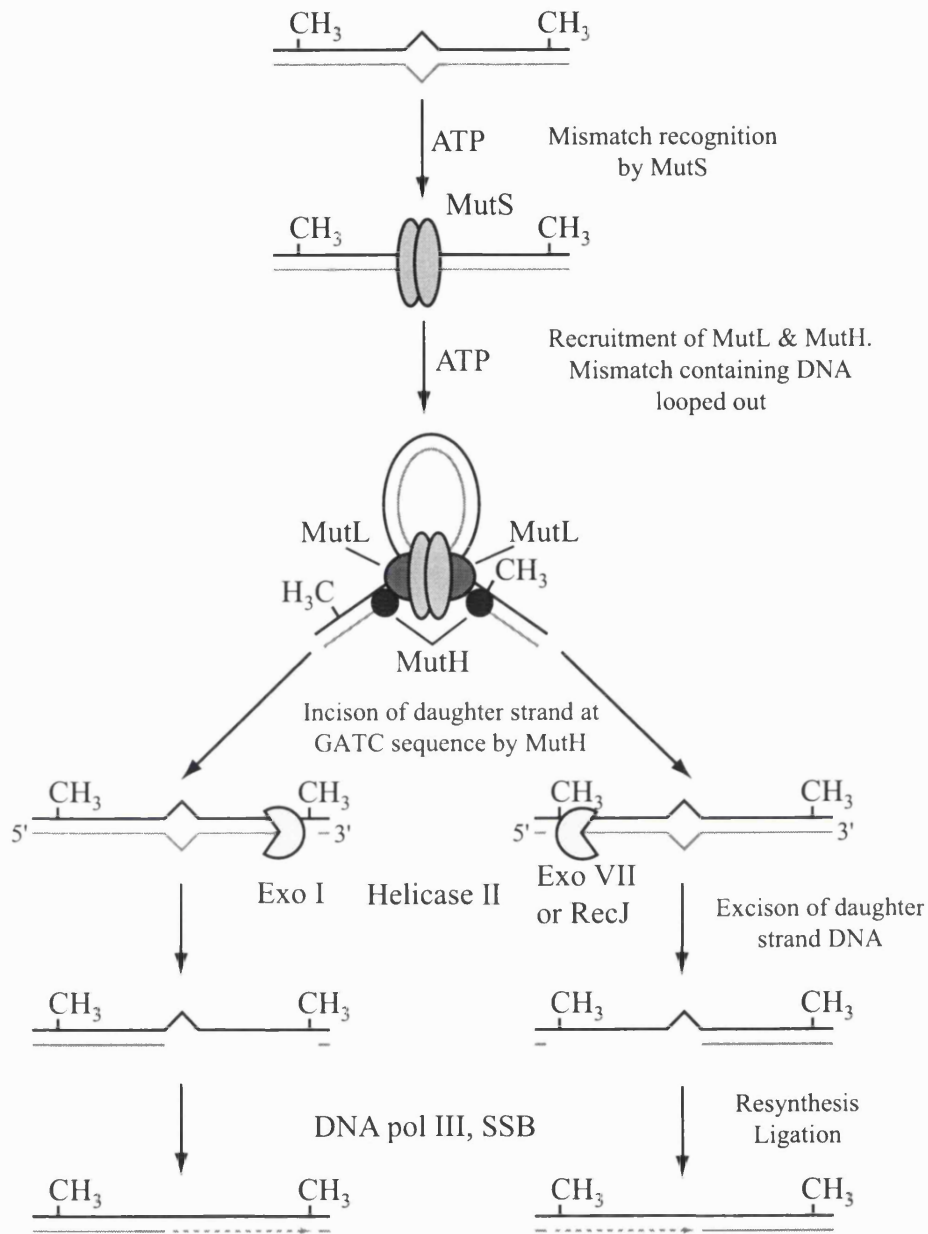


Figure 1.8 Model of Methylation-dependent Mismatch Repair in *E. coli*

See text or details

Parental strand (—), daughter strand (—).

This cleavage can only occur in the unmethylated strand of a hemimethylated duplex. In this way, the MutH protein is able to discriminate the parental and daughter strands during MMR as the newly synthesised DNA remains unmethylated for a short time after DNA replication. *E. coli dam* mutants show an increase in mutations due to their inability to consistently repair the correct DNA strand after replication.

Mammalian Mismatch Repair

In mammalian cells, five homologues of MutS have been identified - MSH2 to 6 but only three of these, MSH2, MSH3 and MSH6, have so far been shown to participate in post-replicative MMR. MSH2 forms heterodimers with MSH6 and MSH3 and these dimers are referred to as MutS α and MutS β respectively (Fig 1.9). This closely parallels the observation that the *E. coli* MutS homodimer functions as a heterodimer. The MutS α and MutS β heterodimers have distinct yet overlapping mismatch recognition properties. MutS α recognises predominantly single base mispairs and 1-2 base pair insertion-deletion loops (IDL) while MutS β recognises 2-5 base pair IDLs. As in yeast, MSH4 and MSH5 appear to be important for some function specific to meiosis.

Upon mismatch binding hMutS α undergoes structural changes that are dependent on the state of the nucleotide bound. The ADP-bound form of hMutS α is proficient for mismatch binding and upon binding to a mismatch, ADP-ATP exchange occurs. ATP-hMutS α no longer remains bound to the mismatch and is free to translocate along the DNA. Two models have been suggested to account for this phenomenon. In the first, hMutS α is suggested to behave like a molecular switch analogous to G-proteins (for example ras or the trimeric G-proteins, (Fishel, 1998; Fishel, 1999)). Upon exchange of ADP for ATP, hMutS α forms a "sliding clamp signalling molecule" and transduces a "mismatch signal" to a downstream effector, such as the DNA polymerase machinery, that controls repair. Hydrolysis of ATP to ADP by the intrinsic ATPase activity of the MutS complexes releases hMutS α from the DNA regenerating it for new mismatch binding. An alternative model suggests that hMutS α behaves like the MutS dimer of *E. coli*. ATP binding by hMutS α releases it

from the mismatch and it then translocates along the DNA in an ATP-dependent fashion (Blackwell *et al.*, 1998a; Blackwell *et al.*, 1998b).

In addition to the MutS homologues, mammalian cells have four homologues of MutL - PMS1 (post-meiotic segregation 1), PMS2, MLH1 and MLH3. MLH1 forms heterodimers with the other three proteins. The heterodimer of MLH1/PMS2 is the major player in post-replication MMR and is referred to as hMutL α . MLH1/PMS1 is believed to have some function in meiosis and no definite function has yet been assigned to the recently discovered MLH1/MLH3 dimer. The role of hMutL α in mammalian mismatch repair is not clear and may, like MutL, serve to recruit the other factors necessary to elicit repair.

Little is known about the additional factors required for MMR but a putative exonuclease, EXO1, has been identified that is homologous to the yeast EXO1 involved in MMR (Tishkoff *et al.*, 1998). Finally, PCNA co-immunoprecipitates with hMSH2, hMLH1 and hPMS2 from cultured cells. This suggests that PCNA may play a key role in the MMR process perhaps in strand discrimination or in tethering POL δ or ϵ to the repair process.

Strand Discrimination in Human MMR

In *E. coli* strand discrimination, as already discussed, is achieved through methylation of adenine in GATC sequences by Dam and the subsequent recognition of this modification by MutH. No such DNA modifications have been identified in mammalian cells nor has a homologue of MutH. *In vitro*, strand discontinuities can direct mammalian MMR to the correct strand but this is also true for MutH defective *E. coli*. This has led some to suggest that single-strand gaps, such as those of Okazaki fragments, could serve as strand discrimination signals. However, this does not account for repair on the leading strand where DNA synthesis is continuous.

The discovery that PCNA interacts with components of the MMR system (MLH1) has led to the suggestion of an alternative model in which MMR is tethered to the advancing replicative polymerase (Jiricny, 1998).

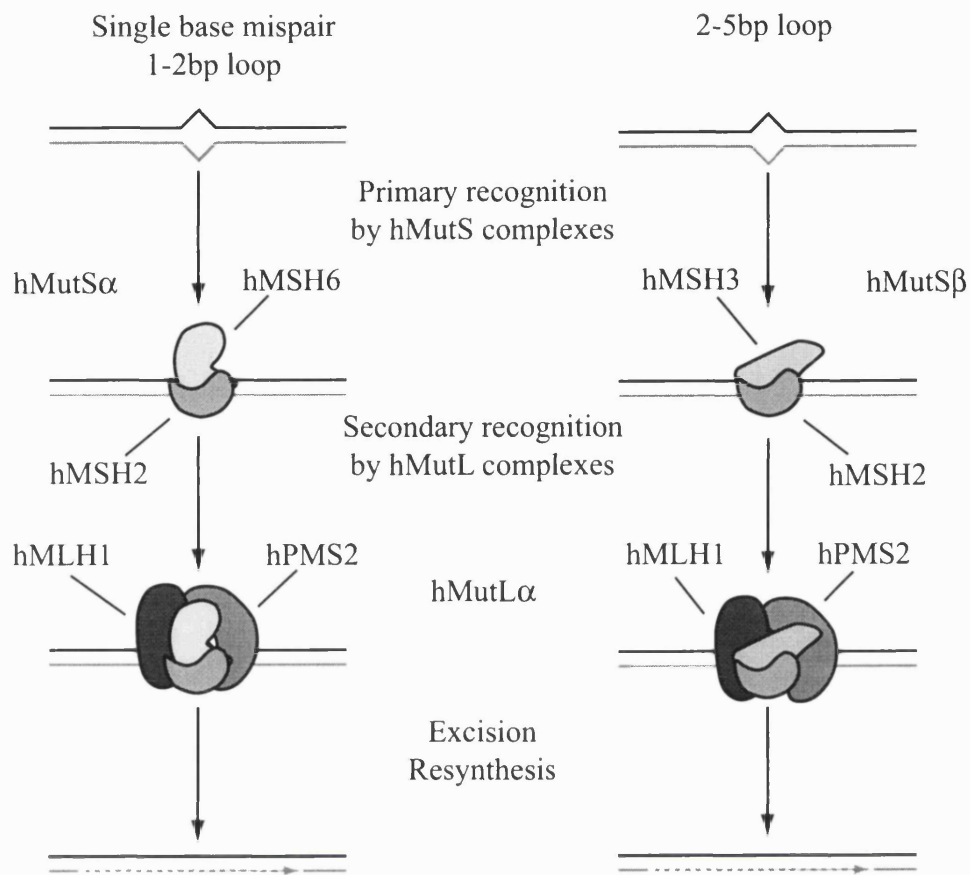


Figure 1.9 Initiation of Mismatch Repair in Human Cells

Illustrated are the two major mismatch recognition complexes hMutS α (hMSH2 / hMSH6) and hMutS β (hMSH2 / hMSH3). Both have distinct yet overlapping substrate specificity's. Only the major secondary recognition complex, hMutL α (hMLH1 / hPMS2), is shown for simplicity. Parental strand (—), daughter strand (---).

Generation of base coding errors by the polymerase that escape proof reading would be recognised by the hMutS α or hMutS β complexes tethered to the back of the polymerase. Such recognition may cause the polymerase to stall and then dissociate leaving the newly synthesised 3' nucleotide free. Degradation of the newly synthesised strand by a 3'→5' exonuclease past the site of the mismatch and reinitiation of DNA synthesis would complete repair. Alternatively, the replication complex may remain bound to the DNA with the MMR complex and instead "back up" the DNA with the 3' to 5' exonuclease degrading the newly synthesised strand until it has passed the error.

Mismatch Repair Gene Mutations and Cancer

Inherited defects in mismatch repair genes underlie an inherited cancer syndrome, hereditary nonpolyposis colorectal cancer (HNPCC). HNPCC is a relatively common autosomal recessive disorder affecting about 1 in 200 to a 1000 people and is characterised by an increased incidence and early onset of cancer of epithelial organs especially the colon (about 80% of cases) (Boland, 1998). Such kindred's harbour a germline mutation in an allele of one of the MMR genes and somatic mutation of the second allele generates a hypermutable phenotype. Hence a characteristic of HNPCC tumours is microsatellite instability (MSI or MIN⁺). MIN⁺ tumours contain mutations in simple repeat sequences like (CA)_n or (A)_n and genes containing microsatellites are often targets for inactivation in these tumours.

Of the >240 HNPCC mutations so far described, ~60% are in *hMLH1* and ~35% in *hMSH2* (Jiricny and Nystrom-Lahti, 2000). Inactivation of either of these genes completely abolishes the repair of both single base mispairs and IDLs generating a strong mutator phenotype and extensive MSI. No *hMSH3* germline mutations and only two kindreds with *hPMS2* mutations have been reported in HNPCC. This may reflect the overlapping substrate specificity of hMutS α and hMutS β , and suggest that a second hMutL complex containing hMLH1 can substitute for hMutL α . Cells mutated in *hMSH6* display elevated mutation rates at the *HGPRT* locus but MSI in these cells is restricted to some mononucleotide repeats due to the overlapping functions of hMutS α and hMutS β . No *hMSH6* germline mutations have been

associated with "classical" HNPCC. However, germline mutations in *hMSH6* have recently been identified in patients with late-onset atypical HNPCC (Kolodner *et al.*, 1999).

HNPCC accounts for about 3% of all colon cancers. Approximately 20% of sporadic (non-HNPCC) colon cancers also exhibit MSI. MSI is not however characteristic of colon cancer or limited to these tumours. Some gastric cancers, endometrial cancers, ovarian tumours, urinary bladder tumours, non-small-cell lung carcinomas, small-cell lung carcinomas, breast cancers, as well as other tumour types exhibit the MIN⁺ phenotype. In the majority of cases, no germline mutations were identified. Inactivation of mismatch repair and the subsequent increase in mutation rate from increased base miscoding events is advantageous in the process of multi-step carcinogenesis.

DNA Mismatch Repair and Acquired Resistance to DNA Damaging Agents

Methylating Agents

As already discussed, S_N1 methylating agents such as MNU and MNNG, and the chemotherapy agent TMZ exert their cytotoxic effects through the methylation of DNA. These agents generate a wide variety of lesions of which the major toxic lesion, O⁶meG (see Fig 1.10A), comprises about 7-8%. O⁶meG is repaired by the enzyme MGMT but persistent exposure to methylating agents is lethal probably due to saturation of this repair system. Cells defective in MGMT-dependent repair of O⁶meG (Mex⁻) are hypersensitive to killing by methylating agents (Fig 1.10B, left panel). Repeated exposure to such agents allows selection of cells that are resistant.

The involvement of MMR in the lethal processing of O⁶meG adducts and the subsequent loss of this pathway in acquired resistance was first inferred from experiments with *E. coli*. *Dam* mutants of *E. coli* are sensitive to killing by the methylating agent MNNG. A second mutation in either the *MutL* or *MutS* gene restores resistance to that of the wild type (Karran and Marinus, 1982). This is

consistent with the idea that O⁶meG is a lethal lesion in *dam* strains but tolerated if the mismatch processing function is abolished.

In mammalian cells, the realisation of two important predictions has highlighted the crucial role of MMR in acquired resistance to these methylating agents.

(1) Cells selected for resistance (tolerance) to S_N1 methylating agents are defective in long-patch mismatch repair (Branch *et al.*, 1993; Hampson *et al.*, 1997; Kat *et al.*, 1993).

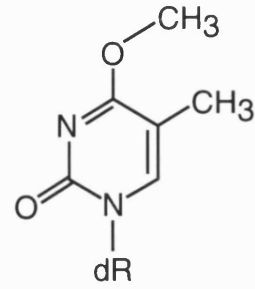
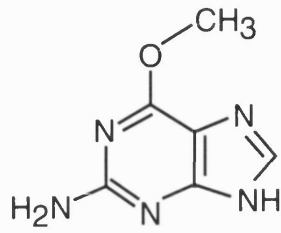
(2) Cells derived from tumours with known defects in MMR are resistant to the cytotoxic effects of S_N1 methylating agents (Branch *et al.*, 1995).

Inactivation of MMR in Mex⁻ cells restores S_N1 methylating agent sensitivity to that of the wild type (Fig 1.10B, right panel). Mismatch repair defective cells are sometimes 50 to 100-times more resistant to these drugs than their MMR-proficient counterparts.

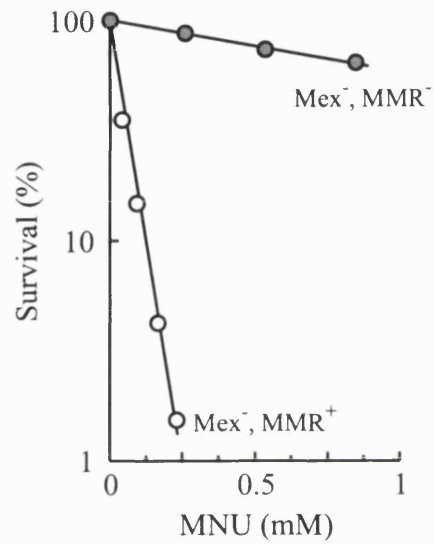
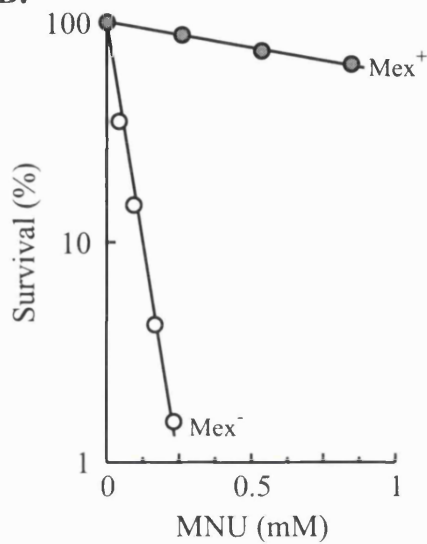
6-thioguanine

6-thioguanine (S⁶G) is used in the treatment of acute leukaemia, autoimmune diseases and also for the management of psoriasis (Elion, 1989). Cells defective in MMR show cross-resistance to S⁶G (Aquilina *et al.*, 1990; O'Driscoll *et al.*, 1999) (Fig 1.10C). MMR defective cells are around 10-fold more resistant to S⁶G than MMR-proficient cells. In order to be toxic, S⁶G must first be incorporated into DNA *via* the HGPRT purine salvage pathway. Upon incorporation, a small number of DNA-S⁶G (between 1 in 10⁴ and 10⁵) undergo S-methylation by S-adenosylmethionine (SAM) to generate DNA-S⁶meG (Fig 1.10D) (Swann *et al.*, 1996). S⁶meG shows an extremely close structural similarity to O⁶meG and thus, resistance to S⁶G can be thought of as a special case of methylation resistance.

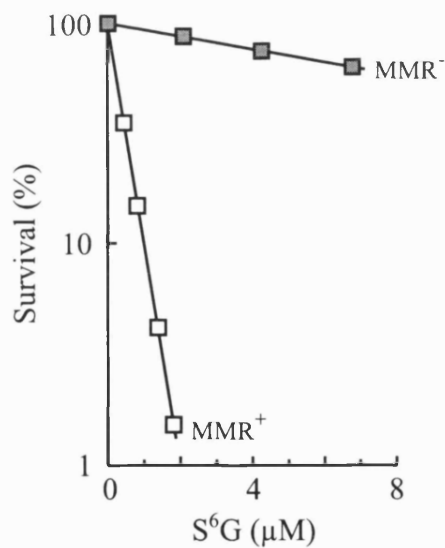
A.



B.



C.



D.

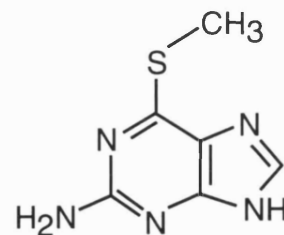
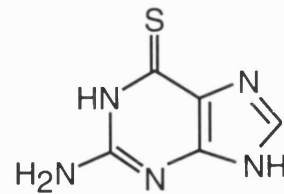


Figure 1.10 Contribution of MMR to Methylating Agent Tolerance

A. Structure of O⁶meG (left) and O⁴meT (right) DNA adducts.

B. Cells defective in MGMT activity (Mex⁻) are sensitive to killing by MNU (left). An additional mutation in MMR (Mex⁻ MMR⁻) restores sensitivity to that of Mex⁺ (right).

C. Cells deficient in MMR function are cross-resistant to S⁶G.

D. Structure of S⁶G and S⁶meG adducts.

Model for O⁶meG / S⁶meG Processing by MMR

O⁶meG and S⁶meG exhibit a striking structural resemblance. This has led to the suggestion of a model in which MMR recognises DNA damage due to its ability to miscode and mimic normal base mispairs (Karran and Bignami, 1996). This is summarised in Fig 1.11. In essence, upon being replicated, both O⁶meG and S⁶meG can miscode. O⁶meG shows about a 4-fold preference for G over C (Tan *et al.*, 1994) while S⁶meG has no real preference for C or T (Swann *et al.*, 1996). Both O⁶meG:C and :T (Duckett *et al.*, 1996; Griffin *et al.*, 1994) and S⁶meG:C and :T (Swann *et al.*, 1996; Waters and Swann, 1997) are recognised by hMutS α and processed by the long-patch mismatch repair pathway. As the damaged base (O⁶meG or S⁶meG) is situated in the parental strand, repair attempts are essentially futile. These futile repair attempts probably generate regions of single-stranded DNA and, after a subsequent round of DNA replication, a double-strand break. These double strand breaks probably induce apoptosis and cell death. O⁶meG adducts have been shown to trigger apoptosis (Meikrantz *et al.*, 1998) and both active MMR and p53 was necessary for this process (Hickman and Samson, 1999). Both O⁶meG and S⁶meG exhibit delayed cytotoxicity. This delayed cytotoxicity suggests that the collapse of the replication fork in the subsequent S-phase is responsible for the generation of a DSB. No evidence exists to support this futile cycling model but it is consistent with the properties of MMR-defective and drug resistant cells. The point, however, that mismatch repair contributes in a major way to the cytotoxic effects of these agents is firmly established.

Other DNA Damaging Agents

Loss of MMR is also implicated in the acquired resistance to other DNA damaging agents namely *cis*-diamminedichloroplatinum(II) (cisplatin), carboplatin, doxorubicin (adriamycin), etoposide (VP-16), *N*-aceotoxy-*N'*-acetyl-2-aminofluorene (AAAF) and benzo[*a*]pyrene-7,8-dihyrdodiol-9,10-epoxides (B[*a*]PDE, (Aebi *et al.*, 1997; Drummond *et al.*, 1996; Wu *et al.*, 1999)). Unlike methylating agents, loss of MMR confers only a small increase, up to about 2-fold, in resistance to these agents. Cisplatin has been the most extensively studied of these agents and only this drug will be examined in great detail here.

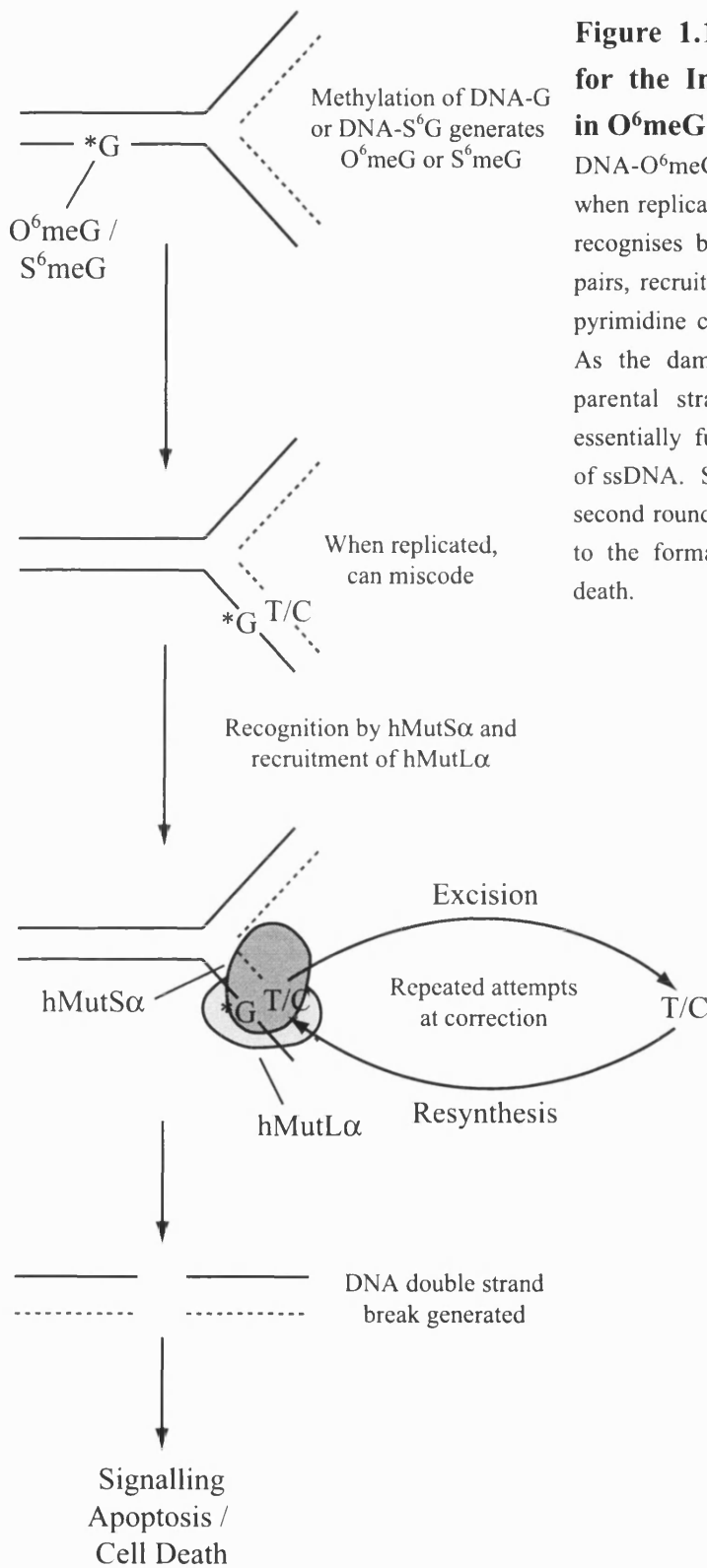


Figure 1.11 Proposed Model for the Involvement of MMR in O⁶meG or S⁶meG Toxicity

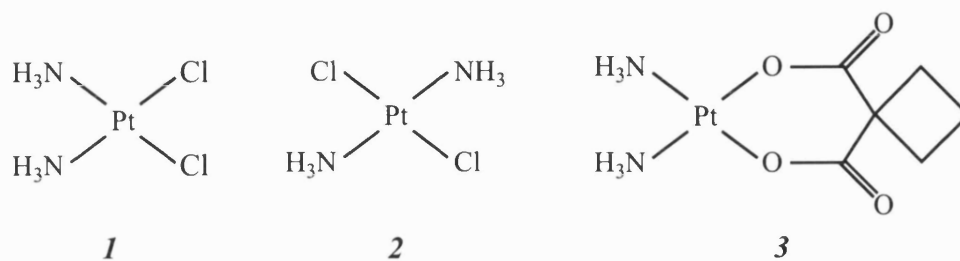
DNA-O⁶meG or DNA-S⁶meG (*G) when replicated can miscode. hMutS α recognises both *G:C and *G:T base pairs, recruits hMutL α and excises the pyrimidine containing daughter strand. As the damage is contained in the parental strand, repair attempts are essentially futile and generate regions of ssDNA. Subsequent processing or a second round of DNA replication leads to the formation of a DSB and cell death.

Cisplatin

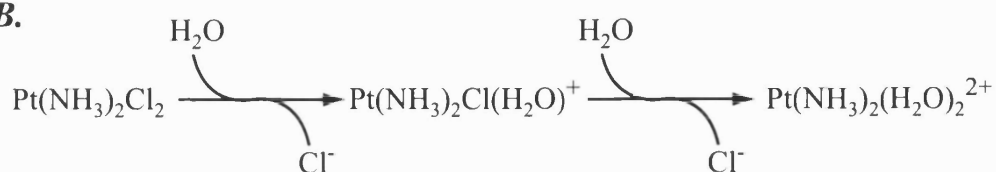
The chemistry of cisplatin and how it interacts with DNA has been extensively reviewed (Jamieson and Lippard, 1999; Trimmer and Essigmann, 1999). Cisplatin shows significant activity against a wide variety of tumours including ovary, bladder, lung, and head and neck and is a common component of many chemotherapy regimes. It has been used most successfully in the treatment of testicular carcinomas with greater than 90% now curable by this drug. The structure of cisplatin, carboplatin and the inactive isomer transplatin are illustrated in Fig 1.12A. Uptake of cisplatin into cells is suggested to occur via passive diffusion. In the bloodstream, due to the high concentration of Cl⁻ ions (~100mM), cisplatin is relatively unreactive. However, in the cell the Cl⁻ concentration is much lower (~ 4mM) and this facilitates the hydrolysis of the two Cl ligands on the cisplatin molecule. Water molecules displace the two Cl ligands in a stepwise fashion to generate an aquated positively charged complex (Fig 1.12B). As water is a good leaving group, the aquated cisplatin complex can react with cellular nucleophiles including DNA, RNA, proteins and cellular thiols (e.g. glutathione and metallothionein). DNA is suggested to be the important target by which cisplatin exerts its cytotoxic effect as *E. coli*, yeast and mammalian cells defective in the repair of cisplatin induced DNA damage are hypersensitive to killing by this drug. The major DNA target is the N⁷-position of purines. The major adducts induced by cisplatin are illustrated in Fig 1.12C and their relative abundance in Table 1.1.

Unlike cisplatin, transplatin shows no anti-tumour activity. Since transplatin does not induce 1,2-dipurine intrastrand crosslinks (1,2{AG} or {GG}) but cisplatin does, these are suggested to be the major cytotoxic lesion *in vivo*. There is also a positive correlation between DNA adduct formation and clinical response. Carboplatin produces an identical spectrum of damage to cisplatin but reacts with slower kinetics.

A.



B.



C.

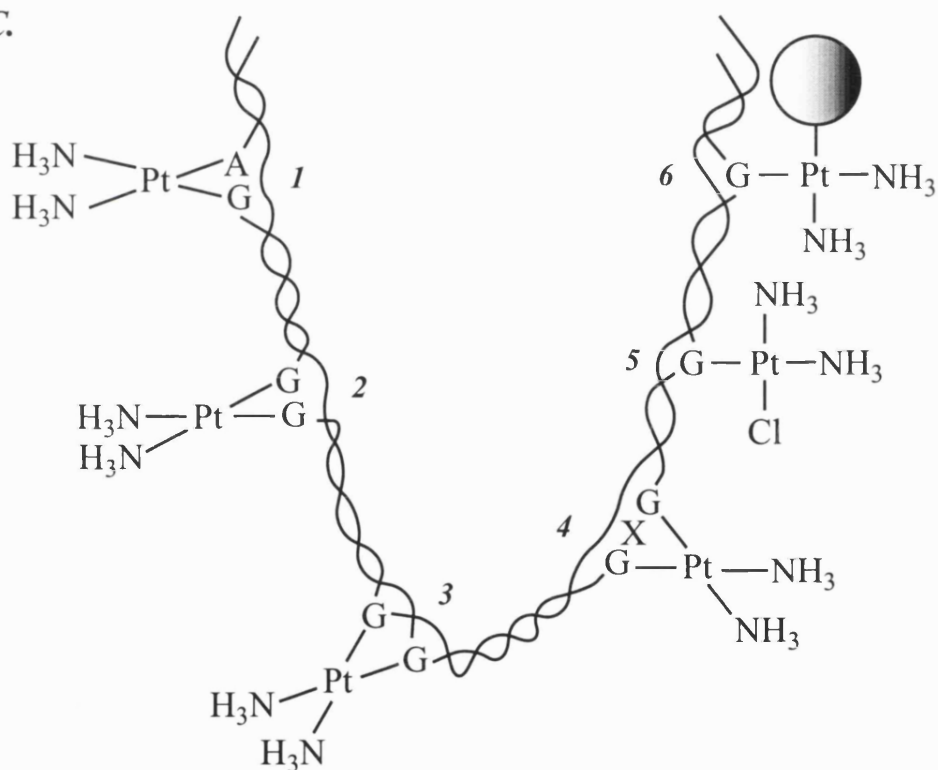


Figure 1.12 Platinum (II) Compounds and DNA Damage

A. Structure of cisplatin (1), transplatin (2) and carboplatin (3).

B. Reaction highlighting the sequential hydrolysis of the Cl ligands of cisplatin.

C. Major DNA lesions induced by cisplatin.

1. 1,2{AG} intrastrand crosslink; 2. 1,2{GG} intrastrand crosslink; 3. G-G interstrand crosslink;

4. 1,3{GNG} intrastrand crosslink; 5. monofunctional adduct; 6. DNA-protein crosslink.

Table 1.1 Comparison of DNA Adducts Formed by Cis- and Transplatin

	Cisplatin	Transplatin
Monofunctional dG	Yes	Yes
Intrastrand		
1,2{GG}	65%	No
1,2{AG}	25%	No
1,3{GNG}	6%	40%
Interstrand	2%	20%

Data taken from (Trimmer and Essigmann, 1999).

Cellular Responses to Cisplatin

The ability of cisplatin to bind DNA and modify its structure suggests that it may interfere with normal cellular functions, namely replication and transcription. Both DNA replication and transcription are essential for normal cellular division and growth, and inhibiting these would be toxic.

Effects on DNA Replication

Inhibition of DNA synthesis, and hence the growth of tumour cells, is suggested to be the major mechanism by which cisplatin exerts its cytotoxic effect. *In vitro* studies using an SV40 replication system indicated that, at similar levels of DNA platination, both cis- and transplatin bifunctional DNA lesions form an effective block to replication (Heiger-Bernays *et al.*, 1990). Using site-specific single DNA lesions, 1,2-dipurine adducts (1,2{GG} or {AG}) of cisplatin were found to be the most effective at blocking DNA replication by a host of polymerases (Comess *et al.*, 1992; Vaisman and Chaney, 2000). These adducts blocked replication by >95%. In contrast, 1,3{GNG} adducts of transplatin blocked replication by only 10-40%. The difference observed between the two systems is suggested to be the result of differential cellular processing of the DNA damage. The ability of cisplatin adducts to preferentially arrest DNA replication and subsequently induce DSBs through replication fork collapse (Zdraveski *et al.*, 2000) is most likely the main mechanism by which cisplatin kills tumour cells.

Effects on Transcription

When treated with cisplatin, cells arrest at the G2/M transition. It has been suggested that, in addition to inhibiting replication and inducing cell cycle checkpoints, part of this G2 arrest results from the inability of cells to transcribe genes necessary to enter mitosis. In addition, transcription by RNA pol II and *E. coli* RNA pol are blocked by cisplatin 1,2{GG}, 1,2{AG}, 1,3{GNG} and interstrand DNA adducts when present on the transcribed strand. Transplatin and mono-adducts do not form a transcription block.

Effects on Telomeres

Telomeres are formed of the G-rich repeat TTAGGG and when critically shortened, cells senesce and die. In a study on HeLa cells treated with cisplatin, the telomeres were shortened and the cells entered senescence. This suggests that cisplatin may inhibit telomerase activity through either binding to the protein or RNA component of the enzyme (Jamieson and Lippard, 1999).

Repair of Cisplatin Adducts

In both *E. coli* and mammalian cells, cisplatin DNA adducts are removed predominantly by the nucleotide excision repair pathway. *In vitro* repair studies have shown that repair of platinum damage was poor when compared to UV-damage and a distinct preference for platinum adducts was observed. 1,3{GNG} adducts were repaired more efficiently than 1,2{GG} adducts (Moggs *et al.*, 1997; Szymkowski *et al.*, 1992; Zamble *et al.*, 1996). Cells defective in this pathway are extremely sensitive to killing by this drug. Recent work has shown that testicular cancers exhibit reduced NER due to decreased expression of XPA. Such tumour cells were more sensitive to killing by cisplatin (Koberle *et al.*, 1997; Koberle *et al.*, 1999). This has been suggested to be a potential reason for the high cisplatin sensitivity of testicular tumours.

Binding by HMG Proteins

HMG domain proteins are another group of proteins that have been shown to recognise cisplatin adducts *in vitro*. These proteins preferentially bind to 1,2{GG} and {AG} cisplatin intrastrand crosslinks. Over expression of HMG domain proteins sensitises cells to killing by cisplatin (He *et al.*, 2000). Several mechanisms have

been suggested for how the binding of HMG proteins to cisplatin adducts modulates sensitivity. These include:

- (1) Cisplatin adducts are bound and shielded by the HMG protein. NER of the damage is therefore reduced, the adducts persist and apoptosis is increased.
- (2) Adducts hijack transcription factors (many contain HMG domains) leading to reduced transcription and death.

The *in vivo* relevance of these observations has not yet been ascertained.

Acquired Resistance to Cisplatin

MMR

Evidence exists to associate loss of MMR function with an increased level of resistance to cisplatin. Several ovarian carcinoma cell lines selected for high levels of cisplatin resistance have an associated defect in MMR (Table 1.2).

Table 1.2 Cisplatin Resistance in Ovarian Carcinoma Cell Lines

Cell Line	RF ^a	MMR Defect	Reference
A2008	~60	hMLH1	(Aebi <i>et al.</i> , 1996)
A2780-CP70	17-31.8	hMLH1	(Johnson <i>et al.</i> , 1994)
A2780-CP30	57.7-143	hMLH1	(Vaisman <i>et al.</i> , 1998)
A2780-CP200	489	hMLH1	
A2780-CP	20.3	hMLH1	

^a RF = relative increase in cisplatin resistance compared to parental cells.

Human carcinoma cell lines with known MMR defects are between 1.5 and 4.7-fold more resistant to the cytotoxic effect of cisplatin than an isogenic line made MMR-proficient by addition of the chromosome coding for a wild-type copy of the defective gene (Table 1.3, top). Immortalised fibroblasts from MMR "knock-out" mice also exhibit a modest increase in cisplatin resistance (Table 1.3, bottom). This does, however, seem to be dependent on the method of immortalisation. Unlike

methylyating agents, defects in MMR seem to only a confer a small increase (of about 2-fold) in resistance to cisplatin.

Table 1.3 Cisplatin Resistance in MMR Defective Cell Lines

Cell Line	RF	MMR Defect	Reference
A2780-CP70	4.7	hMLH1	(Durant <i>et al.</i> , 1999)
HCT116	1.5-2.1	hMLH1	(Fink <i>et al.</i> , 1996)
HEC59	1.8	hMSH2	(Vaisman <i>et al.</i> , 1998)
DLD1	4.7	hMLH1	(Aebi <i>et al.</i> , 1996)
HHUA	2.4	hMSH3/hMSH6	(Aebi <i>et al.</i> , 1996)
mMSH2 ko	2.1	mMSH2	(Fink <i>et al.</i> , 1997a)
mPMS2 ko	1.9	mPMS2	(Fink <i>et al.</i> , 1997a)
Ras/E7 mMSH2 ko	1.0	mMSH2	(Reitmar <i>et al.</i> , 1997)

A closer dissection of the A2780 model ((Branch *et al.*, 2000), summarised in Fig 1.13) indicates that the contribution of MMR to cisplatin resistance is small (only about a 1.3-fold increase). Cells selected for MMR defects through tolerance to the methylating agent MNU were found to be about 4-fold more resistant to cisplatin but had an associated defect in p53. Re-expression of hMLH1 increased the sensitivity of the cells by a factor of about 1.3-fold. Expression of a dominant negative form of p53 in the p53-proficient parental cells increased cisplatin tolerance by a factor of about 2. This suggests, that in this cellular model, loss of MMR function contributes about 1.3-fold to the increased resistance to cisplatin and may be associated with a defect in p53. Interestingly, a recent screen of the NCI anticancer drug cell panel found no correlation between defects in MMR and increased cisplatin resistance in the 60 cell lines tested (Taverna *et al.*, 2000).

The ability of cisplatin to select for MMR defective cells is a prerequisite for the involvement of loss of MMR function in acquired resistance to cisplatin. Evidence for this is two fold. Treatment of a mixed population of MMR-proficient and MMR-deficient HCT116 cells with cisplatin lead to the enrichment of the MMR-deficient variant (Fink *et al.*, 1997b). In addition, single step selection (SCP) (McLaughlin *et al.*, 1991) or multi step selection (MCP) (Anthony *et al.*, 1996) with cisplatin of the

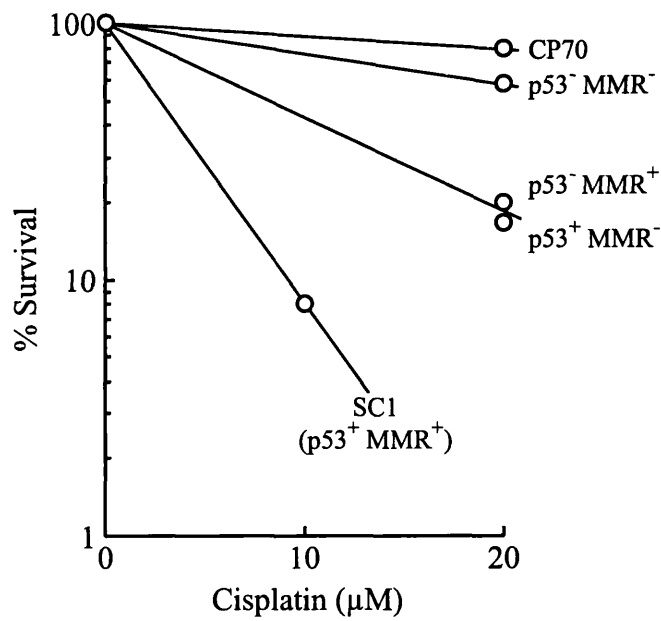


Figure 1.13 Effects of p53 and MMR Defects on Cisplatin Sensitivity in A2780

Adapted from Branch *et al.*, 2000. A2780-SC1 (p53⁺ MMR⁺), A2780-MNU1A (MMR⁻ p53⁻), A2780-SC1 with dominant negative p53 (p53^{val135}, p53⁻ MMR⁺) and A2780-MNU1A transfected with the human hMLH1 cDNA (p53⁻ MMR⁺) were used to dissect the various contributions of loss of MMR and/or p53 function in acquired resistance to cisplatin in the A2780 tumour cell model.

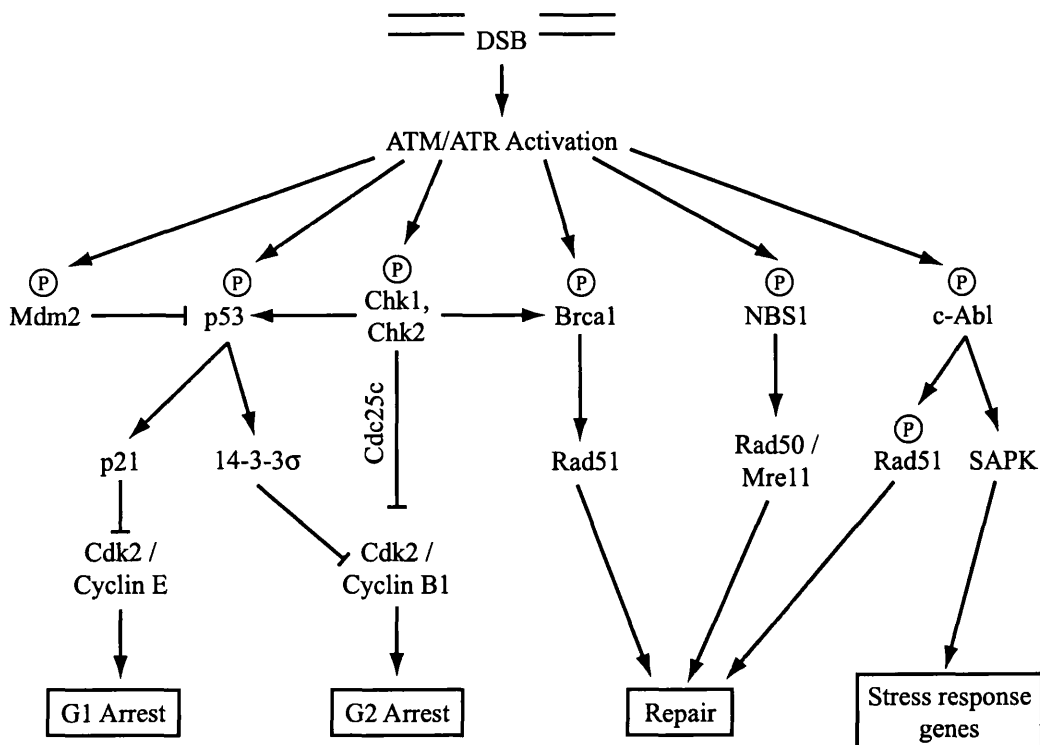


Figure 1.14 Cellular Responses to DSBs Mediated by the ATM/ATR Kinases

A2780 carcinoma cell line generated variants with low levels of cisplatin resistance and an apparent defect in MMR. Of the ten MCP variants generated, 70% of them exhibited defects in hMLH1 but surprisingly, all of them had an associated defect in the p53 pathway (Brown *et al.*, 1997). In the A2780 line, defects in MMR are always associated with loss of expression of hMLH1. The mechanism behind this is suggested to be methylation of the hMLH1 promoter leading to promoter silencing and loss of expression (Strathdee *et al.*, 1999). Tumours in mice derived from the cell line A2780-CP70 are refractory to cisplatin treatment. Re-expression of hMLH1 in these tumours by treatment with DAC (an inhibitor of the methyltransferase) restored cisplatin sensitivity (Plumb *et al.*, 2000).

Two alternative models have been suggested for how MMR interacts with bulky DNA damage induced by chemotherapy drugs like cisplatin. The mismatch recognition complex hMutS α recognises and binds to 1,2{GG} cisplatin adducts *in vitro* (Duckett *et al.*, 1996). This binding is much improved when the 1,2{GG} adduct is mispaired with a C opposite the 5' G and a T opposite the 3' G (Yamada *et al.*, 1997). This has led to a suggestion that the model for MMR induced cell death is identical to that of O⁶meG (Fink *et al.*, 1998). Replication of 1,2{GG} adducts generates mismatched compound lesions that are then recognised by hMutS α and repair attempted. As with O⁶meG, repair generates new compound lesions that are again recognised by hMutS α and these repeated attempts at repair trigger G2 arrest and ultimately apoptosis.

Replication through cisplatin DNA damage, as outlined previously, is extremely poor. Experiments from *S. cerevisiae* and *E. coli* have suggested an alternative explanation for the involvement of MMR in cisplatin-dependent death. *S. cerevisiae* defective in MMR are resistant to killing by both cisplatin and doxorubicin (Durant *et al.*, 1999). More interestingly, however, is the observation that this is epistatic with the Rad52 family of homology-directed repair proteins. In *E. coli*, homologous recombination is essential for cell survival after cisplatin damage. Cells defective in these gene products are extremely sensitive to killing by cisplatin (Zdraveski *et al.*, 2000). These two observations suggest an alternative role for MMR in cisplatin induced toxicity. DNA damage induced by cisplatin blocks an advancing replication fork leading to the collapse of the fork and generation of a DSB. Repair of this fork

is attempted using the HDR pathway of recombination. MMR probably exerts its influence by inhibiting this recombination directed repair.

Alternative Factors that Contribute to Acquired Resistance to Cisplatin

Many factors have been identified that can contribute to increased resistance to cisplatin (see (Perez, 1998) for a summary). The high levels of cisplatin resistance and the multiple defects observed in the A2780 and A2008 models suggest that acquired resistance to cisplatin is multi-factorial.

One such important factor is the p53 DNA damage response pathway. DNA damage induced by a variety of damaging agents can lead to the formation of DSBs and the induction of the ATM/ATR kinases (Fig 1.14, (Shiloh, 2001)). p53 is a target of these kinases and loss of p53 function can lead to increased cisplatin resistance (Branch *et al.*, 2000; Perego *et al.*, 1996; Piovesan *et al.*, 1998). However, in some cell models, loss of p53 function was not always accompanied by an increase in cisplatin resistance (Zamble *et al.*, 1998). The p53 gene, first described in 1979, was the first tumour-suppressor gene to be identified. The exon structure of p53 is illustrated in Fig 1.15A. In most human cancers, p53 has been found to not function correctly and in about half of these tumours, p53 is directly inactivated by mutation. These mutations tend to be clustered at specific hotspots, namely R175, G245, R248, R249, R273 and R282 (Fig 1.15B). Alternative mechanisms of inactivating p53 include C-terminal deletion, Mdm2 gene amplification, viral infection with e.g. HPV, deletion of p14^{ARF} (this leads to loss of MDM2 inhibition) and mislocalisation of p53 to the cytoplasm.

p53 functions as a tetrameric transcription factor (see (Ko and Prives, 1996; May and May, 1999) for reviews) and induces the expression of several genes involved in growth arrest and apoptosis including p21, Bax, Gadd45 and Mdm2. p53 function is negatively regulated by MDM2 via its interaction with the N-terminus. MDM2 is an E3 ubiquitin ligase and promotes the rapid degradation of p53. Binding of p53 by MDM2 leads to p53 ubiquitination, export to the cytoplasm and subsequent degradation by the proteasome. DNA damage leads to post-translational modifications that inhibit the MDM2 : p53 interaction and the shuttling of MDM2 to

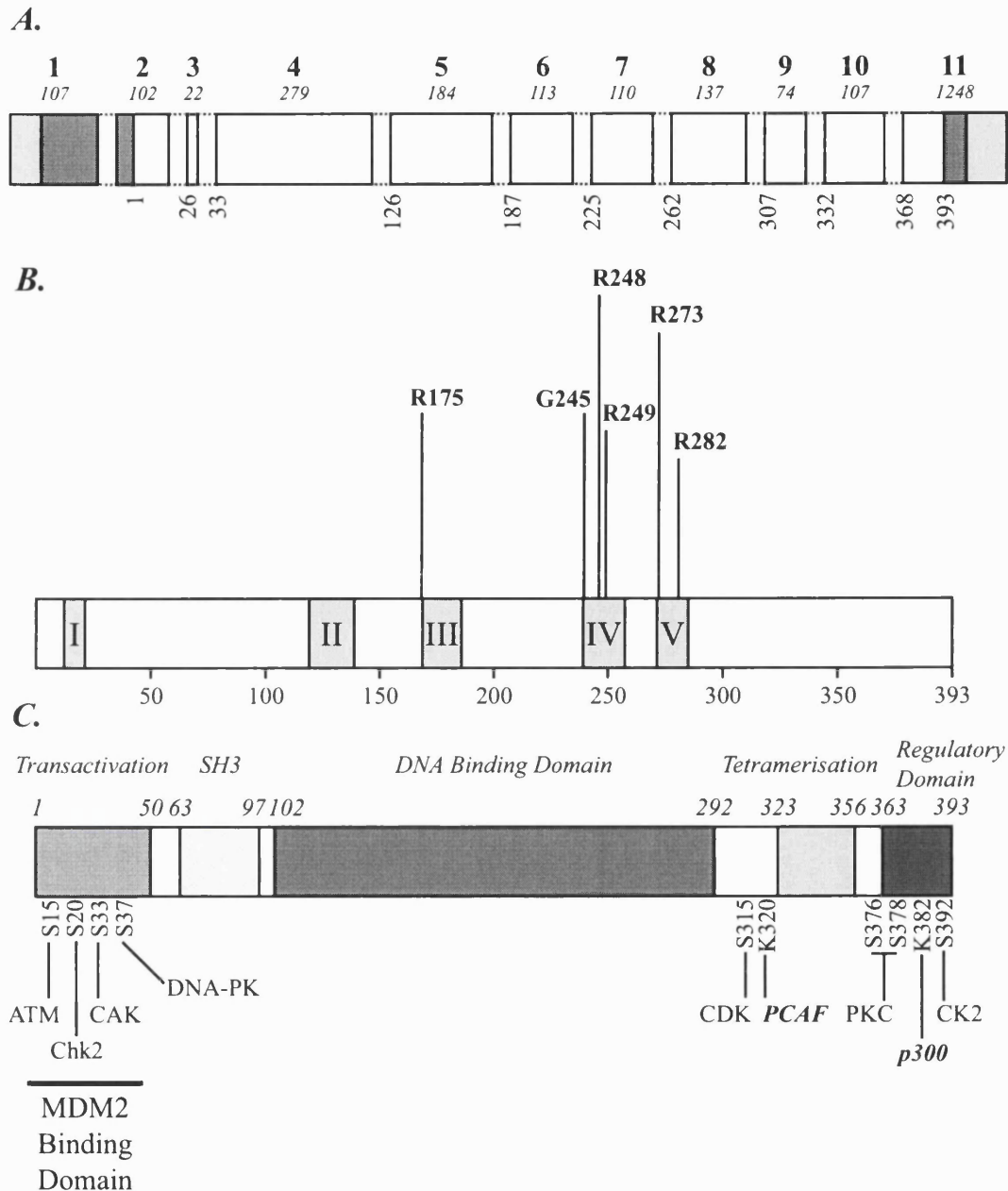


Figure 1.15 Structure of the p53 Gene and p53 Protein

A. Structure of the p53 gene.

The exons are numbered and their size in bp indicated. Light grey areas are non-transcribed sequence and dark grey non-translated. The numbers below indicate the first amino acid coded by each exon.

B. Mutation hotspots in p53.

The positions of the major mutation hotspots in human cancers are indicated. The grey boxes numbered I to V represent evolutionarily conserved regions.

C. p53 domains and post-translational modification sites.

The major protein domains and their amino acid positions are indicated by the grey boxes. The major sites of phosphorylation and the kinases responsible for this phosphorylation are indicated below. Also indicated are two lysine residues (K320 and K382) whose acetylation / deacetylation may be important for p53 function.

the cytoplasm. p53 is thus stabilised and activated. A summary of the major domains of p53 and the sites of post-translational modification are illustrated in Fig 1.15C.

Additional mechanisms that have been implicated in cisplatin resistance include:

1. Decreased accumulation of cisplatin (Lanzi *et al.*, 1998; Loh *et al.*, 1992).
2. Increased efflux of cisplatin from the cell *via* either the human canalicular multispecific organic anion transporter (cMOAT or MRP2) (Chen *et al.*, 1998; Taniguchi *et al.*, 1996) or the copper-transporting P-type adenosine triphosphatase (ATP7B) protein (Komatsu *et al.*, 2000).
3. Increased glutathione levels and glutathione synthesis (Godwin *et al.*, 1992; Mistry *et al.*, 1991).
4. Increased DNA damage tolerance (Johnson *et al.*, 1997).
5. Inhibition of cisplatin induced apoptosis *via* over-expression of Bcl-2 (Miyake *et al.*, 1998).
6. Increased repair of platinum DNA damage (Johnson *et al.*, 1994; Masuda *et al.*, 1990).

This extensive list of potential mechanisms by which cells may become resistant to cisplatin indicate that acquired resistance is truly multi-factorial.

Thiobases and Thionucleosides

The thiopurine 6-thioguanine (S^6G) is used in the treatment of acute leukaemia (Elion, 1989) and is incorporated into DNA *via* the HGPRT purine salvage pathway (Aarbakke *et al.*, 1997). Thymidine analogues including the halogenated pyrimidines (BrUdR and IUdR) and, to a lesser extent, 5FUdR are incorporated into DNA through the thymidine kinase salvage pathway. A summary of the suggested metabolism of thio-substituted purines and pyrimidines is shown in Fig 1.16.

The thiopyrimidine, 4-thiothymidine (S^4TdR) and S^6G absorb preferentially in the UVA range. Their structures and absorption spectra, along with those of thymidine (TdR) and 4-methylthiothymidine (S^4meTdR), are illustrated in Fig 1.17. UVA light consists of wavelengths between 320 and 400nm (Fig 1.18A).

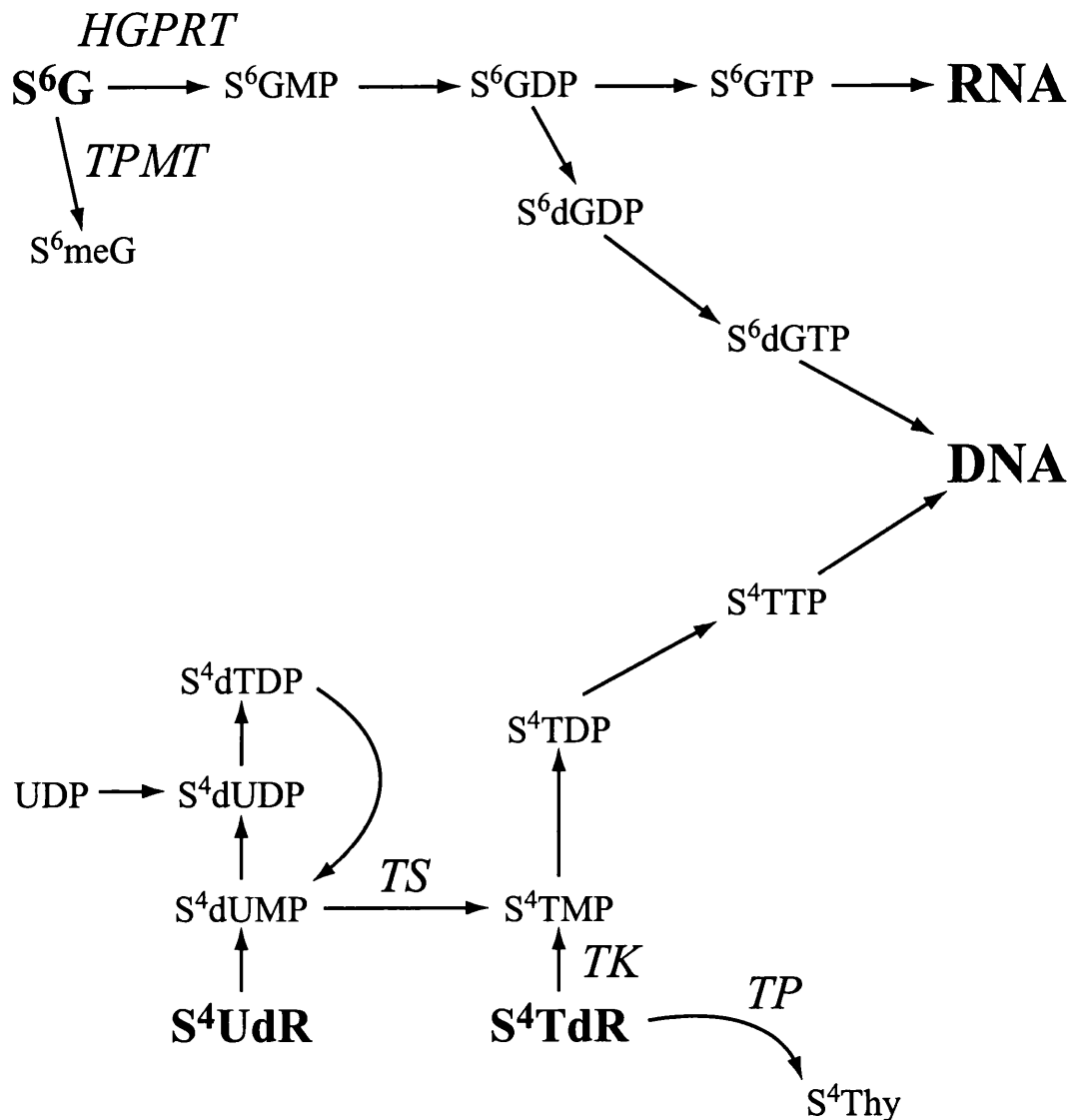
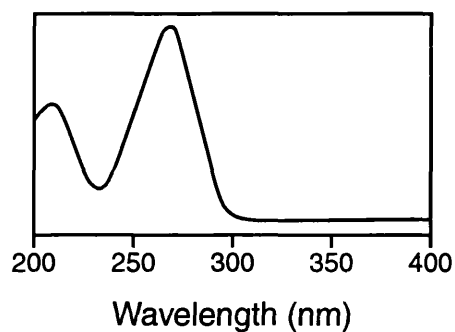
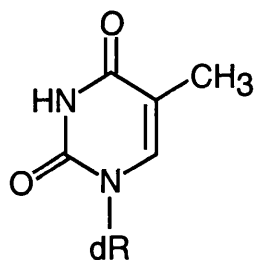


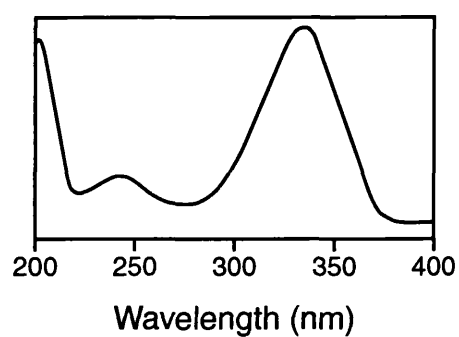
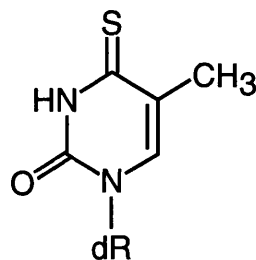
Figure 1.16 S^6G , S^4TdR and S^4UdR Metabolism *in vivo*

Enzymes are indicated in italics. *HGPRT*, hypoxanthine guanine phosphoribosyl transferase; *TPMT*, thiopurine methyl transferase; *TS*, thymidylate synthase; *TK*, thymidine kinase; *TP*, thymidine phosphorylase.

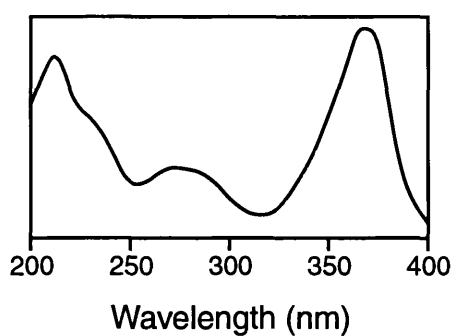
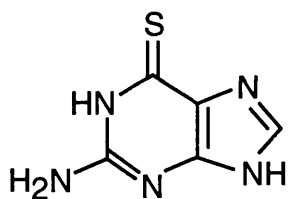
TdR



S⁴TdR



S⁶G



S⁴meTdR

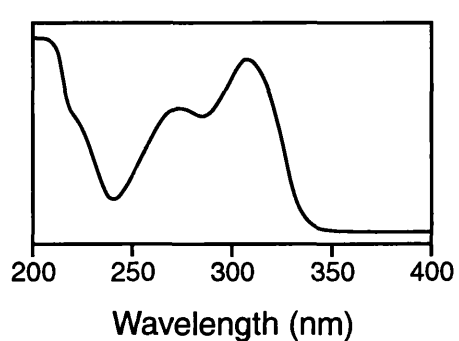
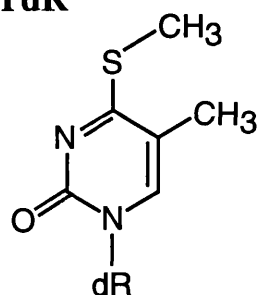


Figure 1.17 Structure and Absorption Spectra of TdR, S⁴TdR, S⁶G and S⁴meTdR

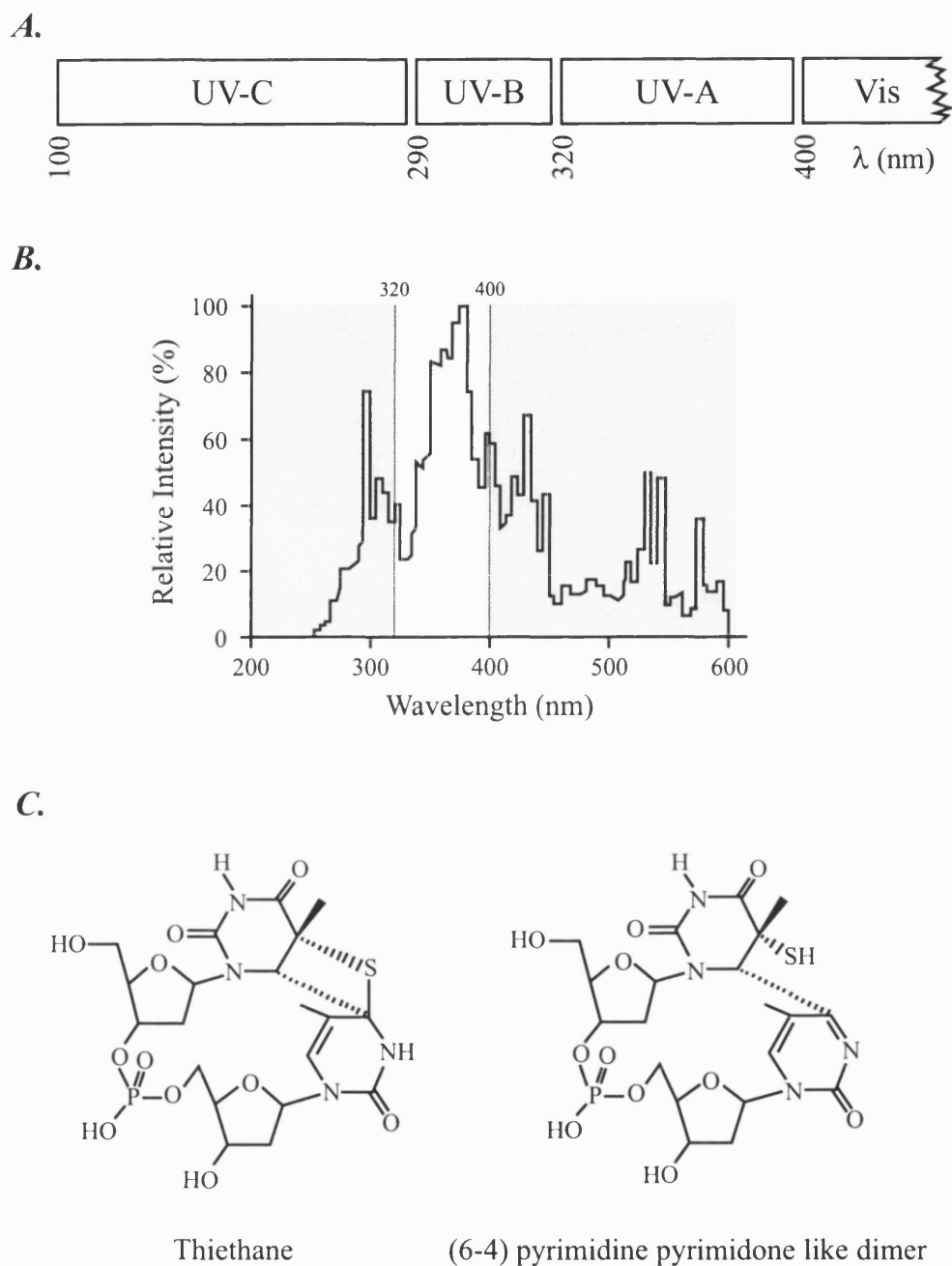


Figure 1.18 Thiobases and UVA

A. Wavelengths of the UV Spectrum.

B. UV Output from UVH-253 Lamp.

The filter supplied allows only the emission of wavelengths between 320 and 400nm.

C. Structure of TpS⁴T Dimers Induced by UVA Light.

An example of the spectral output of a UVA light source (in this case a UVH-253 lamp, UV Light Technology) is illustrated in Fig 1.18B. This lamp uses a combination of a Fe-doped metal halide bulb and a filter. Only wavelengths of 320-400nm are emitted.

Previous studies have indicated that, in combination with UVA light, thiopyrimidines exhibit some toxicity. 4-thiouridine incorporated into the RNA of monkey kidney cells triggered the UVA dependent inhibition of DNA, RNA and protein synthesis (Favre *et al.*, 1993). Additionally, S⁴TdR and UVA exhibited some UVA-dependent inhibition of Vaccinia and Herpes Simplex viruses (Domi *et al.*, 1995) but the effects were quite limited. Irradiation of dinucleotides or oligonucleotides containing TpS⁴T pairs leads to the formation of pyrimidine-pyrimidone intrastrand crosslinked products that resemble (6-4) pyrimidine pyrimidone photoproducts produced in unsubstituted DNA by UVC (Favre *et al.*, 1998; Warren *et al.*, 1998). These structures are shown in Fig 1.18C and should be compared to those for a UVC induced TpT dimer shown in Fig 1.6B.

Phototherapy and Photodynamic Therapy (PDT)

Phototherapy is defined as the use of nonionising electromagnetic radiation for therapeutic effects (Nee, 1997). This now generally refers to the use of UVB light. Narrow band UVB (λ around 313nm) is the currently preferred treatment for the therapeutic clearing of psoriasis and has generally replaced the use of psoralen and UVA. This treatment is effective when applied in 1 or 2 minimally erythematous doses. The mechanism by which this treatment works is not completely understood. DNA damage, however, seems a likely explanation. UVB induces a much greater number of CPDs and (6-4) pyrimidine pyrimidone photoproducts in DNA than UVA (Kielbassa and Epe, 2000; Runger *et al.*, 2000). The UVA dose required to have the same therapeutic effect is approximately 1000 times that of UVB. This would indicate UV-induced DNA damage as the potential source of cytotoxicity. UVB is also a good mutagen with the major sites of mutation corresponding to dipyrimidines.

Photodynamic Therapy (PDT) is the use of photochemotherapy in the treatment of cancer (Dougherty *et al.*, 1998; Levy, 1995; Oleinick and Evans, 1998) and involves oxygen-requiring photosensitised reactions. Three components are required for effective PDT:

1. The preferential accumulation of a photosensitising molecule in the tumour cells.
2. Nonthermal visible light of a wavelength matching the absorption maximum of the photosensitising molecule. This is generally in the red region of the spectrum ($\lambda > 600\text{nm}$).
3. Molecular oxygen.

PDT can involve two types of photochemical reactions. Type I occur via reactive free radicals that are scavenged by O_2 . The second, Type II, result in the direct formation of singlet oxygen ($^1\text{O}_2$) by direct energy transfer from the excited photosensitiser to O_2 . $^1\text{O}_2$ is a non-radical but very reactive form of oxygen.

A derivative of hematoporphyrin, Photofrin (PF), has been licensed for clinical use against cancers of the lung, oesophageal, digestive tract, genitourinary and head and neck. Second generation photosensitisers including benzoporphyrin derivative (BPD), tin-etioapurin (SnET2), lutetium texaphyrin (LuTex) and phthalocyanine Pc4 (Pc4) are currently under evaluation. Their advantage is an absorption maximum at longer wavelengths ($\lambda > 650\text{nm}$) than PF ($\lambda_{\text{max}} = 630\text{nm}$). The mechanism by which the produced oxygen species destroy the tumour can involve three different mechanisms: direct damage of intracellular components, changes to vascularisation, and release of cytokines generating an inflammatory response. This leads to the induction of both apoptosis and necrosis. The extent to which each participates is dependent on both the tumour type and the photosensitising molecule used. The majority of the photosensitising molecules used are lipophilic and localise to membranes. The major targets of damage include the cytoskeleton, lysosomes and mitochondria. As the $^1\text{O}_2$ species generated by a Type II molecule is extremely short lived, DNA localised close to the nuclear envelope may also be damaged.

Aims of Thesis

The work described in Chapters 3 and 4 was an attempt to further understand the role of MMR in acquired resistance to cisplatin. Two model systems (*E. coli dam* mutants and the A2780 carcinoma cell line respectively) were used to investigate the possible selection of MMR defects in acquired resistance to cisplatin. In Chapter 5, I investigated the potential use of 4-thiothymidine as a chemotherapeutic agent analogous to 6-thioguanine. Finally, in Chapter 6 I present an evaluation of the possible use of DNA-thiobases as intrinsic DNA-photosensitisers and their effects on human cells.

Chapter 2

Materials and Methods

Materials

All chemicals were from Sigma and all radiochemicals from Amersham International unless otherwise stated. Standard solutions of 0.5M EDTA, 1M Tris-HCl, 5M NaCl, 10xM9 salts, 10% Glucose, Trypsin/Versene, DMEM, 2% RPMI 1640, Giemsa stain, L-Broth and L-agar were all produced by ICRF central services. All other stock solutions were made according to standard methods (Sambrook *et al.*, 1989; Sambrook and Russell, 2001).

4-thiothymidine (S⁴TdR) was synthesised by Dr. Y.-Z. Xu according to his previously published method (Xu *et al.*, 1991).

Bacterial Techniques

Maintenance of Stocks

Escherichia coli strains were kind gifts from Dr. M. Marinus (Worcester College, MA, USA), Dr. J. Essigmann (MIT, MA, USA) or Dr. B. Sedgwick (ICRF Clare Hall). All were maintained on L-agar plates supplemented with antibiotics where appropriate (50µg/ml Kanamycin or 25µg/ml Tetracycline). Stocks grown from single colonies were stored at -70°C in 10% Glycerol (v/v) / L-broth. Single colonies from fresh streak plates were used for each experiment.

Cisplatin Survival Curves

These were carried out according to the protocol of Dr. J. Mello (MIT, MA, USA). *E. coli* in log phase (OD₆₀₀ = 0.2-0.3, approx. 1-2x10⁸ cells/ml) were pelleted and resuspended in M9 salts (containing 20µg/ml Thymine where necessary) at a concentration of between 1 and 2x10⁸ cells/ml. Cells were then treated with an

appropriate concentration of cisplatin for 2 hours at 37°C before being serially diluted in M9 salts and plated on L-agar. After overnight growth at 37°C, the number of colonies was scored.

Preparation of Cisplatin

Cisplatin (Sigma) was dissolved in dH₂O by incubating at 37°C for 4-6 hours with regular vortexing. Just prior to treatment, undissolved cisplatin was removed by centrifugation and the concentration of aqueous cisplatin determined at A₃₀₁ (E = 131).

Selection of Cisplatin Resistant E. coli

Log phase *E. coli* were treated with 100µM cisplatin prepared as above. After each treatment, the surviving cells were grown overnight in L-broth at 37°C. Cells were then diluted and grown to log phase before being treated again or serially diluted and plated on L-agar. After growth overnight on L-agar plates, single colonies were picked and tested for the various secondary characteristics of *dam*.

2-aminopurine sensitivity was determined by streaking single colonies onto L-agar plates impregnated with 200µg/ml 2-AP. Mutation frequency was assessed by plating approximately 10⁸ cells onto L-agar plates containing 100µg/ml Rifampicin.

Preparation and Digestion of Genomic DNA

Genomic DNA was prepared from 1.5ml of overnight culture of *E. coli* cells using a Genomic-tip 100/G kit (QIAGEN) according to the manufacturer's supplied protocol. Digestion of genomic DNA by *DpnI* was performed using approximately 500ng of genomic DNA and 10U *DpnI* (NEB) in the manufacturer's supplied reaction buffer. Samples were incubated at 37°C for 2 hours before being separated on a 0.5% agarose gel containing 0.5µg/ml ethidium bromide (GibcoBRL). Products were detected under UV light.

Cell Culture Techniques

Maintenance of Cell Cultures

All cells used were obtained from the ICRF central cell services. Lymphoblastoid cell lines were maintained in 2% RPMI 1640 cell culture medium supplemented with 10% foetal calf serum (Gibco BRL). Cells were maintained at a concentration of between 2×10^5 and 2×10^6 cells/ml at 37°C in a humidified atmosphere containing 5% CO₂.

Fibroblast lines, colorectal lines and the variants of A2780 were maintained in Dulbecco's MEM (E4) supplemented with 10% FCS at 37°C and 10% CO₂. Cells were passaged approximately twice a week by detaching the cells with a thin layer of 0.25% Trypsin in 0.1% Versene for 3 to 5 minutes at 37°C. This was neutralised with 10 ml of medium containing 10% FCS and cells replated at dilutions of between 1:5 and 1:12.

Large scale cell culture for cell extracts was performed by the ICRF central cell services laboratory according to their standard methods.

Viable cell numbers were counted using an Improved Neubauer haemocytometer. At least four large squares were counted, the number averaged and multiplied by 10^4 to give the number of viable cells/ml.

Cell Storage

Frozen cell stocks were stored at -70°C and under liquid nitrogen (LN₂). Approximately 2 to 5×10^7 cells were pelleted, the medium removed and the pellet resuspended in the appropriate growth medium containing 10% (v/v) DMSO. Cell suspensions were transferred to cryovials (Nunc), wrapped in tissue paper, placed at -70°C and cooled at a rate of 1°C / minute. After 48 hours, vials were transferred to LN₂ for long term storage.

Cell stocks were recovered by rapidly thawing the cryovial at 37°C and transferring the cells into an appropriate volume of fresh media.

Generation of Cell Cultures From Single Cells

Single cell clones were established by limiting dilution. Essentially, an exponentially growing cell culture was diluted to 20, 40, 60 or 80 cells per ml. 100µl of diluted cells were seeded in each well of a 96 well plate and allowed to grow for 2-3 weeks. Mass cultures were established from wells containing only a single colony.

Selection of Cisplatin Resistant Clones

A medium flask containing an exponentially growing, sub-confluent population of approximately 5×10^6 A2780-SCA5 cells was treated with an appropriate concentration of cisplatin (3.33mM Stock in 1% NaCl, David Bull Laboratories) in growth medium containing 10% FCS. Treatment was for one hour and after this period, the medium was replaced with drug-free medium containing 10% FCS. Cells were then left to recover for about 2-3 weeks before the next treatment. After the cells had recovered from the final treatment, single cell clones were generated.

Dialysis of Foetal Calf Serum

Foetal calf serum was dialysed against 10 x volume of PBSA using SpectraPor7 dialysis tubing (Fisher Scientific) at 4°C for 48 hours with five changes of PBSA before being filter sterilised. The dialysis tubing has a molecular weight exclusion limit of 2KDa.

Cell Survival by Colony Formation Assay

Cisplatin

Cells from an exponentially growing culture were seeded at between 200 and 10^6 per 10cm dish and allowed to attach for about 4 hours. An appropriate concentration of cisplatin was added and cells were incubated for a further hour. The growth medium was then replaced with fresh medium, the cells incubated for a further 10 days and then colonies counted after staining with Giemsa.

S⁴TdR and UVA

Cells were grown for 3 days in medium supplemented with 10% DFCS and the indicated concentration of S⁴TdR. Cells were counted, serially diluted and seeded at between 100 and 10⁵ per well of a 6 well plate. Cells were allowed to attach for 4 hours and then washed once with 5mls of warm PBSA before being irradiated with either a VL-6L (Merck) or a UVH-253 (UV Light Technology, Birmingham, UK) lamp under a thin film (approx. 1mm) of PBSA. The dose rate was calibrated using either a J-221 (UVP) or UV-A (UV Light Technology) meter. After irradiation, the PBSA was replaced with fresh growth medium containing 10% FCS and viable colonies scored after a further 10 days growth by Giemsa staining.

S⁶G and UVA

Experiments were carried out as above except cells were grown in undialysed FCS.

Lymphoblastoid Growth Curves

Cells from exponentially growing cell stocks were seeded at a concentration of 5x10⁵ cells per ml in a 24 well plate and grown in the continuous presence of the drug. S⁶G was dissolved in 0.1M NaOH as a 5mM stock and S⁴TdR as a 20mM stock in dH₂O. Cell numbers were determined by daily cell counts using an improved Neubauer haemocytometer.

UVA Irradiation

Lymphoblasts were grown in medium containing 10% DFCS and the appropriate concentration of S⁴TdR for 3 days. Cells were then washed once with PBSA and irradiated as before as a concentrated suspension (~1-5x10⁶ cells/ml) in PBSA. Cells were pelleted and resuspended in fresh growth medium containing 10% FCS and seeded at a concentration of 5x10⁵ cells per ml in a 24 well plate. Growth was then determined as above.

Mutation Frequency

Mutation frequency was determined at the *APRT* locus using the CHO cell line D422 (Gonclaves *et al.*, 1984). Cells were grown for 3 days in growth medium

supplemented with 10% DFCS and 100 μ M S⁴TdR. After this period, cells were expanded for a further 5 days in growth medium containing 10% FCS and no S⁴TdR. Cells were counted and plated at a concentration of 5x10⁵ per 10cm dish. APRT⁻ mutants were selected using 0.4mM 8-azaadenine and the number of mutants per plate determined after a further 10 days growth. At least 1.5x10⁷ cells were plated per experiment.

Inhibition of Cell Growth by Aminopterin

500 μ l of Raji or Jurkat cells grown in either 10% FCS or 10% DFCS were seeded at a concentration of 4x10⁵ per ml in 24 well plates before being treated with various combinations of 0.4 μ M aminopterin (GibcoBRL), 100 μ M hypoxanthine and various concentrations of TdR or S⁴TdR. Cell numbers were determined after a further 3 days growth.

Molecular and Cellular Biology Techniques

Measurement of Protein Concentrations in Aqueous Solution

Protein concentrations were determined according to the method of Bradford. An appropriately diluted 1 μ l aliquot of extract was added to 100 μ l of dH₂O and to this, 900 μ l of Bradford reagent. After thorough mixing and incubation at room temperature for 5 minutes, the absorbance at 595nm (A₅₉₅) was determined and the background (900 μ l + 100 μ l dH₂O) subtracted. The protein concentration was determined from a standard curve of the A₅₉₅ from known amounts of BSA.

Bradford Reagent: 100mg Coomassie Brilliant Blue
 50ml 95% (v/v) Ethanol
 100ml Orthophosphoric Acid
 dH₂O to 1L

The solution was stored at +4°C, protected from light but was warmed to room temperature prior to use.

Determination of Nucleic Acid Concentrations in Aqueous Solutions

Concentrations of DNA in solution were determined according to the method of (Sambrook *et al.*, 1989). The absorbance of appropriately diluted solutions was determined at 260 and 280nm (A_{260} and A_{280}) in quartz cuvettes (Jencons) using either an UltrospecIII or GeneQuant (both Amersham Pharmacia Biotech, APB) spectrophotometer. An A_{260} equal to 1.0 corresponds to 50 μ g/ml dsDNA or 33 μ g/ml ssDNA or oligonucleotide. The ratio of A_{260}/A_{280} is an estimate of purity and should be between 1.8 and 2.0 for pure dsDNA.

Cell Extracts

Stillman Replication Extract

Cell extracts were prepared from either 20 triple flasks or 5 litres of cell culture (Cell Production Unit, ICRF Clare Hall). The cells were washed first in hypotonic buffer (20mM HEPES-KOH pH 7.5, 5mM KCl, 1.5mM MgCl₂ and 0.5mM DTT) containing 250mM sucrose then in hypotonic buffer alone and allowed to swell on ice for 5 minutes. Cells were then dounce homogenised with a B pestle and centrifuged for 20 min at 10 000 x g at 4°C. The supernatant was centrifuged again at 50 000 x rpm in a Beckman TL100.2 rotor for 1 hour at 4°C. Aliquots of the supernatant were snap frozen and stored at -70°C. All solutions were kept at less than 4°C and all steps carried out on ice.

For DE81 Paper TK Assay

Approximately 10⁷ cells were lysed in Triton extraction buffer (50mM Tris-HCl pH 7.5, 10mM DTT, 1mM EDTA, 0.2% (v/v) Triton X-100) for 5 minutes on ice. Lysates were clarified by centrifugation at 15 000 x g at 4°C for 15 minutes. The protein concentration in the supernatant was determined as before.

For Gel Retardation Assay

Approximately 1 litre (2x10⁸) of cells were harvested, washed with PBSA, pelleted and resuspended in 1ml of ice-cold extraction buffer (25mM HEPES-KOH pH 8.0, 1mM EDTA, 1mM benzamidine, 2mM β -mercaptoethanol, 0.5mM spermidine, 0.1mM spermine). Cells were homogenised in a Dounce homogeniser with 10

strokes of the pestle and an equal volume of ice-cold glycerol added. 11µl of saturated AmSO₄ per 100µl pre-glycerol homogenate was then added, mixed well and left on ice for 20 minutes. The precipitate was removed by centrifugation in a Beckman TL100.2 rotor at 90 000 x rpm for 60 minutes at 4°C. Supernatant was snap frozen and stored at -70°C.

For Western Blots

One medium flask (or around 2x10⁷ cells) were pelleted, washed and resuspended in 100-200µl of extraction buffer (1% NP40, 10mM NaF, 1mM NaV₃O₄, 1mM NaPPO₄, Mini EDTA free protease inhibitor cocktail tablet (Roche) in PBSA) and incubated on ice for 1 hour. Samples were centrifuged at 15 000 x g for 30 mins at 4°C and the protein concentration determined.

Preparation of Genomic DNA

HPLC and PCR

This was prepared from about 2x10⁶ cells using a DNeasy Tissue Kit (QIAGEN) according to the manufacturers instructions.

Platination Levels

About 4x10⁷ cells were harvested, washed and pelleted. Cells were resuspended in 200µl lysis buffer (150mM NaCl, 0.4% SDS, 10mM EDTA, 10mM Tris-HCl pH 8.0) and Proteinase K added to a final concentration of 1mg/ml and incubated overnight at 37°C. After extraction with phenol/chloroform and chloroform, the DNA solution was treated with RNaseA (100µg/ml) for 1 hour at 37°C followed by a second extraction with phenol/chloroform and chloroform. DNA was precipitated with 1/10th volume 3M NaAc and 2 volumes ice cold EtOH, washed twice with 70% EtOH and dried.

Determination of DNA-S⁴TdR by HPLC

2x10⁶ cells were grown in medium containing 100µM S⁴TdR and 10% DFCS for 3 days. DNA was extracted using a DNeasy Tissue kit and converted to deoxynucleosides by successive digestion with DNase I (Sigma), Phosphodiesterase

I (Roche) and alkaline phosphatase (Roche). Products were separated by reverse phase HPLC on a C14 column (Waters) as previously described (Xu *et al.*, 1992).

Thymidine Kinase Assays

By DE81 Paper

30µg of Raji cell extract was incubated in 20µl assay mix (100mM Tris-HCl pH 8.0, 2.5mM MgCl₂, 5mM DTT, 5mM ATP, 10mM NaF) containing the appropriate concentration of [¹⁴C]TdR and unlabelled TdR or S⁴TdR at 37°C for 15 minutes. Reactions were stopped by heating to 70°C for 5 minutes and then rapidly cooled on ice. The reaction mix was spotted onto a 1.5cm² piece of DE81 paper, allowed to dry and washed four times in 500ml of 4mM Tris-HCl pH 8.0 for 5 minutes each. Squares were washed a final time in 200ml of IMS, allowed to dry and scintillation counted in 5ml of EcoscintO (National Daagnostics).

By TLC

HeLa cytoplasmic cell extracts were prepared by the Stillman method. 500µl of extract was dialysed for 24 hours against 1 litre of hypotonic buffer. 30µg of dialysed extract was incubated for 15 minutes at 37°C in 25µl reaction mix (100mM Tris-HCl pH 8.0, 2.5mM MgCl₂, 5mM DTT, 10mM NaF, 0.5mM ATP, 2µCi/ml [³²P]γATP). Reactions were terminated by boiling for 3 minutes and then rapidly cooled on ice. 5µl of reaction was spotted onto PEI-cellulose TLC plates (Camlab) and developed in saturated (NH₄)₂SO₄, pH 3.5. Products were detected using a STORM (Molecular Dynamics) phosphorimager.

Thymidine Phosphorylase Assay

Purified *E. coli* thymidine phosphorylase (Sigma) was incubated in 25µl of reaction mix (20mM KPO₄ pH 8.0, 1mM DTT, 1mM EDTA and 20µM [¹⁴C]TdR) in the presence of various concentrations of unlabelled TdR or S⁴TdR at 37°C for 10 minutes. Reactions were terminated by boiling for 2 minutes and then clarified by centrifugation. 10µl aliquots were spotted onto a Silica 60 TLC plate (0.2mm thickness, Merck) and developed in Chloroform (90) : MeOH (5) : Acetic Acid (5) (v/v/v). Products were detected using a STORM phosphorimager system.

Synthesis of S⁴T and S⁴meT Containing Oligonucleotides

Oligonucleotides containing S⁴T and S⁴meT were synthesised by Dr. Y.-Z. Xu.

S⁴T containing oligomers were synthesised using a 4-thio-dT-CE phosphoramidite (Glen Research) and deprotected with 50mM sodium hydrosulphide (NaSH) in ammonia at room temperature for 2 days. The oligomers were recovered by NENSORB PREP disposable cartridges (perkin elmer) and purified by FPLC chromatography. S⁴meT oligomers were prepared by site-specific methylation of S⁴T using methyl iodide (MeI). 1.0 OD of 34mer oligonucleotide was dissolved in 400µl 0.4M potassium phosphate buffer pH 10 and 20µl of 5% MeI in acetonitrile added. The reaction was followed by removing aliquots at specific time points and monitoring the conversion by FPLC on a Dionex BLOC system. Eluent A: 0.2M NaCl, 10mM NaOH; Eluent B: 1.2M NaCl, 10mM NaOH. Method: First 5 minutes, eluent B = 40% then eluent B increased to 60% for a further 20 minutes. When necessary, additional MeI was added to drive the reaction to completion. The product peak was isolated and immediately neutralised with dilute acetic acid, desalted with a NAP-10 (APB) column and freeze dried.

Gel Retardation Assay

These were carried out according to the previously described protocols of (Duckett *et al.*, 1996; Griffin *et al.*, 1994).

Substrate oligonucleotides

34mer : AAT TCC CGG GGA TCC GTC XGC CTG CAG CCA AGC T

31mer : GCT AGC AAG CTX TCG ATT CTA GAA ATT CGG C

where X = T, S⁴T or S⁴meT. Appropriate amounts of oligonucleotide was 5'-end-labelled with [³²P]γATP / T4 polynucleotide kinase and purified using G50 Sephadex spin column chromatography.

Duplex ³²P-labelled oligonucleotides were formed by annealing a 10-fold excess of complementary strand containing either A or G opposite X. Either HeLa cell extracts or extensively purified hMutSα (P. Macpherson) were incubated for 5 minutes at room temperature with 2 pmol of perfectly matched, non-radioactive

duplex in 20 μ l 10mM Hepes-KOH pH 7.6, 1mM DTT, 5mM MgCl₂, 50mM KCl, 50 μ g/ml BSA and 50 μ g poly(dI.dC). 20 fmol of radiolabelled duplex was then added and incubation continued for a further 20 minutes. 10 μ l aliquots were separated on 6% non-denaturing polyacrylamide gels and the products detected by autoradiography on BioMax MR film (Kodak).

Primer Extension Assay

Primer extension assays were performed using the 34mer gel retardation assay oligomer as the template and a 15mer 5'-³²P end-labelled primer (AGC TTG GCT GCA GGC) that terminated directly prior to the S⁴T or S⁴meT residue. Extension was carried out essentially as described in (Menichini *et al.*, 1994). Briefly, reactions (10 μ l) containing 2nM primer/template in 20mM Tris-HCl pH 7.8, 2mM MgCl₂, 2mM DTT and various concentrations of dNTP were incubated with 0.5nM Klenow fragment (Pharmacia). After 60 seconds at 37°C, reactions were terminated by the addition of an equal volume of 90% formamide in 50mM EDTA, products denatured by heating to 100°C for 3 minutes and separated by electrophoresis on 7M urea / 15% polyacrylamide gels. Reaction products were detected by autoradiography as above.

Extension of mismatched termini was analysed using the same template but with a 16mer primer in which the 3' terminal base, complementary to the S⁴T or S⁴meT, was either A or G. The primer/template was extended as above using 0.5nM exonuclease-deficient Klenow fragment (New England Biolabs) with all four dNTPs (200 μ M). Products were separated and detected as before.

***In vitro* Mismatch Repair Assay**

The substrate was prepared and the assay carried out by Mr. P. Macpherson in the laboratory according to the previously described method (Oda *et al.*, 2000).

Mismatch correction was assayed in 25 μ l 30mM Hepes-KOH pH 8.0, 7mM MgCl₂, 0.5mM DTT, 100 μ M each dNTP, 4mM ATP, 40mM phosphocreatine, 1 μ g creatine phosphokinase (rabbit muscle type I), 70mM KCl, 90ng DNA substrate (T/C mismatch) and up to 200 μ g cell extract. Extracts were prepared according to the

method of Stillman described earlier. Mixtures were incubated at 37°C for 15 minutes and then terminated by the addition of 10mM EDTA, 0.5% SDS. Proteins were removed by proteinase K digestion and phenol extraction and the DNA precipitated with 1/10th volume 3M NaAc and 2 volumes EtOH. After extensive washing with 70% EtOH and drying, the DNA was dissolved in restriction enzyme buffer (NEB) and digested with *MluI* (NEB) which is diagnostic for the removal of the mismatch. Digestion products were separated on a 0.8% agarose gel and detected by ethidium bromide staining.

Western Blotting

Antibodies

Immunogen	Manufacturer	Clone	Concentration (µg/ml)
hMSH2	Pharmingen	G219-1129	1
hMSH6	Santa Cruz	Q-20	2
hPMS2	Pharmingen	A16-4	1
hMLH1	Pharmingen	G168-15	0.5
p53	Pharmingen	FL393	1
p21	Oncogene	EA10	0.1
MDM2	Santa Cruz	SMP14	0.2
Bax	Pharmingen		1:4000*

* concentration of Ab unknown, recommended manufacturer's dilution.

50µg of whole cell extract (total volume of 10µl) per well was loaded onto either 8% (MMR proteins, MDM2), 10% (p53) or 12% (p21, Bax) SDS-PAGE gels along with 10µl of prestained Perfect Protein markers (lane 1) and 10µl Kaleidoscope markers (lane 10, both Biorad). Separated proteins were transferred to a PVDF membrane (Immobilon-P, Millipore) for 1 hour at 18V using a Transblot semi-dry transfer cell (Biorad) and 25mM Tris, 192mM Glycine, 0.037% SDS and 20% MeOH as the transfer buffer. Membranes were blocked overnight in 5% (w/v) non-fat powdered milk in PBS-Tween (0.1% Tween20) at 4°C with gentle rocking. Membranes were washed three times with PBS-Tween before being incubated with the primary antibody diluted in 5% BSA / 0.1% sodium azide / PBS-Tween for 1 hour at room

temperature. Membranes were again washed three times with PBS-Tween and immunoreactive proteins detected using a HRP-conjugated secondary antibody diluted according to the manufacturers instructions in 5% BSA / PBS-Tween; anti-mouse (hMSH2, hMLH1, hPMS2, MDM2, p21 and Bax, Biorad), anti-rabbit (p53, Biorad) or anti-goat (hMSH6, Chemicon). Incubation was for 1 hour at room temperature. Membranes were washed a further four times before antibody complexes were detected using ECL substrate and quantitated on Hyperfilm ECL film (APB). Transfer efficiency was ascertained by staining the membranes with Ponceau after immunogen detection.

PCR Amplification and DNA Sequencing of p53

The primers used to amplify the various exons of p53 are listed below: Due to the small size of the introns between exons 2, 3 and 4, exons 2 to 4 were amplified as a single PCR product.

Exon 2 Forward

TGG AAG TGT CTC ATG CTG GA

Exon 4 Forward

ATC TAC AGT CCC CCT TGC CG

Exon 4 Reverse

CAG GCA TTG AAG TCT CAT GG

Exon 5 Forward

TCT GTT CAC TTG TGC CCT GAC TTT C

Exon 5 Reverse

ACC CTG GGC AAC CAG CCC TGT CGT C

Exon 6 Forward

CAG GGC TGG TTG CCC AGG GTC CCC A

Exon 6 Reverse

ACT GAC AAC CAC CCT TAA CCC CTC C

Exon 7 Forward

CTT GCC ACA GGT CTC CCC AA

Exon 7 Reverse

AGG GGT CAG CGG CAA GCA GAG

Exon 8 Forward

TAG GAC CTG ATT TCC TTA CTG CCT C

Exon 8 Reverse

AAC TGC ACC CTT GGT CTC CTC CAC C

PCR reactions contained 100ng genomic DNA, 2.5mM MgCl₂, 200μM each dNTP, 25 pmol each primer and 2.5U HotStar Taq (QIAGEN) in the manufacturer's buffer to a final volume of 50μl. Efficient amplification of exons 2-4, exon 6 and exon 7 required the addition of Q-solution (QIAGEN) to the PCR reaction. Two different sets of PCR conditions were used dependent on the exon(s) to be amplified. Exon 4 and exons 2-4: 15 minutes at 95°C to activate Taq followed by 35 cycles of 95°C for 1', 55°C for 1' and 72°C for 1' with a final extension of 72°C for 5' in a MJ Research thermal cycler. Exons 5, 6, 7 and 8 were amplified as above except the annealing temperature was increased to 65°C. PCR products were purified using QIAquick PCR purification spin columns (QIAGEN) and checked by agarose gel electrophoresis.

DNA Sequencing Reactions

These were carried out using the ABI Prism BigDye Terminator Cycle Sequencing Ready Reaction Kit (Applied Biosystems) according to the manufacturers instructions. Essentially, reactions contained 8μl of BigDye mix, 20ng PCR product and 3.2 pmol primer in a total volume of 20μl. The DNA was then sequenced in a MJ Research thermal cycler for 25 cycles of 96°C for 30s, 50°C for 15s and 60°C for 4' (at a ramp rate of 1°C/s). At the end of the reaction, excess dye terminators were removed using Centri-Sep (Princeton Separations) spin columns. Electrophoresis was carried out by the ICRF Equipment Park on an ABI Prism 377 Sequencer.

Fluorescence Associated Cell Sorting (FACS) Analysis

FACs analysis was carried out with the help of Mr. D. Davies of the ICRF FACS laboratory, 44 L.I.F.

Exponentially growing cell cultures were treated with 30μM cisplatin for 1 hour. At the appropriate time point (0, 24 or 48 hours), cells were harvested and washed with

PBSA. Approximately 10^6 cells were fixed in 1ml of 70% EtOH at 4°C for 1 hour. EtOH was spun out and the cells washed 3 times with PBSA. To remove RNA, cells were subsequently treated with 100µl of 100µg/ml RNase A. 400µl propidium iodide (50µg/ml) was then added and cells incubated at room temperature for 15 minutes. Analysis by flow cytometry using a FACscan cytometer was then performed.

For apoptosis studies, the sub-G1 apoptotic cell population was measured essentially as above except the cells were now washed in phosphate-citrate buffer (0.192M Na_2HPO_4 , 4mM citric acid pH 7.8) prior to FACs analysis.

Levels of DNA Platination in Cultured Human Cells After Cisplatin Treatment

The levels of DNA platination in the A2780 clonal variants was determined by Atomic Absorption Spectroscopy (AAS) by Dr. Ciaran O'Neill at the CRC Centre for Cancer Therapeutics, Institute of Cancer Research, Sutton, UK.

Approximately one large flask (about 4×10^7 cells) per cell line was treated with 0 to 100µM cisplatin for 2 hours. Medium was removed, the cells washed twice with PBSA and then pelleted. DNA was extracted by phenol chloroform extraction as described previously and precipitated with sodium acetate / EtOH. After extensive washing with 70% EtOH, DNA samples were dried before being dissolved in 500µl 0.2% nitric acid overnight at 37°C. Samples were diluted 1 in 10 for AAS analysis.

Determination of Reduced Glutathione Levels

Assays were performed according to the modified enzyme recycling method outlined in (Akerboom and Sies, 1981).

About 5×10^6 cells were pelleted, washed in PBSA, lysed by sonication in 1ml of PBSA and clarified by centrifugation at 10 000 x g for 10 minutes at 4°C. Protein was precipitated by mixing 1 volume 12% 5-sulphosalicylic acid (SSA) with 3 volumes sonicate and incubated on ice for 4 hours. Precipitate was removed by centrifugation at 10 000 x g for 10 minutes at 4°C.

Reactions contained 700 μ l 0.3mM NADPH, 100 μ l 6mM DTNB, 0.5U glutathione reductase (Sigma), sample and dH₂O to 1ml. NADPH and DTNB were dissolved in 175mM KPO₄ pH 7.5, 6.3mM EDTA. The reaction was followed at 412 nm over a period of 2 minutes and the rate of reaction calculated. A standard curve of rate of reaction versus known concentrations of reduced glutathione (GSH) was constructed and concentrations of GSH in the precipitated extracts determined from this.

Chapter 3: Results I

Role of DNA Mismatch Repair in Cisplatin Sensitivity of *Escherichia coli* Defective in the DNA Adenine Methylase (*dam*) Gene

DNA Adenine Methylation deficient (*dam*) strains of *Escherichia coli* are defective in the specific methylation at the N-6 position of adenine in the sequence GATC. Such strains are sensitive to killing by both the alkylating agent MNNG (Karran and Marinus, 1982) and cisplatin (Fram *et al.*, 1985) but not to carboplatin or iproplatin (Fram *et al.*, 1986). The introduction of a mutation in either the *mutL* or *mutS* genes abolishes the sensitivity of *dam* strains to both MNNG and cisplatin. *E. coli dam* strains are therefore an ideal model to study the role of mismatch repair in acquired resistance to cisplatin. The genotypes of the *E. coli* strains used in this study are described in Table 3.1.

Determination of Secondary Characteristics of *dam E. coli*

E. coli dam mutants lack DNA adenine methylase activity and therefore have no detectable 6-methyladenine in their DNA. In addition, *dam* strains can be discriminated from wild type and *dam mutL/S* by their secondary phenotypes.

Identifying phenotypic properties:

(1) 2-Aminopurine Sensitivity.

As well as being sensitive to MNNG and cisplatin, *dam* strains are also hypersensitive to the base analogue 2-aminopurine. Wild type and *dam mutL/S* are not. Thus wild type and *dam mutL/S* strains can be distinguished from *dam* mutants by screening colonies for the ability to grow on plates containing 2-AP.

(2) Restriction Enzyme Digests

The restriction enzyme *DpnI* cuts at GATC sequences only when the adenines of both strands are methylated. In contrast, *MboI* will cut DNA at GATC sequences

when the adenines of both strands are unmethylated. Neither enzyme shows activity on hemi-methylated DNA.

(3) Mutator Phenotype

Mismatch repair defective *E. coli* are characterised by the high rate of spontaneous mutation due to the lack of repair of DNA replication errors. *Dam* strains also demonstrate a mild mutator phenotype as mismatch repair in these strains can occur in either the parental or daughter strand. Table 3.2 summarises the extent of the mutator phenotype in both *dam* and *dam mutL/S E. coli*.

These properties allow the efficient characterisation of *dam* / mismatch repair defective mutants. A summary of the various characteristics is illustrated in Table 3.3.

Table 3.1 Genotypes of *E. coli* K-12 strains

Strain	Genotype
GM112	<i>F</i> <i>thr-1 ara-14 leuB6 Δ(gpt-proA)62 lacY1 tsx-33 supE44 galK2 hisG4 metB1 rfbD1 mgl-51 rpsL260 kdgK51 mtl-1 thi-1 thyA12 deoB16</i>
GM113	GM112 <i>dam-3</i>
GM150	GM112 <i>dam-3 mutL451</i>
GM169	GM112 <i>dam-3 mutS453</i>
AB1157	<i>F</i> <i>thr-1 ara-14 leuB6 Δ(gpt-proA)62 lacY1 tsx-33 glnV44(AS) galK2(Oc) hisG4(Oc) rfbD1 mgl-51 rpoS396(Am) rpsL31(StrR) kdgK51 xylA5 mtl-1 argE3(Oc) thi-1</i>
GM3819	AB1157 <i>dam-16::Kan</i>
GM5556	AB1157 <i>dam-16::Kan mutS::Tn10</i>
ES1582	AB1157 <i>mutL25</i>
BH200	<i>uvrA</i>

The *dam-3* mutation was induced by mutagenesis with MNNG followed by selection for loss of adenine methylation (Bale *et al.*, 1979). In contrast the *dam-16* strain was constructed by replacement of part of the *dam* gene with a fragment encoding resistance to kanamycin (Parker and Marinus, 1988). GM150 and GM169 were generated from GM113 by conjugation and transduction followed by selection for suppression of secondary phenotypes of *dam* (namely 2-AP sensitivity, (McGraw and Marinus, 1980).

Table 3.2 Mutator phenotypes of *E. coli* K-12 Defective in Mismatch Repair

Strain	Pertinent Genotype	Mutator Effect
GM112	Wild Type	1
GM113	<i>dam</i>	~2
GM150	<i>dam mutL</i>	~10 ⁴
GM169	<i>dam mutS</i>	~10 ⁴

Data summarised from (McGraw and Marinus, 1980). The mutant frequency is determined from the number of rifampicin resistant mutants per number of sensitive cells plated. The mutator phenotype is the fold increase in the mutation frequency over the wild type.

Table 3.3 Summary of Secondary Phenotypes

	2-AP ^a	Mutator	<i>DpnI</i> Digestion ^b
Wild Type	R	–	D
<i>dam</i>	S	+	U
<i>mutL</i> or <i>mutS</i>	R	+++	D
<i>dam mutL / S</i>	R	+++	U

^a S = growth inhibited by 2-AP; R = no inhibition of growth

^b D = genomic DNA sensitive to *DpnI* digestion; U = resistant to digestion

Verification of Selection Strategy

The parental strains (listed in Table 3.1) were checked for *dam* and *dam mutL/S* status using the outlined criteria. Single colonies were streaked onto L-agar containing 2-aminopurine and growth after incubation overnight ascertained (Fig 3.1A). Only strains with a functional Dam methylase or doubly mutated in *dam* and either *mutL* or *mutS* are resistant to 2-AP; *dam* strains (GM113 and GM3819) are sensitive. In order to differentiate wild type from *dam mutL/S* mutants, genomic DNA from GM112 and its derivatives was digested with *DpnI* and then analysed by agarose gel electrophoresis (Fig 3.1B). DNA from strains with a functional Dam

methylase (GM112 and BH200) was sensitive to *DpnI* digestion. The DNA of *dam* strains (GM113, GM150 and GM169) that lack adenine methylation was insensitive to *DpnI* cutting. Comparable results were obtained for the AB1157 family of strains (data not shown).

This primary analysis allows confident identification of the genotypes with respect to *dam* of the *E. coli* strains being investigated.

Sensitivity of *dam* and *dam mutL/S E. coli* to Cisplatin

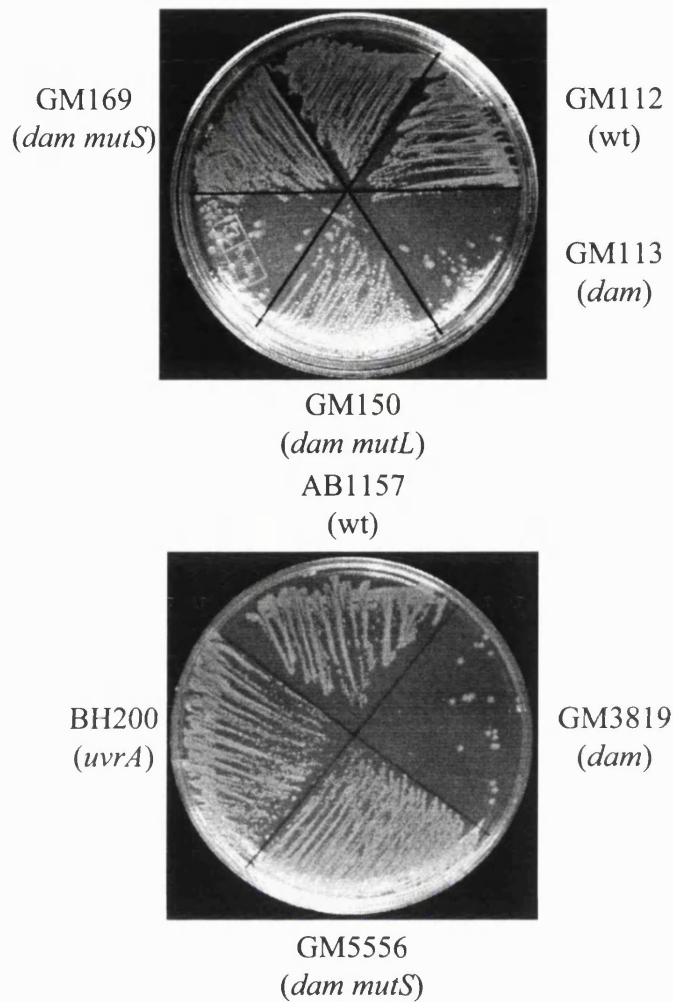
E. coli dam strains are approximately 11-fold more sensitive to killing by cisplatin than the wild type. Introduction of a second mutation in either *mutL* or *mutS* reverses the resistance to wild type levels (Fram *et al.*, 1985). The cisplatin sensitivity of *dam* and *dam mutL/S* strains was reinvestigated as this provides the basis for the examination of a role for mismatch repair in acquired resistance to this drug.

Cytotoxicity was assessed by exposing exponentially growing cultures of wild type, *dam* and *dam mutL/S E. coli* to 0-80 μ M cisplatin for 2 hours (Fig 3.2A). The D_{37} values for wild type, *dam* and *dam mutL/S* were 27, 7 and 14 μ M respectively (Table 3.4).

Dam E. coli were about 3.9-fold more sensitive to killing than the wild type (Table 3.4). *E. coli* defective in nucleotide excision repair (*uvrA*, *uvrB* or *uvrC*) are extremely sensitive to cisplatin. The *uvrA* defective strain BH200 was about 6.4 times more sensitive to cisplatin than the wild type (Table 3.4). Unexpectedly, I found that the introduction of a second mutation in either the *mutL* or *mutS* gene into the *dam* background did not restore full wild type resistance. The double mutants remained about 1.9-fold more sensitive to cisplatin than the wild type. This was confirmed using a different set of *dam / dam mutL/S* mutants (Fig 3.2B) indicating that the result is not due to the host strain's genetic background.

Loss of either *mutL* or *mutS* could sensitise cells to cisplatin and could be responsible for the 1.9-fold sensitivity of *dam mutL/S* strains. No difference in sensitivity to cisplatin was observed in a *mutL* defective strain (Fig 3.2C) indicating that the mismatch repair recognition machinery does not play a role in cisplatin sensitivity independent of *dam*.

A.



B.

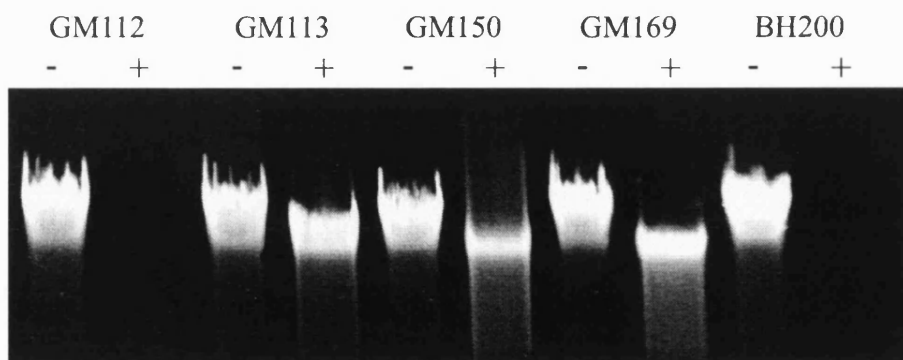


Figure 3.1 Phenotypic Characterisation of Wild Type and Mutant Strains

A. 2-Aminopurine Sensitivity.

Single colonies were streak plated onto L-agar containing 200µg/ml 2-AP. Growth after overnight incubation at 37°C was then ascertained.

B. Sensitivity of Genomic DNA to *DpnI* Digestion.

Approximately 1µg of genomic DNA from wild type and mutant strains was digested with 5 units of *DpnI* at 37°C for 2 hours. Undigested (-) and digested (+) products were analysed on a 0.5% native agarose gel and visualised under UV light by ethidium bromide staining.

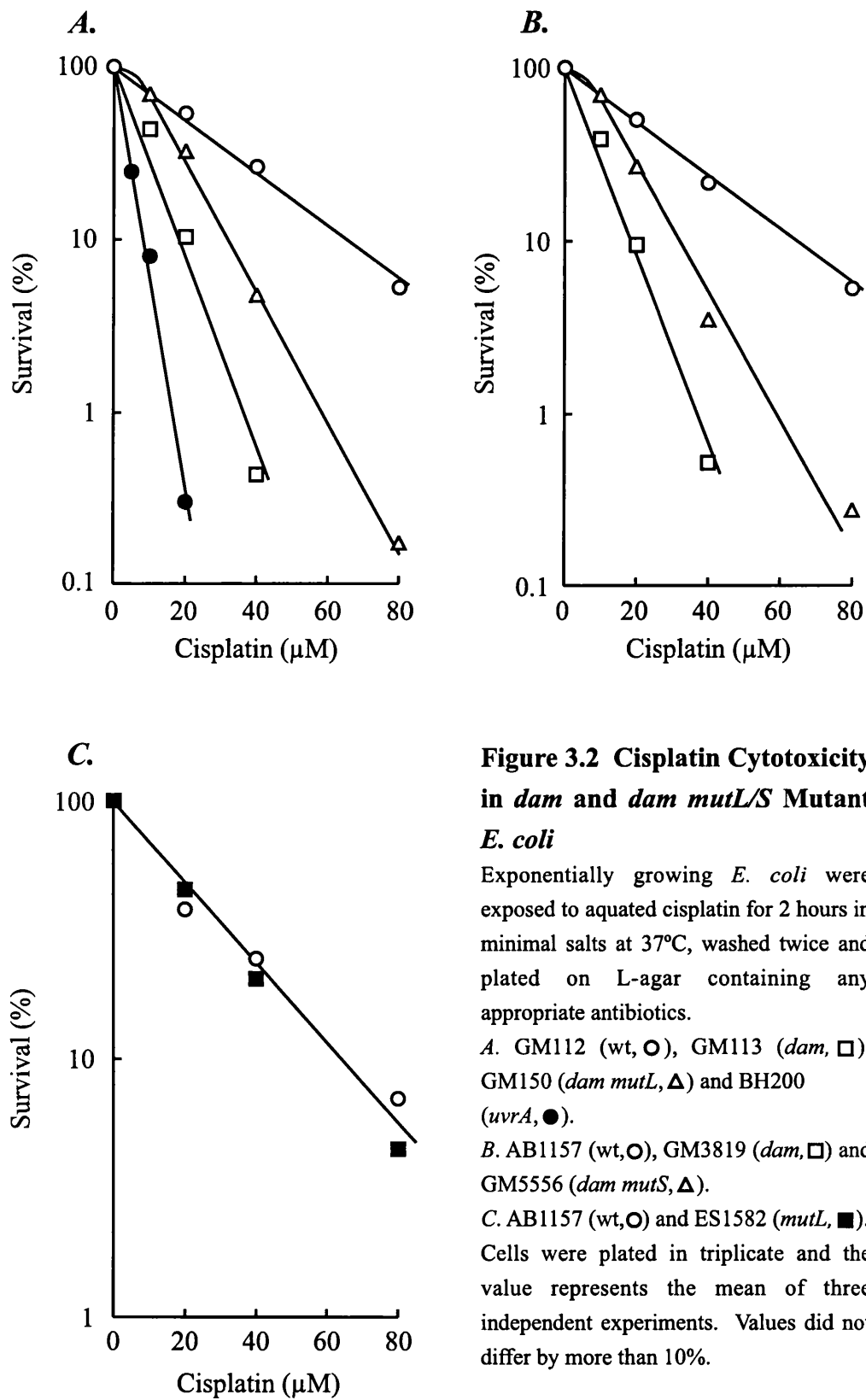


Figure 3.2 Cisplatin Cytotoxicity in *dam* and *dam mutL/S* Mutant *E. coli*

Exponentially growing *E. coli* were exposed to aqated cisplatin for 2 hours in minimal salts at 37°C, washed twice and plated on L-agar containing any appropriate antibiotics.

A. GM112 (wt, ○), GM113 (*dam*, □), GM150 (*dam mutL*, Δ) and BH200 (*uvrA*, ●).

B. AB1157 (wt, ○), GM3819 (*dam*, □) and GM5556 (*dam mutS*, Δ).

C. AB1157 (wt, ○) and ES1582 (*mutL*, ■). Cells were plated in triplicate and the value represents the mean of three independent experiments. Values did not differ by more than 10%.

Table 3.4 Sensitivity of *dam* and *dam mutL/S* *E. coli* to Cisplatin

	Strains	D ₃₇	RF ^a
wild type	GM112, AB1157	27 ± 5.46	1.0
<i>dam mutL</i>	GM150	15 ± 1.25	1.8
<i>dam mutS</i>	GM169, GM5556	13 ± 1.79	2.0
<i>dam</i>	GM113, GM3819	7 ± 1.40	3.9
<i>uvrA</i>	BH200	4.2	6.4

The D₃₇ value (the concentration required to reduce survival to 37%, in μM) was determined from each survival curve. The value represents the mean, ± the standard error.

^a RF = relative fold sensitivity compared to wild type strains.

Selection for Cisplatin Resistance in a *dam* Genetic Background

The previous data confirm that *dam* defective *E. coli* are sensitive to cisplatin and further indicate that this sensitivity is only partially abrogated by a second mutation in either the *mutL* or *mutS* genes. *E. coli dam* strains were used as a model system to investigate whether loss of mismatch repair occurs in acquired resistance to cisplatin.

Exponentially growing cultures of either GM113 or GM3819 were repeatedly exposed to 100μM cisplatin (approximately 10⁻⁶ survival / 2 hour treatment). After each treatment cycle, the phenotype of fifty surviving clones was determined using the three tests outlined previously. The results are outlined in Table 3.5. Each row of Table 3.5 represents an independent experiment and the columns, the number of treatments with cisplatin. The letters B to H indicate treated cultures that were screened for the secondary phenotypes outlined previously and are described in future figures. For example, Expt. B clones were generated by a single selection of GM112 with 100μM cisplatin. E clones were selected from B by a subsequent selection with 100μM cisplatin. Finally, E2 were selected from E by a further two rounds of 100μM cisplatin treatment. Each of the fifty surviving clones was screened initially for 2-AP resistance (that is characteristic of Dam⁺ or *dam mutL/S* bacteria, examples shown in Fig 3.3A). Resistant clones were subsequently screened

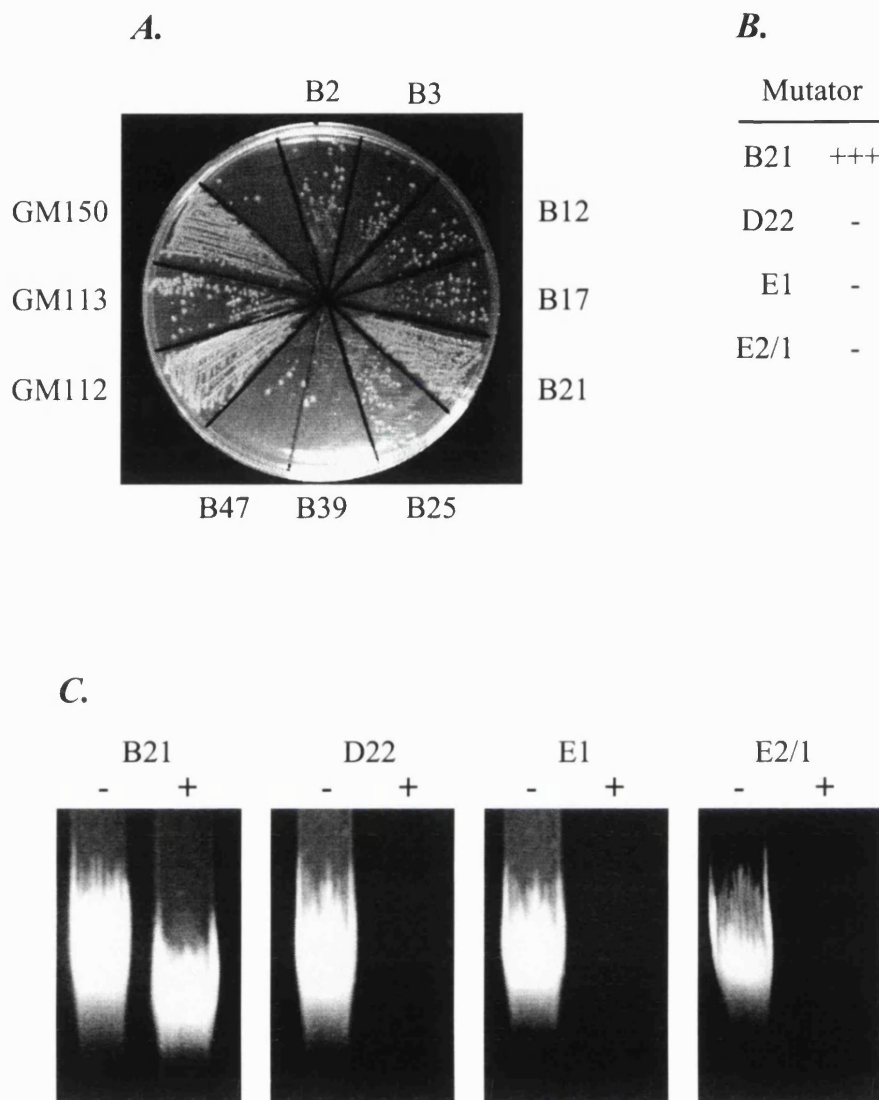


Figure 3.3 Secondary Characteristics of GM113 Selected with Cisplatin

A. 2-Aminopurine Sensitivity.

Single colonies that survived treatment with cisplatin were screened on 200 μ g/ml 2-AP. Examples are shown for experiment B (clones B2, B3, B17, B21, B25, B39 and B47) which have received a single treatment of 100 μ M cisplatin. GM112 (wt), GM113 (*dam*) and GM150 (*dam mutL*) are shown as controls.

B. Summary of Mutator Phenotypes.

Clones resistant to 2-AP were screened for a mutator phenotype as described before.

- = no mutator phenotype, +++ = strong mutator phenotype.

C. Sensitivity of Genomic DNA to *DpnI* Digestion.

DNA from various clones was digested with *DpnI*. Clones deficient in Dam (e.g. B21) are insensitive to cutting by *DpnI*.

for a mutator phenotype on rifampicin containing plates (Fig 3.3B). Analysis of the genomic DNA by *DpnI* digestion was subsequently carried out to confirm the Dam status of these clones (Fig 3.3C).

Table 3.5 Secondary Phenotypes of Cisplatin Selected *E. coli*

Strain	Treatment Cycle								
	1			2			4		
	Expt	Dam ⁺	Dam ⁻ MutL/S ⁻	Expt	Dam ⁺	Dam ⁻ MutL/S ⁻	Expt	Dam ⁺	Dam ⁻ MutL/S ⁻
GM113	B	0	1	E	4	11	E2	49	0
	D	21	0						
		0	2		0	25	G1	0	50
		0	3		0	13	G2	0	50
		0	1		0	24	G3	0	50
		0	0		0	14	G4	0	50
		0	2		0	16	G5	0	50
GM3819	C	0	3	F	0	33	H	0	50

Dam⁺ - number of colonies out of 50 screened resistant to 2-AP but do not show a mutator phenotype.

Dam⁻ MutL/S⁻ - number of colonies out of 50 screened that were 2-AP resistant and showed a mutator phenotype.

To determine the mutator phenotype, approximately 1x10⁸ cells were plated on L-agar plates containing 100µg/ml rifampicin. After growth at 37°C overnight, colonies were counted. Those containing >500 colonies / plate were deemed to have a high mutator phenotype characteristic of *mutL* or *mutS* defective strains.

Selection for cisplatin resistance in *dam* mutant *E. coli* results in a variety of phenotypes illustrating a range of genotypes. Several clones, picked at random, demonstrate a *dam mutL/S* phenotype (e.g. B21) or reversion to Dam⁺ (e.g. D22, E1 and E2/1). The sensitivity of clones D22, E1 and E2/1 to *DpnI* indicate that these clones are indeed wild type and that this reversion occurs with a remarkably high frequency. Revertants of the *dam* gene would also seem to have a greater resistance to cisplatin and is illustrated by the fact that even when the initially selected population contains only *dam mutL/S* clones, subsequent selections lead to a

population containing only Dam⁺ (clone E2/1, Expt. B, Table 3.5). In order to eliminate the effects of reversion, selection was also carried out on GM3819 in which part of the *dam* gene has been replaced by a selectable marker for kanamycin resistance. As expected, analysis of these clones after selection indicate that only *dam mutL/S* clones are generated (Expt C and F, Fig 3.4). Treatment of *dam E. coli* with highly toxic concentrations of cisplatin generates both *dam* revertants and *dam mutL/S* variants at roughly similar frequencies.

Extent of Cisplatin Resistance in Selected Clones

Cytotoxicity to 0-80µM cisplatin was determined for the cisplatin selected clones B21 and D22 (Fig 3.5A) and C45, F21 and F38 (Fig 3.5B). Their D₃₇ values are summarised in Table 3.6.

Table 3.6 Summary of Cisplatin Resistance of Clones Selected for Cisplatin Resistance

Clone	Parent	D ₃₇ (µM)	RF	Phenotype
<i>dam</i>		7	1.0	Dam ⁻
wt		27	3.9	Dam ⁺
B21	GM113	19	2.7	Dam ⁻ MutL/S ⁻
D22	GM113	28	4.0	Dam ⁺
C45	GM3819	24	3.4	Dam ⁻ MutL/S ⁻
F21	GM3819	35	5.0	Dam ⁻ MutL/S ⁻
F38	GM3819	18	2.6	Dam ⁻ MutL/S ⁻

RF = relative fold resistance.

From Fig 3.4 and Table 3.6, it is clear that some of the clones (e.g. F21) selected from GM3819 show resistance equivalent to that of the wild type even though the *dam* mutation was retained. GM3819 is unable to revert easily due to an insertional mutation in the *dam* gene. To investigate if such *dam mutL/S* clones that exhibit wild type cisplatin resistance can be selected from a population that is able to revert at a relatively high frequency, clones G1 to G5 were independently selected by four repeated treatments with 100µM cisplatin. All five selected clones still retain a

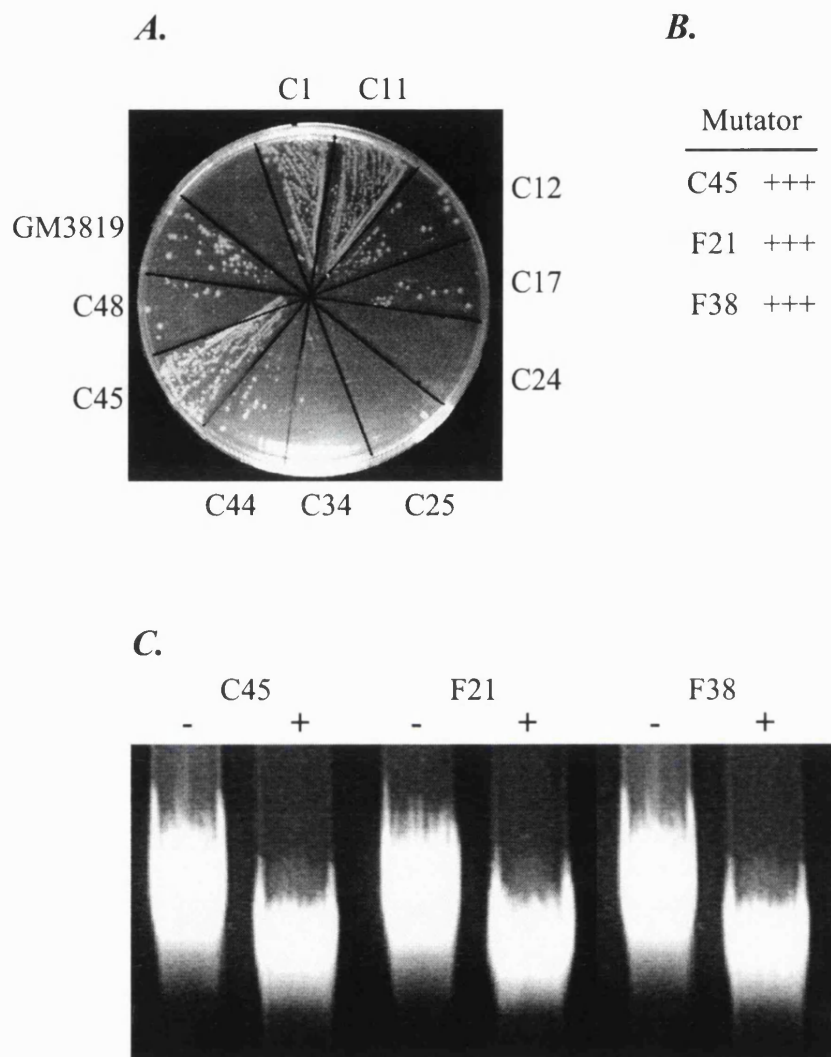


Figure 3.4 Secondary Characteristics of GM3819 Selected With Cisplatin

A. 2-Aminopurine Sensitivity.

Single colonies that survived treatment with cisplatin were screened on 200 μ g/ml 2-AP. Examples are shown for experiment C (clones C1, C11, C12, C17, C24, C25, C34, C44, C45 and C48) which have received a single treatment of 100 μ M cisplatin. GM3819 (*dam*) is shown as a control.

B. Summary of Mutator Phenotypes.

Clones resistant to 2-AP were screened for a mutator phenotype as described before.

- = no mutator phenotype, +++ = strong mutator phenotype.

C. Sensitivity of Genomic DNA to *DpnI* Digestion.

DNA from various clones was digested with *DpnI*. Clones deficient in *Dam* (e.g. C45) are insensitive to cutting by *DpnI*.

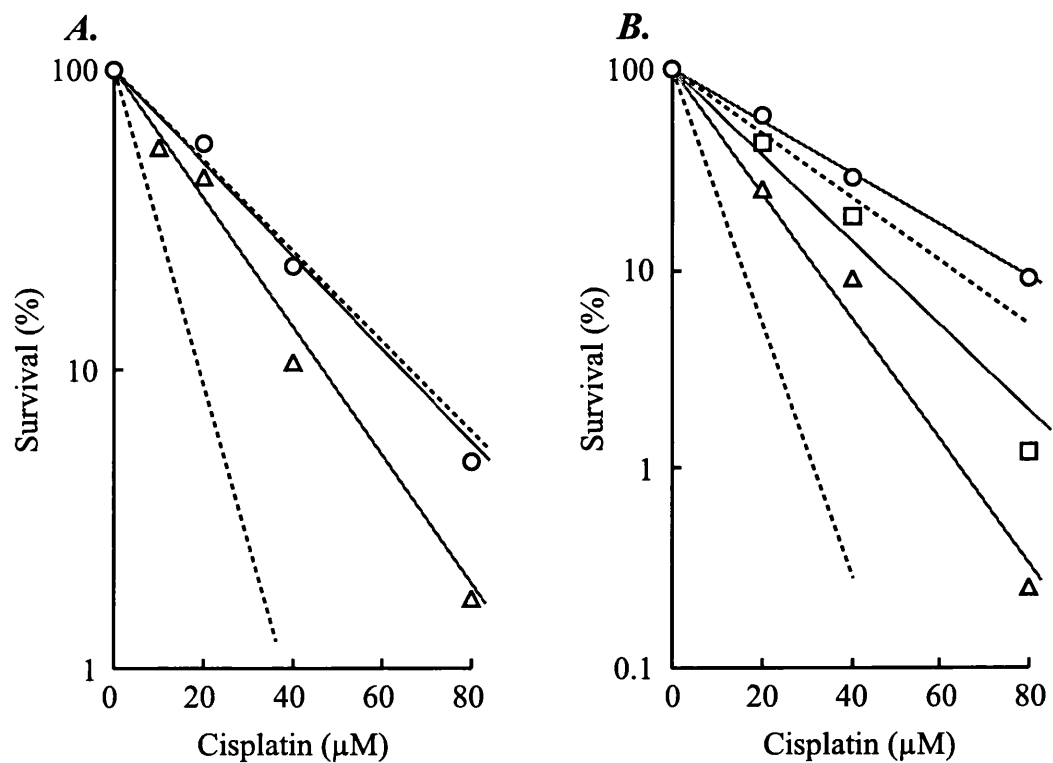


Figure 3.5 Cisplatin Cytotoxicity in Clones Selected for Resistance to Cisplatin

Clones were exposed to cisplatin as described previously.

A. From GM113 - B21 (Δ) and D22 (\circ).

B. From GM3819 - F38 (Δ), C45 (\square) and F21 (\circ).

Cells were plated in triplicate and the mean plotted. Dotted lines indicate the sensitivity of wild-type (upper) or *dam* (lower) strains.

mutated *dam* gene as determined by digestion of the genomic DNA with *DpnI* (Fig 3.6A) and a high mutator phenotype (Fig 3.6B) as judged by rifampicin resistance.

The five clones selected and analysed in Fig 3.7 show a wide variation in cisplatin resistance as judged by clonal survival after treatment with 80µM cisplatin for 2 hours. Closer observation seems to suggest that there are in fact two different populations distinct from both the wild type and the *dam mutL/S* variants. G2 and G5 exhibit cisplatin resistance that is generally greater than that of the wild type whereas G1, G3 and G4 are more sensitive than the wild type but substantially more resistant than the *dam mutL/S* double mutant GM150. This variation in cisplatin resistance is indicative of additional factors being involved in acquired resistance to cisplatin.

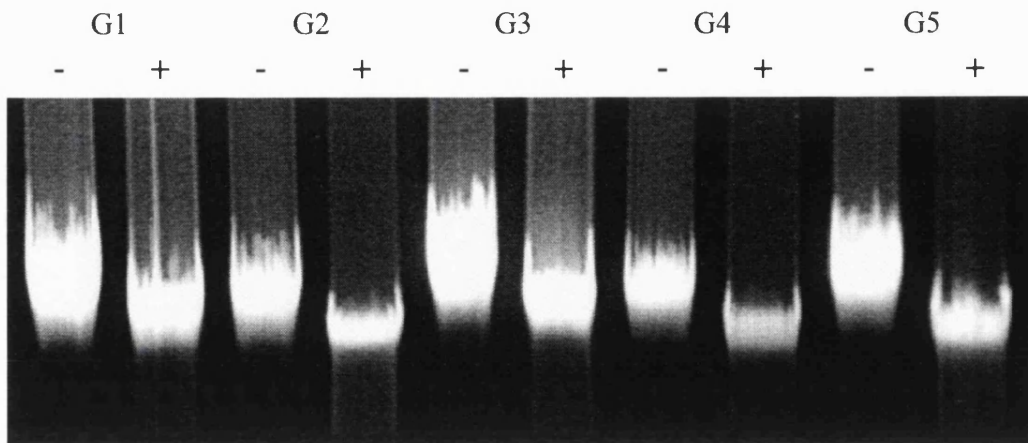
In conclusion, loss of MMR function occurs frequently in *dam* defective strains selected for resistance to cisplatin but additional factors also contribute to cisplatin resistance in these strains.

Summary

E. coli dam strains are sensitive to the chemotherapeutic agent cisplatin. A second mutation in either *mutS* or *mutL* partially reversed the sensitivity of these strains. These cisplatin sensitive *dam* mutants were used as a model system to investigate the possible selection of mismatch repair defects in cisplatin resistant derivatives. The *dam* mutants GM113 and GM3819 were 3.9-fold more sensitive to cisplatin than their wild type counterpart. A *mutS* or *mutL* mutation (GM150, GM169 and GM5556) alleviated about half of the sensitivity (1.9-fold sensitive). A single mutation in one of the MMR genes had no effect on cisplatin sensitivity or resistance (ES1582, *mutL*).

Repeated cisplatin treatment of *dam* defective strains resulted in the selection of Dam⁺ revertants in GM113 but not GM3819. *dam mutL/S* were frequent variants in cisplatin resistant colonies arising after cisplatin selection. They exhibited partial resistance to cisplatin. Some *dam mutL/S* phenotypic variants selected from both strains exhibited wild type cisplatin resistance. At least two distinct populations of

A.



B.

Mutator	
G1	+++
G2	+++
G3	+++
G4	+++
G5	+++

Figure 3.6 Secondary Characteristics of Clones G1 to G5

A. Sensitivity of Genomic DNA to *DpnI* Digestion.

B. Summary of Mutator Phenotypes.

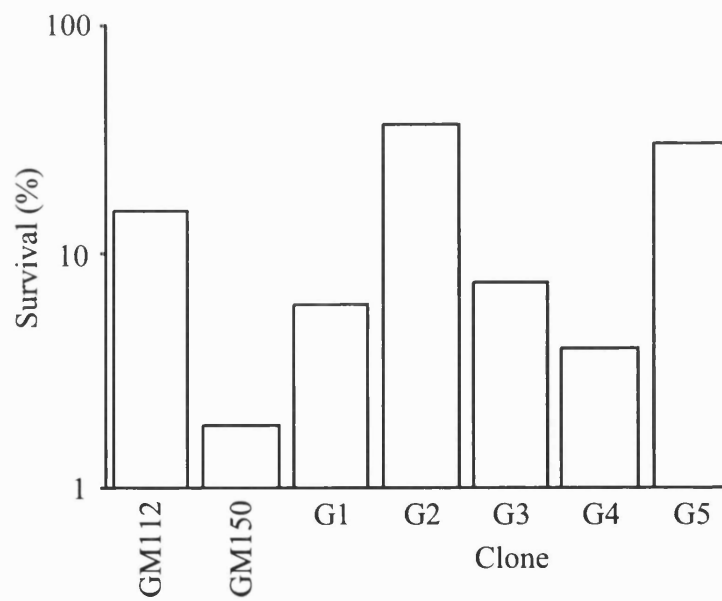


Figure 3.7 Cisplatin Sensitivity of G clones

Clones were exposed to 80 μM cisplatin as described previously.

GM112 (wt) and GM150 (*dam mutL/S*). Cells were plated in triplicate and the value represents the mean of two independent experiments.

these variants exist. One group shows resistance intermediate between *dam mutL/S* and Dam^+ . The second group was significantly more resistant than the wild type. This suggests the contribution of additional factors to cisplatin resistance.

Discussion

Cisplatin sensitive *dam* defective *E. coli* were used to investigate the possible selection of defective mismatch repair in acquired resistance to cisplatin. The *dam* gene encodes a DNA adenine methylase specific for GATC. Strains defective in Dam activity are sensitive to killing by the base analogue 2-AP, the methylating agent MNNG (Karran and Marinus, 1982) and the chemotherapeutic agent cisplatin but not the platinum analogues transplatin, carboplatin or iproplatin (Fram *et al.*, 1986). Inactivation of MMR in *dam* strains restores wild type 2-AP and MNNG resistance. The data presented here indicate that it restores only partial cisplatin resistance. This observation suggests that the mechanism by which MMR modulates cisplatin resistance may be different from that of MNNG or 2-AP.

Cisplatin sensitive *dam* mutants were chosen as a model for the involvement of MMR defects in acquired resistance to cisplatin due to their increased sensitivity to cisplatin. As expected, selection of the point mutant *dam* strain (GM113) generated both Dam^+ revertants and *dam mutL/S* variants. Additionally, only *dam mutL/S* mutants were selected from GM3819 in which *dam* is inactivated by insertion. The frequency of Dam^+ revertants from GM113 is quite high but this may be a consequence of their higher cisplatin resistance and their increased growth rate compared to a *dam mutL/S* mutant. However, *dam mutL/S* variants were still isolated at a high frequency. This suggests that defects in MMR function are a significant contributor to cisplatin resistance in this model.

In my experiments, loss of MMR in a *dam* background restored only partial cisplatin resistance. This is in contrast to the data of Fram *et al.* (Fram *et al.*, 1985) in which resistance was fully restored by mutation of the MMR system. This would appear not to be strain dependent as similar results are obtained with GM3819. Differences in either the growth stage of the cells or subtle differences in experimental procedure may underlie this. In the experiments reported here, the genotype was constantly

monitored using the three tests outlined previously. Cisplatin sensitivity of the selected clones was always compared to control strains for which the genotype is known.

Cisplatin clones (for example F21 and C45), that exhibited the secondary characteristics of *dam mutL/S* strains according to the three tests described previously, showed levels of resistance approximately equivalent to that of the wild type. Such clones were isolated from both GM113 and GM3819 parental strains. Closer inspection of the resistance revealed that this was variable with some clones more sensitive and others more resistant than the wild type. All were always more resistant than the *dam mutL* strain used for comparison. Factors in addition to MMR could contribute to the increased cisplatin resistance in these strains. Potential mechanisms include: (1) Reduced DNA platination through some form of protective mechanism such as inactivation of cisplatin by glutathione. (2) Increased DNA repair. (3) Increased recombination or recombination independent of MMR. (4) Constitutively active SOS-response (Ind^s) due to mutations in the LexA repressor. This would generate increased levels of Pol V and potentially increased bypass of the cisplatin lesions and a reduced number of DSBs. Mechanisms, in addition to MMR defects, may therefore contribute to the greater levels of cisplatin resistance observed in some *dam* clones.

Models for MMR Involvement in O⁶meG and Cisplatin DNA Damage Processing

For the methylating agent MNNG, a high proportion of the total alkylation products are O⁶meG and this lesion is believed to be responsible for its cytotoxic and mutagenic effects (Karran and Marinus, 1982). O⁶meG codes ambiguously during replication showing a 4-fold preference for T over C (Tan *et al.*, 1994). Neither O⁶meG:C nor O⁶meG:T is a preferred base pair and both are recognised by MutS (Fig 3.8A). *Dam* strains do not methylate the strand discrimination sequence and so cannot discriminate the parental strand from the newly synthesised DNA strand. Repair attempts may therefore be simultaneously made on both strands leading to the formation of a DSB (Fig 3.8B).

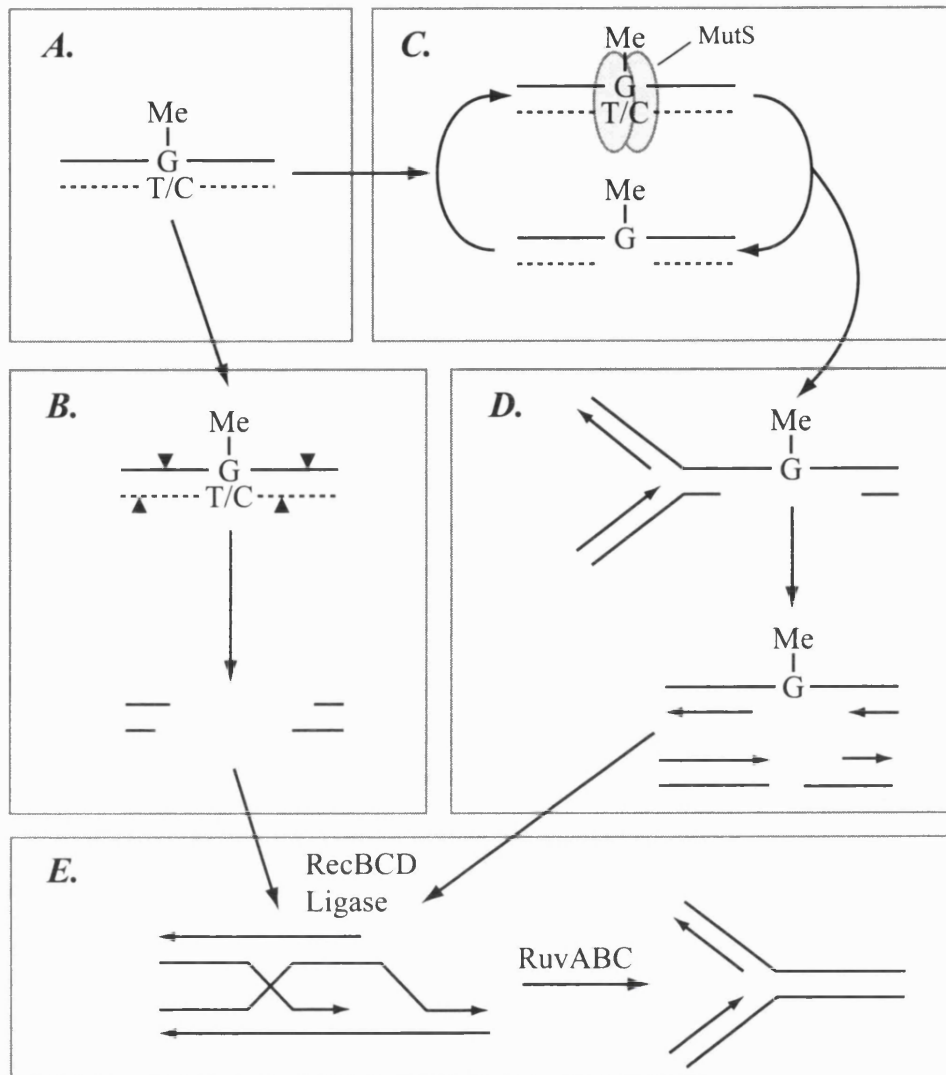


Figure 3.8 Role of Mismatch Repair in the Processing of O⁶meG

A. Replication of O⁶meG-DNA adducts generates both O⁶meG:C and O⁶meG:T base-pairs with T preferred by a factor of about 4-fold. Both combinations are recognised by MutS which recruits MutL and MutH initiating repair.

(—) parental strand, (----) daughter strand

B. In *dam* mutant strains, nicking by MutH may occur simultaneously on both the parental and daughter strands resulting in the generation of a DSB.

C. Excision of the newly synthesised daughter strand generates a daughter strand gap. Subsequent resynthesis and ligation of the gap generates O⁶meG:T/C pairs which are again recognised by MutS. In strains proficient for Dam, this cycle continues until the GATC strand discrimination signal is methylated.

D. A new replication fork encounters a single-strand gap due to incomplete repair causing the replication fork to collapse, the chromosome end to be released and a DSB generated.

E. These DSBs are substrates for RecBCD which acts on the DSB ends to generate 3'-overhangs. RecA dependent synapsing at the nearest Chi sequence generates the recombination intermediate which can be resolved by RuvABC to restore the replication fork. MutL and MutS may act to prevent the RecA dependent synapsing of heterologous DNA sequences.

Alternatively, recognition of the O⁶meG:C or :T by MutS initiates repair. As the damage is located in the parental strand, repair is essentially futile (Fig 3.8C). This alternative model suggests repair will continue until the strand discrimination sequence is methylated preventing further repair attempts. In cells lacking Dam, these repair attempts are likely to be more persistent. This may lead to the generation of single-stranded regions of DNA. The replication fork of a subsequent round of replication may encounter such an incomplete repair patch leading to the collapse of the replication fork and the formation of a DSB (Fig 3.8D). DSBs generated by this mechanism or by simultaneous repair attempts on both strands are potential substrates for RecBCD and RecA dependent homologous recombination (Fig 3.8E). MutS or MutL may prevent the synapsing of heterologous sequences aborting repair. A second mutation in either the *mutL* or *mutS* gene restores resistance by preventing the repeated repair attempts of the O⁶meG:T/C pairs and thus, no DSBs would be generated. No evidence exists to support this futile cycling model but it is consistent with the properties of *dam* and *dam mutL/S E. coli*.

Cisplatin DNA damage can cause the replicative DNA polymerase to stall at the site of damage. Bypass, *in vitro*, of cisplatin DNA damage by *E. coli* DNA Pol I or Pol III is exceptionally poor (1,2{GG} 3.3 and 6%; 1,2{AG} 14 and 9%; 1,3{GCG} 27 and 4% (Comess *et al.*, 1992)). In recent years, several new polymerases involved in the replicative bypass of DNA damage have been identified. In *E. coli* these have been named Pol IV (*dinB*) and Pol V (UmuD'₂C). Synthesis past the adduct by either of these two polymerases could generate a suitable substrate for MMR (Fig 3.9A). Pol IV seems an unlikely candidate as its human homologue pol κ is unable to bypass cisplatin adducts *in vitro* (Ohashi *et al.*, 2000). Pol V on the other hand appears able to do so. Strains defective in Pol V are immutable by cisplatin (Fram *et al.*, 1985). The majority of mutations induced by cisplatin are single-base-pair substitutions occurring at putative 1,2{GG} or {AG} sites (Burnouf *et al.*, 1987). This would be consistent with Pol V bypass. Such bypassed adducts may be a suitable substrate for MMR. In mammalian cells, hMutS α is known to recognise 1,2{GG} intrastrand crosslinks (Duckett *et al.*, 1996). Recognition is improved when the 1,2{GG} adduct is opposite a mispair (Yamada *et al.*, 1997) which is what Pol V would generate. Repeated daughter strand repair attempts, as proposed for O⁶meG, could lead to the formation of DSBs. The involvement of Pol V in repair

synthesis is, however, not known. A second attempt at repair may lead to blockage of the polymerase by the DNA lesion which Pol V may not bypass. MMR may therefore have an alternative involvement in cisplatin toxicity.

An alternative explanation for the involvement of MMR in replication blockage by DNA damage has come from work by Seigneur *et al.* (Seigneur *et al.*, 1998). The stalled DNA polymerase allows the two newly synthesised daughter strands to isomerise and form a cruciform structure resembling a Holliday junction. This structure is bound by the RuvAB dimer leading to its stabilisation. Resolution by RuvC generates a DSB that again is a substrate for RecBCD and RecA dependent recombination (Fig 3.9B). MutS and MutL may again function by binding to and aborting heterologous recombination intermediates. Alternatively, MutS/L may bind the cisplatin damage in the isomerised strand thereby preventing the resolution.

The fact that loss of MMR only partially restores the resistance of *dam* strains to cisplatin suggests that *dam* mutations also contribute to cisplatin sensitivity independently of MMR. *Dam* mutants exhibit uncoordinated DNA replication initiation compared to wild type strains (Boye *et al.*, 1988). This uncoordinated DNA replication may inhibit repair attempts at collapsed replication forks due to the absence of a suitable substrate to recombine with.

In summary, the sensitivity of *dam* strains to cisplatin is partially restored by an additional mutation in either the *mutL* or *mutS* mismatch repair genes. Cisplatin resistant clones defective in mismatch repair could be isolated from *dam* strains. This suggests that loss of MMR function may be a significant, but not exclusive, mechanism by which drug naïve tumour cells may become resistant to cisplatin.

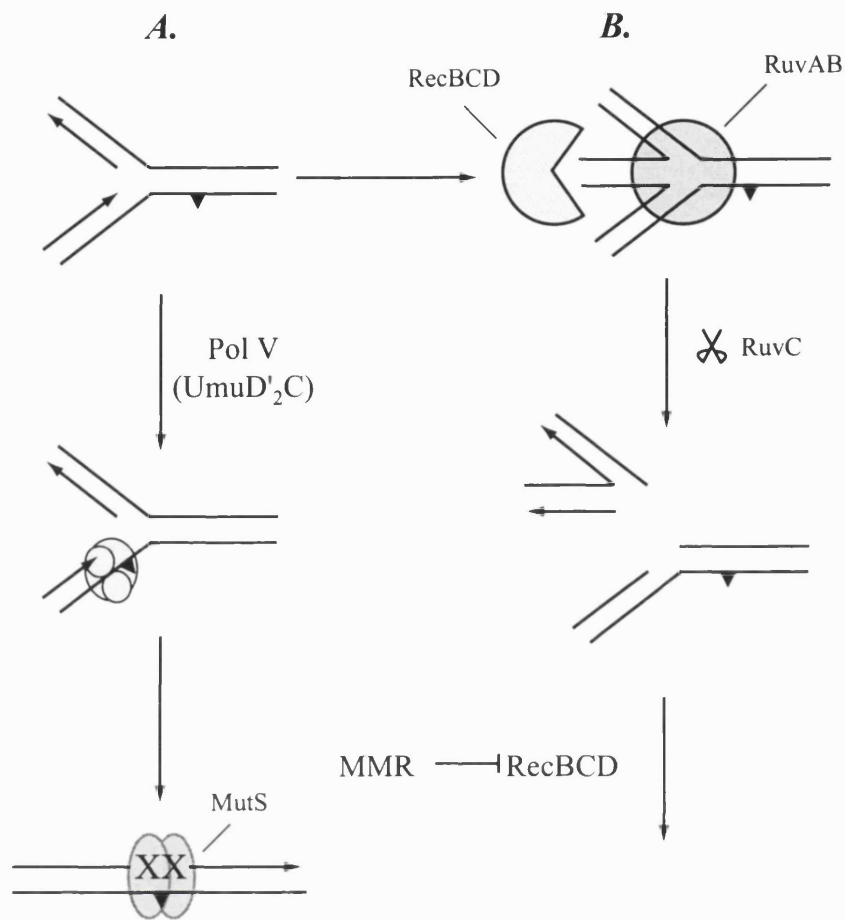


Figure 3.9 Origin of Double-strand Breaks Induced by Cisplatin-DNA Adducts

An advancing replication fork encounters a cisplatin adduct (▼) and stalls.

A. SOS-induction of Pol V ($umuD'_{2}C$) allows the mutagenic bypass of the adduct and the restart of DNA synthesis by Pol I. MutS may recognise the bypassed cisplatin adduct triggering the excision of the daughter strand and the regeneration of the stalled replication fork.

B. The two newly synthesised DNA strands isomerise to form a cruciform structure resembling a Holliday junction that is stabilised by RuvAB binding. There are two possible outcomes for this structure. RecBCD may act on the double-stranded end of the annealed strands to reform the stalled fork. Alternatively, the Holliday junction is resolved by RuvC to generate a DSB (only one conformation is shown).

As before, RecBCD and RecA act to restore the replication fork. MutS and MutL may again work by inhibiting the RecA dependent synapsing of heterologous DNA sequences or resolution by RuvC.

Chapter 4: Results II

Acquired Resistance to Cisplatin in the Ovarian Tumour Cell Line A2780

In the previous chapter, I reported that *Escherichia coli* defective in *dam* were sensitive to cisplatin. Cisplatin resistant clones could be generated from these strains and acquired resistance was associated with the loss of MMR function. This confirmed a previous report of the involvement of MMR in cisplatin sensitivity and further suggested that loss of MMR might be a mechanism by which human tumour cells become resistant to cisplatin.

Loss of MMR function has been demonstrated in human tumour cells selected for high levels of cisplatin resistance (Aebi *et al.*, 1996; Drummond *et al.*, 1996). However, these cell lines generally have multiple defects and the contribution of MMR deficiency to their overall resistance is not always clear. In particular, loss of MMR function and the associated mutator phenotype may provide a selective advantage to cisplatin treated cells by increased mutations in genes that modulate the drugs toxicity.

The ovarian carcinoma cell line A2780 is a commonly used model for the effects of cisplatin. I used A2780 cells to investigate whether MMR defects alone are likely to be a significant factor in cisplatin resistance.

Generation of Clonal Variants of A2780 Resistant to Cisplatin

The human ovarian carcinoma line A2780 harbours a sub-population of cells defective in both hMLH1 and p53. Previous studies using this cell line as a model system for acquired resistance to cisplatin may have selected for this pre-existing population (Anthony *et al.*, 1996; Behrens *et al.*, 1987; Drummond *et al.*, 1996). Of the clones isolated in one of these studies, those with a defect in hMLH1 also had an associated defect in the p53 damage response pathway (Anthony *et al.*, 1996; Brown *et al.*, 1997). Since inactivation of p53 function is an acknowledged

modulator of cisplatin resistance, it is not possible to separate the effects of MMR and p53 in these cells. In order to address this problem, a single cell clone was isolated (designated A2780-SCA5). A2780-SCA5 cells were confirmed to be proficient in both hMLH1 and p53 function. From this clone, resistant variants were selected by repeated exposure to cisplatin. Selection was performed shortly after SCA5 was established in order to minimise the possibility of generating an established sub-population of spontaneous variants. To mimic the selection procedures used to generate MMR deficient, methylation tolerant cells, highly toxic doses of cisplatin were used and exposure time kept to a minimum. This is in contrast to previous selection procedures. For example, the clone A2780-CP70 (Behrens *et al.*, 1987) was 39-times more resistant than the parental line and was isolated by repeated exposure to increasing concentrations of cisplatin over a period of 2 years. A2780-CP70 shows multiple mechanisms of cisplatin resistance. This probably, at least partly, reflects the treatment procedure employed. My selection protocol, I hoped, would minimise the generation of resistant clones through multiple pathways.

Two slightly different selection procedures were employed to generate cisplatin resistant clonal variants of A2780-SCA5. The first set of clones, CP1A to CP6A, were selected with 30 μ M cisplatin (about 0.1% survival) followed by two treatments each with 50 μ M (10^{-5} % survival) for 1 hour. Cells were allowed to recover and repopulate the flask after each treatment. CP7A to CP12A were generated in a similar fashion except the first cisplatin dose used was 10 μ M (10% survival) followed by 20 μ M, 30 μ M and finally two rounds of 50 μ M. Cells were allowed to recover between each treatment as before. After the final selection, single cell clones were isolated and expanded, and it was on these clones that the experiments were performed. All clones came from separate flasks and therefore can be regarded as independent. Similar protocols have been used to generate MMR defective methylation tolerant cells with 100% success rates (e.g. Aquilina *et al.*, 1990; Hampson *et al.*, 1997).

Cisplatin Resistance of A2780 Clonal Variants

The cisplatin sensitivity of a representative clone from each selection protocol (CP3A and CP7A) was determined by clonogenic survival. Both clones were moderately more resistant to cisplatin than the parental SCA5 cells (Fig 4.1A). For SCA5, the D_{37} value was $3.6\mu\text{M}$ and this increased to $5\mu\text{M}$ and $5.6\mu\text{M}$ in CP3A and CP7A respectively corresponding to a 1.4-fold and 1.6-fold increase in resistance. The sensitivity of two additional lines (CP5A and CP8A) was tested at a single dose of $20\mu\text{M}$. These two clones were more resistant than both the parental line SCA5 and the other two clones tested (Fig 4.1B). Their D_{37} values were estimated at $9.3\mu\text{M}$ and $10.8\mu\text{M}$, 2.6-fold and 3-fold higher than SCA5 respectively. The data are summarised in Table 4.1. The plating efficiency of the clones was similar to that of the parental cell. All the clones exhibited a somewhat increased rate of growth compared to SCA5 (data not shown). In conclusion, both of the selection protocols employed isolated clones with modest cisplatin resistance of between 1.4 and 3-fold compared to SCA5.

Table 4.1 Comparative Cytotoxicity in Cisplatin Resistant Clones

Clone	D_{37} (μM)	RF
SCA5	3.6	
CP3A	5.0	1.4
CP5A	9.3	2.6
CP7A	5.6	1.6
CP8A	10.8	3.0

D_{37} values (the dose of cisplatin required to kill 37% of the cells) were estimated from straight line plots.

RF = fold resistance compared to the wild type.

Previous protocols designed to select for cisplatin resistant variants have selected for clones with multiple changes including inactivation of hMLH1 and p53. I analysed whether my selected cisplatin resistant clonal variants were also deficient for these two functions.

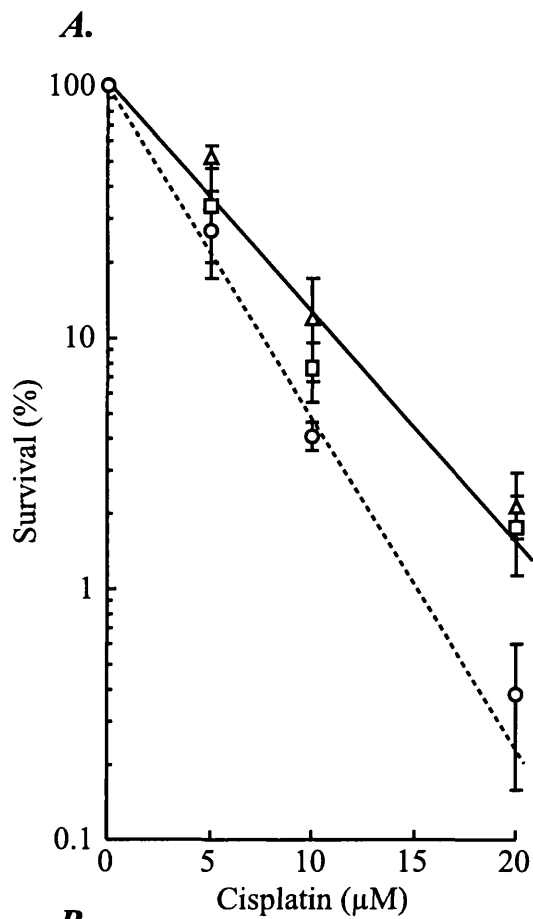
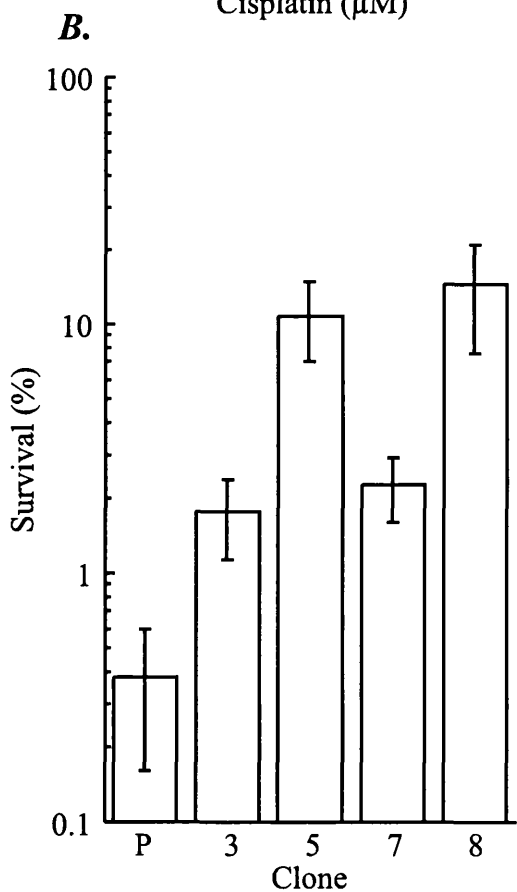


Figure 4.1 Cisplatin Cytotoxicity in A2780 Clonal Variants

A. Parental cell, SCA5 (○) or cisplatin selected clonal variants CP3A (□) or CP7A (△) were treated for 60 min with cisplatin at the concentrations indicated in complete media supplemented with 10% FCS. This was then replaced with fresh, drug-free media containing 10% FCS. After 10 days, surviving colonies were stained and counted.

B. SCA5, CP3A, CP5A, CP7A or CP8A cells were treated with 20 μM cisplatin for 60 min and survival determined as above. The value represents the mean of three independent experiments plus or minus the standard error.



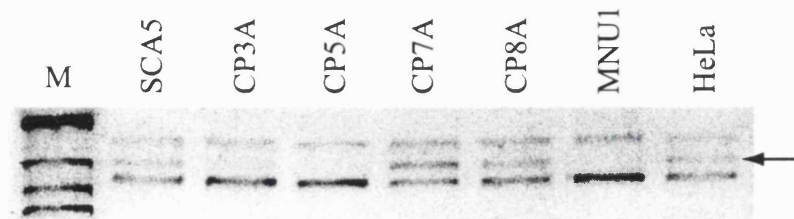
Mismatch Repair Status of Clonal Variants

Mismatch repair status was determined using an *in vitro* assay described previously (Hampson *et al.*, 1997). Extracts from the parental cells SCA5 and three of the clonal variants tested (CP3A, CP7A and CP8A) were proficient in the repair of a T/C mismatch (Fig 4.2A). A previously described clonal variant of A2780, A2780-MNU1 has no demonstrable hMLH1 expression (Branch *et al.*, 2000) and this variant demonstrated no T/C mismatch correction in the repair assay. In addition, one of the isolated variants, CP5A appeared deficient in T/C repair. Three of the four cisplatin-selected clonal variants were therefore clearly proficient for mismatch repair and were comparable to the parental SCA5 cells in this regard. Analysis of the expression of the four major MMR proteins (hMSH2, hMSH6, hMLH1 and hPMS2) was determined by western blotting. All twelve of the cisplatin resistant clonal variants, including the three representatives that were MMR proficient by the *in vitro* assay, showed similar levels of expression of all four proteins to that of the parental line (Fig 4.2B). Lower levels of hMSH6 was observed in clones CP3A, CP4A and CP5A. This was not reproducible and was most likely due to reduced protein transfer during the blotting procedure. Loss of expression of the MMR proteins, especially hMLH1 is associated with acquired resistance to cisplatin. As no difference in the expression of the MMR proteins in CP5A was observed compared to the other clones, it seems likely that this clone may also be proficient in MMR. These cells were still sensitive to S⁶G indicative of functional MMR. This could be further confirmed by checking their sensitivity to MNU. The presence of *in vitro* mismatch correction and expression of all four MMR proteins suggests that all twelve clones are likely to be proficient for mismatch repair.

p53 Response in Cisplatin-resistant Variants

The p53 response of each cisplatin resistant clone was tested after exposure to the drug. Cisplatin elicited a strong induction of p53 in all the clones except CP3A, CP7A and CP10A which showed little increase above the basal level as determined by western blotting (Fig 4.3A). The same treatment also induced expression of p21 in a p53 dependent fashion. In addition to CP3A, CP7A and CP10A, p21 induction was absent or reduced in CP5A, CP8A and CP12A (Fig 4.3B).

A.



B.

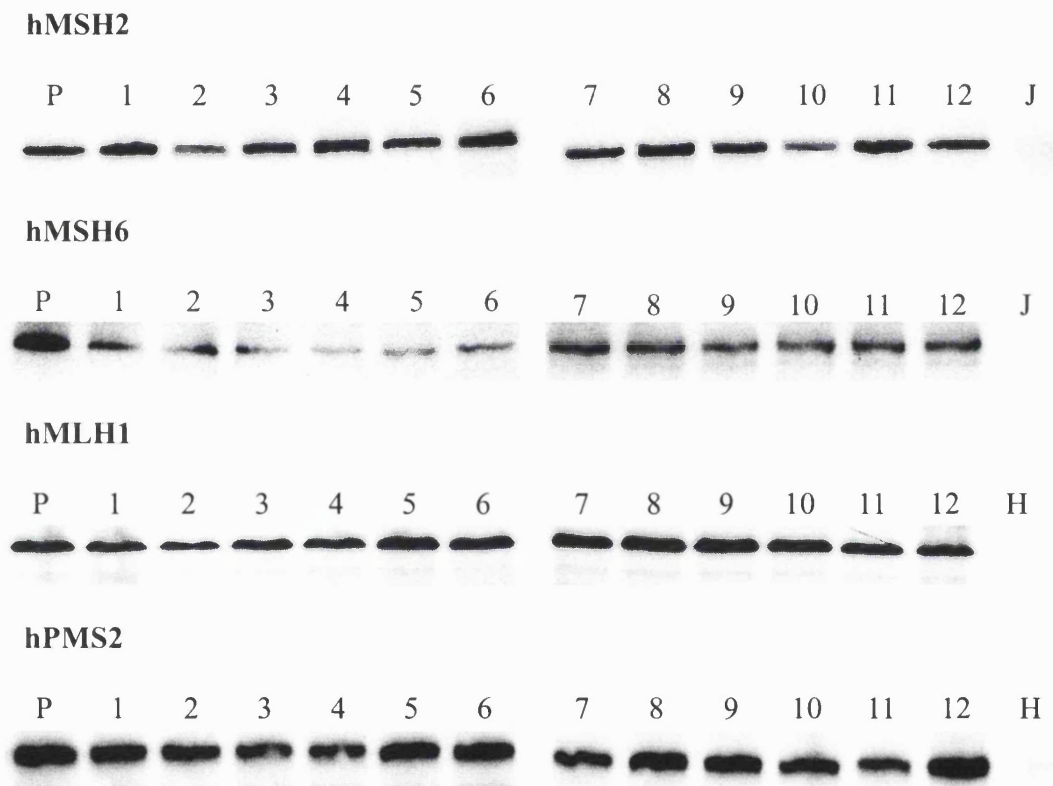


Figure 4.2 Analysis of Mismatch Repair Function

A. Mismatch repair by extracts from cisplatin resistant clones. 150 μ g of extract prepared from A2780-SCA5, CP3A, CP5A, CP7A, CP8A and MNU1 were assayed for the ability to correct a T/C mismatch and restore an *Mlu*I restriction endonuclease site in a standard nicked circular duplex substrate. Following incubation of substrate and extract, DNA was digested with *Mlu*I and the products analysed on a 0.8% agarose gel in the presence of ethidium bromide. The arrowed band corresponds to molecules in which the mismatch has been corrected.

This experiment was carried out by P. Macpherson.

B. Western blot analysis of mismatch repair proteins. Cell extracts were separated on an 8% SDS-PAGE gel, transferred to a PVDF membrane and probed with anti-hMSH2, anti-hMSH6, anti-hMLH1 or anti-hPMS2 antibodies. Immunoreactive proteins were detected using an ECL-detection system as described in materials and methods.

P = SCA5; 1-12 = CP1A to CP12A; J = Jurkat; H = HCT116

CP4A expressed a truncated form of p53. This appears however, to remain functional as p21 induction by cisplatin in CP4A was comparable to that of the parental line with full length p53. From this analysis of p53 and p21 induction after treatment with cisplatin, p53/p21 defects appear to be quite frequent among the cisplatin resistant clones. At least three different phenotypic groups of clones were identified. Group 1 (CP3A, 7A and 12A): severely reduced p53 and p21 induction. Group 2 (CP5A, 8A and 12A): normal p53 response but an abrogated p21 response. Group 3 (CP1A, 2A, 4A, 6A, 9A and 11A): p53 and p21 are induced at comparable levels to the parental line.

Group 1 (Reduced p53 and p21 Induction)

In order to examine whether the p53 induction defect of this group extended to other forms of DNA damage, p53 levels were examined after IR or UV treatment using CP7A as a representative. After treatment with either IR or UV, p53 levels in CP7A were markedly increased and were comparable to those in the parental line SCA5 after similar treatment (Fig 4.4A). This experiment also confirmed the minimal increase in the level of p53 after exposure to cisplatin. This suggests that the response of p53 to some forms of DNA damage in these cells is normal. Analysis of the p53 response to cisplatin in a dose dependent fashion indicates that the p53 response in CP3A and CP7A is attenuated rather than absent (Fig 4.4B). In CP3A, treatment with 20 μ M cisplatin induced p53 to a similar extent as treatment of the parental line (SCA5) with 10 μ M. For CP7A, the cisplatin concentration required to produce the same levels of induction was higher still; about 30-40 μ M. I therefore considered the possibility that the mechanism of cisplatin resistance in these lines is some form of protective mechanism that leads to reduced DNA damage (see later).

Group 2 (Normal p53 Response but Abrogated p21)

CP5A, CP8A and CP12A retain an apparently normal p53 response but show an abrogated p53-dependent p21 response to cisplatin. p53 also controls the levels of MDM2 and Bax after DNA damage. MDM2 and Bax induction after treatment with cisplatin was therefore determined. Induction of MDM2 after cisplatin was comparable in all the clones tested including CP5A, 8A and 12A (Fig 4.5A) and was similar to that in the parental SCA5 cells. The data for Bax induction were less clear. A small increase in Bax expression after cisplatin treatment was observed in SCA5,

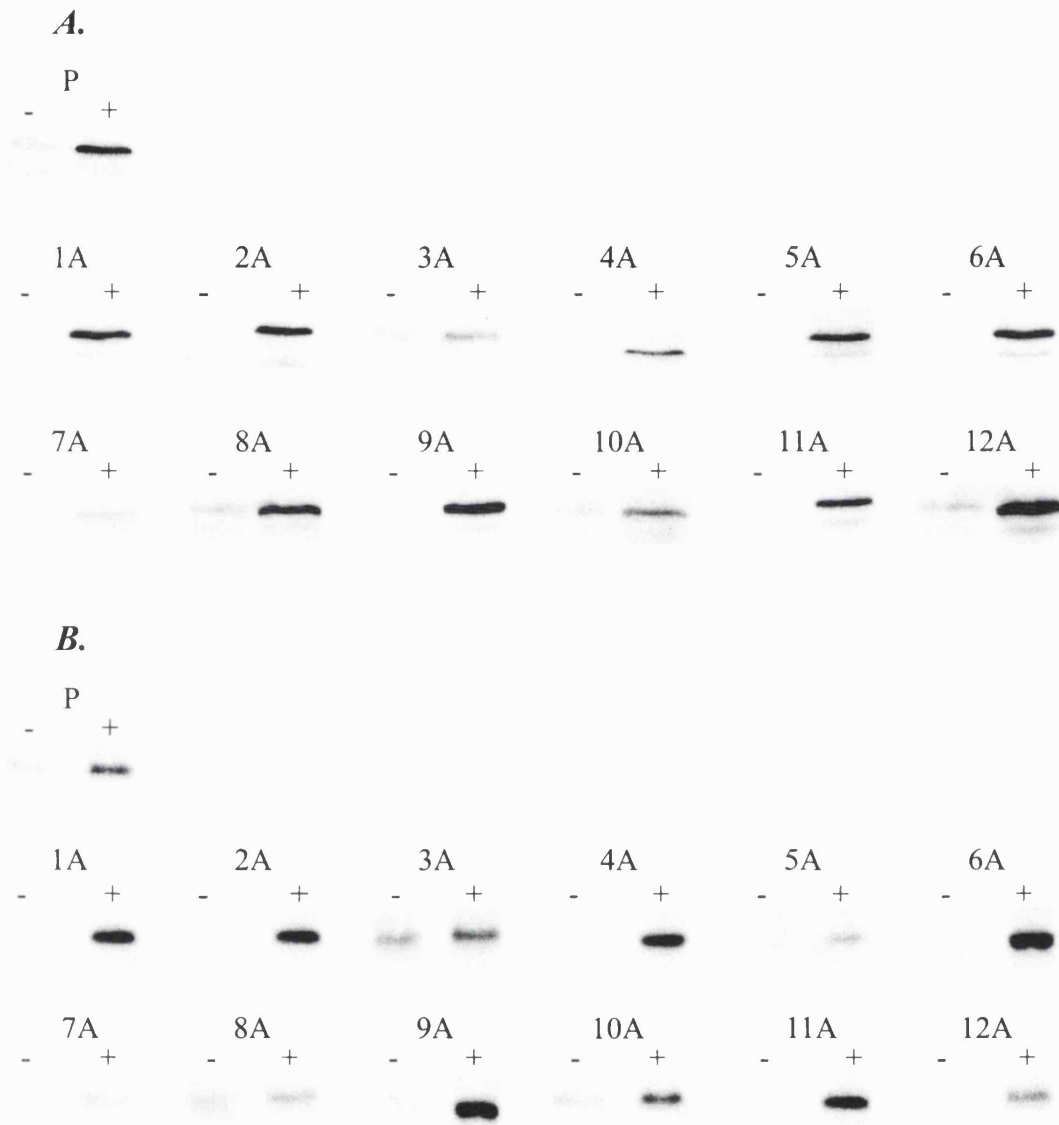


Figure 4.3 Analysis of p53 and p21 Levels After Induction With Cisplatin

Exponentially growing cell cultures were treated without (-) or with (+) 30 μ M cisplatin for 60 min, the drug was then removed and cells grown for a further 24h in drug-free medium before extracts were made. Extracts were separated on either a 10% or 12% SDS-PAGE gel, transferred to PVDF membranes and probed with either anti-p53 (A) or anti-p21 (B) antibodies.

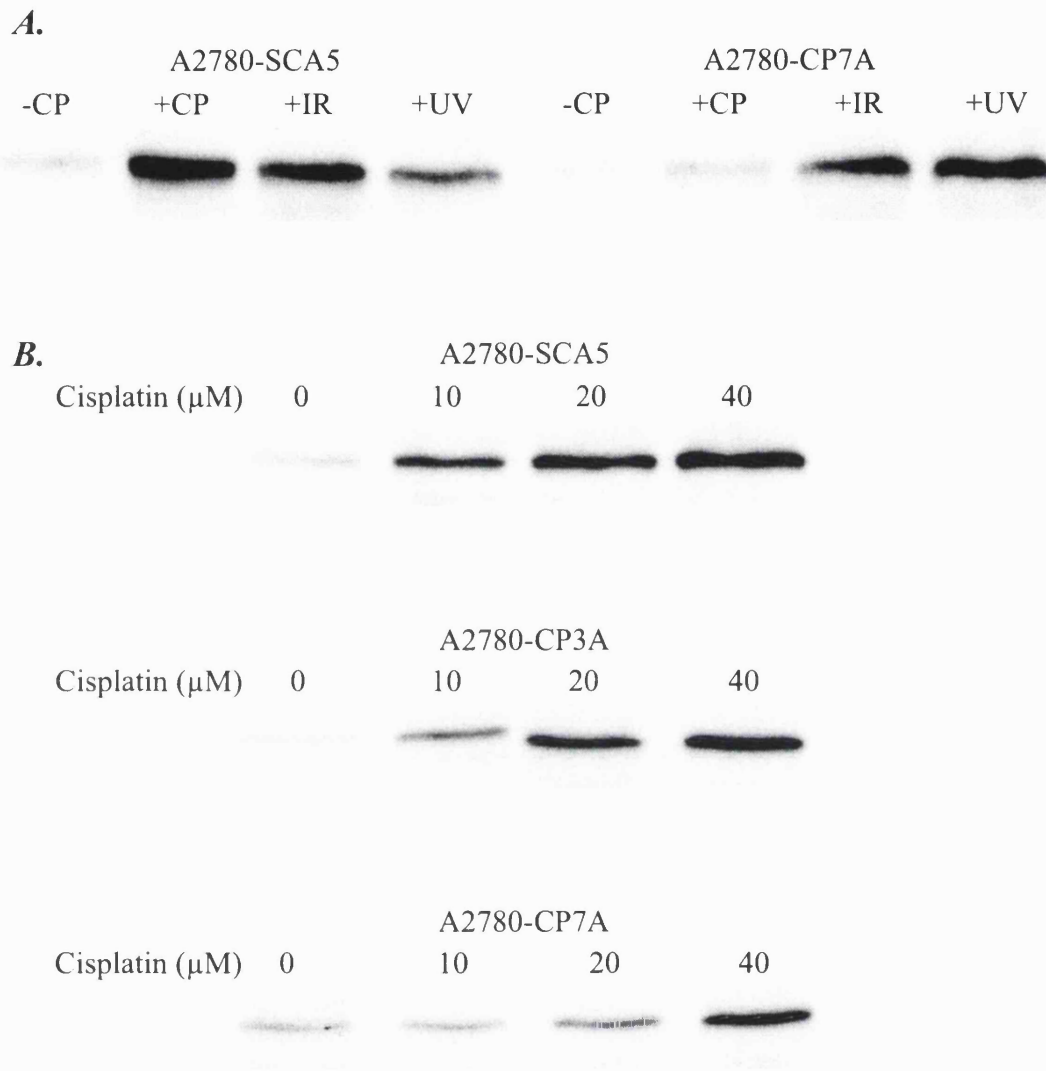


Figure 4.4 p53 Induction in CP3A and CP7A by Different Forms of DNA Damage

A. Cells were treated with cisplatin as before or with 5Gy IR or 20J/m² UVC and harvested 7h after irradiation. Extracts were separated and probed for p53 expression as before.

B. SCA5, CP3A or CP7A cells were treated with 0, 10, 20 or 40 μ M cisplatin for 60 min and cells harvested after 24h as before. Extracts were separated by SDS-PAGE and probed for p53 expression as before.

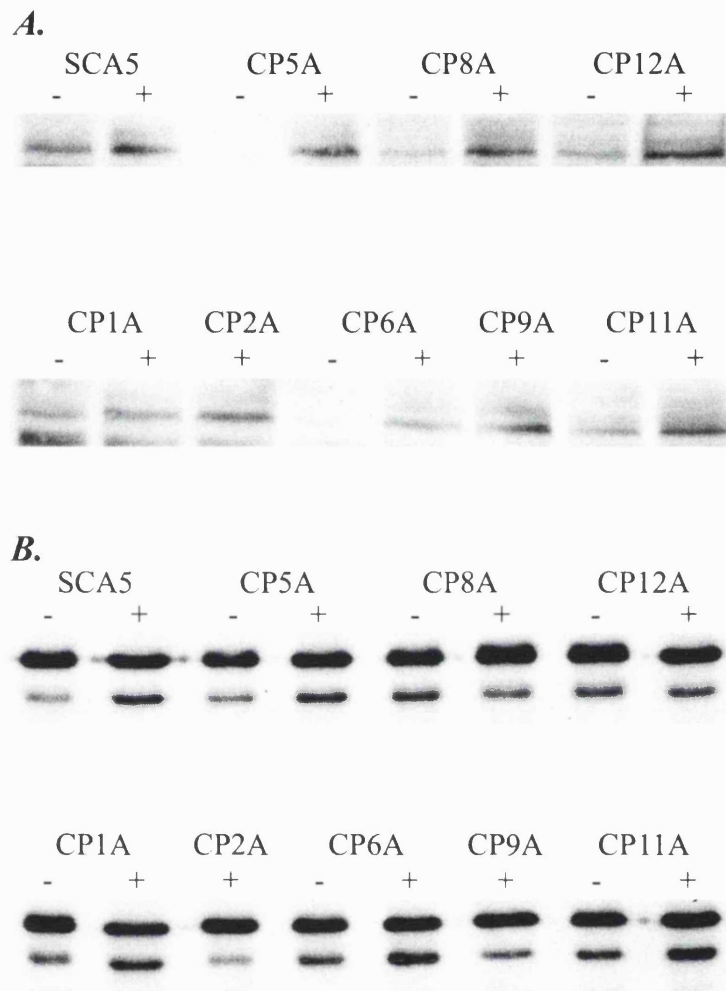


Figure 4.5 Downstream Targets of p53 - Induction of MDM2 and Bax by Cisplatin

Extracts from cisplatin treated cells (30 μ M, 60 min) were separated on 8% (MDM2) or 12% (Bax) SDS-PAGE and transferred to PVDF membranes as before. Membranes were probed with either anti-MDM2 (*A*) or anti-Bax (*B*) antibodies and detected as before.

Three protein isoforms of Bax have been identified: Bax- α (21KDa), - β (24KDa) and - γ (5KDa). The upper band most likely represents Bax- β and the lower band Bax- α .

CP5A, CP1A, CP6A and CP11A but levels were apparently unchanged in CP2A, CP8A, CP9A and CP12A. Constitutive levels of Bax expression (without cisplatin treatment) were high in all the samples making it difficult to be certain that the Bax response was not functional in CP2A, CP8A, CP9A and CP12A. Overall, in view of the apparently normal MDM2 response, it seems reasonable to conclude that there is not a general defect in induction of p53-dependent downstream targets in this group.

Mutations in the p53 Gene

The majority of reported p53 mutations lie in the DNA binding domain between amino acids 100 and 300. This corresponds to exons 4 through to 8 of the p53 gene. In addition, exons 2, 3 and 4 code for the N-terminus transactivation domain which contains several phosphorylation sites thought to be important for p53 activation following DNA damage. Genomic DNA sequencing of the p53 gene was employed to investigate whether the p53 / p21 induction defects observed in Groups 1 and 2 (CP3A, CP5A, CP7A, CP8A, CP10A and CP12A) were due to mutations in p53.

Some p53 mutations are dominant negative (such as the one in A2780-CP70, P. Karran unpublished) and may be missed by cDNA sequencing. The individual exons were therefore directly amplified from genomic DNA by PCR. An example of the PCR products obtained is shown in Fig 4.6. Due to the small size of the introns between exons 2, 3 and 4, exons 2 to 4 were amplified and sequenced as a single PCR product.

PCR products were purified and sequenced using the ABI BigDye terminator cycle sequencing kit and an ABI Prism 377 automatic sequencer (ICRF Equipment Park, L.I.F.). The data generated was analysed using the software ClustalX to compare the generated sequences against the published p53 sequence (NCBI PubMed Nucleotide database). An example of the data generated for SCA5, CP3A and CP5A is shown in Fig 4.7. No mutations in any of the seven exons analysed were found in CP3A, CP5A, CP7A, CP8A, CP10A or CP12A. This indicates that the defects observed in either p53 or p21 induction after cisplatin treatment and cisplatin resistance were not a consequence of mutated p53.

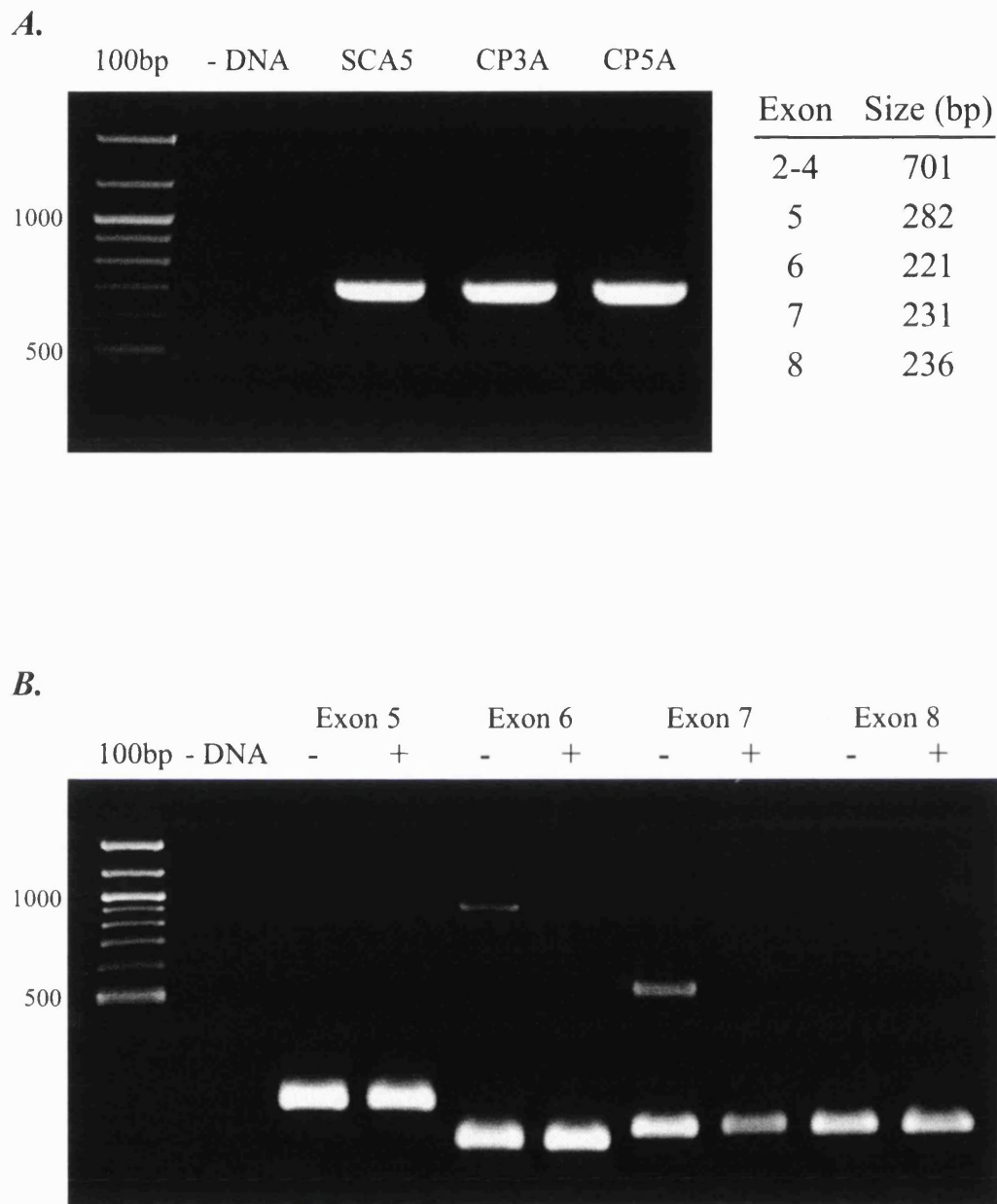


Figure 4.6 PCR Amplification of the *p53* Gene

Genomic DNA from exponentially growing cells was prepared using a DNeasy Tissue Kit according to the manufacturers instructions. Exons 2 to 4 (A) or exons 5, 6, 7 or 8 (B) were amplified using exon specific primers and HotStar Taq in a thermal cycler. Exons 5 to 8 were amplified in the absence (-) or presence (+) of the primer melting point modifier Q-solution. Primers were removed using a QIAquick PCR purification kit, PCR products separated on 1.5% agarose gel and visualised after EtBr staining.

Exon 2

Exon2 CAGCCAGACTGCCTTCCGGGTCAGTCCATGGAGGAGCC
SCA5 CAGCCAGACTGCCTTCCGGGTCAGTCCATGGAGGAGCC
CP3A CAGCCAGACTGCCTTCCGGGTCAGTCCATGGAGGAGCC
CP5A CAGCCAGACTGCCTTCCGGGTCAGTCCATGGAGGAGCC

Exon2 GCAGTCAGATCCTAGCGTCGAGCCCCCTCTGAGTCAGGAAACATTTTCAGACCTATGGAA
SCA5 GCAGTCAGATCCTAGCGTCGAGCCCCCTCTGAGTCAGGAAACATTTTCAGACCTATGGAA
CP3A GCAGTCAGATCCTAGCGTCGAGCCCCCTCTGAGTCAGGAAACATTTTCAGACCTATGGAA
CP5A GCAGTCAGATCCTAGCGTCGAGCCCCCTCTGAGTCAGGAAACATTTTCAGACCTATGGAA

Exon2 ACT
SCA5 ACT
CP3A ACT
CP5A ACT

Exon 3

Exon3 ACTTCCTGAAAACAACGTTCTG
SCA5 ACTTCCTGAAAACAACGTTCTG
CP3A ACTTCCTGAAAACAACGTTCTG
CP5A ACTTCCTGAAAACAACGTTCTG

Exon 4

Exon4 TCCCCCTTGCCGTCCCAA
SCA5 TCCCCCTTGCCGTCCCAA
CP3A TCCCCCTTGCCGTCCCAA
CP5A TCCCCCTTGCCGTCCCAA

Exon4 GCAATGGATGATTTGATGCTGTCCCCGGACGATATTGAACAATGGTTCAGTGAAGACCCA
SCA5 GCAATGGATGATTTGATGCTGTCCCCGGACGATATTGAACAATGGTTCAGTGAAGACCCA
CP3A GCAATGGATGATTTGATGCTGTCCCCGGACGATATTGAACAATGGTTCAGTGAAGACCCA
CP5A GCAATGGATGATTTGATGCTGTCCCCGGACGATATTGAACAATGGTTCAGTGAAGACCCA

Exon4 GGTCCAGATGAAGCTCCCAGAATGCCAGAGGCTGCTCCCGCGCTGGGCCCTGCACCAGCA
SCA5 GGTCCAGATGAAGCTCCCAGAATGCCAGAGGCTGCTCCCGCCCTGGGCCCTGCACCAGCA
CP3A GGTCCAGATGAAGCTCCCAGAATGCCAGAGGCTGCTCCCGCCCTGGGCCCTGCACCAGCA
CP5A GGTCCAGATGAAGCTCCCAGAATGCCAGAGGCTGCTCCCGCCCTGGGCCCTGCACCAGCA

Codon 72

Exon4 GTCCTACACCGGCGGCCCTGCACCAGCCCCCTCCTGGCCCCCTGTCATCTTCTGTCCCT
SCA5 GTCCTACACCGGCGGCCCTGCACCAGCCCCCTCCTGGCCCCCTGTCATCTTCTGTCCCT
CP3A GTCCTACACCGGCGGCCCTGCACCAGCCCCCTCCTGGCCCCCTGTCATCTTCTGTCCCT
CP5A GTCCTACACCGGCGGCCCTGCACCAGCCCCCTCCTGGCCCCCTGTCATCTTCTGTCCCT

Exon4 TCCCAGAAAACCTACCAGGGCAGCTACGGTTTCCGTCTGGGCTTCTTGCACTTCTGGGACA
SCA5 TCCCAGAAAACCTACCAGGGCAGCTACGGTTTCCGTCTGGGCTTCTTGCACTTCTGGGACA
CP3A TCCCAGAAAACCTACCAGGGCAGCTACGGTTTCCGTCTGGGCTTCTTGCACTTCTGGGACA
CP5A TCCCAGAAAACCTACCAGGGCAGCTACGGTTTCCGTCTGGGCTTCTTGCACTTCTGGGACA

Exon4 GCCAAGTCTGTGACTTGCACG
SCA5 GCCAAGTCTGTGACTTGCACG
CP3A GCCAAGTCTGTGACTTGCACG
CP5A GCCAAGTCTGTGACTTGCACG

Exon 5

Exon5 TACTCCCCTGCCCTCA
SCA5 TACTCCCCTGCCCTCA
CP3A TACTCCCCTGCCCTCA
CP7A TACTCCCCTGCCCTCA

Exon5 ACAAGATGTTTTGCCAACTGGCCAAGACCTGCCCTGTGCAGCTGTGGGTTGATTCCACAC
SCA5 ACAAGATGTTTTGCCAACTGGCCAAGACCTGCCCTGTGCAGCTGTGGGTTGATTCCACAC
CP3A ACAAGATGTTTTGCCAACTGGCCAAGACCTGCCCTGTGCAGCTGTGGGTTGATTCCACAC
CP7A ACAAGATGTTTTGCCAACTGGCCAAGACCTGCCCTGTGCAGCTGTGGGTTGATTCCACAC

Exon5 CCCCGCCCGGCACCCGCGTCCGCGCCATGGCCATCTACAAGCAGTCACAGCACATGACGG
SCA5 CCCCGCCCGGCACCCGCGTCCGCGCCATGGCCATCTACAAGCAGTCACAGCACATGACGG
CP3A CCCCGCCCGGCACCCGCGTCCGCGCCATGGCCATCTACAAGCAGTCACAGCACATGACGG
CP7A CCCCGCCCGGCACCCGCGTCCGCGCCATGGCCATCTACAAGCAGTCACAGCACATGACGG

Exon5 AGGTTGTGAGGCGCTGCCCCACCATGAGCGCTGCTCAGATAGCGATG
SCA5 AGGTTGTGAGGCGCTGCCCCACCATGAGCGCTGCTCAGATAGCGATG
CP3A AGGTTGTGAGGCGCTGCCCCACCATGAGCGCTGCTCAGATAGCGATG
CP7A AGGTTGTGAGGCGCTGCCCCACCATGAGCGCTGCTCAGATAGCGATG

Exon 6

Exon6 GTCTGGCCCCCTCCTCAGCATCTTA
SCA5 GTCTGGCCCCCTCCTCAGCATCTTA
CP3A GTCTGGCCCCCTCCTCAGCATCTTA
CP7A GTCTGGCCCCCTCCTCAGCATCTTA

Exon6 TCCGAGTGGAAGGAAATTTGCGTGTGGAGTATTTGGATGACAGAAACACTTTTCGACATA
SCA5 TCCGAGTGGAAGGAAATTTGCGTGTGGAGTATTTGGATGACAGAAACACTTTTCGACATA
CP3A TCCGAGTGGAAGGAAATTTGCGTGTGGAGTATTTGGATGACAGAAACACTTTTCGACATA
CP7A TCCGAGTGGAAGGAAATTTGCGTGTGGAGTATTTGGATGACAGAAACACTTTTCGACATA

Exon6 GTGTGGTGGTGCCCTATGAGCCGCCTGAG
SCA5 GTGTGGTGGTGCCCTATGAGCCGCCTGAG
CP3A GTGTGGTGGTGCCCTATGAGCCGCCTGAG
CP7A GTGTGGTGGTGCCCTATGAGCCGCCTGAG

Exon 7

Exon7 GTTGGCTCTGACTGTACCACCATC
SCA5 GTTGGCTCTGACTGTACCACCATC
CP3A GTTGGCTCTGACTGTACCACCATC
CP5A GTTGGCTCTGACTGTACCACCATC

Exon7 CACTACAAC TACATGTGTAACAGTT CCTGCATGGGCGGCATGAACCGGAGGCCCATCCTC
 SCA5 CACTACAAC TACATGTGTAACAGTT CCTGCATGGGCGGCATGAACCGGAGGCCCATCCTC
 CP3A CACTACAAC TACATGTGTAACAGTT CCTGCATGGGCGGCATGAACCGGAGGCCCATCCTC
 CP5A CACTACAAC TACATGTGTAACAGTT CCTGCATGGGCGGCATGAACCGGAGGCCCATCCTC

Exon7 ACCATCATCACACTGGAAGACTCCAG
 SCA5 ACCATCATCACACTGGAAGACTCCAG
 CP3A ACCATCATCACACTGGAAGACTCCAG
 CP5A ACCATCATCACACTGGAAGACTCCAG

Exon 8

Exon8 TGGTAATCTACTGGGACGGAACAGCTT
 SCA5 TGGTAATCTACTGGGACGGAACAGCTT
 CP3A TGGTAATCTACTGGGACGGAACAGCTT
 CP5A TGGTAATCTACTGGGACGGAACAGCTT

Exon8 TGAGGTGCGTGTTTGTGCCTGTCCTGGGAGAGACCGGCGCACAGAGGAAGAGAATCTCCG
 SCA5 TGAGGTGCGTGTTTGTGCCTGTCCTGGGAGAGACCGGCGCACAGAGGAAGAGAATCTCCG
 CP3A TGAGGTGCGTGTTTGTGCCTGTCCTGGGAGAGACCGGCGCACAGAGGAAGAGAATCTCCG
 CP5A TGAGGTGCGTGTTTGTGCCTGTCCTGGGAGAGACCGGCGCACAGAGGAAGAGAATCTCCG

Exon8 CAAGAAAGGGGAGCCTCACCACGAGCTGCCCCAGGGAGCACTAAGCGAG
 SCA5 CAAGAAAGGGGAGCCTCACCACGAGCTGCCCCAGGGAGCACTAAGCGAG
 CP3A CAAGAAAGGGGAGCCTCACCACGAGCTGCCCCAGGGAGCACTAAGCGAG
 CP5A CAAGAAAGGGGAGCCTCACCACGAGCTGCCCCAGGGAGCACTAAGCGAG

Figure 4.7 Direct Genomic Sequencing of p53

20ng of PCR product was sequenced using the ABI Prism BigDye Terminator cycle sequencing ready reaction kit according to the manufacturers instructions. Extension products were purified using Centri-sep spin columns and loaded onto an ABI Prism 377 automatic sequencer. Sequence data was analysed using ClustalX software. An example of the data produced is shown for SCA5, CP3A and CP5A. The top line (Exon *n*) represents the published DNA sequence for p53 from the NCBI PubMed Nucleotide database.

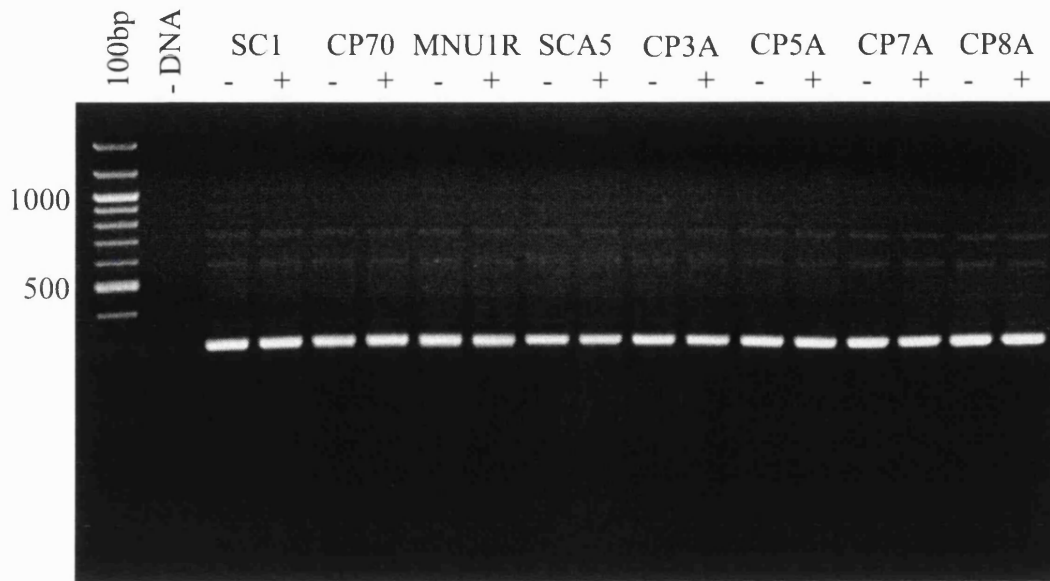
Codon 72 Polymorphisms and Cisplatin Resistance

The p73 protein is a close homologue of p53 and may activate p53-responsive promoters and induce apoptosis after cisplatin treatment (Gong *et al.*, 1999). Some tumour derived p53 mutants can bind to and inactivate p73 function. The binding of such mutants to p73 is dependent on whether codon 72 (in exon 4) of p53 encodes Arg or Pro. The ability of mutant p53 to bind and neutralise p73 is enhanced when codon 72 encodes Arg (Marin *et al.*, 2000). From my sequencing data, it appears that the parental line and all the resistant clones are Pro / Pro. This was analysed more closely using restriction enzyme digestion of PCR amplified exon 4 and compared to other A2780 clonal variants harbouring known p53 mutations. Alleles that harbour the Pro polymorphism (CCC) at codon 72 are resistant to *BstUI* digestion. Arg polymorphisms (CGC) are not. All the clonal variants analysed were homozygous for Pro at codon 72 including A2780-CP70 and A2780-MNU1 which contain mutant p53 (Fig 4.8). The p53 defects do not reflect the presence of an altered codon 72 in the cisplatin resistant variants.

DNA Platination Levels in A2780 Clonal Variants

Protective mechanisms that prevent the reaction of cisplatin with DNA are an acknowledged contributor to cisplatin resistance. As the p53 response was attenuated in cisplatin resistant variants from group 2, this seemed a likely mechanism of resistance. Exponentially growing cell cultures were treated for 2 hours with increasing concentrations of cisplatin and DNA extracted.

DNA platinum levels were determined by Atomic Absorption Spectroscopy (AAS) by Dr. Ciaran O'Neill, ICR, Sutton, UK. Platination levels were plotted as a function of cisplatin concentration (Fig 4.9). Dose responses were approximately linear and significant differences were identified between the different clones. The slope of the line gives the amount of platination per mg DNA per μM cisplatin per hour. The results are also summarised in Table 4.2.



*Bst*UI Recognition sequence

CG[↓]CG cuts if Arg

Codon 72

C[□]CGC[□]GT Arg

C[□]CCC[□]GT Pro

Figure 4.8 Analysis of the Codon 72 Polymorphism in A2780 Clonal Variants

Exon 4 was amplified from genomic DNA as described previously to generate a 298bp fragment. Approximately 200ng of purified PCR product was digested with (+) or without (-) 5U of *Bst*UI at 60°C for 2 hours. Products were then separated on a 1.8% agarose gel and visualised by EtBr staining.

Table 4.2 DNA Platination Levels in A2780 Clonal Variants

Clone	ng Pt / mg DNA / μ M CP / hr	RPt	RF
SCA5	1.6		
CP3A	1.2	0.7	1.4
CP5A	1.9	1.2	2.6
CP7A	0.9	0.7	1.6
CP8A	2.0	1.2	3.0

DNA platination levels were determined from the slope of plots of cisplatin concentration vs. DNA platination in Fig 4.9.

RPt = level of DNA platination compared to the parental SCA5 cells.

RF = fold resistance by clonal survival compared to SCA5

Both CP3A and CP7A exhibit reduced levels (around 70%) of DNA platination compared to the parental line SCA5. This correlates with their increased cisplatin resistance. CP7A was slightly more resistant than CP3A (Table 4.1) and shows the lowest level of DNA platination. This is consistent with the existence of protective mechanisms in CP3A and CP7A that reduces the levels of cisplatin reaction with DNA. This protective mechanism in Group 1 variants was inferred from the p53 / p21 studies described in Fig 4.3. In contrast, CP5A and CP8A do not exhibit levels of DNA platination less than the parental line and the mechanism of platinum resistance in these lines is most likely different.

GSH, A Protective Mechanism Against DNA Damage Induced by Cisplatin

Attempts were made to try to identify the cellular mechanism behind the reduced levels of DNA platinum damage induced by cisplatin treatment in CP3A and CP7A. Reduced glutathione (GSH) can modify the reaction of cisplatin with DNA. This occurs by the direct reaction of the intracellular, aquated cisplatin with the cysteine moiety of the GSH molecule. An increased cellular level of GSH is a common factor associated with resistance to cisplatin (Godwin *et al.*, 1992; Mistry *et al.*, 1991). GSH levels before and after treatment with cisplatin were determined in the parental clone SCA5 and four of the cisplatin resistant variants CP3A, CP5A, CP7A and

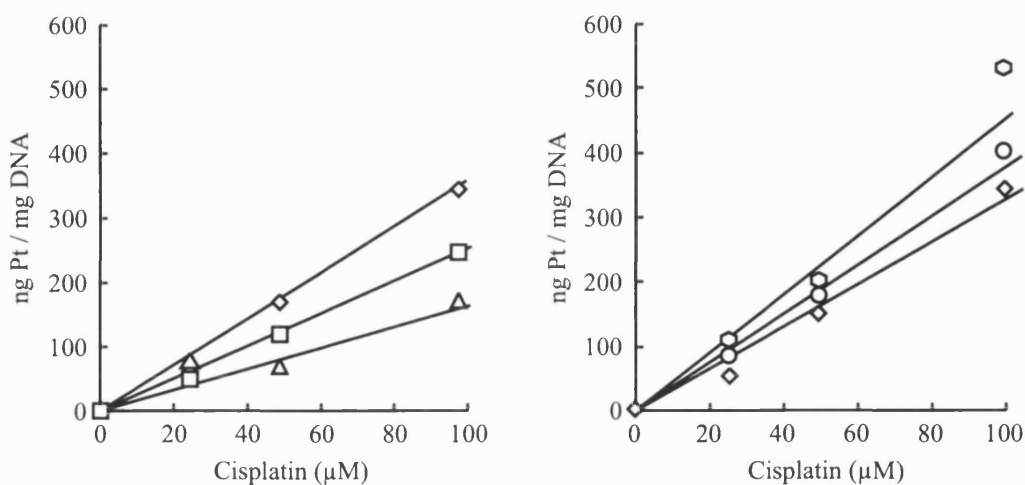


Figure 4.9 Determination of DNA-Platinum Levels After Treatment With Cisplatin

About 10^8 SCA5 (\diamond), CP3A (\square), CP5A (\circ), CP7A (\triangle) or CP8A (\circ) cells were treated with 0, 25, 50 or $100\mu\text{M}$ cisplatin for 2 hours. Cells were harvested and genomic DNA prepared and hydrolysed in 0.2% nitric acid at 37°C for 18 hours. DNA platination levels were determined by atomic absorption spectroscopy by C. O'Neill at the ICR, Sutton, UK.

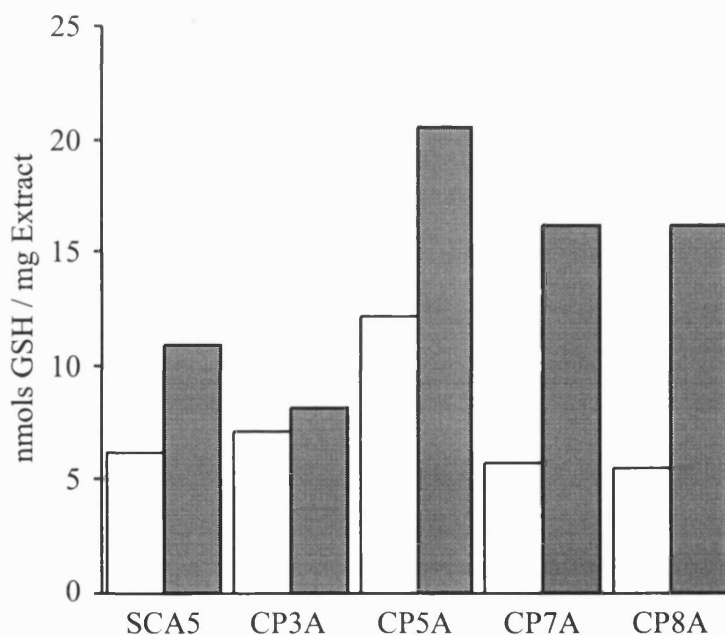


Figure 4.10 GSH Levels in A2780 Clonal Variants Before and After Cisplatin Treatment

Reduced glutathione levels were determined according to the modified enzyme recycling method (Akerboom *et al.*, 1981). The amount of GSH in sonicated cell extracts before (\square) or after (\blacksquare) treatment with $30\mu\text{M}$ cisplatin for 24 hours was determined from a standard curve generated with known concentrations of GSH.

CP8A. Cisplatin treatment caused an increase in cellular GSH levels in all five clones (Fig 4.10). Increased levels of GSH was observed in CP5A, CP7A and CP8A after cisplatin treatment compared to the parental SCA5 cells. No difference was observed between CP3A and SCA5. No correlation between cellular GSH levels after cisplatin treatment, DNA platination levels or cell survival were observed (Table 4.2). This suggests, that in CP3A at least, increases in glutathione levels are not responsible for the decreased levels of DNA platination.

Cell Cycle Analysis of A2780 Clonal Variants After Cisplatin Treatment

After treatment with cisplatin, human cells arrest at the G2/M transition. The effect of cisplatin on my cisplatin resistant variants was determined using propidium iodide staining and FlowJo software (Dean Jett Fox algorithms, D. Davies, ICRF FACs laboratory) to determine the proportion of cells in each stage of the cell cycle. In SCA5, treatment with 30 μ M cisplatin for one hour caused efficient arrest of the cells at the G2/M boundary after 24 hours and the cells remained in this arrested state for at least 48 hours (Fig 4.11). Group 1 variants (including CP3A and CP7A) exhibit a pattern of arrest similar to the parental SCA5 cells. In Group 2 variants (including CP5A and CP8A) the G2/M arrest appears transient. Cells from these two clones arrest at the G2/M boundary 24 hours after cisplatin treatment in a fashion identical to the other three clones. This arrest, however, was short lived. A large proportion of the cells have exited G2 (33% and 29%) and re-entered the G1-phase of the cell cycle after 48 hours (17% and 12%). More importantly, a similar fraction (16% and 17%) of the cells have also entered S-phase indicative of a new round of DNA synthesis. This suggests that CP5A and CP8A retain the processes necessary for activating the G2/M checkpoint but the mechanism for maintaining the checkpoint after initiation has been compromised. Consistent with their resistance to cisplatin, both CP5A and CP8A showed reduced levels of apoptosis 72 hours after cisplatin treatment (Fig 4.12). In CP5A, this was about 1.8-fold lower and in CP8A, about 1.4-fold.

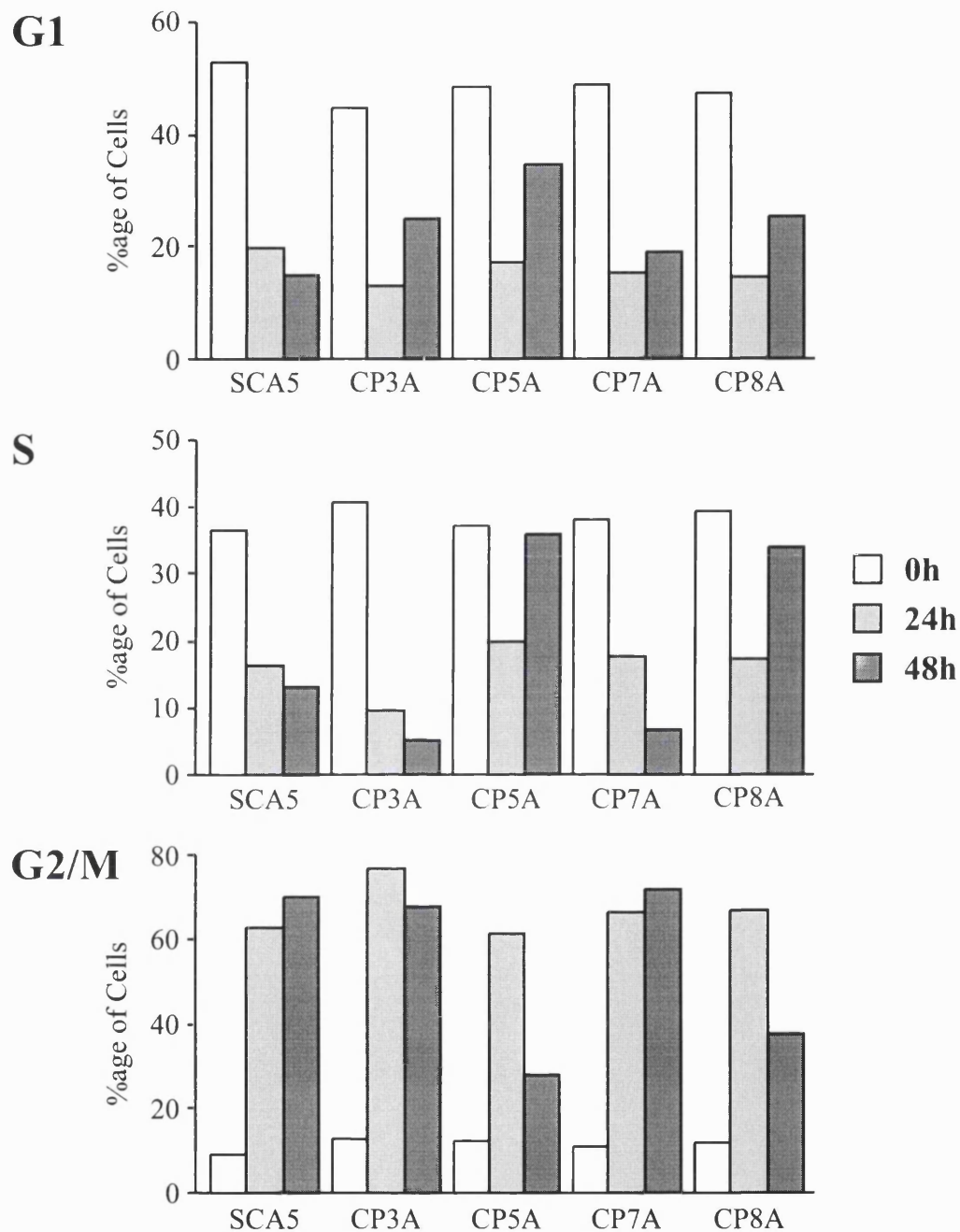


Figure 4.11 Cell Cycle Response to Cisplatin in A2780 Clonal Variants

Exponentially growing cultures of SCA5, CP3A, CP5A, CP7A or CP8A were treated with 30 μ M cisplatin for 60 min. This was then replaced with drug-free medium and cells harvested 0 (□), 24 (▤) or 48 (▥) hours after treatment. About 10⁶ harvested cells were fixed in 70% EtOH for 1 hour and then analysed for cell cycle status using Propidium Iodide staining (D. Davies, ICRF FACs Laboratory). Data was analysed using FlowJo software.

Mechanism of p21 Inactivation in Group 2 Clonal Variants

Although decreased expression of p21 is often detected in human cancer cells, mutations or allelic loss of the p21 gene are rarely observed (Gartel and Tyner, 1999). Two alternative mechanisms have been suggested for the inactivation of p21: methylation of the promoter region and changes to an inactive chromatin configuration by histone deacetylation.

Histone acetylation allows the separation of the DNA from the histones creating a more open DNA conformation and easier access for transcription factors. Naturally occurring compounds such as *n*-butyric acid (butyrate) induce this transcriptionally active chromatin structure through their ability to inhibit histone deacetylases (HDACs). Formation of inactive chromatin seems to be the general mechanism by which the gene is inactivated in gastric cancers (Shin *et al.*, 2000). In addition to inhibiting HDACs, *n*-butyric acid can also activate the p21 gene promoter through the Sp1 sites in a p53-independent fashion (Nakano *et al.*, 1997). Treatment of cells with *n*-butyric acid in which the p21 gene is inactivated by histone acetylation but not methylation should lead to the induction of p21 protein levels.

After treatment with *n*-butyric acid, a strong induction of p21 was observed in the parental cell line SCA5. In the clonal variants CP5A, CP8A and CP12A no induction of p21 above the basal level was observed (Fig 4.13). The previous result showing the lack of p21 induction by cisplatin in CP5A, CP8A and CP12A was confirmed. This suggests that p21 inactivation in CP5A, CP8A and CP12A may be *via* promoter methylation of the CpG islands.

Summary

Twelve independent clones were selected from the ovarian carcinoma line A2780 by repeated exposure to lethal doses of cisplatin. The parental cells were proficient in both mismatch repair and p53. Direct investigation of MMR protein expression and MMR activity in cell extracts did not provide convincing evidence of MMR defects in any clone. Resistance could be assigned to 3 distinct groups according to the p53 and p21 response of the clones after cisplatin treatment. No mutations in p53 were

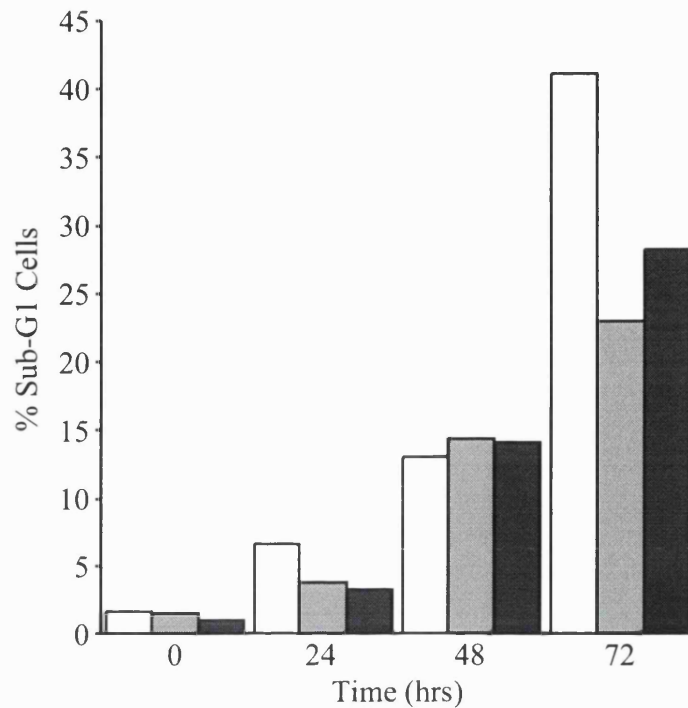


Figure 4.12 Cisplatin Induced Apoptosis in A2780 Clonal Variants

SCA5 (□), CP5A (▒) or CP8A (■) cells were treated with 30 μ M cisplatin for 60 min and fixed after the various time points as above. Sub-G1 DNA content was determined by Propidium Iodide staining by the ICRF FACs laboratory.

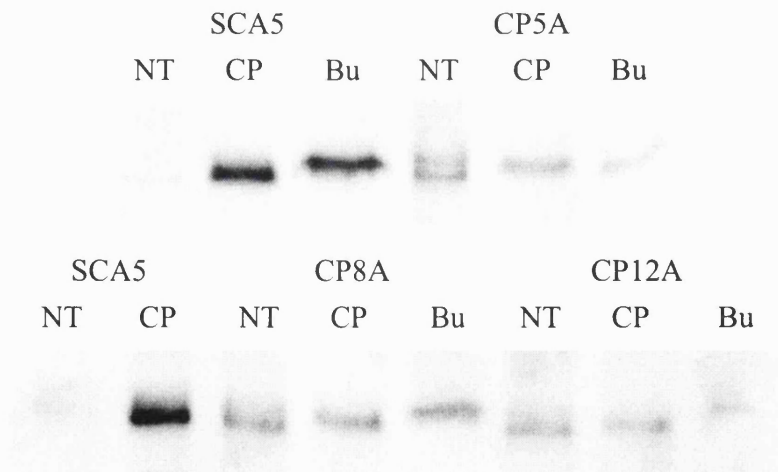


Figure 4.13 Induction of p21 Protein Levels by *n*-butyric Acid

Exponentially growing cell cultures were untreated (NT), treated with 30 μ M cisplatin (CP) for 60 minutes as before or with 5mM *n*-butyric acid (Bu) for 24h. Extracts were prepared and separated on a 12% SDS-PAGE gel, transferred to PVDF membranes and probed with anti-p21 antibodies as described previously.

found in any group.

Members of the first group, comprising CP3A, CP7A and CP10A, were approximately 1.5-fold more resistant to cisplatin. Induction of p53 and p21 by cisplatin was attenuated. These functions were normal after either IR or UV treatment. DNA-platinum levels in these lines were reduced compared to the parental line but this was not a consequence of altered levels of GSH.

CP5A, CP8A and CP12A are characteristic of the second group of variants. These were approximately 3-fold more resistant to cisplatin than the parental line. After cisplatin treatment, p53 induction was normal as was the p53 dependent induction of MDM2 and probably Bax. However, these variants showed no detectable induction of p21 after cisplatin treatment. No mutations in the exons of p53 analysed were uncovered, and unlike the Group 1 clones, the DNA-platinum levels after cisplatin treatment were similar to those of the parental cells. Group 2 clones exhibited a cell cycle response to cisplatin that differed from that of the parental cell line. These variants arrested normally at the G2/M transition but, unlike the parental cells, the arrest was transient and cells had re-entered the cell cycle 48 hours after cisplatin treatment. Their levels of cisplatin induced apoptosis were reduced compared to the parental line.

The remaining six clones have been placed, arbitrarily, into a third group. Little has been determined about their levels of cisplatin resistance or phenotype due to the lack of clues. Group 3 clones show normal p53, p21 and MDM2 induction after cisplatin treatment and so have a different mechanism of cisplatin resistance than group 1 or 2.

Discussion

Cisplatin and its analogue carboplatin are highly active cytotoxic drugs widely used in the treatment of many malignancies. Clinically their effectiveness is compromised by intrinsic tumour drug resistance and additionally many tumours become refractory to chemotherapy through acquired resistance. Many mechanisms of acquired resistance have been identified through the use of *in vitro* tumour models. These can be divided into three broad groups. (1) Altered cellular pharmacology including decreased uptake, increased efflux and inactivation of the drug through reaction with sulphurhydryl containing molecules like GSH and metallothionein. (2) Increased

repair of the cisplatin induced DNA damage. (3) Tolerance to cisplatin induced DNA damage. Tolerance can occur through a variety of mechanisms including loss of p53 function, inactivation of MMR, alterations in cell cycle responses and decreased apoptosis.

In previous work using the A2780 model system and multi-step selection for cisplatin resistance (Anthony *et al.*, 1996; Brown *et al.*, 1997), 8 out of the 9 multiple cisplatin treated (MCP) clones isolated were deficient in hMLH1 expression. Of these 8 clones, 7 exhibited additional defects in the p53 pathway as determined by decreased p21 induction, reduced apoptosis and attenuation of G2/M arrest after cisplatin or IR treatment. These clones exhibited a heterogeneous level of resistance which varied between 1.3 and 4.7-fold more than the parental cells and is suggestive of multiple alterations contributing to the cisplatin resistance phenotype. The close association between loss of hMLH1 and p53 function has been interpreted as selection of a pre-existing sub-population defective in both functions. My work was an attempt to understand the separate roles of MMR and p53 in acquired resistance to cisplatin. To do this, I started with a homogenous population of drug naïve cells that did not harbour any doubly defective sub-population.

Twelve independent cisplatin resistant cell lines were selected and at least three different sub-groups identified according to their phenotype. Of these, two groups were characterised and some insight into the underlying mechanism of cisplatin resistance was obtained. The first group, composed of CP3A, CP7A and CP10A, is characterised by reduced levels of DNA platination and subsequently DNA damage after cisplatin treatment. A suggested mechanism by which this could occur is through increased GSH production and hence inactivation of intracellular cisplatin (Godwin *et al.*, 1992). No correlation between DNA platination levels and cellular GSH was observed suggesting that this is unlikely to be the mechanism by which these cell lines have acquired cisplatin resistance. Alternative mechanisms that warrant investigation include reduced drug accumulation (Lanzi *et al.*, 1998), inactivation of cellular cisplatin by metallothionein or increased export of platinum complexes by membrane pumps such as MRP-2 (cMOAT) (Ishikawa *et al.*, 1996; Taniguchi *et al.*, 1996) or the copper-transporting P-type adenosine triphosphate (ATP7B) (Komatsu *et al.*, 2000).

The second group of clones, composed of CP5A, CP8A and CP12A, appear defective in p21 induction after cisplatin treatment even though they have wild type p53 and the p53 response appears normal as judged by the induction of p53 itself and other downstream targets. A characteristic of these variants is a defect in the maintenance, but not the initiation, of the G2/M checkpoint after cisplatin treatment. This is consistent with a role for p21 in maintaining but not triggering the G2/M checkpoint after cisplatin DNA damage. Induction of p21 is normally associated with the arrest of cells at the G1/S checkpoint. Cisplatin, however, arrests cells predominantly at the G2/M boundary and probably requires an S-phase for the cisplatin DNA damage to become lethal. Evidence exists that suggests a role for p21 in the G2/M checkpoint after γ -irradiation (Bunz *et al.*, 1998). p21 is synthesised in G2, this promotes a pause in G2 under normal growth conditions and when expressed exogenously, cells undergo G2 arrest. A potential model for the involvement of p21 in G2/M arrest is shown in Fig 4.14A (adapted from (Dulich *et al.*, 1998)). p21 potentially exerts its effects by inhibiting CAK and the phosphorylation of T161 necessary for activation of the Cdc2/CycB kinase complex (Fig 4.14B, (Taylor and Stark, 2001)).

My data suggest, that after DNA damage by cisplatin, p21 is not necessary to cause the G2 "pause" (1 in Fig 4.14A) that initiates the G2/M checkpoint. Both CP5A and CP8A initially undergo G2/M arrest after cisplatin. However, p21 does appear to be necessary for maintenance of these cells in the G2 arrested state (2 in Fig 4.14A). Both CP5A and CP8A do not remain arrested in G2/M after cisplatin treatment and have re-entered the cell cycle less than 24 hours after cisplatin treatment. It would appear that loss of p21, in these cells, overrides other signals that activate the G2/M checkpoint such as the activation of Chk1/Chk2 by ATM/ATR. Chk1/Chk2 phosphorylate Cdc25c on S216 generating a 14-3-3 binding site. Cdc25c is then exported to the cytoplasm where it is unable to dephosphorylate T14 and Y15 of Cdc2 necessary to activate the Cdc2/CycB kinase complex (Shiloh, 2001). ATM/ATR and Chk1/Chk2 may function as the initiator signal of the G2/M checkpoint and the subsequent induction of p21 by p53 is essential to maintain cellular arrest.

What is the advantage of loss of the G2/M checkpoint and how may this contribute to the increased survival of these cells? Arrest at the G2/M boundary and the subsequent maintenance of this arrest in cells with heavily damaged DNA may be necessary to initiate apoptosis. Cells lacking DNA damage appear to arrest initially at the G2/M transition but this arrest is not maintained (Dulich *et al.*, 1998). The loss of the maintenance of G2/M arrest may allow cells with DNA damage to enter mitosis and escape the apoptotic pathway. Such cells may not complete cytokinesis due to mechanical defects. Those that complete cytokinesis probably exhibit a high number of chromosome aberrations (CIN phenotype).

If p21 inactivation is a frequent event in acquired resistance to cisplatin, as the above cell model would suggest, why is inactivation of p21 function in drug resistant tumours a rare event? Induction of p21 after DNA damage by cisplatin requires p53. A large proportion of human tumours have abrogated p53 function through a wide variety of mechanisms. In a human tumour, loss of p53 function is a better promoter of tumourigenesis than loss of p21 function. Cisplatin treatment *in vivo* probably selects not only for tumour cells resistant to cisplatin but also for tumour cells with other beneficial factors such as increased growth rate. p53 fulfils this criteria much more readily than p21 due to its central position in many pathways controlling cell growth and death. Loss of p53 confers a significant selective advantage compared to p21. Perhaps previous models, where pre-existing populations were selected, are in fact a better model of acquired resistance *in vivo*.

In summary, in the cell system and with the selection conditions used, inactivation of MMR or loss of p53 function were found not to be significant contributors in acquired resistance to cisplatin. In 3 of 12 resistant cell lines DNA platination was reduced indicative of protective mechanism. An additional 3 out of the 12 clones were defective in p21 induction after cisplatin treatment and this was correlated with a subsequent inability to maintain a cisplatin-induced G2/M arrest. The remaining 6 clones have not been fully characterised but are resistant through mechanism(s) different from the other two described.

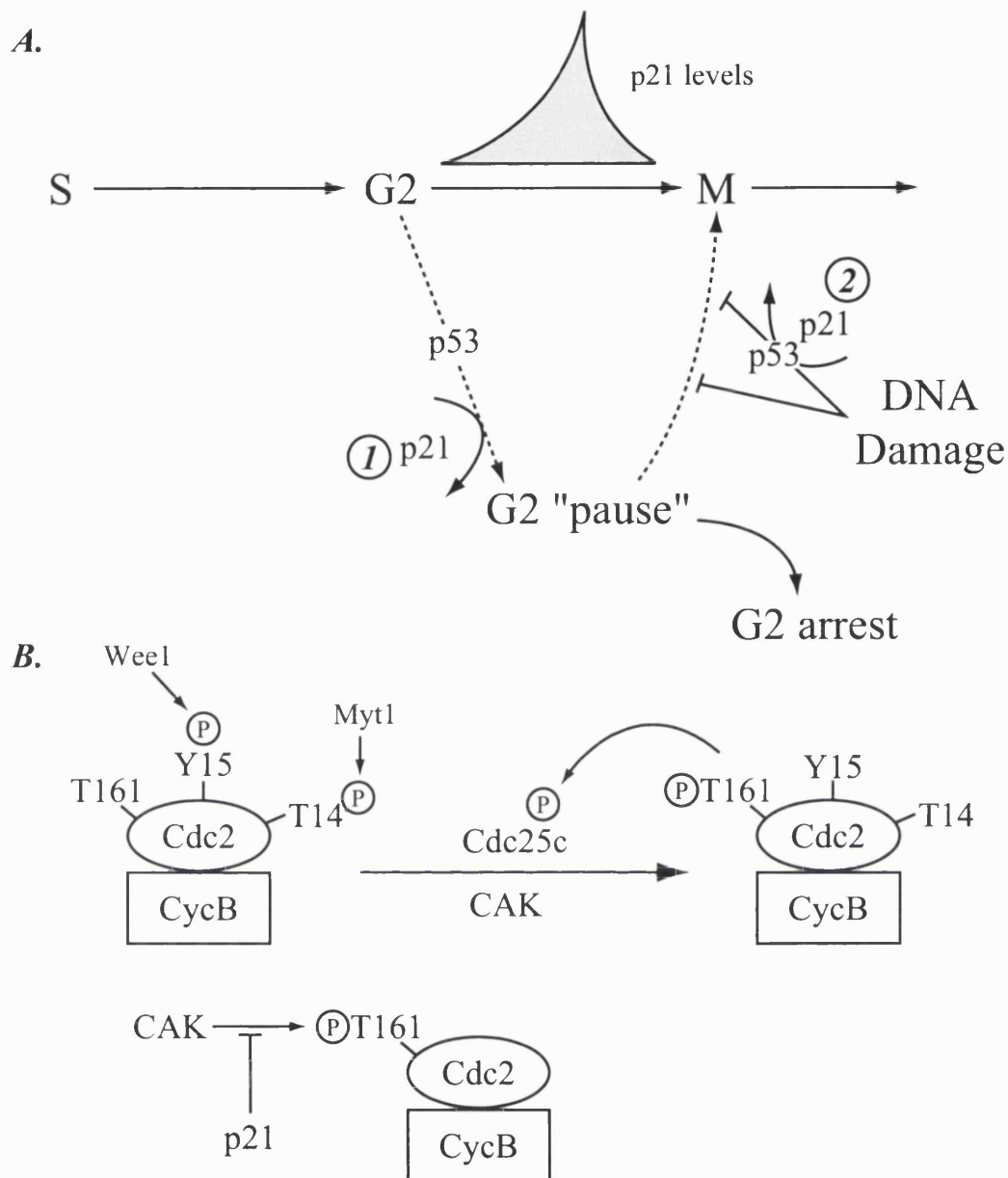


Figure 4.14 Model for the involvement of p21 in the G2 / M checkpoint control

A. Accumulation of p21 during the G2-phase of the cell cycle may cause a G2 "pause" that allows for the integration of the G2 checkpoint signals before mitosis. In response to DNA damage, induction of p53 leads to p21 induction and the subsequent maintenance of the G2 pause leading to G2/M arrest. (Adapted from Dulic *et al*, 1998).

B. Molecular events required to activate the cyclin dependent kinase Cdc2 and entry into mitosis. Cdc2 is kept inactive by phosphorylation of Y15 by Wee1 and T14 by Myt1. At the onset of mitosis, both residues are dephosphorylated by the phosphatase Cdc25c. Phosphorylation of T161 by CDK-activating kinase (CAK) is also required to activate Cdc2/CycB. Cdc2/CycB can also phosphorylate Cdc25c further activating it and initiating a positive feedback loop. p21 may inhibit Cdc2 by either directly binding it like with the G1 CDKs or by inhibiting the phosphorylation of T161 by CAK.

The inability of cisplatin to select for MMR defects in the A2780 model is in direct contrast to the results obtained with the *dam* mutant *E. coli*. In the *E. coli* model, loss of MMR was a common defect associated with cisplatin resistance and thus an important contributor to acquired resistance. Additional, unidentified factors also contributed to cisplatin resistance in this model. In the human model, it was perhaps these defects and not MMR that were the major factors identified in acquired resistance to cisplatin. This difference between the two organisms may be a reflection of the relative contribution of MMR to acquired resistance in each.

Chapter 5: Results III

The Interaction Between DNA Mismatch Repair and the Thiopyrimidine, 4-Thiothymidine

The thiopurines 6-mercaptopurine and 6-thioguanine (S^6G) are used in the treatment of acute leukaemia (Elion, 1989). In order to be toxic, S^6G must be salvaged by the HGPRT pathway and a significant proportion of this salvaged S^6G is incorporated into DNA. DNA- S^6G can undergo facile methylation on the S^6 position by *S*-adenosylmethionine (SAM). SAM is a normal constituent of mammalian cells where it provides methyl groups for enzymatic reactions. It can also act as a weak S_N2 methylating agent and, while it shows no detectable methylation of the O^6 position of guanine, methylation at the S^6 position of S^6G can occur due to the increased nucleophilicity of the sulphur (Swann *et al.*, 1996). This reaction produces DNA-6-methylthioguanine (S^6meG).

When replicated, S^6meG forms base pairs with both C and T with approximately equal efficiency. DNA mismatch repair recognises either combination and signals the removal of the incorporated pyrimidine (Swann *et al.*, 1996; Waters and Swann, 1997). Repair of the gap by either polymerase δ or ϵ regenerates the $S^6meG:C/T$ pair. It has been hypothesised that these repeated rounds of attempted repair trigger cell death. Resistance to S^6G is an acknowledged property of mismatch repair defective cells. Tumour cells defective in components of either the hMutS α (hMSH2 or hMSH6) or the hMutL α (hMLH1 or hPMS2) are resistant to the drug (Aquilina *et al.*, 1990; Hawn *et al.*, 1995).

Previous studies have shown that O^6meG and S^6meG share similar structural, biochemical and, ultimately, biological properties. I have investigated whether S^4TdR can be incorporated into DNA, undergo *in situ* S-methylation and provoke MMR-dependent toxicity in a fashion analogous to S^6G . In this way, I hope to

understand if S⁴meT mimics S⁶meG and thus might have potential as an alternative chemotherapeutic agent.

Cytotoxicity of S⁴TdR

S⁴TdR was not cytotoxic. Continuous growth in 100µM S⁴TdR did not inhibit the proliferation of the TK-proficient, MMR-competent Burkitt's Lymphoma line, Raji, over a seven day period (Fig 5.1A). In direct comparison, growth of the same cells in 1µM S⁶G caused significant cytotoxicity after day 3 (Fig 5.1B). There was no evidence of S⁴TdR toxicity in several other cell lines, including the fibroblasts MRC5VA and XP12RO, the A2780 ovarian carcinoma and its MMR-deficient variant A2780-MNU1, and the MMR-defective HCT116 colon carcinoma.

Metabolism of S⁴TdR

In order to be toxic, S⁶G must be incorporated into DNA by the HGPRT salvage pathway. Thymidine and its analogues are salvaged by the thymidine kinase pathway and incorporated into DNA *via* this route. S⁴TdR was shown to be a substrate for phosphorylation by thymidine kinase by two different methods.

A cytoplasmic extract of HeLa cells converted ¹⁴C-labelled TdR to phosphorylated forms which were separated from the unphosphorylated forms by their tight binding to DE81 paper. Both cold TdR and S⁴TdR decreased the amount of phosphorylated [¹⁴C]TdR by directly competing for TK in the HeLa extract (Fig 5.2). Based on the comparison of the ability to compete with [¹⁴C]TdR for phosphorylation, I estimate that S⁴TdR was about a 6-fold poorer substrate than TdR for TK. This technique, however, does not exclude the possibility of S⁴TdR being an inhibitor of TK and not a direct substrate.

In the second approach, direct phosphorylation of both TdR and S⁴TdR was determined using [³²P]γATP and thin layer chromatography (TLC). In the presence of [³²P]γATP, HeLa cell extracts converted TdR or S⁴TdR to ³²P-labelled phosphorylated forms which can be separated by TLC. The TLC system used separates nucleotides and nucleosides according to their hydrophobicity.

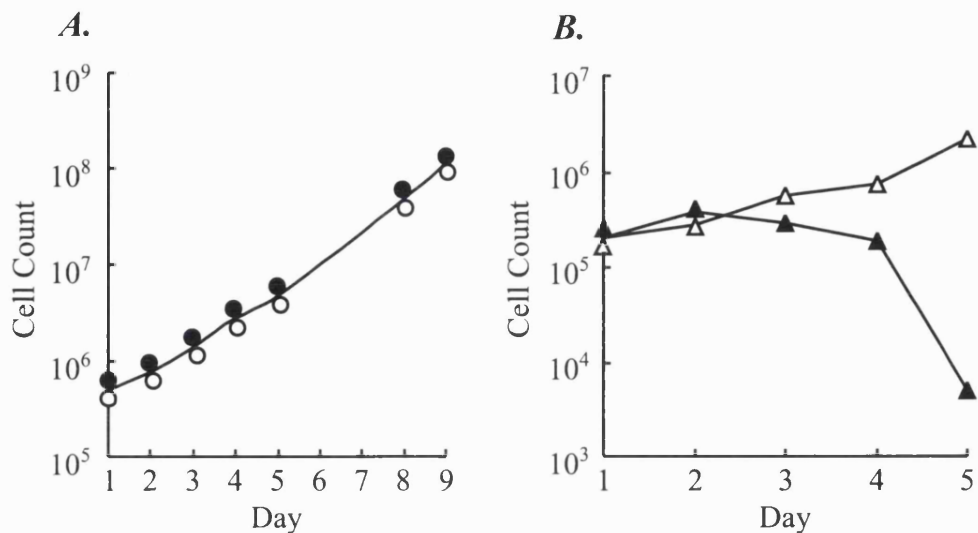


Figure 5.1 Cytotoxicity of S⁴TdR

Approximately 5×10^5 exponentially growing Raji cells were plated in the presence (●▲) or absence (○△) of $100 \mu\text{M}$ S⁴TdR (A) or $1 \mu\text{M}$ S⁶G (B) in dialysed calf serum. Cell number was determined by daily haemocytometer counts for up to 9 days.

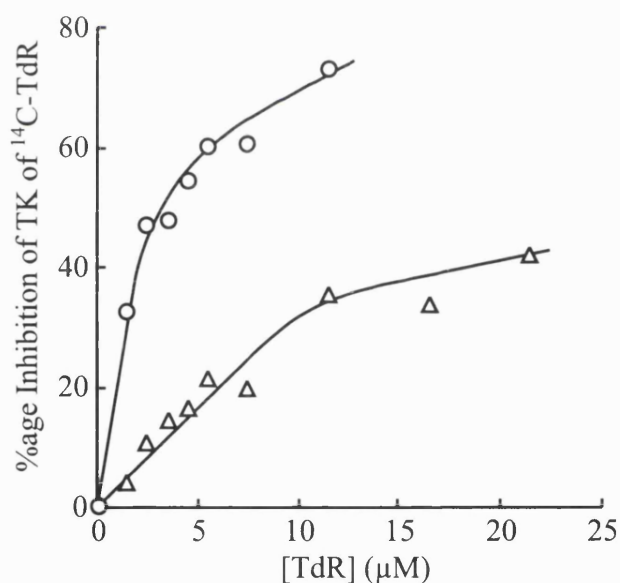


Figure 5.2 Inhibition of Phosphorylation of [¹⁴C]TdR by Cold TdR or S⁴TdR

The ability of either TdR (○) or S⁴TdR (△) to inhibit the conversion of ¹⁴C-labelled TdR to phosphorylated forms by a dialysed HeLa extract was assayed. Assays containing $1.5 \mu\text{M}$ [¹⁴C]TdR and increasing concentrations of unlabelled TdR or S⁴TdR were incubated at 37°C for 15 min and then stopped. Reactions were spotted onto DE81 paper squares and non-phosphorylated [¹⁴C]TdR washed off with 4mM Tris-HCl (pH 8). The amount of [¹⁴C]TdR converted to [¹⁴C]TNP was determined by scintillation counting.

The percentage inhibition is determined as:

$$\frac{\text{CPM without inhibitor} - \text{CPM with inhibitor}}{\text{CPM without inhibitor}} \times 100\%$$

S^4TdR is significantly more hydrophobic (partition coefficient (P) = 0.855) than TdR (P = 0.055) (Palomino *et al.*, 1990) or ATP and is well separated from the unused, labelled ATP. S^4TdR was converted to phosphorylated forms with about 10% the efficiency of TdR (Fig 5.3A and B). No phosphorylated forms of either TdR or S^4TdR could be detected with extracts from TK deficient Raji cells (Fig 5.3A and B). From the Michaelis-Menten plots (Fig 5.3C and D), the apparent K_m for TdR was estimated to be $3\mu M$. The corresponding value for S^4TdR was estimated to be $30\mu M$. Their V_{max} were not reliably different: 200 and 232 $pmols^{-1}mg^{-1}min^{-1}$ respectively. Estimates of the utilisation of S^4TdR by TK using the two different approaches correspond reasonably well to published values for rabbit thymus TK which has a four-fold higher K_i for S^4TdR than its apparent K_m for TdR (Palomino *et al.*, 1990). In most of the subsequent experiments, the concentration of S^4TdR used was more than 3 times that of the apparent K_m .

Several problems exist with this TLC based approach. No genuine markers exist for the phosphorylated forms of S^4TdR and the position of potential phosphorylated products is estimated from the migration of S^4TdR . In addition, crude extracts are used which contain all three enzymes necessary to convert S^4TdR to S^4TTP namely TK, thymidylate kinase and TDP kinase. Since all phosphorylated nucleotides were quantified, the apparent K_m is therefore not a direct measure of TK activity but an apparent value for all three enzymes.

I examined whether the absence of toxicity might be due to the degradation of S^4TdR . Thymidine phosphorylase (TP) catalyses the breakdown of TdR to thymine (Thy) and could serve as a potential mechanism for S^4TdR degradation. Purified bacterial TP efficiently converts [^{14}C]TdR to [^{14}C]Thy. Substrate and products are easily separated by TLC on Silica60 plates and detected and quantified using a phosphorimager (Fig 5.4A). An enzyme concentration in the linear range (Fig 5.4B) was selected and the conversion of [^{14}C]TdR to Thy inhibited with increasing concentrations of TdR . The K_m for TP is high (about $100\mu M$ (el Kouni *et al.*, 1993)) hence large quantities of cold nucleoside were required to achieve significant inhibition of the degradation of the labelled substrate.

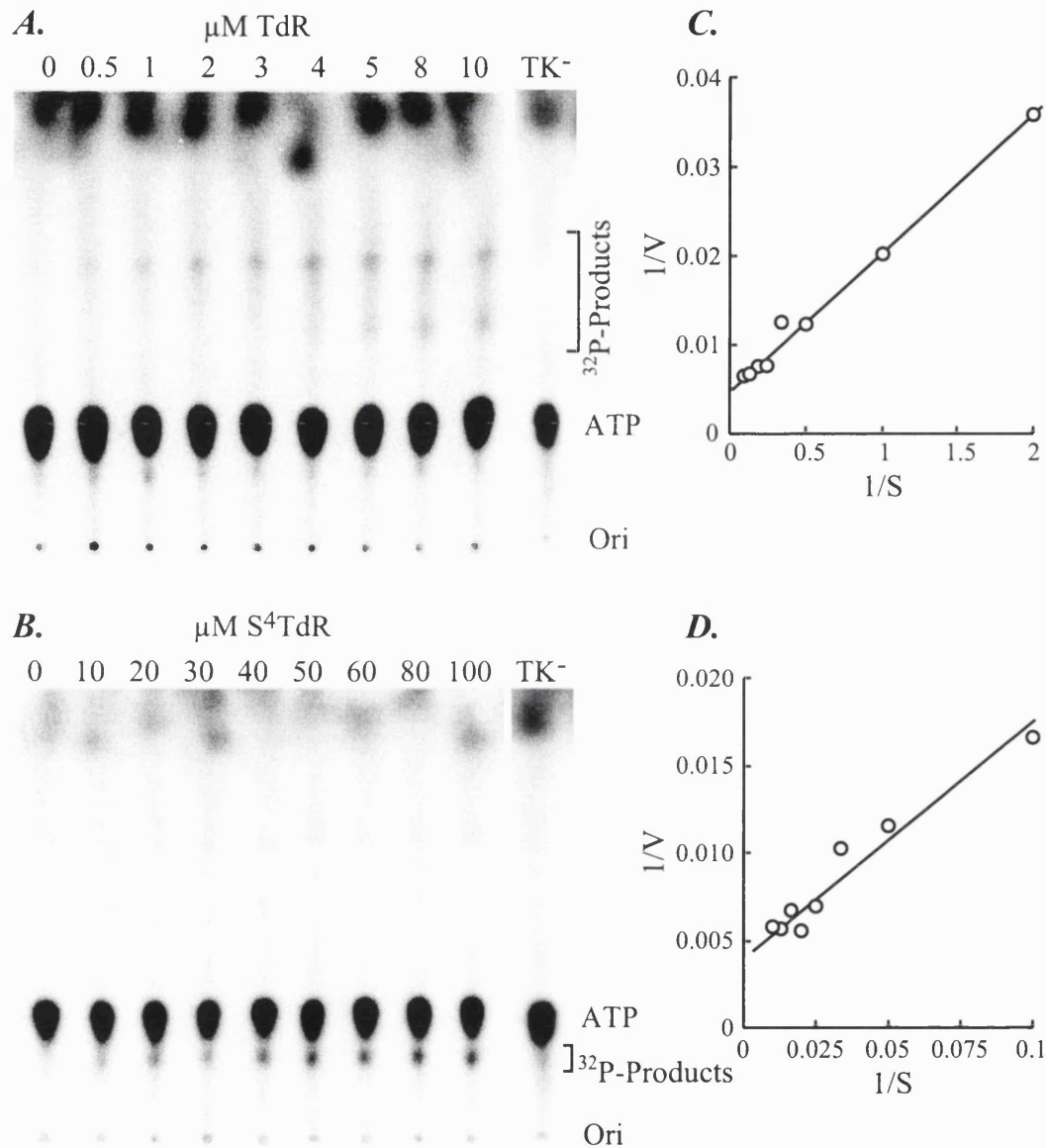


Figure 5.3 Direct Phosphorylation of TdR and S⁴TdR by [³²P]γATP

TdR (*A*) or S⁴TdR (*B*) was converted to phosphorylated forms by a dialysed HeLa extract using [³²P]γATP as the phosphate source. Phosphorylated TdR or S⁴TdR were separated from labelled ATP on PEI-cellulose using saturated AmSO₄, pH3.5 as the mobile phase and detected and quantified using a STORM phosphorimager. From the double reciprocal plots for TdR (*C*) and S⁴TdR (*D*), the K_r and V_{max} values for both nucleotides could be calculated.

Dialysed extracts deficient in thymidine kinase from the Burkitt's lymphoma line Raji TK⁻ (TK⁻) were incubated with either 10μM TdR (*A*) or 100μM S⁴TdR (*B*) and separated as above.

The position of genuine markers (detected under UV₂₅₄ light) are: ATP (R_f = 0.28), TNP (R_f = 0.49), TTP (R_f = 0.64) and S⁴TdR (R_f = 0.24). The position of the origin (Ori) is also indicated.

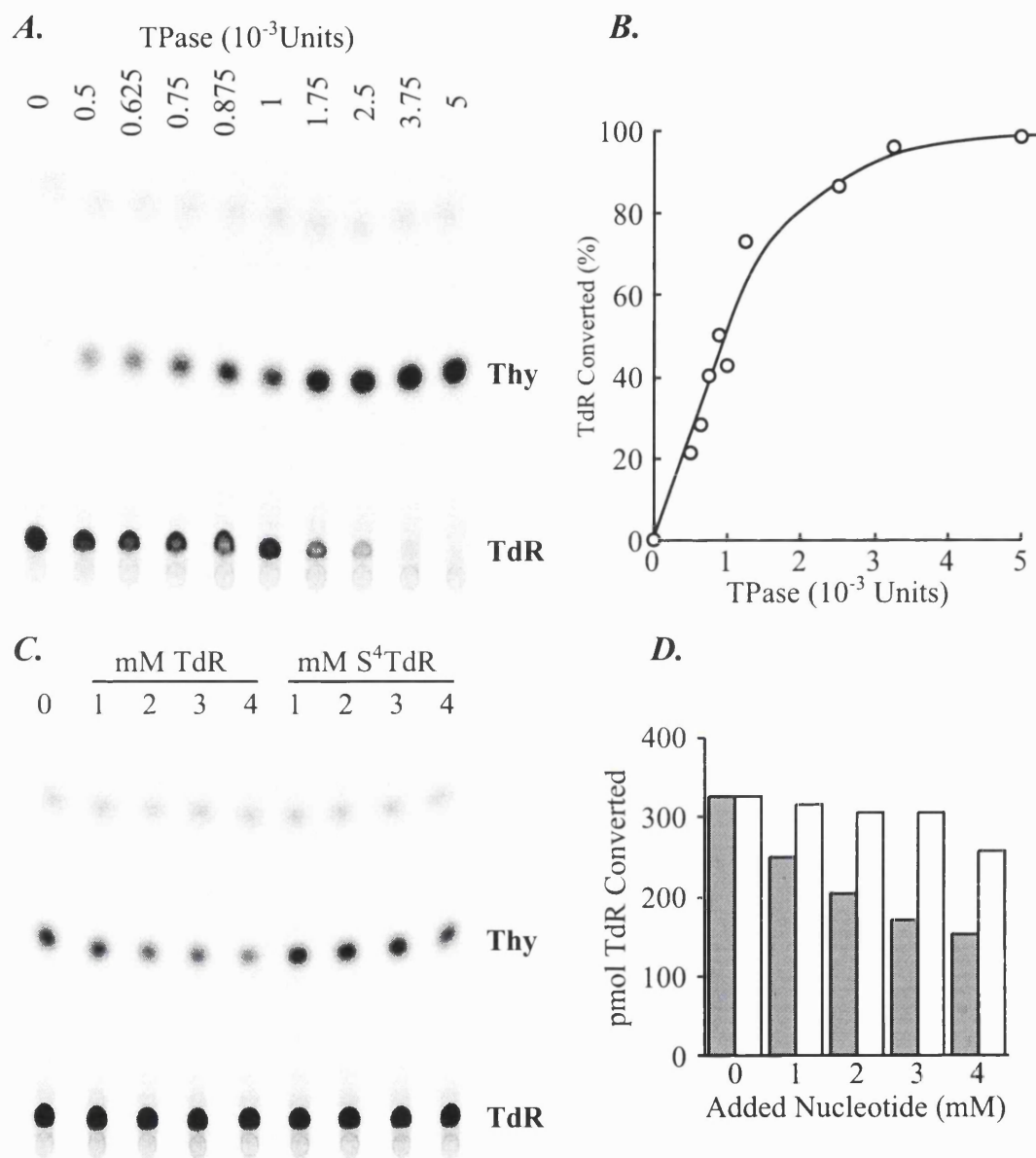


Figure 5.4 Degradation of Nucleosides by Thymidine Phosphorylase

^{14}C -labelled TdR was converted to $[^{14}\text{C}]\text{Thy}$ by purified bacterial thymidine phosphorylase. $[^{14}\text{C}]\text{Thy}$ was efficiently separated from $[^{14}\text{C}]\text{TdR}$ by thin layer chromatography on Si-60 plates with CHCl_3 (90) : MeOH (5) : Acetic Acid (5) (v/v/v) as the mobile phase (A). Products were detected and quantified by STORM phosphorimager and the percentage TdR converted to Thy calculated (B). The positions of genuine markers for TdR ($R_f = 0.07$) and Thy ($R_f = 0.47$) are indicated.

Reaction mixes containing 1nmol $[^{14}\text{C}]\text{TdR}$, 1.5×10^{-3} units of TP and increasing concentrations of cold nucleoside were incubated at 37°C for 10 minutes. Reactions were terminated and products separated and quantitated as before (C). The amount of TdR converted was calculated and plotted (D). TdR (■), S⁴TdR (□).

Cold TdR effectively inhibited the conversion of [¹⁴C]TdR to Thy with approximately 50% inhibition at 3.5mM (Fig 5.5). No significant inhibition was seen with S⁴TdR at concentrations less than 4mM. The highest concentration used (4mM) only slightly reduced the amount of [¹⁴C]TdR converted (by ≤ 20%).

I conclude that S⁴TdR is a poor substrate for TP. Degradation by this enzyme should not serve as a mechanism by which the availability of S⁴TdR for incorporation into DNA is reduced.

S⁴TdR Incorporation into DNA

S⁴TdR was a substrate for thymidine kinase with a K_m of approximately 10-times that of TdR but a poor substrate for thymidine phosphorylase. There appears to be no obvious impediment to the formation of S⁴TTP and incorporation into DNA. Incorporation of the phosphorylated S⁴TdR into DNA of growing cells was examined directly using reverse phase HPLC. The SV40 transformed fibroblasts MRC5VA were grown in medium containing 100μM S⁴TdR and DFCS for 3 days. DNA was extracted and enzymatically digested to deoxynucleosides which were then separated by reverse phase HPLC. S⁴TdR has an absorption maximum of 335nm at which the other deoxynucleosides do not absorb significantly. Eluates were therefore monitored at both 260nm and 335nm. S⁴TdR eluted late and was well separated from the unmodified deoxynucleosides (Fig 5.5). From the height of the S⁴TdR and TdR peaks corrected for their relevant extinction coefficients ($E_{TdR} \approx 8000 @ \lambda_{260nm}$ and $E_{S^4TdR} \approx 20\ 000 @ \lambda_{335nm}$), the amount of S⁴TdR relative to TdR incorporated can be calculated. This was estimated to be about 1%. Similar analyses were performed with DNA from the Raji Burkitt's Lymphoma, the SV40 transformed XPA defective fibroblast XP12RO and the hMSH2 defective derivative of XP12RO, XP12ROB4 (data not shown). The average replacement of DNA thymine was estimated to be about 0.5% (range 0.2 to 1.3%, four determinations). This compares favourably with the approximately 3% substitution of guanine by S⁶G after growth in highly toxic S⁶G concentrations (Swann *et al.*, 1996).

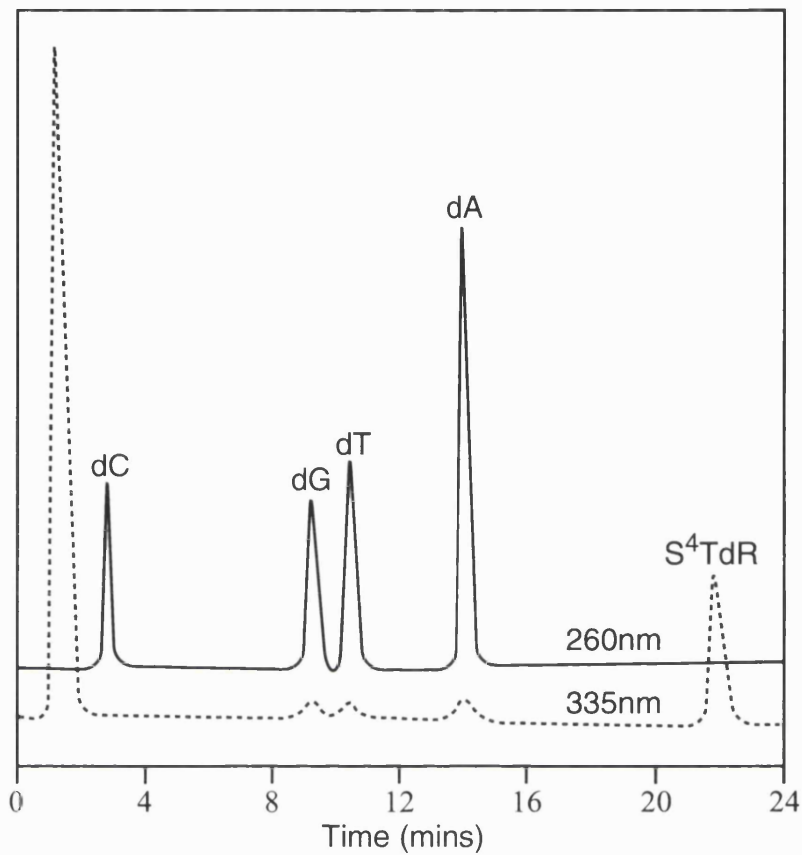


Figure 5.5 Incorporation of S⁴TdR into Genomic DNA

MRC5VA cells were grown in medium containing 10% dialysed calf serum and 100 μ M S⁴TdR for 3 days. DNA was extracted and digested to nucleosides by DNaseI, Phosphodiesterase I and Alkaline Phosphatase. The eluate was separated by reverse phase HPLC and monitored simultaneously at 260nm (upper trace, —) and 335nm (lower trace, ----) as previously described (Xu *et al.*, 1992). S⁴TdR absorbs maximally at 335nm and elutes at approximately 22 mins. The other major deoxynucleoside peaks are indicated. The sensitivity levels of detection at the two different wavelengths differ by a factor of 100.

S-methylation of S⁴TdR

The lethality of DNA-S⁶G requires non-enzymatic S-methylation by SAM. An estimated 1 in 10⁴ to 10⁵ of the incorporated S⁶G is S-methylated (Swann *et al.*, 1996). The sensitivity of the MMR-proficient Raji cells to killing by S⁶G indicates that they contain sufficient SAM to methylate the incorporated S⁶G. Nevertheless, I considered whether lack of S-methylation by SAM of the incorporated S⁴TdR may be responsible for the absence of MMR dependent toxicity. S-methylation shifts the absorption maximum of S⁴TdR from 335nm to around 315nm. Assuming that the rate of methylation is similar to S⁶G, the number of incorporated S⁴TdR residues methylated is likely to be small (of the order of 10⁻⁵). No products could be detected by monitoring the HPLC eluate at 315nm (data not shown). This is consistent with the amount of methylated S⁴TdR being small or even absent. The likelihood of *in vivo* methylation of DNA-S⁴TdR was therefore determined using a different method.

The ability of the model S_N2 methylating agent methyl iodide (MeI) to methylate a synthetic oligonucleotide containing a single S⁴TdR base was determined *in vitro* by Dr. Y.-Z. Xu. MeI was incubated with a 34mer containing a single S⁴TdR residue and samples removed at various times. These were analysed using FPLC conditions that separate the methylated and unmethylated forms. Approximately 50% conversion was observed after 50 minutes and by 140 minutes, more than 80% of the S⁴TdR containing oligonucleotide had been converted to the methylated form (Fig 5.6). This rate of methylation is very similar to that of an oligonucleotide containing a single S⁶G under identical conditions (Xu, 1996) and therefore suggests that S⁴meTdR should be formed with a significant frequency *in vivo*.

To investigate further whether the absence of toxicity reflected the lack of a suitable methylating agent *in vivo*, the ability of S⁴TdR to sensitise cells to S_N1 and S_N2 methylating agents was determined. SAM behaves like a weak S_N2 methylating agent. MMS and MNU are S_N2 and S_N1 methylating agents respectively. Treatment with these compounds should increase the levels of DNA-S⁴meTdR and hence, their cytotoxicity. The XPA defective fibroblasts XP12RO were grown for 3 days with and without 100 μM S⁴TdR and DFCS.

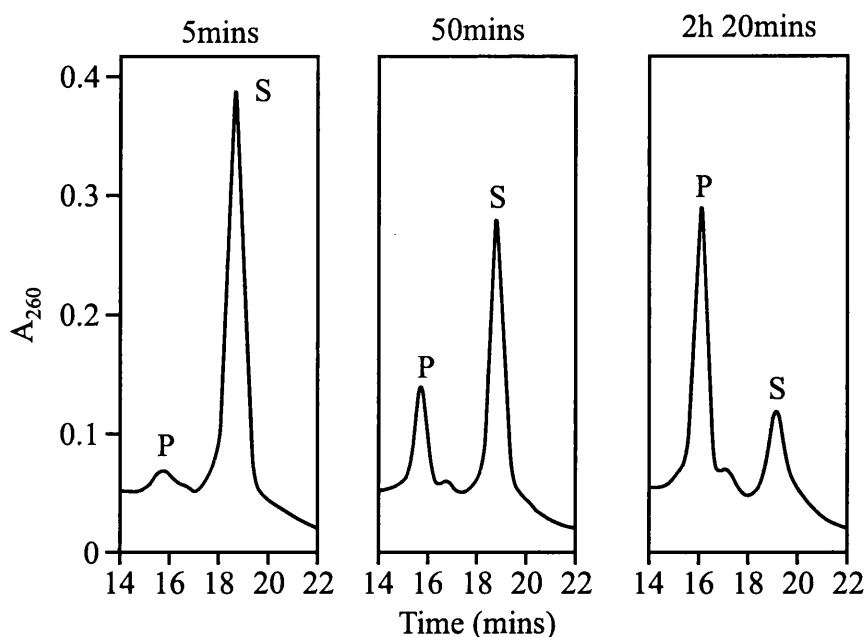


Figure 5.6 *In situ* Methylation of a S⁴TdR Containing Oligonucleotide by Methyl Iodide

The 34mer AAT TCC CGG GGA TCC GTA XGC CTG CAG CCA AGC T, where X = S⁴TdR was dissolved in 0.4M K Phosphate (pH10) and incubated with 0.25% MeI. At the various times indicated, aliquots were withdrawn and the unmethylated substrate (S, $R_m = 18.5$ min) separated from the methylated product (P, $R_m = 15.5$ min) by FPLC on a DIonex BIOLC FPLC system and Mono Q HR 5/5 column. This experiment was performed by Dr. Y.-Z. Xu.

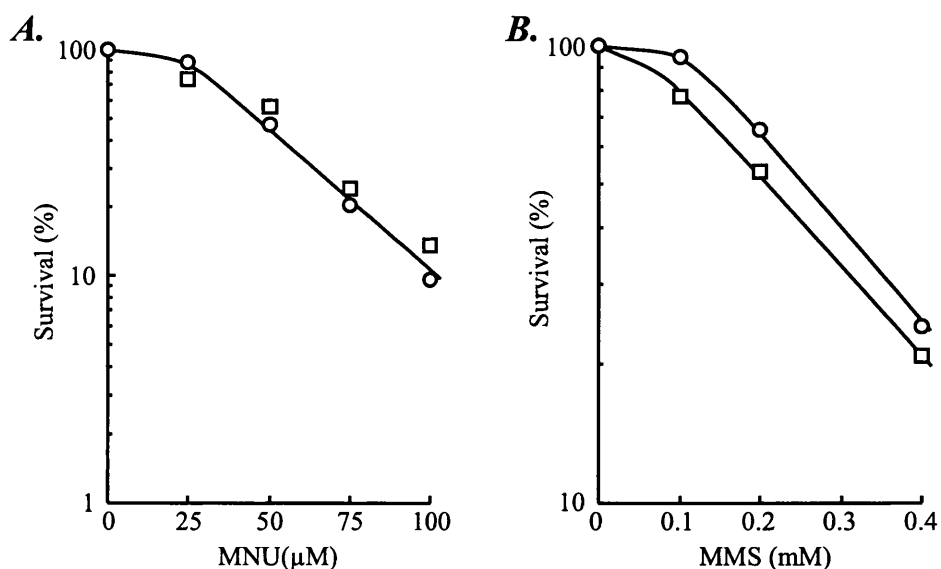


Figure 5.7 S⁴TdR Does Not Increase Sensitivity to Either S_N1 or S_N2 Methylating Agents

XP12RO cells were grown in the presence (□) or absence (○) of 100 μM S⁴TdR in media containing 10% dialysed calf serum for 3 days. Appropriate numbers of cells were plated in 10cm dishes and treated with increasing concentrations of MNU (A) or MMS (B). After 10 days growth, colonies were stained and scored. Cells were plated in triplicate and each point is the mean of two independent experiments.

Appropriate numbers of cells were seeded in 10cm dishes and the sensitivity to MNU and MMS determined by clonal survival (Fig 5.7). No increased sensitivity to either form of methylating agent was observed after treatment with S⁴TdR.

I conclude that S⁴TdR is incorporated into DNA where it is likely to undergo non-enzymatic methylation by SAM at similar rates to S⁶G. The absence of S⁴TdR induced cell killing is not due to insufficient *in situ* methylation.

Coding Properties of S⁴TdR and S⁴meTdR During DNA Synthesis

The coding properties of both S⁴TdR and S⁴meTdR were determined using a primer / template system containing a single thiopyrimidine residue. Insertion of a single base opposite the thiobase by the exonuclease-proficient Klenow fragment of pol I was determined. As expected, when the template contained a T, the preference for A over G was more than a 100-fold (Fig 5.8A). A was also the preferred base in the presence of a template S⁴T. The preference for A over G was again ≥ 100 -fold. Incorporation was efficient but reduced when compared to the template T (Fig 5.8B). Incorporation opposite a template S⁴meT was again extremely efficient but in contrast to the unmethylated base, S⁴meT preferentially directed the incorporation of G over A by a factor of greater than 30-fold (Fig 5.8C).

The coding properties of S⁴TdR closely resembled those of TdR in that it directs the incorporation of A. This suggests that S⁴TMP will be incorporated into DNA in the place of TMP and should not substitute to any great extent for dCMP. This is consistent with the observation that S⁴TTP is efficiently utilised by the Klenow fragment and HIV-1 reverse transcriptase and incorporated into a poly(dA).poly(dT) template (Rao *et al.*, 2000). My data further indicate that when replicated, S⁴TdR preferentially (>99%) forms base pairs with A.

S⁴meTdR also exhibits highly selective base pairing. S⁴meT:G was overwhelmingly (> 30-fold) favoured. Therefore S⁴meTdR appears to be accommodated well in the S⁴meT:G pair and is unlikely to resemble a mismatch. This is in direct contrast to S⁶meG which shows no preference for the complementary pyrimidine and directs incorporation of C and T with approximately equal efficiency (Swann *et al.*, 1996).

Mismatched base pairs are poorly extended by exonuclease-deficient Klenow fragment. This property can be used to investigate how closely a modified base pair resembles a mismatch. The ability of exonuclease-deficient Klenow fragment to extend TdR, S⁴TdR and S⁴meTdR terminal base pairs was therefore examined (Fig 5.9). In the presence of all 4 dNTPs, a T:A terminal base pair was rapidly extended and the reaction was complete in less than 30 seconds. A S⁴T:A pair was extended with similar kinetics. In direct contrast, no extension of a terminal S⁴meT:A pair was observed in the 2 minute incubation period. As expected, a T:G pair was also very poorly extended. In the presence of all 4 dNTPs incorporation of the first base (a T) after the T:G pair was observed. No subsequent extension beyond this occurred in the 2 minute incubation period. Extension of a S⁴T:G pair occurred with relative ease and the reaction was essentially complete in less than 30 seconds. The rate of extension is only slightly slower than a T:A or S⁴T:A pair. Under identical conditions, S⁴meT:G base pairs were also extended rapidly with the reaction again complete in 15 to 30 seconds. The kinetics of extension of the S⁴meT:G pair were not significantly different from those of a T:A pair.

Thermal Stability of S⁴T:A Base Pairs

Thermal stability studies of self-complementary oligonucleotides carried out by Dr. Y.-Z. Xu were in agreement with the preferential formation and stability of the S⁴T:A base pair. The T_m of the oligonucleotide AGCGAATTCGCT was reduced by only a single degree (from 64.5°C to 63.5°C) when the indicated T was replaced by S⁴T to form an S⁴T:A base pair. In contrast, replacement of the indicated G by S⁶G to generate a S⁶G:C base pair decreased the T_m by 13.3°C.

Mutagenicity of S⁴TdR

The mutagenicity of S⁴TdR was investigated. The preferential pairing of S⁴meTdR with G should be highly mutagenic. The cell line CHO-D422 is hemizygous for the *APRT* gene. Mutation of the remaining *APRT* allele renders cells resistant to killing by the purine analogue 8-azaadenine.

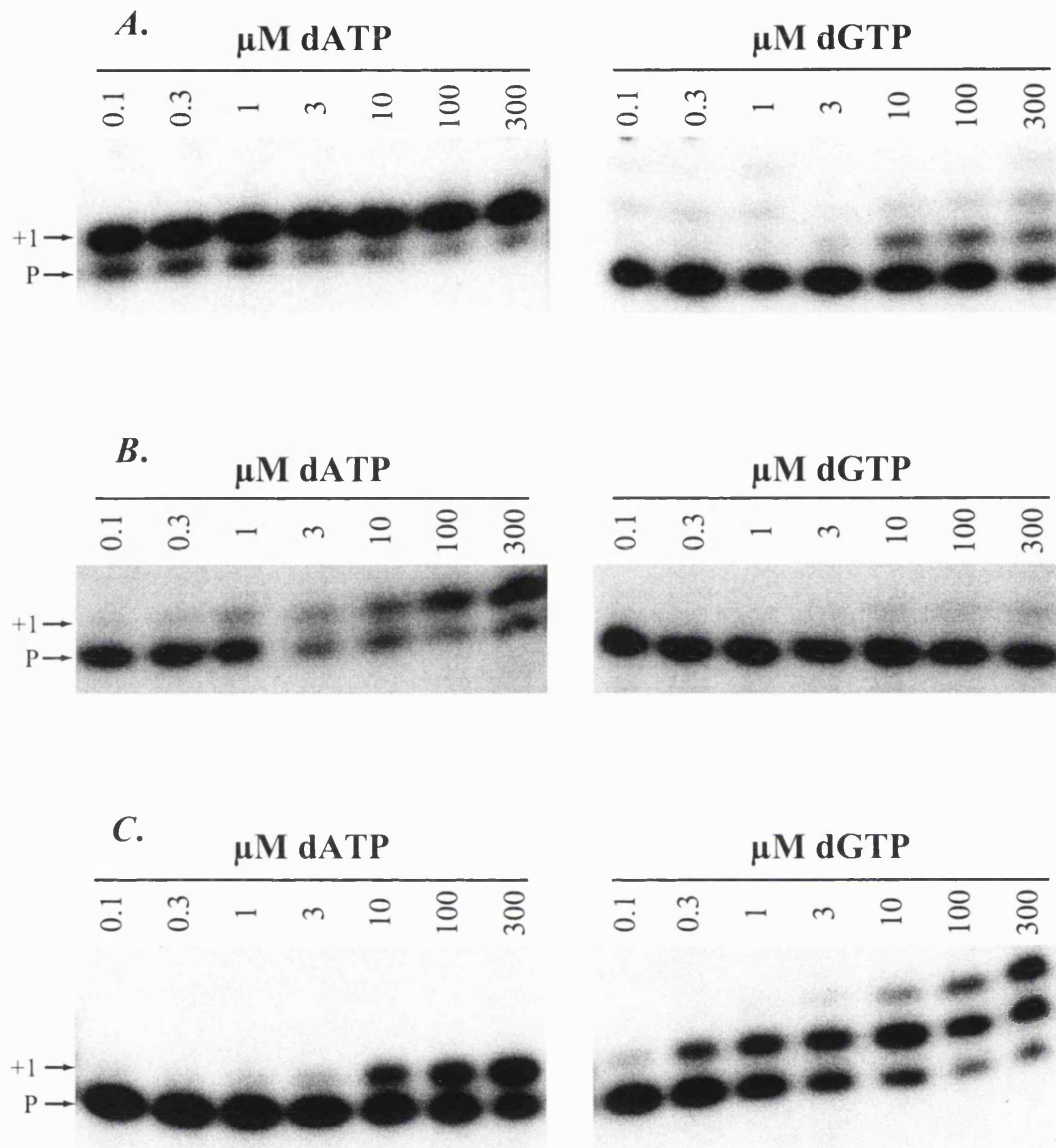


Figure 5.8 Coding Properties of S⁴TdR and S⁴meTdR

The template AAT TCC CGG GGA TCC GTA XGC CTG CAG CCA AGC T where X = T (A), S⁴T (B) or S⁴meT (C) was annealed to a 5'-³²P end-labelled 15mer primer that terminated at the base prior to the modified residue. The primer was extended by exonuclease-proficient Klenow fragment in the presence of increasing concentrations of dATP (left panel) or dGTP (right panel) for 60 seconds at 37°C. Products were denatured and separated on a 7M Urea / 15% polyacrylamide gel and detected by autoradiography. The position of the primer (P) and the primer extended by one base (+1) are indicated.

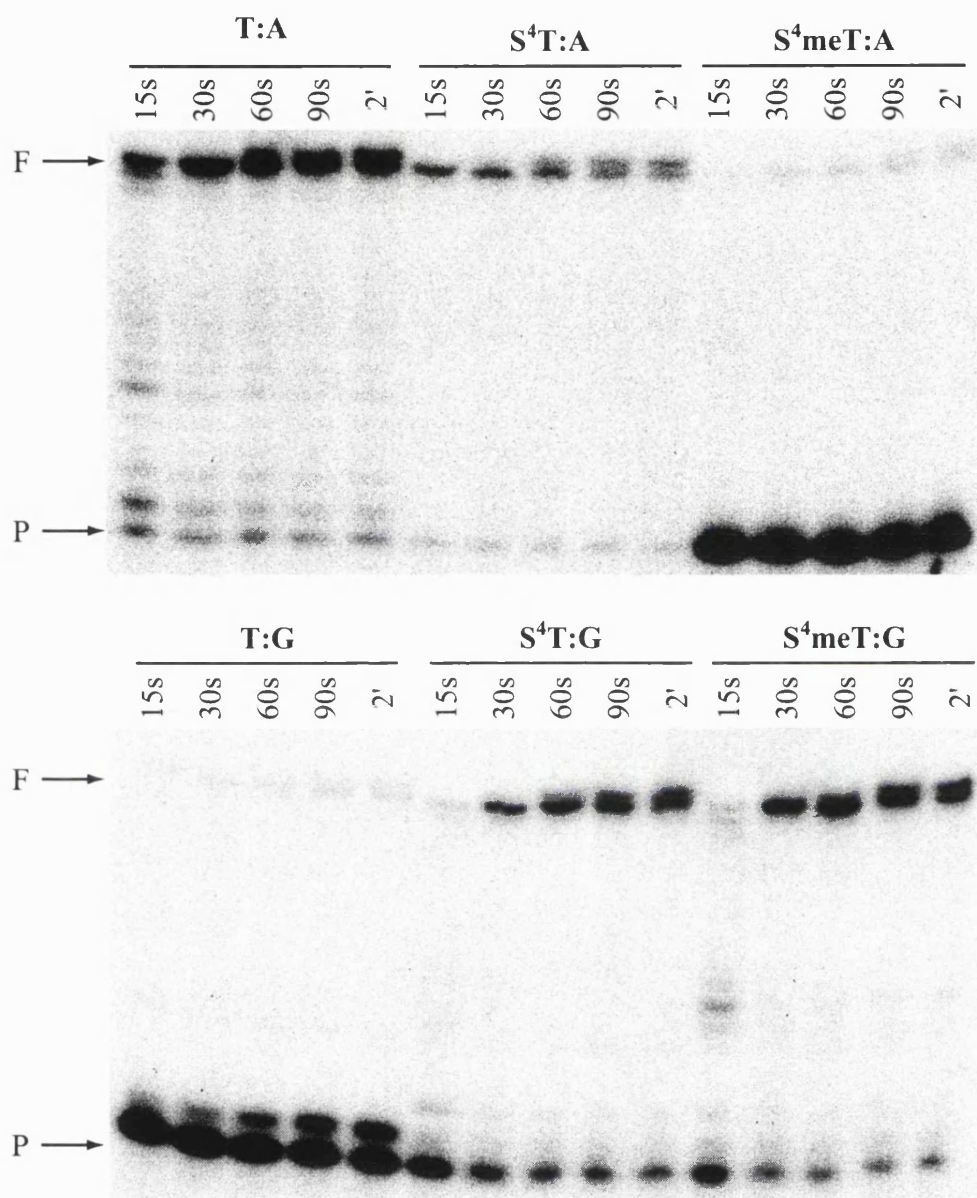


Figure 5.9 Extension of Terminal Base Pairs by Exonuclease-deficient Klenow Fragment

Conditions for determining the extension of mismatched termini were essentially the same as Fig 5.8 except that that a 5'-³²P end-labelled 16mer primer was used. The terminal base of the primer was either A generating T:A, S⁴T:A or S⁴meT:A terminal mismatches (top panel) or G (lower panel). Annealed template:primer pairs were extended by exonuclease-deficient Klenow fragment in the presence of all 4 dNTPs for 15 to 120 seconds at 37°C. Products were denatured and separated as before.

The position of the primer (P, 16 bases) or the full length product (F, 34 bases) are indicated.

CHO-D422 were grown for 3 days in the presence of 100 μ M S⁴TdR in DFCS and then for a further 5 days in the absence of S⁴TdR to allow for expression of the mutant phenotype. Cells were plated in 8-azaadenine and the number of 8-azaadenine resistant colonies scored. The results are summarised in Table 5.1.

The results of the three experiments indicate that S⁴TdR is a poor mutagen. Growth in 100 μ M S⁴TdR increased the frequency of 8-azaadenine resistant cells by only 1.4-2 fold. S⁶G is also a poor mutagen. Growth in non-toxic concentrations of S⁶G increases the frequency of HGPRT mutations by a factor of around 2-fold (Glaab *et al.*, 1998). It seems likely that the weak mutagenicity of both thiobases reflects both the ability of the non-methylated base to code as a normal base (i.e. S⁶G as G and S⁴TdR as TdR) and/or the small fraction of DNA-S⁶G or -S⁴TdR that undergo S-methylation to premutagenic products.

Table 5.1 Mutation Frequency Induced by S⁴TdR

	Mutation Frequency ($\times 10^{-5}$)	Average ($\times 10^{-5}$)	Relative Increase
- S ⁴ TdR	1.9, 3.3, 5.2	3.5	
+ S ⁴ TdR	4.0, 3.9, 7.3	5.1	1.5

CHO-D422 cells were grown in media containing 10% DFCS and 100 μ M S⁴TdR for 3 days. Cells were then transferred to complete media without S⁴TdR and grown for a further 5 days and then plated at a density of 5×10^5 per 10cm dish in 0.4mM 8-azaadenine. Colonies were scored after a further 10 days growth.

At least 30 dishes (1.5×10^7 cells) were analysed per experiment and three independent determinations are shown.

Recognition of S⁴TdR and S⁴meTdR Base Pairs by hMutS α

Recognition of S⁶meG:C/T base pairs is a prerequisite for the engagement of mismatch repair and the subsequent toxicity of S⁶G. Using a gel retardation assay that detects binding to both a single G:T mismatch (Griffin *et al.*, 1994) and to S⁶meG:T base pairs (Waters and Swann, 1997), no binding was seen to a S⁴T:G,

S⁴meT:A or S⁴meT:G base pair by a HeLa cell extract (Fig 5.10A). Under the same conditions, binding was observed to a S⁴T:A base pair. In order to test the specificity of this binding, competition experiments using an oligonucleotide containing a labelled G:T mismatch were performed (Fig 5.10B). Binding to the labelled G:T mismatch was reduced by a 10-fold excess of unlabelled G:T competitor and abolished by the addition of a 50-fold excess of the same competitor. No reduction in binding was observed with up to 100-fold excess of cold G:C, S⁴T:G, S⁴meT:A or S⁴meT:G. Single-stranded S⁴TdR- or TdR-containing oligonucleotides also had no effect. In contrast, cold S⁴T:A competitor reduced binding to the labelled G:T substrate in a dose dependent fashion. Addition of a 50-fold excess of S⁴T:A reduced binding to about 50% and 100-fold to 25%. Direct binding by extensively purified hMutS α produced similar results (Fig 5.10C). No binding was observed to either S⁴T:G, S⁴meT:A or S⁴meT:G (data not shown for S⁴meT:G). As before, S⁴T:A was bound weakly. Binding to the modified base pair was approximately 3-fold less efficient than to a single G:T mispair. Under these conditions, S⁴T:A base pairs are a weak substrate for recognition by hMutS α .

To investigate any potential effects due to sequence, a second set of oligonucleotides were prepared. S⁴TdR or S⁴meTdR was placed in a sequence in which G:T, O⁶-meG:C/T and O⁴meT:A base pairs are recognised (Duckett *et al.*, 1996). Using these conditions, binding by cell extracts was observed to G:T and S⁴meT:G pairs but not to S⁴T:A, S⁴T:G or S⁴meT:A (Fig 5.11A). Binding to S⁴meT:G base pairs occurred with an efficiency comparable to a G:T mispair. Jurkat cells are defective in one member of the hMutS α heterodimer, hMSH2, and are unable to bind to a G:T mispair (Lane 1, Fig 5.11B). No hMutS α dependent binding was seen to any of the S⁴TdR or S⁴meTdR containing oligonucleotides. These data suggest that, in this sequence, hMutS α is able to recognise and bind to a S⁴meT:G base pair.

Despite the reproducibility of the binding experiments, the feeble binding and apparent dependence on sequence indicates that caution must be applied when attempting to interpret these results. In a particular 34mer sequence, hMutS α is able to recognise a S⁴T:A containing base pair but not when the same base pair is in a different 31mer sequence.

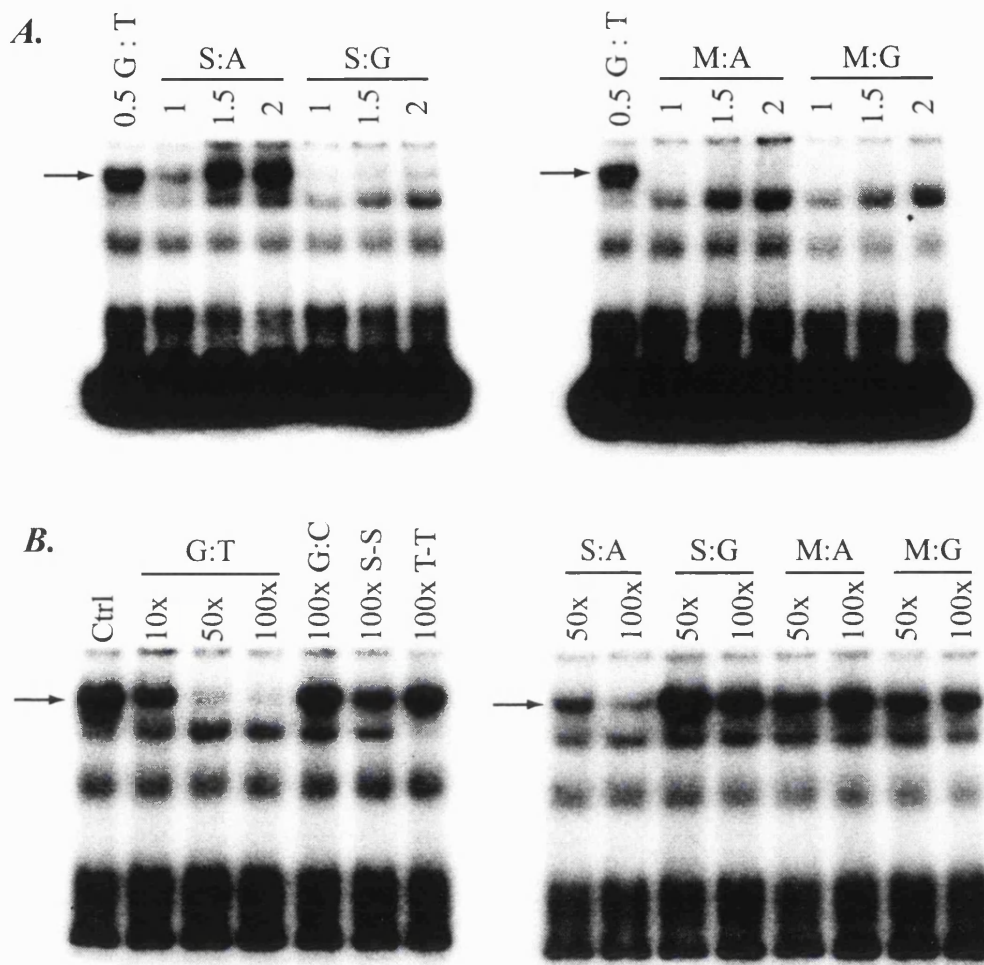


Figure 5.10 hMutS α Binding to a 34mer Containing S⁴TdR or S⁴meTdR Base Pairs

The oligonucleotide AAT TCC CGG GGA TCC GTA XGC CTG CAG CCA AGC T where X = T, S⁴TdR (S) or S⁴meTdR (M) was annealed to the complementary strand to generate G:T, S:A, S:G, M:A or M:G pairs.

A. Oligonucleotide duplexes were incubated with increasing amounts of HeLa extract for 20 min at room temperature and products were then separated on 6% native polyacrylamide gels. The number above the gel indicates the volume (in μ l) of extract used.

B. 0.5 μ l HeLa extract was incubated with ³²P end-labelled G:T duplex and no competitor (lane 1) or increasing amounts of cold G:T (lanes 2-4), G:C (lane 5), single stranded S⁴TdR (lane 6), single stranded TdR (lane 7), S⁴T:A (lanes 8 & 9), S⁴T:G (lanes 10 & 11), S⁴meT:A (lanes 12 & 13) or S⁴meT:G (lanes 14 & 15) competitor duplexes at the fold excesses indicated.

C. ³²P-labelled Oligonucleotide duplexes containing a single G:T, S⁴T:A, S⁴T:G or S⁴meT:A were incubated with extensively purified hMutS α at the volumes indicated (see P.140).

The position of the hMutS α : mismatch complex is indicated by an arrow.

Figure 5.10 C.

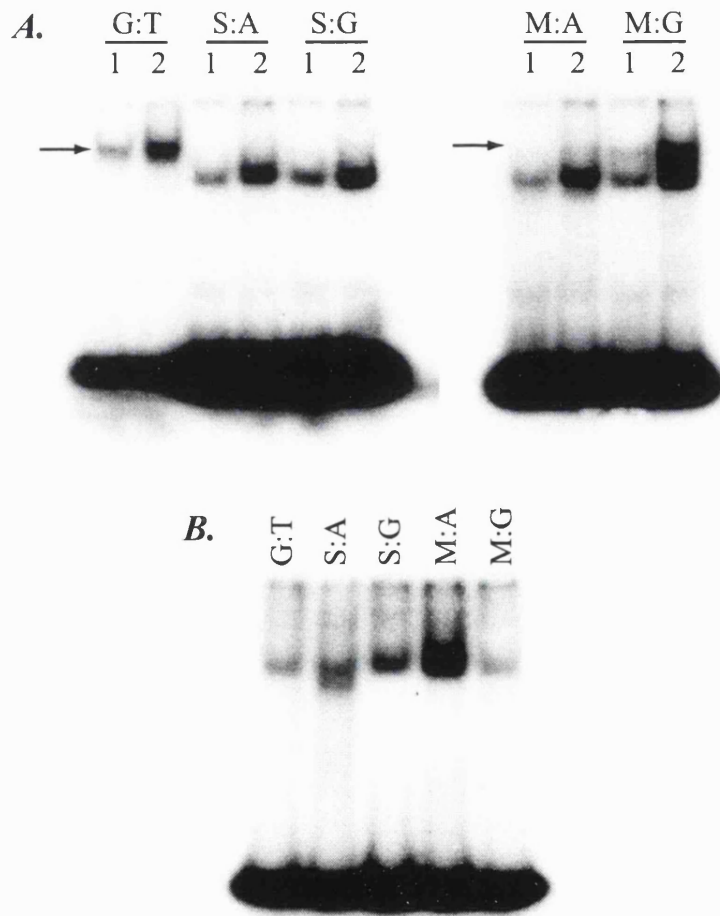
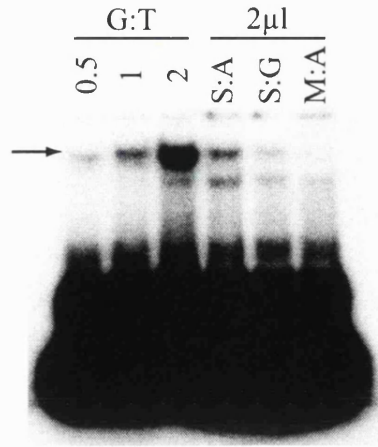


Figure 5.11 hMutS α Binding to a 31mer Containing S⁴TdR or S⁴meTdR Base Pairs

Binding conditions are identical to those in Fig 5.10 except the oligonucleotide sequence:

GCT AGC AAG CTX TCG ATT CTA GAA ATT CGG C is used where X = T, S⁴TdR (S) or S⁴meTdR (M) as before.

A. hMutS α dependent binding in Raji extracts to G:T, S⁴T:A, S⁴T:G, S⁴meT:A or S⁴meT:G duplexes. The number above the gel indicates the volume (in μ l) of extract used.

B. Binding to duplexes by 1.5 μ l of Jurkat extract was performed as in *A.*

Likewise, binding is observed when the 31mer contains a S⁴meT:G base pair but not when the same base pair is contained in the 34mer sequence. From the primer extension data, S⁴T:A and S⁴meT:G are the base pairs favoured by the Klenow fragment of pol I. In addition, the S⁴T:A base pair is thermally stable. Furthermore, both S⁴T:A and S⁴meT:G were efficiently extended.

Finally, if S⁴meT:G was a genuine substrate for MMR *in vivo*, S⁴TdR would be expected to show MMR-dependent cytotoxicity. The ability of MMR to recognise S⁴T:A would be consistent with the absence of toxicity by preventing the incorporation of S⁴TdR into DNA. However, significant substitution of TdR for S⁴TdR is observed. It therefore seems likely that neither S⁴T:A, S⁴T:G, S⁴meT:A or S⁴meT:G is a substrate for hMutS α to a significant degree *in vivo*.

Summary

Unlike the thiopurine S⁶G, S⁴TdR does not display any MMR dependent toxicity at concentrations up to 100 μ M. S⁴TdR was a reasonable substrate for thymidine kinase but a poor substrate for degradation by thymidine phosphorylase. Incorporation of S⁴TdR into DNA occurred at levels of approximately 0.5 to 1% of DNA-thymine. Oligonucleotides containing S⁴TdR underwent *in situ* methylation by MeI with approximately the same efficiency as those containing S⁶G. The presence of S⁴TdR in DNA did not further sensitise cells to either S_N1 or S_N2 methylating agents. Primer extension studies indicate that DNA-S⁴TdR has the same base pairing preferences as TdR; incorporation of A over G was preferred by a factor of greater than a 100-fold. In contrast, S⁴meTdR shows a greater than 30-fold preference for G over A. *In vivo* S⁴TdR was not very mutagenic; growth in 100 μ M caused only a small increase in the mutation frequency. No consistent hMutS α dependent binding was observed. In one sequence, S⁴T:A pairs were a weak substrate for hMutS α but in a different sequence, only S⁴meT:G pairs were recognised.

Thus despite the obvious similarities in the properties of S⁶G and S⁴TdR, the thiopyrimidine is non-toxic. I conclude that DNA-S⁴meT is not a toxic lesion unlike DNA-S⁶meG. Analysis of the coding properties of the thiopyrimidine has revealed important differences in the behaviour of DNA-S⁴meT compared to S⁶meG that may explain their discrepant toxicities.

Discussion

The thiopurines, 6-mercaptopurine and 6-thioguanine are used in the treatment of acute leukaemia. They are metabolised by the purine salvage pathway to 2'-deoxy-6-thioguanosine triphosphate and incorporated into DNA. Both exhibit delayed cytotoxicity consistent with the need for incorporation and subsequent replication. One favoured model for the cytotoxic action of 6-thioguanine suggests that following incorporation into DNA, a small fraction of the incorporated S⁶G undergoes *in situ* methylation by SAM. This generates DNA-S⁶meG. Replication of DNA-S⁶meG produces substrates for MMR. Interaction of these substrates with MMR leads to cell death (Swann *et al.*, 1996).

S⁶meG is structurally similar to, and closely mimics the behaviour of, O⁶meG. This type of DNA base damage is induced by S_N1 methylating agents like MNU and MNNG. Like S⁶G, S_N1 methylating agents show delayed cytotoxicity that is thought to depend on the DNA replication of the DNA-O⁶meG residues and the subsequent interaction of MMR with the resultant base pairs. It is hypothesised that repeated repair attempts trigger cell death through the generation of double strand breaks (Karran and Bignami, 1996). Consequently cells defective in mismatch repair show resistance to killing by S_N1 methylating agents and exhibit cross-resistance to S⁶G (Aquilina *et al.*, 1990).

Despite meeting many of the necessary criteria for a potential cytotoxic agent, S⁴TdR was not cytotoxic. The only significant difference identified between S⁴meTdR and S⁶meG was their base pairing properties. I suggest that this is responsible for the lack of S⁴TdR dependent toxicity. The two bases that are known to provoke MMR-dependent cell killing, O⁶meG and S⁶meG, both code ambiguously. O⁶meG preferentially directs the incorporation of T over C by a factor of about 3 to 4 (Tan *et al.*, 1994) while S⁶meG shows no preference for C or T (Swann *et al.*, 1996). None of the base pairs formed by O⁶meG or S⁶meG are thermodynamically favoured and they also exhibit altered geometries. These base pairs therefore resemble DNA mismatches and all considerably destabilise the DNA duplex. This is consistent with their recognition by mismatch repair as neither methylated base:pyrimidine combination resembles a perfect base pair. Both O⁶meG:C and O⁶meG:T are

recognised by hMutS α in *in vitro* binding assays with a preference of T over C (Duckett *et al.*, 1996; Griffin *et al.*, 1994). hMutS α preferentially binds S⁶meG:T pairs (Swann *et al.*, 1996) and shows very little activity on S⁶meG:C pairs except curiously in the sequence CpS⁶meG (Waters and Swann, 1997). Tan *et al.* (Tan *et al.*, 1994) suggest that the critical factor for the preferred base is not the thermodynamic stability of the base pair or the number of H-bonds but the conformation of the phosphodiester bond. For O⁶meG, base pairing with C produces the most energetically stable pair with the greatest number of H-bonds but T is the base that is preferentially inserted during replication. From NMR studies, O⁶meG:C forms a wobble base pair while O⁶meG:T retains, more or less, the Watson-Crick conformation. The distorted phosphodiester links and the stereochemical problems encountered are consistent with the slow incorporation of C opposite O⁶meG by Klenow Fragment of *E. coli* Pol I in a primer-template system (Tan *et al.*, 1994).

Methylation by SAM is essential for the toxicity of S⁶G. Unmethylated S⁶G does not particularly miscode. S⁶G preferentially directs the insertion of C during replication by a factor of at least 100-fold (Rappaport, 1993). S⁶G:T base pairs are recognised by hMutS α (Griffin *et al.*, 1994) but the frequency of misincorporation is likely to be too low for S⁶G:T to be responsible for the MMR-dependent toxicity (Swann *et al.*, 1996). Similarly S⁴TdR shows a very strong preference for the 'correct' base, an A, by a factor of at least 100-fold. Without prior methylation, neither S⁶G nor S⁴TdR is likely to code ambiguously like O⁶meG.

In contrast to the ambiguous coding properties of both O⁶meG and S⁶meG, S⁴meTdR exhibits a strong preference for the incorporation of G over A by a factor of at least 30. S⁴meTdR resembles a minor product of S_N1 DNA methylation, O⁴meTdR. Primer extension studies examining the base pairing properties of O⁴meTdR reveal that like S⁴meTdR, O⁴meTdR shows a significant preference for G over A. Additionally, O⁴meT:A terminal mismatches are not extended by exonuclease deficient Klenow fragment whereas O⁴meT:G pairs are extended with an efficiency comparable to T:A (Dosanjh *et al.*, 1993). This preference is probably due to the Watson-Crick confirmation being retained in the O⁴meT:G pair whereas O⁴meT:A adopts Wobble pairing. Significantly, the hMutS α MMR recognition complex

recognises O⁴meT:A but not O⁴meT:G (Duckett *et al.*, 1996). It seems likely that the close resemblance of O⁴meT:G and S⁴meT:G pairs to a matched T:A pair underlies their inability to interact with MMR.

Consistent with these base pairing properties, comparative mutagenesis studies in *E. coli* indicate that DNA-O⁴meT is more mutagenic than DNA-O⁶meG (Dosanjh *et al.*, 1991; Pauly *et al.*, 1998). DNA-O⁴meT caused predominantly T → C transitions which is consistent with the known coding properties of this base. Subsequently, S⁴meTdR would be expected to be highly mutagenic and exhibit a T → C transition mutation spectra. My experiments indicate that S⁴TdR causes a very small increase in the frequency of mutation at the CHO *APRT* locus. Examination of the data for S⁶G (Glaab *et al.*, 1998) indicate that S⁶G is also only weakly mutagenic even in a MMR-defective background at high S⁶G concentrations. This can be explained by the calculations of Swann *et al.* (Swann *et al.*, 1996) who estimate the number of S⁶meG to be about 1.2 per 10⁶ nucleotides or about 10³ per cell. Assuming the value to be similar for S⁴TdR, this would account for the very modest increase in mutation frequency that I observe.

In conclusion, S⁴TdR shows no MMR dependent cytotoxicity. I attribute its lack of toxic effect to the inability of both DNA-S⁴TdR and DNA-S⁴meTdR to code ambiguously during replication. S⁴T:A and S⁴meT:G base pairs are formed with a preference of at least 30-fold over the other pyrimidine (c.f. O⁶meG / S⁶meG which show no real preference). Neither of these preferred base pairs is recognised by MMR and subsequently is therefore unable to induce cell death.

By combining this work with that of Peter Swann's group, is it possible to identify any common factors that determine what MMR recognises? In addition to binding its natural substrates (single base mismatches and 1 or 2 base pair loops (Macpherson *et al.*, 1998), hMutS α has been shown to bind to DNA damage that resembles base mispairs namely O⁶meG:C, O⁶meG:T, O⁴meT:A, S⁶G:T, S⁶meG:C and S⁶meG:T pairs (Duckett *et al.*, 1996; Griffin *et al.*, 1994). In addition, it has also been shown *in vitro* to bind a wide diversity of DNA damage including 1,2-intrastrand cisplatin (Duckett *et al.*, 1996; Yamada *et al.*, 1997), AAF and AAAF (Li *et al.*, 1996), benz(a)pyrene (Wu *et al.*, 1999) and even exocyclic DNA adducts that are the

products of lipid oxidation (Johnson *et al.*, 1999). This has led to suggestions that MMR is a general sensor of DNA damage. My observations with S⁴TdR and S⁴meTdR do not support this conclusion. Instead, I suggest that rather than being a general sensor of DNA damage, hMutS α recognises, in a highly selective manner, structures generated within the DNA by incorrectly paired bases. Is it possible to further define the features required for interaction with hMutS α ?

Comparing O⁶meG with O⁴meT indicates that the confirmation of the base pair is not the feature that MMR recognises (Fig 5.12). O⁴meT:A and O⁶meG:C adopt the wobble confirmation while O⁴meT:G and O⁶meG:T maintain the Watson-Crick confirmation (see Fig 5.12 for structures, (Kalnik *et al.*, 1988a; Kalnik *et al.*, 1988b; Tan *et al.*, 1994)). However, both O⁶meG:C and T and O⁴meT:A are bound by hMutS α indicating that there is no discrimination between a wobble or Watson-Crick pairing. Similarly, the number of H-bonds does not define which bases are recognised. Both O⁴meT:A and O⁴meT:G have one H-bond but hMutS α recognises only the A pairing thus ruling out this feature. Thermostability is another property that can be easily eliminated. Substitution of a G for S⁶G in a perfectly matched 12-mer reduces the melting temperature by 13.3°C. S⁶G:C base pairs are not recognised by hMutS α (Griffin *et al.*, 1994) eliminating this as a potential factor.

Under the conditions tested S⁴T:G, even though expected to resemble a mismatch (c.f. S⁶G:T), was not bound by hMutS α . A potential explanation for this is the behaviour of the mismatched termini. S⁴T:G termini, even though rarely formed, were extended by exonuclease-deficient Klenow fragment with about the same efficiency as a perfectly matched T:A. For O⁶meG, extension of O⁶meG:T pairs is much more efficient than for O⁶meG:C due to the positioning of the 3'-OH. Perhaps the same is true for S⁴T:G. The extension is efficient because the 3'-OH is in the correct orientation to allow addition of the next base. Even though the 3'-OH of O⁶meG:T is in the correct orientation, this pairing is better recognised so the distortion with respect to the 3' base is not critical.

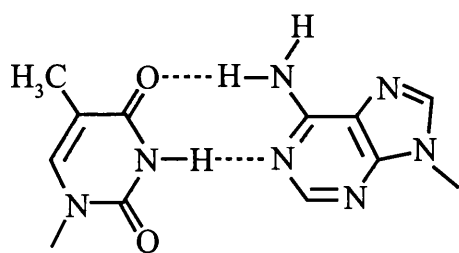
S⁴meT:A base pairs were rarely formed but in contrast to S⁴T:G these were not extended by Klenow fragment. From the O⁴meT data, this was also expected to be a

good substrate for MMR. However no binding was seen. Perhaps in this case, the extra size of the sulphur atom causes too much extra helical distortion rendering it a substrate for NER rather than MMR.

In the last twelve months, the crystal structure of *Escherichia coli* MutS complexed with a G:T mismatch (Lamers *et al.*, 2000) and *Thermus aquaticus* MutS complexed with a single unpaired T residue (Obmolova *et al.*, 2000) have been reported. The general structure has been suggested to resemble a pair of praying hands (Jiricny, 2000) and behave as a functional heterodimer in which only one of the subunits binds to and recognises the mismatch. MutS makes direct contact with the G:T mismatch *via* insertion of a phenylalanine residue stacking onto the thymine and direct H-bonding to the thymine from a glutamate sidechain. An interesting and potentially relevant observation is that on mismatch binding, the MutS dimer bends the DNA by approximately 60° in order to gain access to the minor groove. The energy required to do this is most likely lower at mismatch sites than in regular B-form DNA (Sixma, 2001). It is therefore believed that the MutS dimer scans DNA testing for weakened Watson-Crick H-bonding and base-base stacking interactions.

DNA bending studies looking at global distortions of the DNA molecule (Georgiadis *et al.*, 1991; Voigt and Topal, 1990) have discovered an interesting property of mismatches and methylated base pairs. G:T, A:C, O⁶meG:C, O⁶meG:T and O⁴meT:A but not O⁴meT:G have an anisotropic (asymmetrical) component to the helical distortion induced by these lesions. This results in the DNA being bent. Similarly, a 1,2{GG} cisplatin adduct bends DNA by approximately 70° (Jamieson and Lippard, 1999). All the DNA lesions that are recognised by mismatch repair (G:T, A:C, O⁶meG:C, O⁶meG:T, O⁴meT:A and 1,2{GG}) induce some asymmetrical DNA bending. O⁴meT:G, which is not recognised by MutS α , does not induce any distortion. MutS α may recognise these because the energy required to bend the DNA to about the 60° angle required for interaction with MSH6 is reduced due to the bending already induced by the lesion. It is not possible to correlate the degree of binding by MutS α with the amount of bending as both are dependent on sequence contexts.

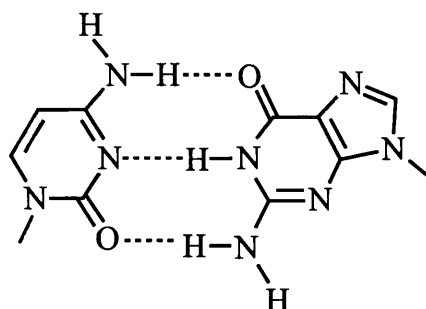
1.



T

A

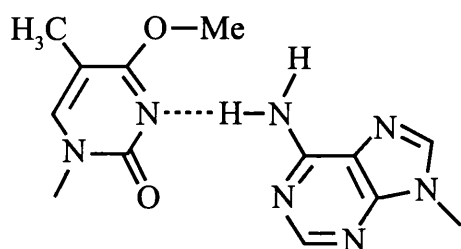
2.



C

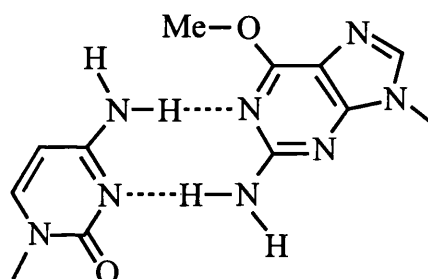
G

3.

O⁴meT

A

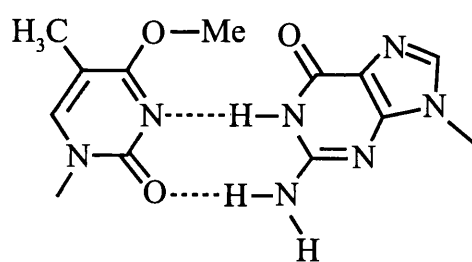
4.



C

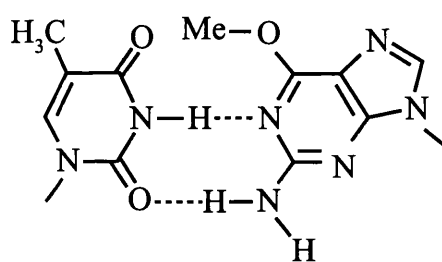
O⁶meG

5.

O⁴meT

G

6.



T

O⁶meG

Figure 5.12 Structure of Base-pairing Confirmations

1. T:A Watson-Crick

2. C:G Watson-Crick

3. O⁴meT:A Wobble

4. C:O⁶meG Wobble

5. O⁴meT:G Watson-Crick

6. T:O⁶meG Watson-Crick

These observations would suggest that mismatch repair does not recognise localised DNA perturbations due to either DNA damage or base mispairing but the more global effects on the DNA molecule (i.e. bending) induced by the heterogeneity. In summary, DNA lesions that provoke MMR dependent cell death must fulfil two requirements.

Firstly they must be efficiently replicated but upon replication code ambiguously and secondly, that these ambiguous base pairs structurally resemble normal mismatched (i.e. G:T or A:C) base pairs.

Chapter 6: Results IV

4-thiothymidine And Other DNA Thiobases As UVA Photosensitisers

S⁴TdR preferentially absorbs light in the UVA range with a maximum at around 335nm (Fig 1.17). This distinguishes it from normal DNA constituents and endows it with distinctive photochemical properties. Upon UVA irradiation, S⁴TdR can undergo a number of chemical reactions including reaction with an adjacent pyrimidine base to form a structure resembling a (6-4) pyrimidine-pyrimidone dimer. Here, I demonstrate that S⁴TdR incorporated into DNA dramatically sensitises cells to non-toxic doses of UVA light. Cells deficient in NER show enhanced sensitivity indicative of a role for NER in the removal of DNA thiothymidine photoproducts.

Synergistic Toxicity of 4-thiothymidine and UVA Light

UVA light, in the absence of any photosensitising molecule, is not particularly toxic to cultured human fibroblasts. NER-proficient human cells (MRC5VA) were not detectably sensitive to UVA doses below 10kJ/m² and their D₃₇ value for UVA was around 70kJ/m² (Fig 6.1A) which is comparable to published values for NER-proficient, cultured human fibroblasts (Otto *et al.*, 1999). Although not directly toxic, several days growth in S⁴TdR dramatically sensitised cultured human cells to subsequent exposure to non-toxic doses of UVA light ($\lambda = 320-400\text{nm}$). The photosensitising effect of S⁴TdR with UVA was dependent on both UVA dose and nucleoside concentration (Fig 6.1B). Increasing UVA sensitivity was observed between 1 and 300 μM S⁴TdR. At 300 μM S⁴TdR, the D₃₇ value for UVA was reduced to 0.5kJ/m² - a sensitisation factor of greater than 100-fold compared to cells irradiated with UVA alone.

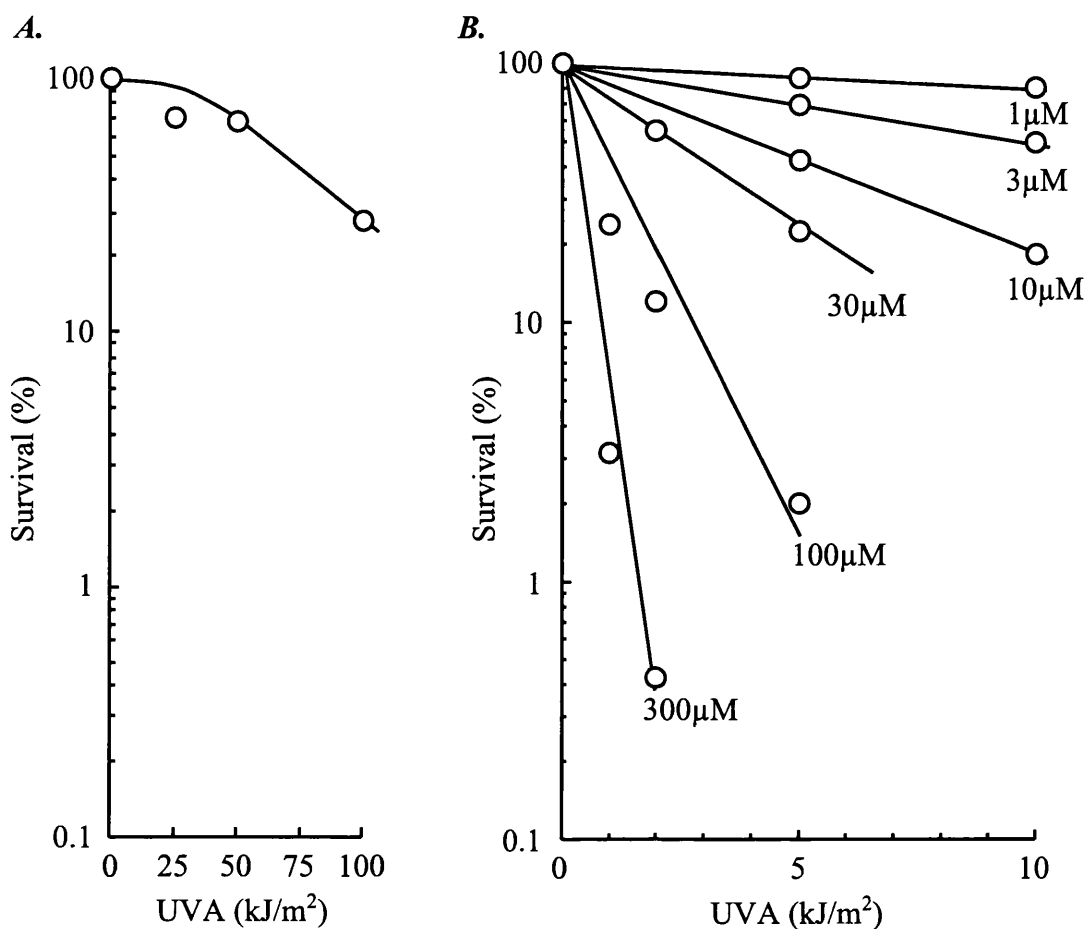


Figure 6.1 Synergistic Toxicity of S⁴TdR and UVA Light in MRC5VA Fibroblasts

A. Exponentially growing MRC5VA cells were washed, trypsinised and appropriate numbers replated in fresh media containing 10% FCS and no S⁴TdR in 6-well plates (4cm well). Cells were allowed to attach for 4-6 hours, washed with PBSA and irradiated under a thin film (≈ 1 mm) of PBSA with a UVH-253 UVA lamp. The dose rate of 0.25 kJ/s/m^2 was calibrated using a UV-A meter. After irradiation, the PBSA was replaced with fresh media containing 10% FCS. Surviving colonies were stained and scored after 10 days.

B. MRC5VA cells were grown for 3 days in medium containing 10% dialysed fetal calf serum and the concentration of S⁴TdR indicated. Cells were irradiated at a dose rate of 0.1 kJ/s/m^2 and survival determined as above.

Sensitivity was assessed by D_{37} values (the UVA dose required to reduce survival to 37%). One 6-well plate per UVA dose was used and each value represents the mean of two independent experiments.

Synergistic Toxicity Requires Active Thymidine Kinase

In order to sensitise cells to UVA light, S⁴TdR must first be salvaged by the thymidine kinase dependent pyrimidine salvage pathway. Raji cells grown in 100µM S⁴TdR for 3 days before being exposed to 8kJ/m² UVA underwent growth arrest and cell death (Fig 6.2A). TK⁻ variant Raji cells treated under identical conditions proliferated for ≥ 7 days. Their rate of proliferation was indistinguishable from control cells grown in the absence of S⁴TdR before being irradiated with 8kJ/m² UVA (Fig 6.2B). As expected, neither Raji variant was affected by growth in 100µM S⁴TdR (Fig 5.1).

Effects of NER Deficiency on the Cytotoxicity of S⁴TdR and UVA

NER-defective *xeroderma pigmentosum* (XP) human fibroblasts were slightly more sensitive to UVA than MRC5VA probably due to the generation of some photodimers by this wavelength (Kielbassa and Epe, 2000). The D₃₇ value for UVA in XP12RO was about 25kJ/m² (Fig 6.3A). UVA alone was not detectably toxic at fluences less than 5kJ/m² which is 50-fold higher than the highest dose used in combination with S⁴TdR. XP12RO and GM04429F (both XP complementation group A) and GM08437B (XP complementation group F) fibroblasts were substantially more sensitive to the combined effects of S⁴TdR / UVA than the NER-proficient line MRC5VA (Fig 6.3B). Under standard conditions of 100µM S⁴TdR in dialysed FCS, XP12RO was the most sensitive of the lines with a D₃₇ value for UVA of 0.04kJ/m². For GM04429F and GM08437B the D₃₇ values were 0.07 and 0.16kJ/m² respectively. For MRC5VA, under identical conditions, the D₃₇ value was 1.2kJ/m². S⁴TdR and UVA treatment is approximately 10-30 times more toxic in NER-deficient cells than in NER proficient fibroblasts grown under identical conditions. Since NER-proficient cells are sensitised ~100-fold to UVA by S⁴TdR, UVA dose modifications of the order of 1000-fold are therefore possible in NER-defective fibroblasts grown in non-toxic doses of S⁴TdR.

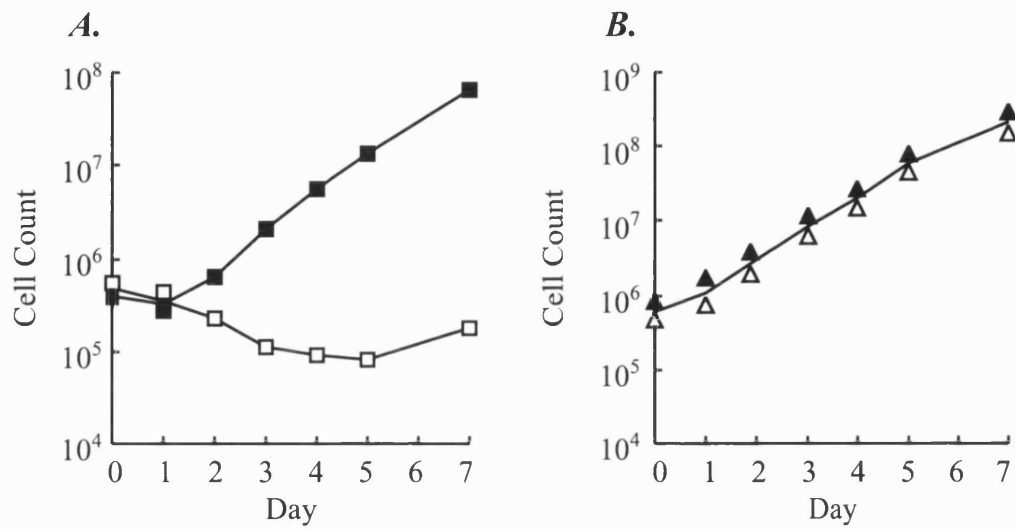


Figure 6.2 S⁴TdR / UVA Cytotoxicity Depends on Active TK

Raji Burkitt's lymphoma cells (A) or the TK⁻ variant (B) were grown for 3 days in medium containing 100 μ M S⁴TdR and 10% dialysed FCS. Cells were washed with PBSA and irradiated on day 0 with 8kJ/m² UVA (□△) as a suspension in PBSA. Identical cultures were prepared in the absence of S⁴TdR and irradiated in the same manner (■▲). Approximately 5x10⁵ cells/ml were returned to full growth medium without S⁴TdR and daily cell counts determined using a haemocytometer. The experiment was carried out twice. A representative experiment is shown.

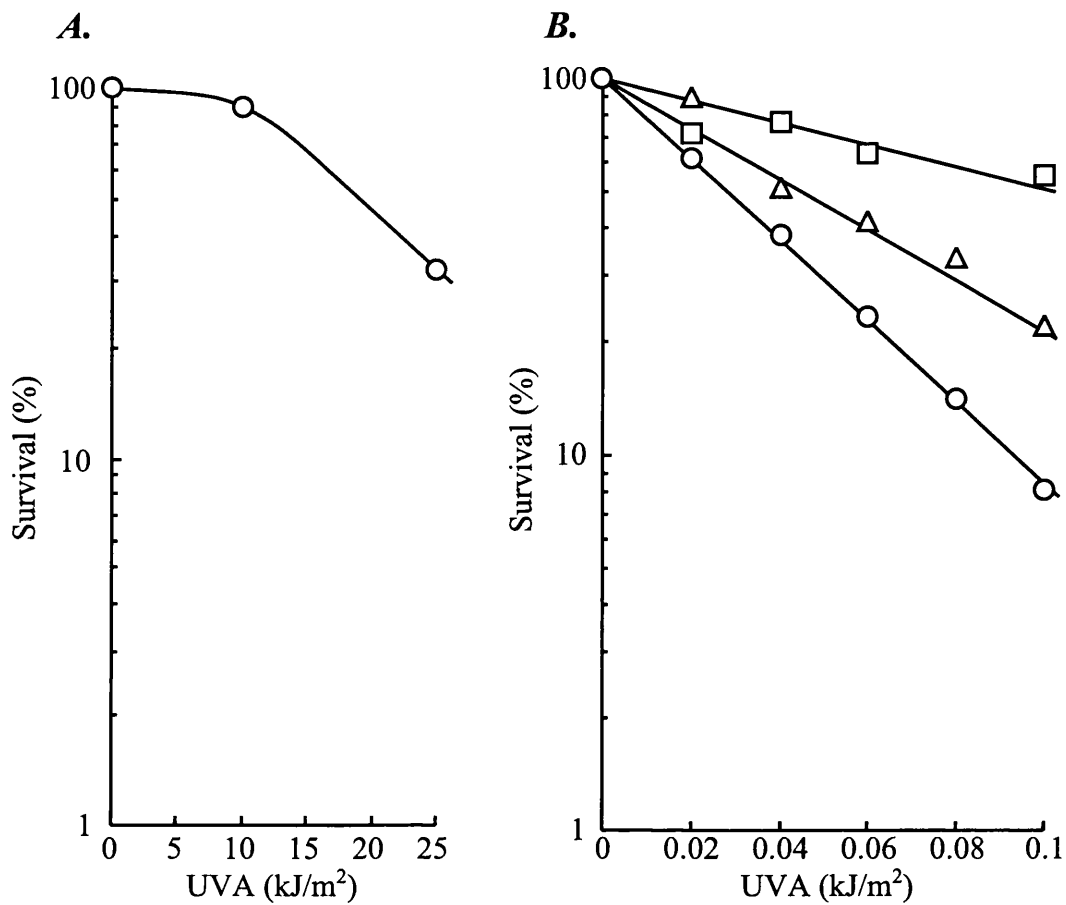


Figure 6.3 Sensitivity of NER-defective XP Fibroblasts to S⁴TdR / UVA

A. XP12RO cells, grown in the absence of S⁴TdR, were irradiated with a UVH-253 lamp at a dose rate of 0.25kJ/s/m². Survival was determined as described previously.

B. XP12RO (○), GM04429F (Δ) and GM08437B (□) were grown for 3 days in media containing 10% dialysed FCS and 100μM S⁴TdR. Cells were washed and plated as before and then irradiated with a VL-6L UVA lamp at a dose rate of 2J/s/m². The dose rate was calibrated using a J-221 meter. Survival was determined as before. Values represent the means of two independent experiments.

GM04429F and GM08437B survivals were carried out by P. Branch.

An Indication of Possible Lethal DNA Lesion - XP129

The XPA 'revertant' XP129 was originally selected from XP12RO. Although XP129 cells have a complex phenotype, they have regained wild type (non-XP) resistance to UVC light as well as the ability to excise DNA (6-4) pyrimidine pyrimidone photoproducts but not cyclobutane pyrimidine dimers (Cleaver *et al.*, 1987). The D_{37} value for S^4TdR / UVA increased from 0.04kJ/m^2 to 0.5kJ/m^2 in XP129 cells (Fig 6.4), an increase of greater than 10-fold. These cells were still 2.4-fold more sensitive than the wild type to the combined effects of S^4TdR / UVA. This result is consistent with a role for a (6-4) pyrimidine pyrimidone like photoproduct in S^4TdR / UVA induced cell death.

Effects of Defective MMR on S^4TdR / UVA Toxicity

It has been suggested that mismatch repair plays an active role in preventing the incorporation of the thymidine analogues bromodeoxyuridine and iododeoxyuridine into DNA (Berry *et al.*, 2000; Berry *et al.*, 1999). From my work in the previous chapter, the gel retardation assays (Fig 5.10 and 5.11) suggest that hMutS α may recognise $S^4T:A$ pairs in certain sequences. If MMR acts to reduce the incorporation of S^4TdR to a significant degree, MMR defective cell lines should be more sensitive to the combined effects of S^4TdR and UVA. Three different matched pairs of human cells were used to investigate the effects of mismatch repair on S^4TdR / UVA survival.

XP12ROB4 is a MMR defective variant of XP12RO and is doubly defective in XPA and hMSH2 (O'Driscoll *et al.*, 1999). After growth in $100\mu\text{M}$ S^4TdR , the D_{37} value for XP12ROB4 was reduced to 0.01kJ/m^2 , a sensitisation of approximately 3-4 fold compared to the matched MMR-proficient line XP12RO (Fig 6.5A). XP12ROB4 showed the same levels of resistance to UVC (O'Driscoll *et al.*, 1999) and UVA light (data not shown) as the parental line XP12RO. The ovarian carcinoma line A2780-MNU1 is defective in hMLH1. MMR function can be restored by the introduction of a plasmid containing the hMLH1 cDNA (A2780-Clone 1pMLH1A) (Branch *et al.*, 2000).

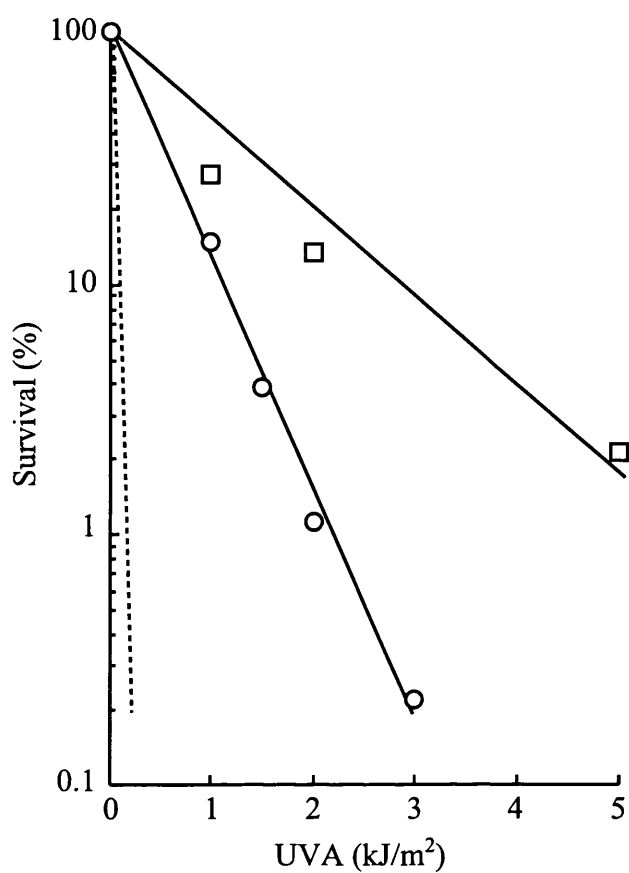


Figure 6.4 Sensitivity of XP129 to S⁴TdR / UVA

The XPA revertant XP129 (○) was grown for 3 days in complete media supplemented with 10% dialysed FCS and 100µM S⁴TdR. Cells were washed, plated and irradiated with a UVH-253 lamp as before. Surviving colonies were stained and scored after 10 days. MRC5VA (□, from Fig 6.1) and XP12RO (....., from Fig 6.3) are shown for comparison.

Values represent the mean of two independent experiments.

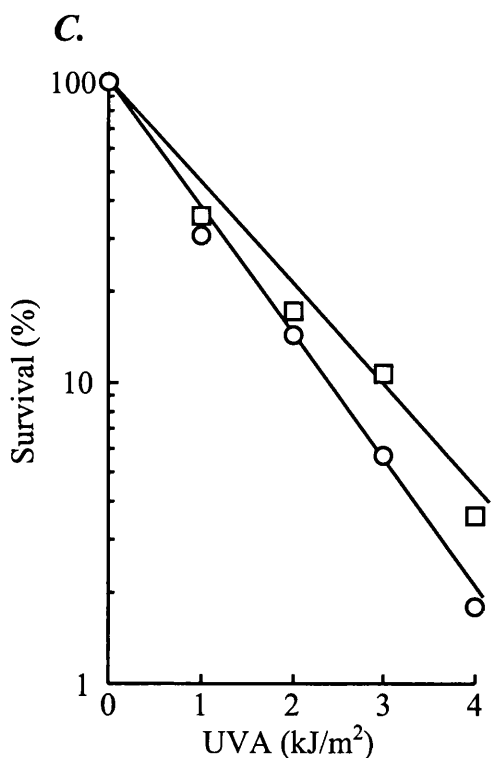
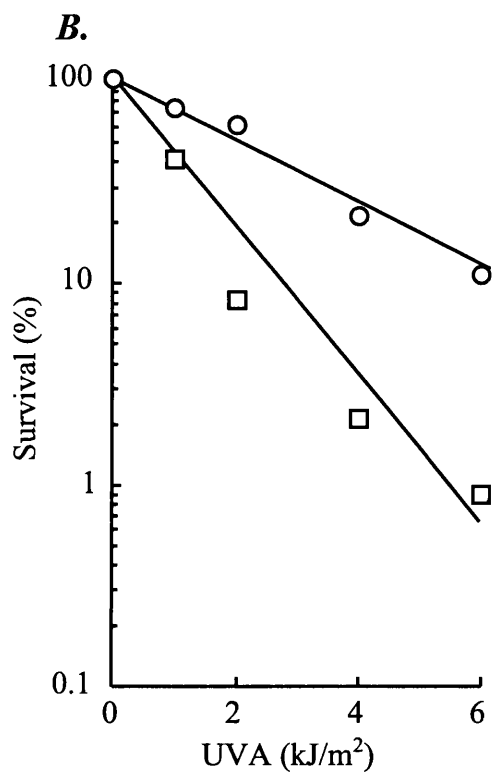
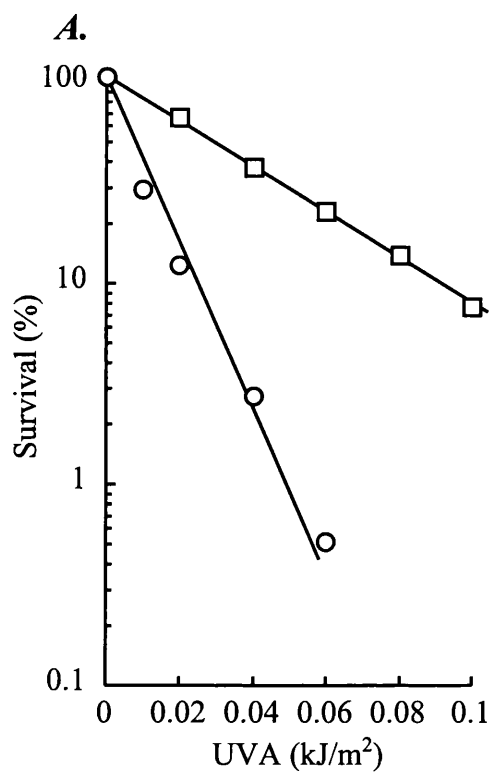


Figure 6.5 Effects of Defective MMR in S⁴TdR / UVA Toxicity

A. XP12ROB4 (MMR⁻, ○) and XP12RO (MMR⁺, □) were grown in media containing 10% dialysed FCS and 100μM S⁴TdR for 3 days. Cells were washed and plated as before and then irradiated with a VL-6L UVA lamp at a dose rate of 2J/s/m².

B. A2780-MNU1 (MMR⁻, ○) and A2780-Clone 1pMLH1A (MMR⁺, □) were grown as above. Cells were irradiated with a UVH-253 UVA lamp at a dose rate of 0.1kJ/s/m². The hMLH1 containing pCMV vector was maintained by the presence of 700μg/ml G418.

C. HeLa Clone 7 (MMR⁻, ○) and HeLa Clone 7#7 (MMR⁺, □) were grown and treated as in B. Chromosome 7 in Clone 7#7 was maintained by the addition of 1mg/ml G418.

The values represent the mean of two independent experiments.

Survivals B and C were performed by P.

Branch.

In this pair of lines, the MMR-defective variant was more resistant ($D_{37} = 2.7\text{kJ/m}^2$) than the MMR-proficient variant ($D_{37} = 1.0\text{kJ/m}^2$, Fig 6.5B). In this case, a defect in MMR increased resistance to $S^4\text{TdR}$ / UVA by a factor of 2.7.

In a third pair of lines, inactivation of MMR had no detectable effect on $S^4\text{TdR}$ / UVA survival. HeLa Clone 7 cells are defective in hPMS2 (Aquilina *et al.*, 1995). MMR was restored by the introduction of a normal copy of chromosome 7 (HeLa Clone 7#7) which contains the hPMS2 gene. Clone 7 ($D_{37} = 0.9\text{kJ/m}^2$) was marginally more sensitive than Clone 7#7 ($D_{37} = 1.2\text{kJ/m}^2$, Fig 6.5C) but this small difference was not deemed to be significant.

In summary, inactivation of MMR did not consistently affect the toxicity of $S^4\text{TdR}$ and UVA light. In the three different pairs of lines tested, MMR defects made the cells more sensitive (XP12ROB4), more resistant (A2780-MNU1) or had no significant effect (HeLa Clone7). Although a contribution of MMR cannot be excluded, the differences observed may be due to small differences in growth rates between the MMR proficient and deficient variants and hence incorporation of $S^4\text{TdR}$.

Exogenous Thymidine Inhibits the Synergistic Toxicity

My preliminary experiments with $S^4\text{TdR}$ and UVA indicated that the extent of synergistic lethality was somewhat variable. In the previous chapter, I presented data that suggest that $S^4\text{TdR}$ is an approximately 10-fold poorer substrate for TK (Fig 5.3). Small quantities of exogenous TdR would be expected to have a significant effect on incorporation of $S^4\text{TdR}$ into DNA, and hence UVA lethality. The concentration in undialysed serum was thought to be low (around $10\mu\text{M}$) and would therefore not have a significant effect. The TS inhibitor aminopterin was used to estimate the concentration of TdR in calf serum. Aminopterin blocks *de novo* TMP synthesis and inhibits cellular growth. This inhibition can be overcome by supplementing the growth media with hypoxanthine and thymidine. The concentration of TdR required to overcome the growth inhibition of Raji cells in medium containing 10% dialysed FCS and $100\mu\text{M}$ hypoxanthine was about $8\mu\text{M}$ (Fig 6.6A). The same cells grown in medium supplemented with 10% undialysed

FCS and 100 μ M hypoxanthine required no additional TdR to overcome the growth inhibitory effects of aminopterin (Fig 6.6B). This indicates that FCS contains at least 80 μ M TdR. Growth in medium containing 10% undialysed calf serum and 100 μ M S⁴TdR reduced the efficiency of killing by UVA compared to cells grown in dialysed FCS. For XP12RO, the D₃₇ was 15-fold higher (0.6kJ/m²) and in MRC5VA, the D₃₇ was 8.7kJ/m² (an 7.3-fold increase, Fig 6.6C). Nevertheless, even in non-dialysed calf serum, a dose-dependent UVA sensitivity was observed between 20 and 100 μ M S⁴TdR (Fig 6.6D).

Effect of Thymidylate Synthase Inhibitors on S⁴TdR / UVA Toxicity

As shown in Chapter 5, S⁴TdR was incorporated into DNA through the thymidine kinase salvage pathway. Inhibition of *de novo* synthesis reduces the contribution of *de novo* synthesis to the thymidine nucleotide pool and could, in principle, facilitate the incorporation of S⁴TdR into DNA. TS inhibitors might potentially enhance S⁴TdR / UVA toxicity still further.

As shown in Fig 6.6A, the growth inhibitory effect of aminopterin can be overcome by supplementing the cells with 100 μ M hypoxanthine and 8 μ M thymidine. Active TK was essential for this reversal. Replacement of TdR by S⁴TdR in combination with aminopterin and hypoxanthine could dramatically increase the amount of DNA-S⁴TdR and hence the sensitivity of cells to UVA. Replacement of TdR with S⁴TdR achieved only a partial restoration of growth at concentrations of 1mM or more (Fig 6.7A). However, examination of the cells under a microscope indicated that the majority generally remained blocked in G2. As discussed previously, MMR may play a role in reducing the incorporation of S⁴TdR into DNA. If this is the case, MMR may be responsible for preventing S⁴TdR reversing the aminopterin block. Jurkat cells are defective in hMSH2. No additional relief of aminopterin induced growth arrest was observed in this cell line (Fig 6.7B). Under the conditions tested, S⁴TdR could not completely reverse the aminopterin-induced block.

5-fluorodeoxyuridine (5FUdR) inhibits TS through a different mechanism to aminopterin. 5FUdR is converted to 5FdUMP by the TK salvage pathway. 5FdUMP binds irreversibly to TS in place of the normal substrate dUMP.

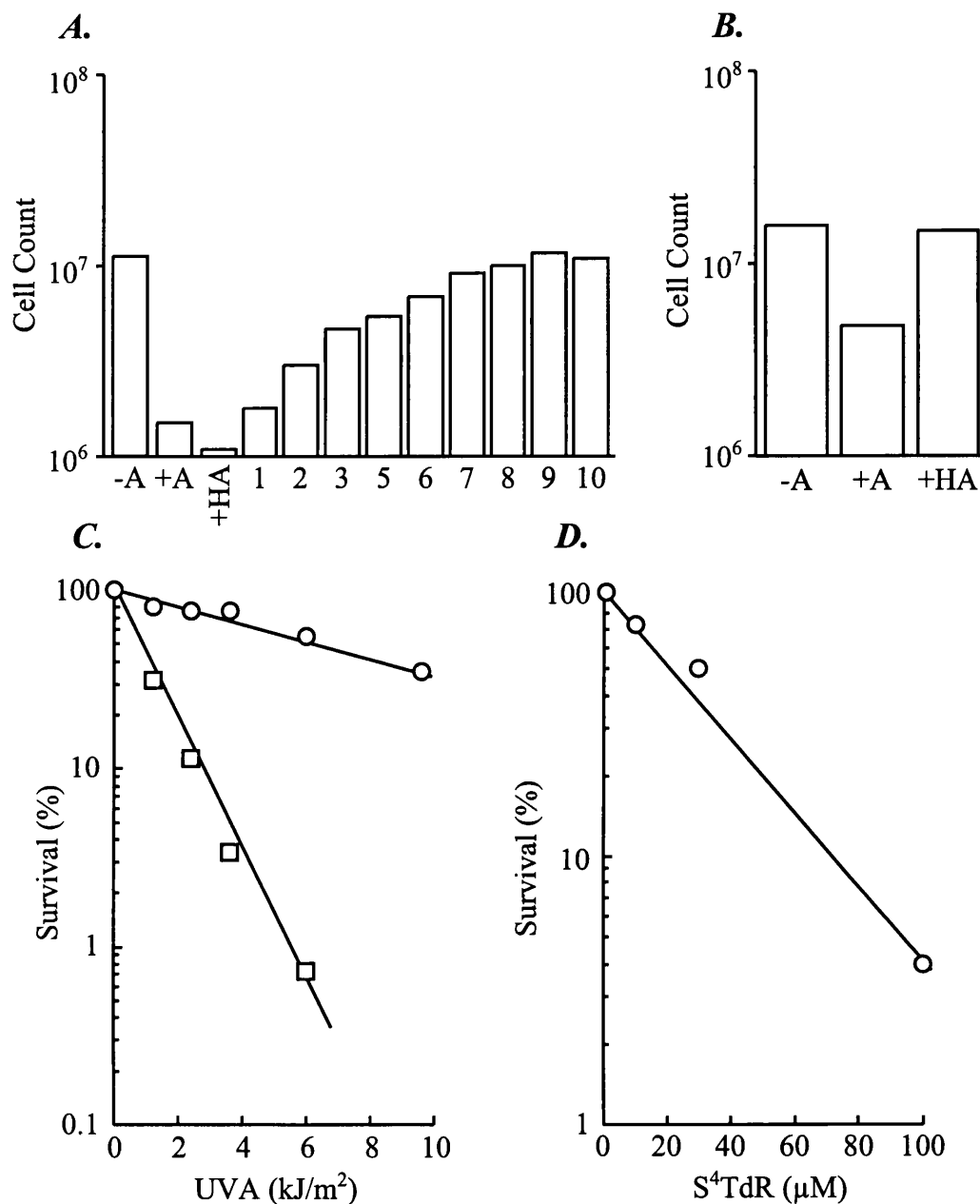


Figure 6.6 Inhibition of S⁴TdR / UVA Toxicity by Exogenous TdR

A. 2×10^5 Raji cells were plated in the absence of any additives (-A), $0.4 \mu\text{M}$ aminopterin (+A), $0.4 \mu\text{M}$ aminopterin / $100 \mu\text{M}$ hypoxanthine (+HA) or $0.4 \mu\text{M}$ aminopterin, $100 \mu\text{M}$ hypoxanthine and increasing concentrations of thymidine (1 to $10 \mu\text{M}$) in media containing 10% dialysed FCS. Growth 3 days later was determined by haemocytometer counts.

B. 2×10^5 Raji cells were plated as above in media containing non-dialysed 10% FCS and growth again determined after 3 days.

C. MRC5VA (○) and XP12RO (□) cells were grown in media supplemented with $100 \mu\text{M}$ S⁴TdR and 10% undialysed FCS for 3 days. Cells were plated, washed, irradiated with a UVH-253 lamp and survival after 10 days determined as before.

D. XP12RO cells were grown as in A in medium containing varying concentrations of S⁴TdR and 10% undialysed FCS and then irradiated as before with 4kJ/m^2 UVA. Survival was determined as previously. Values represent the mean of two independent experiments.

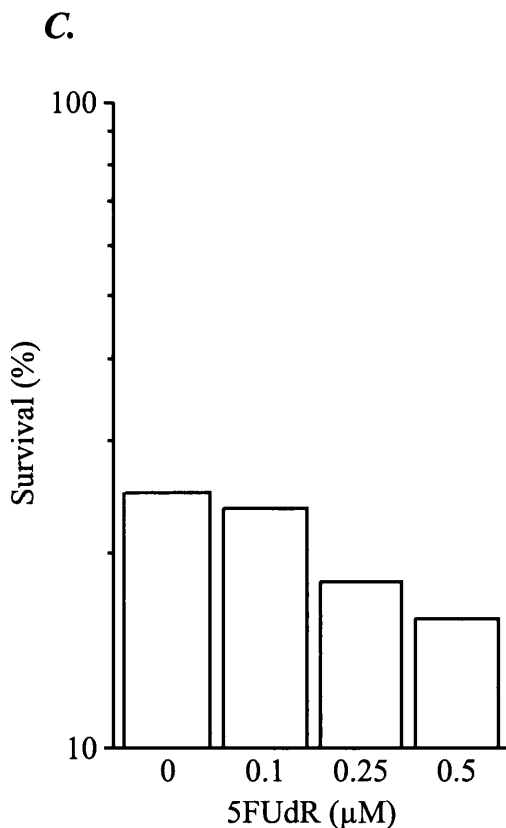
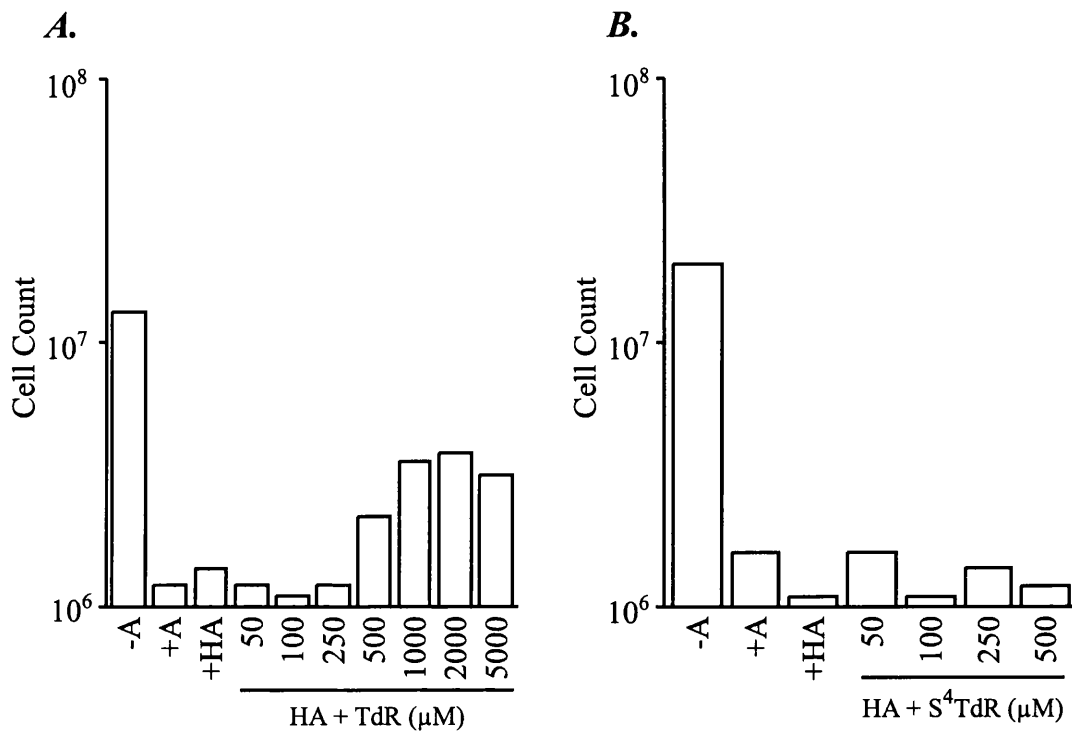


Figure 6.7 Use of TS Inhibitors to Increase the Cytotoxicity of S⁴TdR / UVA

A. 2×10^5 Raji cells were plated in medium containing 10% dialysed FCS, $0.4 \mu\text{M}$ aminopterin, $100 \mu\text{M}$ hypoxanthine and varying concentrations of S⁴TdR ($50 \mu\text{M}$ to 5mM). Growth was determined after 3 days by haemocytometer counts.

B. 2×10^5 Jurkat cells were plated as above. The maximum S⁴TdR concentration used was $500 \mu\text{M}$. Growth was again determined after 3 days.

C. MRC5VA fibroblasts were grown in media containing 10% dialysed FCS, $30 \mu\text{M}$ S⁴TdR and the indicated concentration of 5FUdR for 3 days. Cells were washed and plated as before and then irradiated with 5KJ/m^2 UVA from a UVH-253 lamp. Surviving colonies were stained and scored after 10 days subsequent growth. The value represents the mean of two independent experiments.

5FUdR also exhibits some toxicity independent of its ability to inhibit TS. This is probably through incorporation of the nucleotide into DNA. MRC5VA fibroblasts were grown in the presence of increasing, non-toxic concentrations of 5FUdR and 30 μ M S⁴TdR before being irradiated with UVA. Addition of 5FUdR to the treatment regime did not dramatically increase the sensitivity of cells to S⁴TdR / UVA (Fig 6.7C).

Under the conditions tested, the two TS inhibitors aminopterin and 5FUdR did not markedly increase the cytotoxicity of S⁴TdR / UVA. It should be noted that this analysis is not exhaustive and other TS inhibitors that are in clinical use (for example Tomudex produced by Astra-Zeneca) may prove more useful in this regard.

4-thiodeoxyuridine as a Photosensitiser

Like S⁴TdR, S⁴UdR is probably phosphorylated by TK. S⁴dUMP then enters the *de novo* pathway of pyrimidine synthesis at the TS stage (Kalman *et al.*, 1973) and incorporates into DNA as S⁴TMP. 4-thiodeoxyuridine (S⁴UdR) also exhibited synergistic cytotoxicity with UVA although its effects were more modest when compared to S⁴TdR. Like S⁴TdR, S⁴UdR was non-toxic in the absence of UVA light (data not shown). Growth of XP12RO in 100 μ M S⁴UdR decreased the D₃₇ value for UVA from 25kJ/m² to about 1.8kJ/m², a sensitisation of approximately 14-fold (Fig 6.8). NER-proficient MRC5VA fibroblasts were also slightly sensitised to UVA by S⁴UdR at the highest UVA dose tested (100 μ M S⁴UdR with 10kJ/m² UVA, Fig 6.8). UVA alone shows little toxicity at doses less than about 70kJ/m² and the maximum dose of UVA used (10kJ/m²) was significantly less. S⁴UdR could still have a significant photosensitising effect at higher doses of UVA.

Photosensitising Effects of DNA-6-thioguanine

S⁶G also absorbs in the UVA region with a λ_{\max} of around 365nm and can act as a UVA photosensitiser. I have made a preliminary study of the photosensitising activity of S⁶G towards human cells. This work is much less extensive and many of the experiments have only been carried out once.

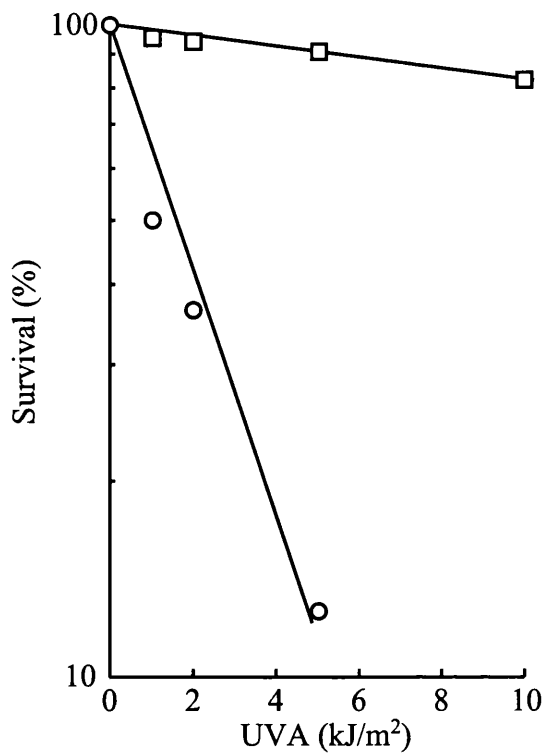


Figure 6.8 S⁴UdR as an Alternative Photosensitiser
 XP12RO (○) and MRC5VA (□) fibroblasts were grown for 3 days in complete media containing 10% dialysed FCS and 100μM S⁴UdR. Cells were plated and washed as before and then irradiated with a UVH-253 lamp at a dose rate of 0.1kJ/s/m². Survival was determined by staining colonies after 10 days growth.

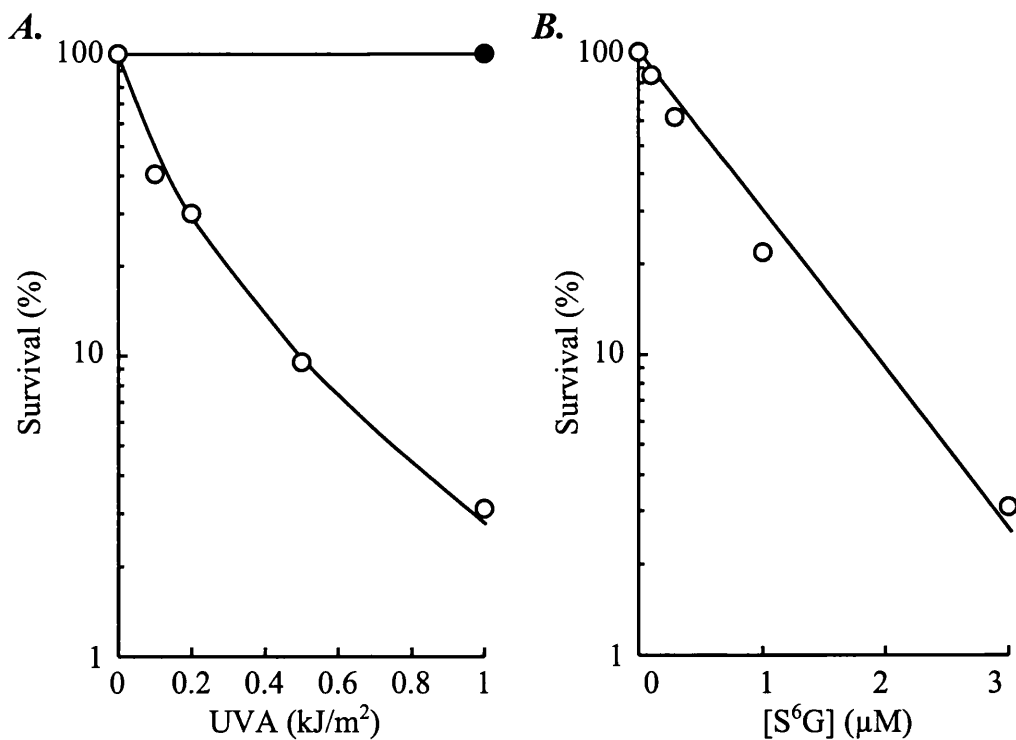


Figure 6.9 S⁶G Sensitises XP12ROB4 Cells to UVA

A. Mismatch repair defective XP12ROB4 cells were grown for 3 days in medium supplemented with (○) or without (●) a non-toxic concentration of S⁶G (3μM) and 10% undialysed FCS. Cells were harvested, irradiated with either a VL-6L (<1kJ/m²) or UVH-253 (>1kJ/m²) lamp and survival determined as described previously.

B. XP12ROB4 cells were grown in the indicated concentration of S⁶G for 3 days before being irradiated with 0.5kJ/m² UVA light from a VL-6L lamp at a dose rate of 5J/m²/s. Survival was determined as above. Values represent the mean of two independent experiments.

MMR defective cells incorporate S⁶G into their DNA without detriment (Aquilina *et al.*, 1990). The hMSH2-defective variant of XP12RO, XP12ROB4 was used to study the phototoxicity of DNA-S⁶G. Growth in 3μM S⁶G was non-toxic to XP12ROB4 and significantly sensitised cells to UVA doses ≥ 0.02kJ/m² (Fig 6.9A) and the D₃₇ value was reduced from 25kJ/m² to approximately 0.2kJ/m², a sensitisation factor of over 100-fold. Like S⁴TdR, the photosensitising effect of S⁶G was dose-dependent and increasing UVA sensitivity was seen at concentrations between 0.1 and 3μM S⁶G (Fig 6.9B).

S⁶G is salvaged through the purine salvage pathway and requires active hypoxanthine guanine phosphoribosyl transferase (HGPRT) for its incorporation into nucleic acids. Active HGPRT was essential for S⁶G / UVA toxicity. An HGPRT defective variant of XP12RO has been isolated that has no detectable HGPRT activity (M. O'Driscoll, PhD Thesis). Growth for 3 days in 10μM S⁶G followed by irradiation with 5kJ/m² UVA had no effect on cell survival (data not shown). I conclude that, like S⁴TdR, S⁶G mediates its synergistic cytotoxicity through incorporation into nucleic acids.

Modulation of S⁶G / UVA Toxicity by NER

HeLa cells are proficient in NER. A MMR defective variant, HeLa Clone 7, does not express detectable levels of hPMS2. Like XP12ROB4, S⁶G combined with UVA light was cytotoxic to HeLa Clone 7 cells. The NER-proficient HeLa Clone 7 was sensitised to a similar extent as the NER-defective XP12ROB4 (Fig 6.10). Although this is a single observation, it suggests that NER may not play a role in processing S⁶G-DNA photoproducts.

S⁶G / UVA Toxicity in MMR-proficient Fibroblasts

Both the toxicity of S⁶G alone, and the combined S⁶G / UVA synergistic cytotoxicity is dependent on the amount of S⁶G incorporated into DNA. The optimal growth time in S⁶G for UVA dependent killing was determined.

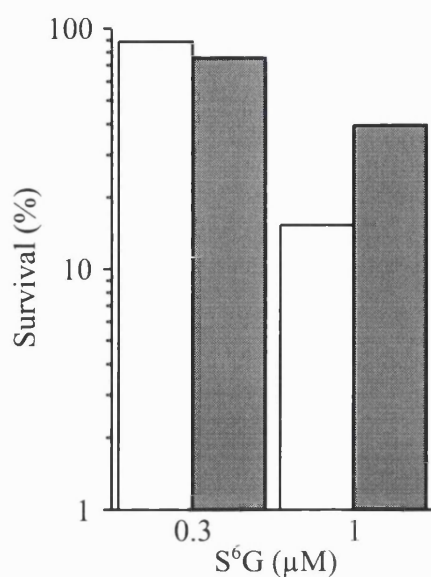


Figure 6.10 Involvement of NER in Processing S⁶G-DNA Photoproducts

HeLa Clone 7 cells (□) were grown in either 0.3μM or 1μM S⁶G for 3 days in media containing 10% undialysed FCS. Cells were washed, plated, irradiated with 0.5kJ/m² UVA (VL-6L lamp) and survival determined as described previously. XP12ROB4 (■) data is shown for comparison. Values represent the mean of two independent experiments.

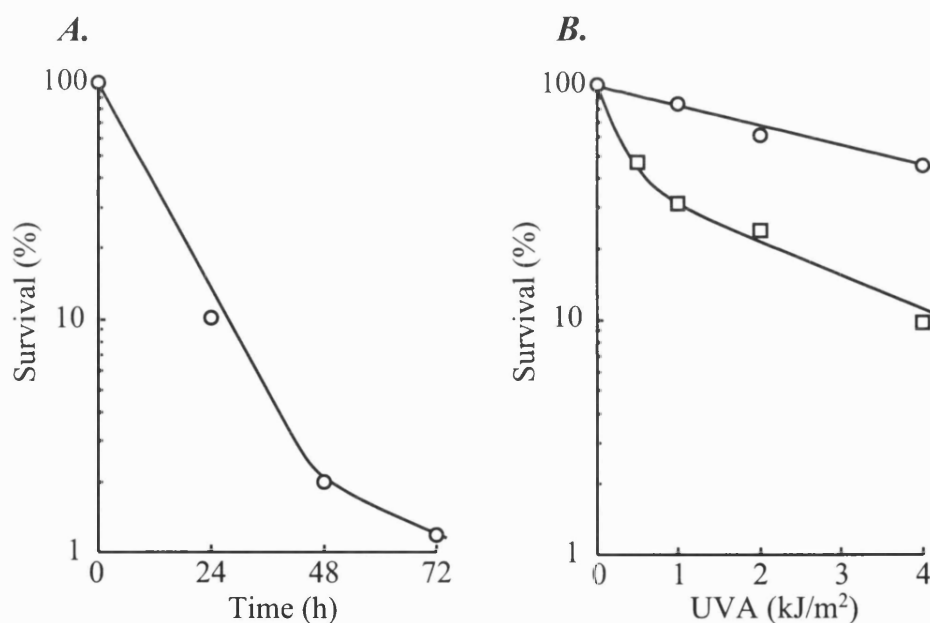


Figure 6.11 Modulation of S⁶G / UVA Cytotoxicity in MMR-proficient MRC5VA Cells

A. XP12ROB4 cells were grown for 24, 48 or 72 hours in medium supplemented with 3μM S⁶G and 10% undialysed FCS. Cells were harvested, irradiated with 1kJ/m² UVA and survival determined as described previously.

B. MMR-proficient MRC5VA cells were grown for 48 hours in medium containing either 0.5μM (○) or 0.75μM (□) S⁶G and 10% undialysed FCS. Cells were harvested, irradiated and survival determined as above.

XP12ROB4 were grown in 3 μ M S⁶G for 24, 48 or 72 hours before being irradiated with 0.5kJ/m² UVA (Fig 6.11A). S⁶G / UVA toxicity increased exponentially up to 48 hours and appeared to plateau thereafter.

MRC5VA fibroblasts were grown in a non-toxic concentration of S⁶G for 48 hours before being irradiated as before. Growth in 0.75 μ M S⁶G reduced the D₃₇ for UVA from about 70kJ/m² to 1kJ/m², a sensitisation of about 70-fold (Fig 6.11B). At concentrations less than 0.75 μ M, UVA-sensitisation appears to diminish quite dramatically. At 0.5 μ M, the D₃₇ value increased to an estimated 5kJ/m².

Table 6.1 Summary of D₃₇ Values

Cell Line	Mutations	D ₃₇ Value (kJ/m ²)			
		UVA	+S ⁴ TdR (100 μ M)	+S ⁴ UdR (100 μ M)	+S ⁶ G
MRC5VA	wt	70	1.2		1.0 (0.75 μ M)
XP12RO	XPA	25	0.04	1.8	
XP12RO- MNUB4	XPA, hMSH2	25	0.01		0.2 (3 μ M)
GM04429F	XPA		0.07		
GM08437B	XPF		0.16		
XP129	XPA-rev		0.5		
HeLa CL7	hPMS2		0.9		
HeLa CL7#7	wt		1.2		
A2780-MNU1	hMLH1		2.7		
A2780- Clone1pMLH1A	wt		1.0		

Summary

In this chapter, I demonstrated that although incorporated into DNA, S⁴TdR was not significantly toxic to human cells. I report that despite its non-toxicity, S⁴TdR dramatically sensitises cultured human cells to non-lethal doses of UVA light by a factor of 100-fold or more. This light-dependent toxicity required S⁴TdR incorporation into DNA *via* thymidine kinase. NER-defective xeroderma pigmentosum fibroblasts were markedly more sensitive and exhibited UVA dose

enhancements of 1000-fold. MMR status did not predictably influence the synergistic S⁴TdR / UVA killing. Exogenous thymidine in the serum dramatically reduced the effectiveness of combined S⁴TdR and UVA. Co-operative UVA cytotoxicity was also observed with S⁴UdR and S⁶G. Dose modifications of greater than a 100-fold were achieved in MMR defective cells with S⁶G and normal fibroblasts were also sensitised. The toxicity of S⁶G with UVA depended on incorporation into nucleic acids but my preliminary data suggest that XP cells are not significantly hypersensitive to S⁶G and UVA.

Discussion

Previous work has shown that the thiopyrimidine, 4-thiouridine is incorporated predominantly into the RNA of monkey kidney cells and the subsequent irradiation with UVA light causes modest inhibition of DNA, RNA and protein synthesis (Favre *et al.*, 1993). S⁴TdR and UVA has also been shown to exhibit modest anti-viral activity against Vaccinia and Herpes Simplex viruses (Domi *et al.*, 1995). I have demonstrated that S⁴TdR and other thiobases can combine with non-toxic doses of UVA light to produce a truly co-operative cytotoxic effect against cultured human cells. This effect was significantly more pronounced than that previously reported for 4-thiouridine in human cells or of S⁴TdR against the viruses.

Mechanism of S⁴TdR and UVA Cytotoxicity

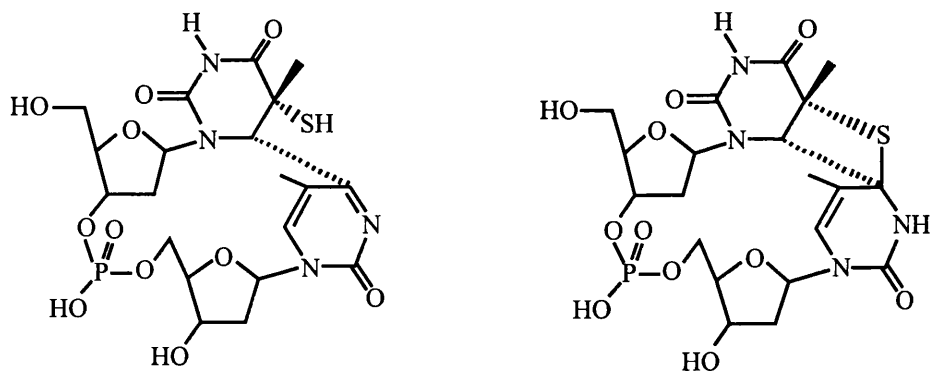
The combined cytotoxicity of S⁴TdR / UVA is dependent on an active pyrimidine nucleoside salvage pathway. This strongly suggests that incorporation of S⁴TdR into DNA is essential for the synergistic effect and that UVA induced DNA damage is responsible for toxicity. The marked sensitivity of the three XP cell lines is consistent with this and further suggests that the toxic lesion can be removed by NER. UVA irradiation of S⁴TdR in oligonucleotides promotes their reaction with nucleophilic groups of proteins to form DNA-protein crosslinks (Bartholomew *et al.*, 1994; Nikiforov and Connolly, 1992). The marked sensitivity of NER defective fibroblasts might reflect their inability to excise DNA-protein crosslinks. Alternatively, the lethal DNA damage may be an intramolecular DNA lesion. When S⁴TdR is placed 3' to a thymine in either di- or oligonucleotides, UVA induces

photo-crosslinks between the two bases (Favre *et al.*, 1998; Warren *et al.*, 1998). S⁴TdR is also able to photo-ligate the ends of two oligonucleotides when one contains S⁴TdR at the 5'-end and the other a thymine at the 3'-end (Liu and Taylor, 1998).

The photo-dimers generated by UVA and S⁴TdR are close structural homologues of the (6-4) pyrimidine pyrimidone photoproducts generated by irradiation of unsubstituted DNA by UVC light (Fig 6.12). This suggests that irradiation of cells grown in S⁴TdR with UVA light generates photo-dimers that resemble a (6-4) pyrimidine pyrimidone photoproduct and are a major contributor to toxicity. The properties of XP129 are in agreement with this suggestion. XP129 is a phenotypic revertant of XP12RO generated by chemical mutagenesis followed by selection for resistance to UVC. Although these cells have a complex phenotype, it is generally accepted that they have regained UVC resistance along with the ability to excise UVC-induced (6-4) pyrimidine pyrimidone photoproducts but not cyclobutane pyrimidine dimers (CPDs) (Cleaver *et al.*, 1987). In my experiments with XP129, resistance to S⁴TdR and UVA was closer to that of NER-proficient cells than to the NER-defective XP12RO parental cells. This suggests that a photoadduct resembling a (6-4) pyrimidine pyrimidone photoproduct generated in unsubstituted DNA by UVC may be a significant contributor to the toxicity of S⁴TdR and UVA.

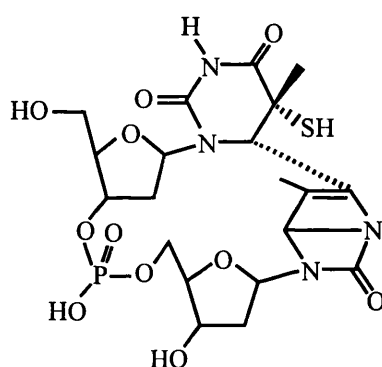
Direct chemical quantification of the photoadducts induced by S⁴TdR and UVA is necessary before an exact understanding of the mechanism of toxicity can be ascertained. Additionally, studying cell lines with more subtle defects in NER such as those derived from patients with defects in XPC, Cockayne syndrome or trichothiodystrophy may provide valuable insights into the mechanism.

Defects in mismatch repair are sometimes associated with increased resistance to chemotherapeutic agents (Fink *et al.*, 1998). Bromodeoxyuridine (BrdUrd) and iododeoxyuridine (IdUrd) are thymidine analogues that can replace TdR in DNA and sensitise cells to ionising radiation (IR). On irradiation, both halopyrimidines produce reactive uracil radicals that are believed to induce strand breaks at adjacent sugar residues. Recent work suggests that MMR defective human and mouse cells are more sensitive to the combined effects of halogenated pyrimidines and IR (Berry *et al.*, 2000; Berry *et al.*, 1999).



1. (6-4) pyrimidine pyrimidone like dimer

2. Thiethane



3. Dewar Isomer

Figure 6.12 Structure of Photodimers Induced in Oligonucleotides Containing a TpS⁴T Dimer

Structures are taken from (Warren *et al.*, 1998). The oligonucleotide ACT CGG ACC TS⁴TC GCT GTG AT was irradiated with 350nm UV light. The major products, the S⁵-(6-4) (1) and the thiethane (2) exist in an equilibrium mixture. Further irradiation of the S⁵-(6-4) at 300nm generates the Dewar isomer (3). These structures are present at the central, underlined TpS⁴T.

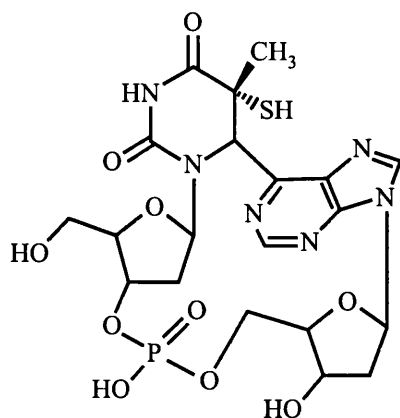


Figure 6.13 Structure of Tpds⁶I Dinucleotide After UVA Irradiation

Structure is taken from (Woisard *et al.*, 1992).

MMR is thought to participate in the removal of BrdUrd or IdUrd from DNA. From my gel retardation assays (Fig 5.10A and C), it appears that hMutS α may recognise S⁴T:A base pairs in certain DNA sequences. As S⁴T:A is the likely product of S⁴TMP incorporation into DNA, it is possible that hMutS α plays a role in reducing the amount of S⁴TdR in DNA. If this is the case, MMR defective cells should be more sensitive to the combined effects of S⁴TdR and UVA. My data does not support this possibility. The effect of defective MMR on S⁴TdR plus UVA treatment was unpredictable. The differences between cell lines may be governed by other factors that determine the amount of S⁴TdR utilised. These include the levels of thymidine kinase, the growth rate of the cells, and their thymidine nucleotide pools. These factors appear to override any effect of MMR deficiencies.

4-thiothymidine is an alternative source of DNA-S⁴TdR. S⁴dUdR is probably phosphorylated and enters the *de novo* pathway of pyrimidine synthesis at the thymidylate synthase step. S⁴dUMP is subsequently converted to S⁴TMP and would then be incorporated into DNA. S⁴dUdR is a substrate for TS but has a K_m approximately 14-fold higher than that of the natural substrate dUdR (Kalman *et al.*, 1973). The 25-fold lower effectiveness of S⁴dUdR as a UVA sensitiser compared to S⁴TdR is probably a reflection of discrimination against the nucleoside at the phosphorylation step, methylation step or both.

S⁶G and UVA Light - A Common Cytotoxic Mechanism for Thiobases and UVA?

I found that like S⁴TdR and S⁴UdR, the thiopurine S⁶G dramatically sensitised human cells to UVA light. The mechanism by which 6-thioguanine and UVA combine to exert a cytotoxic effect is not clear. Free S⁶G, S⁶G nucleotides or DNA-S⁶G are all potential photosensitisers. 6-mercaptopurine (6-MP), a close structural analogue of 6-thioguanine, is used in the treatment of acute leukaemia. 6-MP is salvaged by the HGPRT pathway and is subsequently incorporated into both DNA and RNA. 6-MP, once converted to S⁶dGMP, has the same biological effects as S⁶G. Free 6-MP can participate in photochemical reactions after irradiation with UVA. It is suggested that free radicals including $\cdot\text{OH}$ and $\text{O}_2^{\cdot-}$ are the major contributor to this phototoxicity. Thus, free thiopurines might be responsible for the cytotoxicity through their induction of oxidative DNA damage. My observations do not support

this hypothesis. Active HGPRT is essential for the co-operative cytotoxicity of S⁶G and UVA. The XP12RO HGPRT defective cells are unable to incorporate S⁶G into DNA or RNA despite growth in potentially lethal concentrations of S⁶G. These cells do not exhibit UVA-dependent S⁶G toxicity. Furthermore, washing the cells prior to irradiation ensures that the amount of free S⁶G in HGPRT proficient cells is low compared to the amount in DNA. Since phosphorylation by HGPRT will trap S⁶G in the cell, photosensitisation by free S⁶G nucleotides cannot be ruled out. Their contribution to the intracellular nucleotide pool in HGPRT proficient cells is likely to be quite small. It seems more probable that S⁶G + UVA is cytotoxic through some form of DNA damage. RNA damage and the subsequent inhibition of transcription cannot be eliminated as the reason for the cytotoxicity. However, these effects are likely to be very transient as only transcripts containing S⁶G at the time of irradiation will be affected.

S⁶G induced DNA damage could occur through one of several different mechanisms.

1. Type I Photosensitiser

S⁶G could act as a Type I photosensitiser, like riboflavin, which intercalates into DNA. The sensitiser, usually in the triplet state, interacts directly with the substrate through electron transfer reactions. Type I photosensitisers induce 8-oxo-dG predominantly at the 5' site in 5'-GG-3' sequences (Ito *et al.*, 1993). Electron transfer from sensitiser to substrate is not restricted to the proximal base and 8-oxo-dG generation at GG sites has been observed up to 13 bases (or 37Å) away from the electron source (Hall *et al.*, 1996). 8-oxo-dG, despite being very mutagenic, is not very cytotoxic and is efficiently repaired (Friedberg *et al.*, 1995) and thus an alternative form of DNA damage may be responsible for the cytotoxicity of S⁶G and UVA.

2. Type II Photosensitiser

S⁶G may photosensitise cells *via* a mechanism similar to that of carbonyl compounds. The triplet states of carbonyl compounds like acetone and acetophenone are highly reactive. The energy of these triplet states are higher than that of DNA bases and can react with DNA by triplet energy transfer (Friedberg *et al.*, 1995). In the case of acetophenone, only thymidine has a triplet state of lower energy. Irradiation of a mixture of DNA and acetophenone with UVA results in the

predominant formation of thymine-pyrimidine cyclobutane dimers (Eep *et al.*, 1993). If the triplet state energy of DNA-S⁶G is greater than that of the other bases, energy transfer from S⁶G may occur. This could result in the formation of DNA damage such as CPDs.

3. Direct Photosensitisation

The final possible mechanism involves direct cross-linking of the photo-excited S⁶G molecule with an adjacent base. This is directly analogous to S⁴TdR. Irradiation of a 5'-thymine-6-thioedeoxyinosine (TpdS⁶I) dinucleotide produces a purine-pyrimidine (6-6) adduct that closely resembles a (6-4) pyrimidine-pyrimidone photoproduct (Fig 6.13, (Woisard *et al.*, 1992)). Additionally, *E. coli* defective in either NER (*uvrA*) or recombination (*recA*) are more sensitive to the combined effects of 6-MP and UVA (Komeda *et al.*, 1997). This would be consistent with a major cytotoxic lesion that resembles a (6-4) pyrimidine-pyrimidone photoproduct. None of these models appears to be supported by my data. The NER proficient line examined (HeLa CL7) was as sensitive to the combined effects of S⁶G and UVA as the NER defective line (XP12ROB4). Two factors may account for this. The toxic adduct produced may be poorly repaired by NER (like a cisplatin 1,2{GG} intrastrand crosslink) and thus, loss of NER does not sensitise cells. Alternatively, HeLa cells may incorporate S⁶G more extensively than XP12ROB4. In order to address this problem, DNA-S⁶G could be quantitated by HPLC and survival determined as a function of DNA-S⁶G incorporation.

It should be noted that S⁶G is also able to react with the nucleophilic groups of proteins to form DNA-protein crosslinks (Nikiforov and Connolly, 1992). Although NER is a possible participant, little is known about how DNA-protein crosslinks are repaired. This type of DNA lesion cannot therefore be ruled out as a contributor to the cytotoxic effect. In summary, S⁶G and UVA exert their synergistic cytotoxicity *via* nucleic acids and most probably through DNA damage. Overall, the similarities between S⁴TdR and S⁶G make it probable that in combination with UVA they kill cells by a common mechanism.

Possible Clinical Implications

UVA sensitisation appears to be a general property of DNA thionucleosides. Might it be possible to exploit this property in a clinical setting? DNA-S⁴TdR toxicity is dependent on active TK and UVA. TK is up regulated by a factor of about 10-fold during S-phase (Sherley and Kelly, 1988) and elevated levels of TK are associated with malignant cells. S⁴TdR combined with UVA light will selectively target rapidly proliferating cells and might be worth evaluating as a therapy for hyperproliferative disorders. My data indicate that exogenous levels of TdR affect the efficiency of S⁴TdR / UVA cytotoxicity. This should not prove a problem for systemic use of S⁴TdR in humans as the plasma concentration of TdR is estimated to be <0.1µM (Cao *et al.*, 1999). In mice, however, the serum concentration of TdR is significantly higher (≈1.3µM). Thus, data derived from models using human tumour xenografts in mice will need to be evaluated with caution. The observation that TS inhibitors do not increase the efficacy of S⁴TdR with UVA in the cell culture models was surprising. In principle, this should provide an ideal method for increasing the efficiency *in vivo*. Alternative TS inhibitors such as Raltitrexed (Tomudex or ZD1694, Astra-Zeneca) certainly merit further investigation in this regard.

In my studies, the dose of UVA used never exceeded 10kJ/m². Under these conditions, S⁴UdR was a less effective sensitiser than S⁴TdR. However, UVA alone is not significantly toxic below 50kJ/m² (see Fig 6.1A). In the clinic, it should be possible to use higher doses of UVA than investigated here. This should improve the efficiency of all the thionucleosides investigated. Even S⁴UdR may prove clinically useful if used in conjunction with a high dose (≈ 40kJ/m²) of UVA.

One clear advantage of S⁶G over S⁴TdR is that it is already licensed for use in the clinic. It is used in the treatment of leukaemia, autoimmune diseases and also for the management of psoriasis (Zackheim *et al.*, 1994). DNA-S⁶G itself is relatively non-toxic and its MMR dependent toxicity arises from the small fraction, about 1 in 10⁴ to 10⁵, that undergo S-methylation by SAM to DNA-S⁶meG (Swann *et al.*, 1996). In blood leukocyte DNA, non-toxic steady state levels of about 10⁴-10⁵ S⁶G per cell are possible (Warren *et al.*, 1995). In principle, non-toxic levels of DNA-S⁶G in target cells could still be sufficient to generate a cytotoxic interaction with UVA. DNA

thiobases, in particular S⁴TdR, combined with UVA light warrant further evaluation as a therapeutic approach for the treatment and clinical management of accessible tumours and hyperproliferative skin disorders like psoriasis.

Skin Cancer in Patients Receiving Azathioprine - A Role for S⁶G and UVA Light?

Azathioprine (aza) is a commonly used immunosuppressive drug in transplant patients. It is also used in the management of many autoimmune diseases such as rheumatoid arthritis and Crohn's disease. Prolonged treatment with aza is associated with an increased risk of developing cancer, predominantly of the skin. Kidney and liver transplant patients receiving aza and prednisone show at least a 100-fold increase in the incidence of skin cancer compared to the age matched population. Squamous cell carcinoma and basal cell carcinoma are the two commonest malignancies but melanoma, Kaposi's sarcoma and other rarer malignancies may occur (Otley and Pittelkow, 2000). Part of this increased incidence of skin cancers is almost certainly directly due to immunosuppression. Kaposi's sarcoma, for example, is commonly associated with HIV infected patients due to their suppressed immune system. Aza has been suggested as a major factor in the remaining malignancies. The evidence for this is as follows:

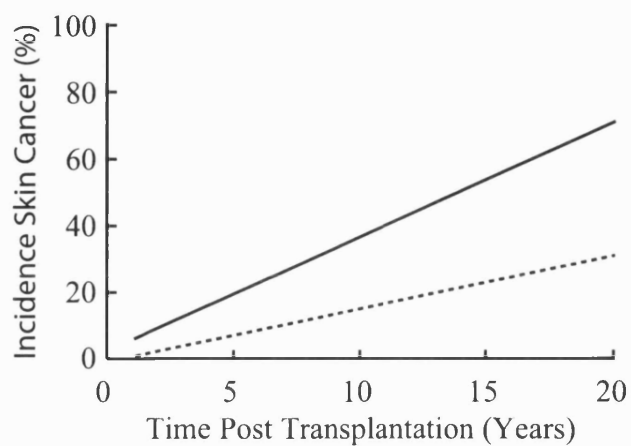
1. The incidence of skin cancer correlates with the amount of aza and its metabolites in the blood.
 2. Substitution of aza by other immunosuppressive agents leads to a decrease in the incidence of cancer.
 3. Non-transplant patients receiving aza alone also have an increased incidence of skin cancer.
 4. Skin cancers in aza treated patients occur almost exclusively on sun-exposed sites.
- The incidence of skin-cancer is remarkably dependent on the latitude of the country in which the transplant patient resides. A particularly striking example of this is the relative incidence of skin cancer in Australian and Dutch transplant recipients (Fig 6.14A).

Azathioprine is metabolised in the cell to 6-mercaptopurine (6-MP) and 1-methyl-4-5-nitroimidazole (MNI) (Fig 6.14B). In the mouse model, both aza and 6-MP but not MNI were phototoxic and photocarcinogenic (Kelly *et al.*, 1989) indicating that the

thiopurine moiety is the active component. 6-MP generated by the metabolism of aza is salvaged by the HGPRT pathway and converted to DNA-S⁶G. The interaction of this DNA-S⁶G with sunlight generates an as yet identified carcinogenic DNA lesion. Mutations in p53 in post-transplant skin cancer have been shown to occur predominantly at dipyrimidine sites (McGregor *et al.*, 1997) which suggests that the carcinogenic lesion is not a TpS⁶G dimer but is consistent with Type II photosensitisation. Identification of the principal DNA adducts and the major signature mutations induced after S⁶G / UVA treatment are essential prerequisites for understanding the mechanism of DNA-S⁶G / UV carcinogenesis.

In summary, my data suggest that DNA thiobases with UVA warrant investigation as a novel therapeutic option for the clinical management of accessible skin tumours or hyperproliferative skin disorders (like psoriasis). Understanding the chemistry and biology of S⁶G / UVA interactions may provide insights into the carcinogenic effects of azathioprine and sunlight.

A.



B.

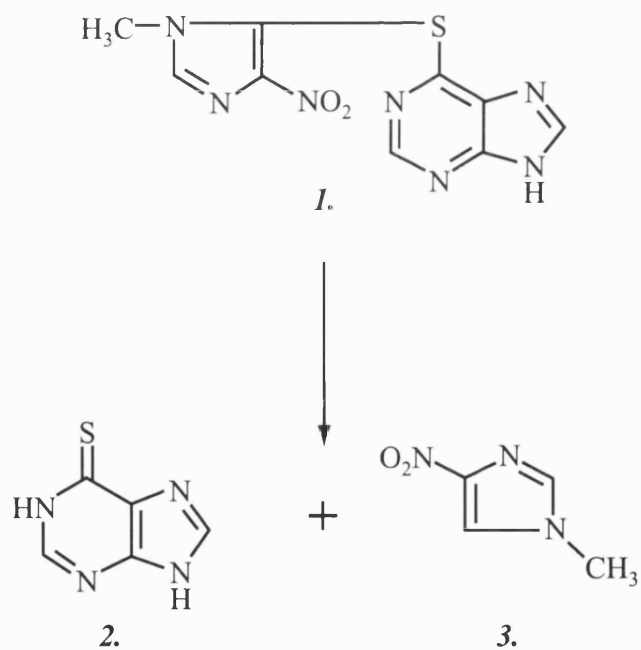


Figure 6.14 Azathioprine and Skin Cancer

A. Prevalence of skin cancer in Dutch (----) and Australian (—) transplant recipients with time after transplantation. Adapted from (Otley *et al.*, 2000).

B. Metabolism of Azathioprine (1) to 6-mercaptopurine (2) and 1-methyl-4-nitroimidazole (3).

References

- Aarbakke, J., Janka-Schaub, G. and Elion, G.B. (1997) Thiopurine Biology and Pharmacology. *Trends Pharmacol. Sci.*, **18**, 3-7.
- Aebi, S., Fink, D., Gordon, R., Kim, H.K., Zheng, H., Fink, J.L. and Howell, S.B. (1997) Resistance to Cytotoxic Drugs in DNA Mismatch Repair-deficient Cells. *Clin. Cancer Res.*, **3**, 1763-1767.
- Aebi, S., Kurdi-Haidar, B., Gordon, R., Cenni, B., Zheng, H., Fink, D., Christen, R.D., Boland, C.R., Koi, M., Fishel, R. and Howell, S.B. (1996) Loss of DNA Mismatch Repair in Acquired Resistance to Cisplatin. *Cancer Res.*, **56**, 3087-3090.
- Akerboom, T.P.M. and Sies, H. (1981) Assay of Glutathione, Glutathione Disulfide, and Glutathione Mixed Disulfides in Biological Samples. *Methods in Enzymol.*, **77**, 373-382.
- Anthony, D.A., McIlwrath, A.J., Gallagher, W.M., Edlin, A.R.M. and Brown, R. (1996) Microsatellite Instability, Apoptosis, and Loss of p53 Function in Drug-resistant Tumour Cells. *Cancer Res.*, **56**, 1374-1381.
- Aquilina, G., Giammarioli, A.M., Zijno, A., Di Muccio, A., Dogliotti, E. and Bignami, M. (1990) Tolerance to O⁶-Methylguanine and 6-Thioguanine Cytotoxic Effects: A Cross-resistant Phenotype in *N*-Methyl-*N*-nitrosourea-resistant Chinese Hamster Ovary Cells. *Cancer Res.*, **50**, 4248-4253.
- Aquilina, G., Hess, P., Fiumicino, S., Ceccotti, S. and Bignami, M. (1995) A Mutator Phenotype Characterises One of Two Complementation Groups in Human Cells Tolerant to Methylation Damage. *Cancer Res.*, **55**, 2569-2575.
- Bale, A., d'Alarcao, M. and Marinus, M.G. (1979) Characterisation of DNA Adenine Methylase Mutants of *Escherichia coli* K12. *Mutat. Res.*, **59**, 157-165.
- Barras, F. and Marinus, M.G. (1989) The Great GATC: DNA Methylation in *E. coli*. *Trends Genet.*, **5**, 139-143.
- Bartholomew, B., Braun, B.R., Kassavetis, G.A. and Geiduschek, E.P. (1994) Probing Close DNA Contacts of RNA Polymerase III Transcription Complexes with the Photoactive Nucleoside 4-Thiodeoxythymidine. *J. Biol. Chem.*, **269**, 18090-18095.
- Batty, D.P. and Wood, R.D. (2000) Damage Recognition in Nucleotide Excision Repair of DNA. *Gene*, **241**, 193-204.

- Baumann, P. and West, S.C. (1998) Role of the Human RAD51 Protein in Homologous Recombination and Double-stranded-break Repair. *Trends Biochem. Sci.*, **23**, 247-251.
- Behrens, B.C., Hamilton, T.C., Masuda, H., Grotzinger, K.R., Whang-Peng, J., Louie, K.G., Knutsen, T., McKoy, W.M., Young, R.C. and Ozols, R.F. (1987) Characterisation of a *cis*-Diamminedichloroplatinum(II)-resistant Human Ovarian Cancer Cell Line and its Use in Evaluation of Platinum Analogues. *Cancer Res*, **47**, 414-418.
- Berry, S.E., Davis, T.W., Schupp, J.E., Hwang, H.-S., de Wind, N. and Kinsella, T.J. (2000) Selective Radiosensitisation of Drug-resistant MutS Homologue-2 (MSH2) Mismatch Repair-deficient Cells by Halogenated Thymidine (dThd) Analogues: Msh2 Mediates dThd Analogue DNA Levels and the Differential Cytotoxicity and Cell Cycle Effects of the dThd Analogues and 6-Thioguanine. *Cancer Res.*, **60**, 5773-5780.
- Berry, S.E., Garces, C., Hwang, H.-S., Kunugi, K., Meyers, M., Davis, T.W., Boothman, D.A. and Kinsella, T.J. (1999) The Mismatch Repair Protein hMLH1, Mediates 5-Substituted Halogenated Thymidine Analogue Cytotoxicity, DNA Incorporation, and Radiosensitisation in Human Colon Cancer Cells. *Cancer Res*, **59**, 1840-1845.
- Blackwell, L.J., Bjornson, K.P. and Modrich, P. (1998a) DNA-dependent Activation of the hMutS α ATPase. *J. Biol. Chem.*, **273**, 32049-32054.
- Blackwell, L.J., Martik, D., Bjornson, K.P., Bjornson, E.S. and Modrich, P. (1998b) Nucleotide-promoted Release of hMutS α from Heteroduplex DNA is Consistent with an ATP-dependent Translocation Mechanism. *J. Biol. Chem.*, **273**, 32055-32062.
- Boland, C.R. (1998) Hereditary Nonpolyposis Colorectal Cancer. In Vogelstein, B. and Kinzler, K.W. (eds.), *The Genetic Basis of Human Cancer*. McGraw Hill, New York, pp. 333-346.
- Bootsma, D., Kraemer, K.H., Cleaver, J.E. and Hoeijmakers, J.H.J. (1998) Nucleotide Excision Repair Syndromes: Xeroderma Pigmentosum, Cockayne Syndrome and Trichothiodystrophy. In Vogelstein, B. and Kinzler, K.W. (eds.), *The Genetic Basis of Disease*. McGraw-Hill, New York, pp. 245-274.
- Boye, E., Lobner-Olsen, A. and Skarstad, K. (1988) Timing of Chromosomal Replication in *Escherichia coli*. *Biochim. Biophys. Acta*, **951**, 359-364.

- Branch, P., Aquilina, G., Bignami, M. and Karran, P. (1993) Defective Mismatch Binding and a Mutator Phenotype in Cells Tolerant to DNA Damage. *Nature*, **362**, 652-654.
- Branch, P., Hampson, R. and Karran, P. (1995) DNA Mismatch Binding Defects, DNA Damage Tolerance, and Mutator Phenotypes in Human Colorectal Carcinoma Cell Lines. *Cancer Res.*, **55**, 2304-2309.
- Branch, P., Masson, M., Aquilina, G., Bignami, M. and Karran, P. (2000) Spontaneous Development of Drug Resistance: Mismatch Repair and p53 Defects in Resistance to Cisplatin in Human Tumour Cells. *Oncogene*, **19**, 3138-3145.
- Brown, R., Hirst, G.L., Gallagher, W.M., McIlwraith, A.J., Margison, G.P., van der Zee, A.G.J. and Anthoney, D.A. (1997) hMLH1 Expression and Cellular Responses of Ovarian Tumour Cells to Treatment with Cytotoxic Anticancer Agents. *Oncogene*, **15**, 45-52.
- Bunz, F., Dutriaux, A., Lengauer, C., Waldman, T., Zhou, S., Brown, J.P., Sedivy, J.M., Kinzler, K.W. and Vogelstein, B. (1998) Requirement for p53 and p21 to Sustain G2 Arrest After DNA Damage. *Science*, **282**, 1497-1501.
- Burnouf, D., Daune, M. and Fuchs, R.P.P. (1987) Spectrum of Cisplatin-induced Mutations in *Escherichia coli*. *Proc. Natl. Acad. Sci. USA*, **84**, 3758-3762.
- Cao, S., McGuire, J.J. and Rustum, Y.M. (1999) Antitumour Activity of ZD1694 (Tomudex) Against Human Head and Neck Cancer in Nude Mouse Models: Role of Dosing Schedule and Plasma Thymidine. *Clin. Cancer Res.*, **5**, 1925-1934.
- Chen, Z.-S., Mutoh, M., Sumizawa, T., Furukawa, T., Haraguchi, M., Tani, A., Saijo, N., Kondo, T. and Akiyama, S.-I. (1998) An Active Efflux System for Heavy Metals in Cisplatin-Resistant Human KB Carcinoma Cells. *Exp. Cell Res.*, **240**, 312-320.
- Cleaver, J.E., Cortes, F., Lutze, L.H., Morgan, W.F., Player, A.N. and Mitchell, D.L. (1987) Unique DNA Repair Properties of a Xeroderma Pigmentosum Revertant. *Mol. Cell Biol.*, **7**, 3353-3357.
- Comess, K.M., Burstyn, J.N., Essigmann, J.M. and Lippard, S.J. (1992) Replication Inhibition and Translesion Synthesis on Templates Containing Site-Specifically Placed cis-Diamminedichloroplatinum(II) DNA Adducts. *Biochemistry*, **31**, 3975-3990.
- Critchlow, S.E. and Jackson, S.P. (1998) DNA End-joining: from Yeast to Man. *Trends Biochem. Sci.*, **23**, 394-398.

- de Boer, J. and Hoeijmakers, J.H.J. (2000) Nucleotide Excision Repair and Human Syndromes. *Carcinogenesis*, **21**, 453-460.
- de Laat, W.L., Jaspers, N.G.J. and Hoeijmakers, J.H.J. (1999) Molecular Mechanism of Nucleotide Excision Repair. *Genes Dev.*, **13**, 768-785.
- Domi, A., Siromachkova, M., Fourrey, J.-L., Favre, A. and Beaud, G. (1995) Photoinactivation (365nm) of Vaccinia and Herpes Simplex Viruses Induced by a New Built-in DNA Photosensitiser: 4-Thiothymidine. *Photochem. Photobiol.*, **61**, 463-470.
- Dosanjh, M.K., Menichini, P., Eritja, R. and Singer, B. (1993) Both O⁴-Methylthymine and O⁴-Ethylthymine Preferentially Form Alkyl T:G Pairs that do not Block *in vitro* Replication in a Defined Sequence. *Carcinogenesis*, **14**, 1915-1919.
- Dosanjh, M.K., Singer, B. and Essigmann, J.M. (1991) Comparative Mutagenesis of O⁶-Methylguanine and O⁴-Methylthymine in *Escherichia coli*. *Biochemistry*, **30**, 7027-7033.
- Dougherty, T.J., Gomer, C.J., Henderson, B.W., Jori, G., Kessel, D., Korbelik, M., Moan, J. and Peng, Q. (1998) Photodynamic Therapy. *J. Natl. Cancer I.*, **90**, 889-905.
- Drummond, J.T., Anthoney, A., Brown, R. and Modrich, P. (1996) Cisplatin and Adriamycin Resistance are Associated with MutL α and Mismatch Repair Deficiency in an Ovarian Tumour Cell Line. *J. Biol. Chem.*, **271**, 19645-19648.
- Duckett, D.R., Drummond, J.T., Murchie, A.I.H., Reardon, J.T., Sancar, A., Lilley, D.M.J. and Modrich, P. (1996) Human MutS α Recognises Damaged DNA Base Pairs Containing O⁶-Methylguanine, O⁴-Methylthymine, or the Cisplatin-d(GpG) Adduct. *Proc. Natl. Acad. Sci. USA*, **93**, 6443-6447.
- Dulic, V., Stein, G.H., Farahi Far, D. and Reed, S.I. (1998) Nuclear Accumulation of p21^{Cip1} at the Onset of Mitosis: A Role at the G2/M-Phase Transition. *Mol. Cell Biol.*, **18**, 546-557.
- Durant, S.T., Morris, M.M., Illand, M., McKay, H.J., McCormick, C., Hirst, G.L., Borts, R.H. and Brown, R. (1999) Dependence on *RAD52* and *RAD1* for Anticancer Drug Resistance Mediated by Inactivation of Mismatch Repair Genes. *Curr. Biol.*, **9**, 51-54.

- Eep, B., Henzl, H., Adam, W. and Saha-Moller, C.R. (1993) Endonuclease-sensitive DNA Modifications Induced by Acetone and Acetophone as Photosensitisers. *Nucleic Acids Res.*, **21**, 863-869.
- el Kouni, M.H., el Kouni, M.M. and Naguib, F.N.M. (1993) Differences in Activities and Substrate Specificity of Human and Murine Pyrimidine Nucleoside Phosphorylases: Implications for Chemotherapy with 5-Fluoropyrimidines. *Cancer Res.*, **53**, 3687-3693.
- Elion, G.B. (1989) The Purine Path to Chemotherapy. *Science*, **244**, 41-47.
- Favre, A., Moreno, G., Salet, C. and Vinzens, F. (1993) 4-Thiouridine Incorporation into the RNA of Monkey Cells (CV-1) Triggers Near-UV Light Long-Term Inhibition of DNA, RNA and Protein Synthesis. *J. Photochem. Photobiol.*, **58**, 689-694.
- Favre, A., Saintome, C., Fourrey, J.-L., Clivio, P. and Laugaa, P. (1998) Thionucleobases as Intrinsic Photoaffinity Probes of Nucleic Acid Structure and Nucleic Acid-Protein Interactions. *J. Photochem. Photobiol.*, **42**, 109-124.
- Fink, D., Aebi, S. and Howell, S.B. (1998) The Role of DNA Mismatch Repair in Drug Resistance. *Clin. Cancer Res.*, **4**, 1-6.
- Fink, D., Nebel, S., Aebi, S., Nehme, A. and Howell, S. (1997a) Loss of DNA Mismatch Repair due to Knockout of MSH2 or PMS2 Results in Resistance to Cisplatin and Carboplatin. *Int. J. Oncol.*, **11**, 539-542.
- Fink, D., Nebel, S., Aebi, S., Zheng, H., Cenni, B., Nehme, A., Christen, R.D. and Howell, S.B. (1996) The Role of DNA Mismatch Repair in Platinum Drug Resistance. *Cancer Res*, **56**, 4881-4886.
- Fink, D., Zheng, H., Nebel, S., Norris, P.S., Aebi, S., Lin, T.-P., Nehme, A., Christen, R.D., Haas, M., MacLeod, C.L. and Howell, S.B. (1997b) *In Vitro* and *in Vivo* Resistance to Cisplatin in Cells That Have Lost DNA Mismatch Repair. *Cancer Res*, **57**, 1841-1845.
- Fishel, R. (1998) Mismatch Repair, Molecular Switches, and Signal Transduction. *Genes Dev.*, **12**, 2096-2101.
- Fishel, R. (1999) Signalling Mismatch Repair in Cancer. *Nature Med.*, **5**, 1239-1241.
- Fram, R.J., Cusick, P.S. and Marinus, M.G. (1986) Studies on Mutagenesis and Repair Induced by Platinum Analogs. *Mutat. Res.*, **173**, 13-18.

- Fram, R.J., Cusick, P.S., Wilson, J.M. and Marinus, M.G. (1985) Mismatch Repair of *cis*-Diamminedichloroplatinum(II)-Induce DNA Damage. *Mol. Pharmacol.*, **28**, 51-55.
- Friedberg, E.C., Walker, G.C. and Siede, W. (1995) *DNA Repair and Mutagenesis*. ASM Press, Washington DC.
- Gartel, A.L. and Tyner, A.L. (1999) Transcriptional Regulation of the *p21 (WAF1/CIP1)* Gene. *Exp. Cell Res.*, **246**, 280-289.
- Georgiadis, P., Xu, Y.-Z. and Swann, P.F. (1991) Nitrosamine-Induced Cancer: O⁴-Alkylthymine Produces Sites of DNA Hyperflexibility. *Biochemistry*, **30**, 11725-11732.
- Glaab, W.E., Risinger, J.I., Umar, A., Barrett, J.C., Kunkel, T.A. and Tindall, K.R. (1998) Resistance to 6-thioguanine in Mismatch Repair-deficient Human Cancer Cell Lines Correlates with an Increase in Induced Mutations at the *HGPRT* locus. *Carcinogenesis*, **19**, 1931-1937.
- Godwin, A.K., Meister, A., O'Dwyer, P.J., Huang, C.S., Hamilton, T.C. and Anderson, M.E. (1992) High Resistance to Cisplatin in Human Ovarian Cancer Cell Lines is Associated with Marked Increase of Glutathione Synthesis. *Proc. Natl. Acad. Sci. USA*, **89**, 3070-3074.
- Gonclaves, O., Drobetsky, E. and Meuth, M. (1984) Structural Alterations of the *aprt* Locus Induced by Deoxyribonucleoside Triphosphate Pool Imbalances in Chinese Hamster Ovary Cell. *Mol. Cell Biol.*, **4**, 1792-1799.
- Gong, J.G., Costanzo, A., Yang, H.-Q., Melino, G., Kaelin Jr, W.G., Levrero, M. and Wang, J.Y.J. (1999) The Tyrosine Kinase c-Abl Regulates p73 in Apoptotic Response to Cisplatin-induced DNA Damage. *Nature*, **399**, 806-809.
- Griffin, S., Branch, P., Xu, Y.-Z. and Karran, P. (1994) DNA Mismatch Binding and Incision at Modified Guanine Bases by Extracts of Mammalian Cells: Implications for Tolerance to DNA Methylation Damage. *Biochemistry*, **33**, 4487-4793.
- Hall, D.B., Holmin, R.E. and Barton, J.K. (1996) Oxidative DNA Damage Through Long-range Electron Transfer. *Nature*, **382**, 731-735.
- Hampson, R., Humbert, O., Macpherson, P., Aquilina, G. and Karran, P. (1997) Mismatch Repair Defects and O⁶-Methylguanine-DNA Methyltransferase Expression in Acquired Resistance to Methylating Agents in Human Cells. *J. Biol. Chem.*, **272**, 28596-28606.

- Harfe, B.D. and Jinks-Robertson, S. (2000) DNA Mismatch Repair and Genetic Instability. *Annu. Rev. Genet.*, **34**, 359-399.
- Hawn, M.T., Umar, A., Carethers, J.M., Marra, G., Kunkel, T.A., Boland, C.R. and Koi, M. (1995) Evidence for a Connection Between the Mismatch Repair System and the G2 Cell Cycle Checkpoint. *Cancer Res.*, **55**, 3721-3725.
- He, Q., Liang, C.H. and Lippard, S.J. (2000) Steroid Hormones Induce HMG1 Overexpression and Sensitise Breast Cancer Cells to Cisplatin and Carboplatin. *Proc. Natl. Acad. Sci. USA*, **97**, 5768-5772.
- Heiger-Bernays, W.J., Essigmann, J.M. and Lippard, S.J. (1990) Effect of the Antitumour Drug *cis*-Diamminedichloroplatinum(II) and Related Platinum Complexes on Eukaryotic DNA Replication. *Biochemistry*, **29**, 8461-8466.
- Hickman, M.J. and Samson, L.D. (1999) Role of DNA Mismatch Repair and p53 in Signalling Induction of Apoptosis by Alkylating Agents. *Proc. Natl. Acad. Sci. USA*, **96**, 10764-10769.
- Ishikawa, T., Bao, J.-J., Yamane, Y., Akimaru, K., Frindrich, K., Wright, C.D. and Kuo, M.T. (1996) Co-ordinated Induction of *MRP/GS-X* Pump and γ -Glutamylcysteine Synthetase by Heavy Metals in Human Leukaemia Cells. *J. Biol. Chem.*, **271**, 14981-14988.
- Ito, K., Inoue, S., Yamamoto, K. and Kawanshi, S. (1993) 8-Hydroxydeoxyguanosine Formation at the 5' Site of 5'-GG-3' Sequences in Double-Stranded DNA by UV Radiation with Riboflavin. *J. Biol. Chem.*, **268**, 13221-13227.
- Jamieson, E.R. and Lippard, S.J. (1999) Structure, Recognition, and Processing of Cisplatin-DNA Adducts. *Chem. Rev.*, **99**, 2467-2498.
- Jiricny, J. (1998) Replication errors: Cha(lle)nging the Genome. *EMBO J.*, **17**, 6427-6436.
- Jiricny, J. (2000) Mismatch Repair: The Praying Hands of Fidelity. *Curr. Biol.*, **10**, R788-R790.
- Jiricny, J. and Nystrom-Lahti, M. (2000) Mismatch Repair Defects in Cancer. *Curr. Opin. Genet. Dev.*, **10**, 157-161.
- Johnson, K.A., Mierzwa, M.L., Fink, S.P. and Marnett, L.J. (1999) MutS Recognition of Exocyclic DNA Adducts that are Endogenous Products of Lipid Oxidation. *J. Biol. Chem.*, **274**, 27112-27118.

- Johnson, S.W., Laub, P.B., Beesley, J.S., Ozols, R.F. and Hamilton, T.C. (1997) Increased Platinum-DNA Damage Tolerance is Associated with Cisplatin Resistance and Cross-resistance to Various Chemotherapeutic Agents in Unrelated Human Ovarian Cancer Cell Lines. *Cancer Res.*, **57**, 850-856.
- Johnson, S.W., Swiggard, P.A., Handel, L.M., Brennan, J.M., Godwin, A.K., Ozols, R.F. and Hamilton, T.C. (1994) Relationship Between Platinum-DNA Adduct Formation and Removal and Cisplatin Cytotoxicity in Cisplatin-sensitive and -resistant Human Ovarian Cancer Cells. *Cancer Res.*, **54**, 5911-5916.
- Kalman, T.I., Bloch, A., Szekeres, G.L. and Bardos, T.J. (1973) Methylation of 4-thio-2'-deoxyuridylate by Thymidylate Synthase. *Biochem. Biophys. Res. Commun.*, **55**, 210-217.
- Kalnik, M.W., Kouchakjian, M., Li, B.F.L., Swann, P.F. and Patel, D.J. (1988a) Base Pair Mismatches and Carcinogen-Modified Bases in DNA: An NMR Study of A:C and A:O⁴meT Pairing in Dodecanucleotide Duplexes. *Biochemistry*, **27**, 100-108.
- Kalnik, M.W., Kouchakjian, M., Li, B.F.L., Swann, P.F. and Patel, D.J. (1988b) Base Pair Mismatches and Carcinogen-Modified Bases in DNA: An NMR Study of G:T and G:O⁴meT Pairing in Dodecanucleotide Duplexes. *Biochemistry*, **27**, 108-115.
- Karran, P. (2000) DNA Double Strand Break Repair in Mammalian Cells. *Curr. Opin. Genet. Dev.*, **10**, 144-150.
- Karran, P. and Bignami, M. (1996) Drug-related Killings: a Case of Mistaken Identity. *Chem. & Biol.*, **3**, 875-879.
- Karran, P. and Marinus, M.G. (1982) Mismatch Correction at O⁶-Methylguanine Residues in *E. coli* DNA. *Nature*, **296**, 868-869.
- Kat, A., Thilly, W.G., Fang, W.-H., Longley, M.J., Li, G.-M. and Modrich, P. (1993) An Alkylation-tolerant, Mutator Human Cell Line is Deficient in Strand-specific Mismatch Repair. *Proc. Natl. Acad. Sci. USA*, **90**, 6424-6428.
- Kelly, G.E., Meikle, W.D. and Moore, D.E. (1989) Enhancement of UV-induced Skin Carcinogenesis by Azathioprine: Role of Photochemical Sensitisation. *Photochem. Photobiol.*, **49**, 59-65.
- Khanna, K.K. and Jackson, S.P. (2001) DNA Double-strand Breaks: Signalling, Repair and the Cancer Connection. *Nat. Genet.*, **27**, 247-254.

- Kielbassa, C. and Epe, B. (2000) DNA Damage Induced by Ultraviolet and Visible Light and Its Wavelength Dependence. *MethodsEnzymol.*, **319**, 359-366.
- Ko, L.J. and Prives, C. (1996) p53: Puzzle and Paradigm. *Gene. Dev.*, **10**, 1054-1072.
- Koberle, B., Grimaldi, K.A., Sunters, A., Hartley, J.A., Kelland, L.R. and Masters, J.R.W. (1997) DNA Repair Capacity and Cisplatin Sensitivity of Human Testis Tumour Cells. *Int. J. Cancer*, **70**, 551-555.
- Koberle, B., Masters, J.R.W., Hartley, J.A. and Wood, R.D. (1999) Defective Repair of Cisplatin-induced DNA Damage Caused by Reduced XPA Protein in Testicular Germ Cell Tumours. *Curr. Biol.*, **9**, 273-276.
- Kolodner, R.D., Tytell, J.D., Schmeits, J.L., Kane, M.F., Gupta, R.D., Weger, J., Wahlberg, S., Fox, E.A., Peel, D., Ziogas, A., Garber, J.E., Syngal, S., Anton-Culver, H. and Li, F.P. (1999) Germ-line *msh6* Mutations in Colorectal Cancer Families. *Cancer Res.*, **59**, 5068-5074.
- Komatsu, M., Sumizawa, T., Mutoh, M., Chen, Z.-S., Terada, K., Furukawa, T., Yang, X.-L., Gao, H., Miura, N., Sugiyama, T. and Akiyama, S.-i. (2000) Copper-transporting P-Type Adenosine Triphosphatase (ATP7B) is Associated with Cisplatin Resistance. *Cancer Res.*, **60**, 1312-1316.
- Komeda, K., Iwamoto, S., Kominami, S. and Ohnishi, T. (1997) Induction of Cell Killing, Mutation and *umu* Gene Expression by 6-Mercaptopurine or 2-Thiouracil with UVA Irradiation. *Photochem. Photobiol.*, **65**, 115-118.
- Lamers, M.H., Perrakis, A., Enzlin, J.H., Winterwerp, H.H.K., de Wind, N. and Sixma, T.K. (2000) The Crystal Structure of DNA Mismatch Repair Protein MutS Binding to a G:T Mismatch. *Nature*, **407**, 711-717.
- Lanzi, C., Perego, P., Supino, R., Romanelli, S., Pensa, T., Careni, N., Viano, I., Colangelo, D., Leone, R., Apostoli, P., Cassinelli, G., Gambetta, R.A. and Zunino, F. (1998) Decreased Drug Accumulation and Increased Tolerance to DNA Damage in Tumour Cells with a Low Level of Cisplatin Resistance. *Biochem. Pharmacol.*, **55**, 1247-1254.
- Levy, J.G. (1995) Photodynamic Therapy. *Trends Biotechnol.*, **13**, 14-18.
- Li, G.-M., Wang, H. and Romano, L.J. (1996) Human MutS α Specifically Binds to DNA Containing Aminofluorene and Acetylaminofluorene Adducts. *J. Biol. Chem.*, **271**, 24084-24088.

- Lindahl, T., Karran, P. and Wood, R.D. (1997) DNA Excision Repair Pathways. *Curr. Opin. Genet. Dev.*, **7**, 158-169.
- Lindahl, T. and Wood, R.D. (1999) Quality Control by DNA Repair. *Science*, **286**, 1897-1905.
- Liu, J. and Taylor, J.-S. (1998) Template-directed Photoligation of Oligodeoxyribonucleotides via 4-thiothymidine. *Nucleic Acids Res.*, **26**, 3300-3304.
- Loh, S.Y., Mistry, P., Kelland, L.R., Abel, G. and Harrap, K.R. (1992) Reduced Drug Accumulation as a Major Mechanism of Acquired Resistance to Cisplatin in a Human Ovarian Carcinoma Cell Line: Circumvention Studies Using Novel Platinum (II) and (IV) Ammine/Amine Complexes. *Br. J. Cancer*, **66**, 1109-1115.
- Macpherson, P., Humbert, O. and Karran, P. (1998) Frameshift Mismatch Recognition by the Human MutS α Complex. *Mutat. Res.*, **408**, 55-66.
- Marin, M.C., Jost, C.A., Brooks, L.A., Irwin, M.S., O'Nions, J., Tidy, J.A., James, N., McGregor, J.M., Harwood, C.A., Yulug, I.G., Vousden, K.H., Allday, M.J., Gusterson, B., Ikawa, S., Hinds, P.W., Crook, T. and Kaelin Jr, W.G. (2000) A Common Polymorphism Acts as an Intragenic Modifier of Mutant p53 Behaviour. *Nat. Genet.*, **25**, 47-54.
- Masson, J.-Y. and West, S.C. (2001) The Rad51 and Dmcl1 Recombinases: a Non-identical Twin Relationship. *Trends Biochem. Sci.*, **26**, 131-136.
- Masuda, H., Tanaka, T., Matsuda, H. and Kusaba, I. (1990) Increased Removal of DNA-bound Platinum in a Human Ovarian Cancer Cell Line Resistant to *cis*-Diamminedichloroplatinum (II). *Cancer Res.*, **50**, 1863-1866.
- May, P. and May, E. (1999) Twenty Years of p53 Research: Structural and Functional Aspects of the p53 Protein. *Oncogene*, **18**, 7621-7636.
- McGraw, B.R. and Marinus, M.G. (1980) Isolation and Characterisation of Dam⁺ Revertants and Suppressor Mutations that Modify Secondary Phenotypes of *dam-3* Strains of *Escherichia coli* K-12. *Mol. Gen. Genet.*, **178**, 309-315.
- McGregor, J.M., Berkhout, R.J.M., Rozycka, M., ter Schegget, J., Bavinck, J.N.B., Brooks, L. and Crook, T. (1997) p53 Mutations Implicate Sunlight in Post-transplant Skin Cancer Irrespective of Human Papillomavirus Status. *Oncogene*, **15**, 1737-1740.
- McLaughlin, K., Stephens, I., McMahon, N. and Brown, R. (1991) Single Step Selection of *cis*-Diamminedichloroplatinum(II) Resistant Mutants from a Human Ovarian Carcinoma Cell Line. *Cancer Res.*, **51**, 2242-2245.

- Meikrantz, W., Bergon, M.A., Memisoglu, A. and Samson, L. (1998) O⁶-Alkylguanine DNA Lesions Trigger Apoptosis. *Carcinogenesis*, **19**, 369-372.
- Menichini, P., Mroczkowska, M.M. and Singer, B. (1994) Enzyme-dependent Pausing During *in vitro* Replication of O⁴-Methylthymine in a Defined Oligonucleotide Sequence. *Mutat. Res.*, **307**, 53-59.
- Mistry, P., Kelland, L.R., Abel, G., Sidhar, S. and Harrap, K.R. (1991) The Relationships Between Glutathione, Glutathione-S-Transferase and Cytotoxicity of Platinum Drugs and Melphalan in Eight Human Ovarian Carcinoma Cell Lines. *Br. J. Cancer*, **64**, 215-220.
- Miyake, H., Hanada, N., Nakamura, H., Kagawa, S., Fujiwara, T., Hara, I., Eto, H., Gohji, K., Arakawa, S., Kamidono, S. and Saya, H. (1998) Overexpression of Bcl-2 in Bladder Cancer Cells Inhibits Apoptosis Induced by Cisplatin and Adenoviral-mediated p53 Gene Transfer. *Oncogene*, **16**, 933-943.
- Moggs, J.G., Szymkowski, D.E., Yamada, M., Karran, P. and Wood, R.D. (1997) Differential Human Nucleotide Excision Repair of Paired and Mismatched Cisplatin-DNA Adducts. *Nucleic Acids Res.*, **25**, 480-490.
- Nakano, K., Mizuno, T., Sowa, Y., Orita, T., Yoshino, T., Okuyama, Y., Fujita, T., Ohanti-Fujita, N., Matsukawa, Y., Tokino, T., Yamagishi, H., Oka, T., Nomura, H. and Sakai, T. (1997) Butyrate Activates the *WAF1/Cip1* Gene Promoter Through Sp1 Sites in a p53-negative Human Colon Cancer Cell Line. *J. Biol. Chem.*, **272**, 22199-22206.
- Nee, T.S. (1997) Phototherapy. *Clin. Dermatol.*, **15**, 753-767.
- Nikiforov, T.T. and Connolly, B.A. (1992) Oligodeoxynucleotides Containing 4-thiothymidine and 6-thiothioxyguanosine as Affinity Labels for the EcoRV Restriction Endonuclease and Modification Methylase. *Nucleic Acids Res.*, **20**, 1209-1214.
- O'Driscoll, M., Martinelli, S., Ciotta, C. and Karran, P. (1999) Combined Mismatch and Nucleotide Excision Repair Defects in a Human Cell Line: Mismatch Repair Processes Methylation but not UV- or Ionising-induced DNA Damage. *Carcinogenesis*, **20**, 799-804.
- Obmolova, G., Ban, C., Hsieh, P. and Yang, W. (2000) Crystal Structures of Mismatch Repair Protein MutS and its Complex with a Substrate DNA. *Nature*, **407**, 703-710.

- Oda, S., Humbert, O., Fiumicino, S., Bignami, M. and Karran, P. (2000) Efficient Repair of A/C Mismatches in Mouse Cells Deficient in Long-patch Mismatch Repair. *EMBO J.*, **19**, 1711-1718.
- Ohashi, E., Ogi, T., Kusumoto, R., Iwai, S., Masutani, C., Hanaoka, F. and Ohmori, H. (2000) Error-prone Bypass of Certain DNA Lesions by the Human DNA Polymerase κ . *Genes Dev.*, **14**, 1589-1594.
- Oleinick, N.L. and Evans, H.H. (1998) The Photobiology of Photodynamic Therapy: Cellular Targets and Mechanisms. *Radiat. Res.*, **150 (Suppl.)**, S146-S156.
- Otley, C.C. and Pittelkow, M.R. (2000) Skin Cancer in Liver Transplant Recipients. *Liver Transplantation*, **6**, 253-262.
- Otto, A.I., Riou, L., Marionnet, C., Mori, T., Sarasin, A. and Magnaldo, T. (1999) Differential Behaviours Toward Ultraviolet A and B Radiation of Fibroblasts and Keratinocytes from Normal and DNA-Repair-deficient Patients. *Cancer Res*, **59**, 1212-1218.
- Palomino, E., Meltsner, B.R., Kessel, D. and Horwitz, J.P. (1990) Synthesis and *in Vitro* Evaluation of Some Modified 4-Thiopyrimidine Nucleosides for Prevention or Reversal of AIDS-Associated Neurological Disorders. *J. Med. Chem.*, **33**, 258-263.
- Parker, B. and Marinus, M.G. (1988) A Simple and Rapid Method to Obtain Substitution Mutations in *Escherichia coli*: Isolation of a *dam* Deletion / Insertion Mutation. *Gene*, **73**, 531-535.
- Pauly, G.T., Hughes, S.H. and Moschel, R.C. (1998) Comparison of Mutagenesis by O⁶-Methyl- and O⁶-Ethylguanine and O⁴-Methylthymine in *Escherichia coli* using Double-stranded and Gapped Plasmids. *Carcinogenesis*, **19**, 457-461.
- Perego, P., Giarola, M., Righetti, S.C., Supino, R., Caserini, C., Delia, D., Pierotti, M.A., Miyashita, T., Reed, J.C. and Zunino, F. (1996) Association Between Cisplatin Resistance and Mutation of p53 Gene and Reduced Bax Expression in Ovarian Carcinoma Cell Systems. *Cancer Res.*, **56**, 556-562.
- Perez, R.P. (1998) Cellular and Molecular Determinants of Cisplatin Resistance. *Eur. J. Cancer*, **34**, 1535-1542.
- Piovesan, B., Pennell, N. and Berinstein, N.L. (1998) Human Lymphoblastoid Cell Lines Expressing Mutant p53 Exhibit Decreased Sensitivity to Cisplatin-induced Cytotoxicity. *Oncogene*, **17**, 2339-2350.

- Plumb, J.A., Strathdee, G., Sludden, J., Kaye, S.B. and Brown, R. (2000) Reversal of Drug Resistance in Human Tumour Xenografts by 2'-Deoxy-5-azacytidine-induced Demethylation of the *hMLH1* Gene Promoter. *Cancer Res.*, **60**, 6039-6044.
- Rao, T.V.S., Haber, M.T., Sayer, J.M. and Jerina, D.M. (2000) Incorporation of 4-Thiothymidine Into DNA by the Klenow Fragment and HIV-1 Reverse Transcriptase. *Bioorg. Med. Chem. Lett.*, **10**, 907-910.
- Rappaport, H.P. (1993) Replication of the Base Pair 6-Thioguanine/5-Methyl-2-pyrimidinone with the Large Klenow Fragment of *Escherichia coli* DNA Polymerase I. *Biochemistry*, **32**, 3047-3057.
- Reitmar, A.H., Risley, R., Bristow, R.G., Wilson, T., Ganesh, A., Jang, A., Peacock, J., Benchimol, S., Hill, R.P., Mak, T.W., Fishel, R. and Meuth, M. (1997) Mutator Phenotype in *Msh2*-deficient Murine Embryonic Fibroblasts. *Cancer Res.*, **57**, 3765-37771.
- Runger, T.M., Moller, K., Jung, T. and Dekant, B. (2000) DNA Damage Formation, DNA Repair, and Survival after Exposure of DNA Repair-proficient and Nucleotide Excision Repair-deficient Human Lymphoblasts to UVA1 and UVB. *Int. J. Radiat. Biol.*, **2000**, 789-797.
- Sambrook, J., Fritsch, E.F. and Maniatis, T. (1989) *Molecular Cloning A Laboratory Manual*. Cold Spring Harbour Laboratory Press, New York.
- Sambrook, J. and Russell, D.W. (2001) *Molecular Cloning A Laboratory Manual*. Cold Spring Harbour Laboratory Press, New York.
- Seigneur, M., Bidnenko, V., Ehrlich, S.D. and Michel, B. (1998) RuvAB Acts at Arrested Replication Forks. *Cell*, **95**, 419-430.
- Sherley, J.L. and Kelly, T.J. (1988) Human Cytosolic Thymidine Kinase: Purification and Physical Characterisation of the Enzyme from Hela Cells. *J. Biol. Chem.*, **263**, 375-382.
- Shiloh, Y. (2001) ATM and ATR: Networking Cellular Responses to DNA Damage. *Curr. Opin. Genet. Dev.*, **11**, 71-77.
- Shin, J.-Y., Kim, H.-S., Park, J., Park, J.-B. and Lee, J.-Y. (2000) Mechanism for Inactivation of the KIP Family Cyclin-dependent Kinase Inhibitor Genes in Gastric Cancer Cells. *Cancer Res.*, **60**, 262-265.
- Sixma, T.K. (2001) DNA Mismatch Repair: MutS Structures Bound to Mismatches. *Curr. Opin. Struct. Biol.*, **11**, 47-52.

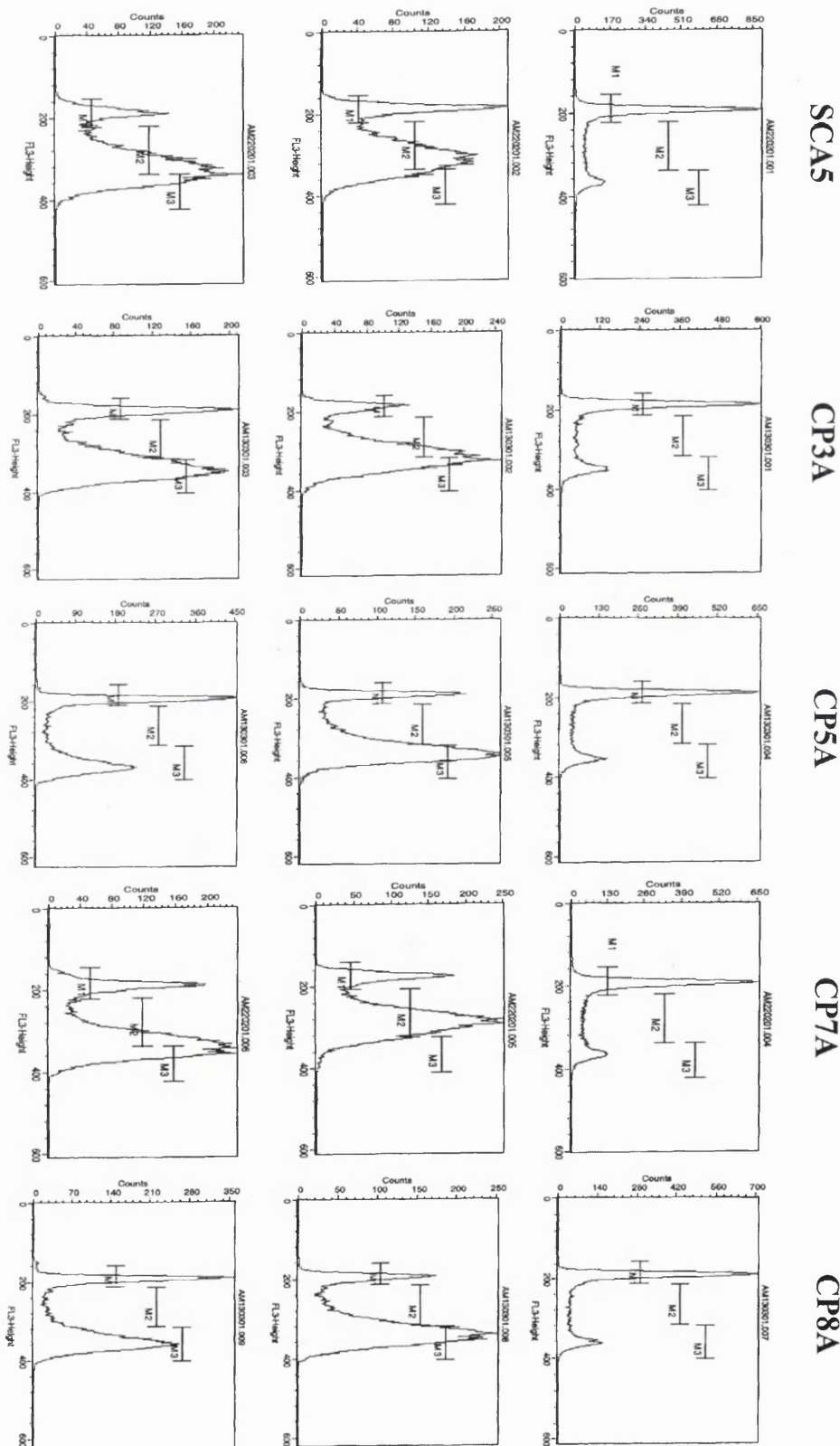
- Sonoda, E., Sasaki, M.S., Morrison, C., Yamaguchi-Iwai, Y., Takata, M. and Takeda, S. (1999) Sister Chromatid Exchanges Are Mediated by Homologous Recombination in Vertebrate Cells. *Mol. Cell. Biol.*, **19**, 5166-5169.
- Strathdee, G., MacKean, M.J., Illand, M. and Brown, R. (1999) A Role for Methylation of the *hMLH1* Promoter in Loss of hMLH1 Expression and Drug Resistance in Ovarian Cancer. *Oncogene*, **18**, 2335-2341.
- Swann, P.F., Waters, T.R., Moulton, D.C., Xu, Y.-Z., Zheng, Q., Edwards, M. and Mace, R. (1996) Role of Postreplicative DNA Mismatch Repair in the Cytotoxic Action of Thioguanine. *Science*, **270**, 1109-1111.
- Szymkowski, D.E., Yarema, K., Essigmann, J.M., Lippard, S.J. and Wood, R.D. (1992) An Intrastrand d(GpG) Platinum Crosslink in Duplex M13 DNA is Refractory to Repair by Human Cell Extracts. *Proc. Natl. Acad. Sci. USA*, **89**, 10772-10776.
- Tan, H.-B., Swann, P.F. and Chance, E.M. (1994) Kinetic Analysis of the Coding Properties of O⁶-Methylguanine in DNA: The Crucial Role of the Conformation of the Phosphodiester Bond. *Biochemistry*, **33**, 5335-5346.
- Taniguchi, K., Wada, M., Kohno, K., Nakamura, T., Kawabe, T., Kawakami, M., Kagotani, K., Okumura, K., Akiyama, S.-i. and Kuwano, M. (1996) A Human Canicular Multispecific Organic Anion Transporter (cMOAT) Gene is Overexpressed in Cisplatin-resistant Human Cancer Cell Lines with Decreased Drug Accumulation. *Cancer Res.*, **56**, 4124-4129.
- Taverna, P., Liu, L., Hanson, A.J., Monks, A. and Gerson, S.L. (2000) Characterisation of MLH1 and MSH2 DNA Mismatch Repair Proteins in Cell Lines of the NCI Anticancer Drug Screen. *Cancer Chemoth. Pharmacol.*, **46**, 507-516.
- Taylor, W.R. and Stark, G.R. (2001) Regulation of the G2/M Transition by p53. *Oncogene*, **20**, 1803-1815.
- Tishkoff, D.X., Amin, N.S., Viars, C.S., Arden, K.C. and Kolodner, R.D. (1998) Identification of a Human Gene Encoding a Homologue of *Saccharomyces cerevisiae* EXO1, an Exonuclease Implicated in Mismatch Repair and Recombination. *Cancer Res.*, **58**, 5027-5031.
- Trimmer, E.E. and Essigmann, J.M. (1999) Cisplatin. *Essays Biochem*, **34**, 191-211.

- Vaisman, A. and Chaney, S.G. (2000) The Efficiency and Fidelity of Translesion Synthesis past Cisplatin and Oxaliplatin GpG Adducts by Human DNA Polymerase β . *J. Biol. Chem.*, **275**, 13017-13025.
- Vaisman, A., Varchenko, M., Umar, A., Kunkel, T.A., Risinger, J.I., Barrett, J.C., Hamilton, T.C. and Chaney, S.G. (1998) The Role of hMLH1, hMSH3, and hMSH6 Defects in Cisplatin and Oxaliplatin Resistance: Correlation with Replicative Bypass of Platinum-DNA Adducts. *Cancer Res.*, **58**, 3579-3585.
- Voigt, J.M. and Topal, M.D. (1990) O⁶-Methylguanine And A:C and G:T Mismatches Cause Asymmetric Structural Defects in DNA That are Affected by DNA Sequence. *Biochemistry*, **29**, 5012-5018.
- Warren, D.J., Andersen, A. and Slordal, L. (1995) Quantitation of 6-Thioguanine Residues in peripheral Blood Leukocyte DNA Obtained from Patients Receiving 6-Mercaptopurine-based Maintenance Therapy. *Cancer Res.*, **55**, 1670-1674.
- Warren, M.A., Murray, J.B. and Connolly, B.A. (1998) Synthesis and Characterisation of Oligodeoxynucleotides Containing Thio analogues of (6-4) Pyrimidine-Pyrimidone Photo-dimers. *J. Mol. Biol.*, **279**, 89-100.
- Waters, T.R. and Swann, P.F. (1997) Cytotoxic Mechanism of 6-Thioguanine: hMut α , the Human Mismatch Binding Heterodimer, Binds to DNA Containing S⁶-Methylthioguanine. *Biochemistry*, **36**, 2501-2506.
- Woisard, A., Favre, A., Clivio, P. and Fourrey, J.-L. (1992) Hammerhead Ribozyme Tertiary Folding: Intrinsic Photolabelling Studies. *J. Am. Chem. Soc.*, **114**, 10072-10074.
- Wu, J., Gu, L., Wang, H., Geacintov, N.E. and Li, G.-M. (1999) Mismatch Repair Processing of Carcinogen-DNA Adducts Triggers Apoptosis. *Mol. Cell Biol.*, **19**, 8292-8301.
- Xu, Y.-Z. (1996) Post-synthetic Introduction of Labile Functionalities onto Purine Residues via 6-Methylthiopurines in Oligodeoxyribonucleotides. *Tetrahedron*, **52**, 10737-10750.
- Xu, Y.Z., Zheng, Q. and Swann, P.F. (1991) Simple Synthesis of 4-Thiothymidine, 4-Thiouridine and 6-Thio-2'-deoxyguanosine. *Tetrahedron Lett.*, **32**, 2817-2820.
- Xu, Y.Z., Zheng, Q. and Swann, P.F. (1992) Synthesis of DNA Containing Modified Bases by Postsynthetic Substitution. Synthesis of Oligomers Containing 4-

- Sustituted Thymine: O⁴-Alkylthymine, 5-Methylcytosine, N⁴-(Diethylamino)-5-methylcytosine and 4-Thiothymine. *J. Org. Chem.*, **57**, 3839-3845.
- Yamada, M., O'Regan, E., Brown, R. and Karran, P. (1997) Selective Recognition of a Cisplatin-DNA Adduct by Human Mismatch Repair Proteins. *Nucleic Acids Res.*, **25**, 491-495.
- Zackheim, H.S., Glogau, R.G., Fisher, D.A. and Maibach, H.I. (1994) 6-Thioguanine Treatment of Psoriasis: Experience in 81 Patients. *J. Am. Acad. Dermatol.*, **30**, 452-458.
- Zamble, D.B., Jacks, T. and Lippard, S.J. (1998) p53-dependent and -Independent Responses to Cisplatin in Mouse Testicular Teratocarcinoma Cells. *Proc. Natl. Acad. Sci. USA*, **95**, 6163-6168.
- Zamble, D.B., Mu, D., Reardon, J.T., Sancar, A. and Lippard, S.J. (1996) Repair of Cisplatin-DNA Adducts by the Mammalian Excision Nuclease. *Biochemistry*, **35**, 10004-10013.
- Zdraveski, Z.Z., Mello, J.A., Marinus, M.G. and Essigmann, J.M. (2000) Multiple Pathways of Recombination Define Cellular Responses to Cisplatin. *Chem. Biol.*, **7**, 39-50.

Appendix

FACs Data for Fig 4.9



Apoptosis Data for Fig 4.10

